

OPTIMIZATION DESIGN  
WORKFLOW FOR LARGE ROOF  
SHADING SYSTEMS

---

MASTER THESIS

MARIANNA PORCELLI







ABT B.V.

Ingenieursbureau Delft

TU Delft supervisors

Dr. MArch. Michela Turrin | TU Delft

Prof. ir. R. Nijssse | TU Delft

Dr.ir. H.R. Schipper | TU Delft

Dr. Truus Hordijk | TU Delft

Company supervisors

ir. Annebeth Muntinga | ABT b.v.

---

COMMITTEE INFORMATION

Student Name	Marianna Porcelli
Student Number	4627911
Master Programme	Civil Engineering
Track	Building Engineering
Specialisation	Building Technology and Physics
Faculty	Civil Engineering
E-mail	marianna.ramd@gmail.com
Telephone number	+31643658847

---

## STUDENT INFORMATION



## ACKNOWLEDGEMENTS

First of all, I want to thank my graduation committee.

Dr. Michela Turrin for the assistance, the extensive knowledge in the computational field and continuous feedback. The intense meeting helped me through hard moment of this research.

Annebeth Muntinga, for her availability and experience in the building physics part. Her advice has been extremely helpful.

Dr. Truus Hordijk providing me with deep knowledge in the daylight field. The suggested practical experiments and advices made my approach to the daylighting design more practical .

Prof. ir Rob Nijse and Dr. ir Roel Schipper for their guidance, assistance and critical thinking during the whole research period.

I would like to thank ABT for giving me the unique opportunity to conduct this research in their name and their contribution to shape this thesis. Furthermore, I thank all my colleagues not only for their help, but mainly for the friendly and warm environment.

Special thanks to Bas, Berk and Eve who patiently assisted me with the computational design.

I want to thanks all my closest and far away friends, for the patience, the kindness and for always been there in the most needed moments.

I am extremely thankful to my parents, Rocco and Angela and my brother Davide, who always believed in me. Without their support and love nothing of this could have been possible.

Last but not least, I want to express my immense gratitude to Earnest, the person that most of all was able to understand me. During this year he helped me to find the strength to overcome the most challenging obstacles.

Delft, October 2019



## ABSTRACT

Recently, sustainability is becoming a more important aspect in the building sector. The use of performance-driven approaches are progressively growing interest among architects and engineers. Proper design of a large span roof shading system can positively influence the micro-climate of the space underneath, representing a significant source of daylight and reducing the building energy demands. To support the decision making process and steer towards high-performing solutions, the adoption of computational design processes has the potential of being a fast and reliable approach. This project was undertaken to propose a computational workflow and evaluate its effectiveness as supportive decision-making tool from the early design stage of large roof shading systems.

The proposed Computational Design Exploration (CDE) is adopted to evaluate three different concept alternatives in terms of daylight and thermal performances. Based on the visualization and analyses of the data, the best performing morphological features of the three alternatives are identified and the design is refined to create an optimal fourth concept. In a second phase, the Computational Design Optimization (CDO) workflow is applied to obtain high performing solutions in terms of daylight objectives, by varying geometrical and material inputs. 50 configurations are selected as optimal. The post process of the CDO consists of a second CDE, in which the selected samples are evaluated in terms of energy performance. The final shading system is chosen by identifying the input settings that allow the lowest energy consumption. As result, the daylight requirements are fulfilled and the thermal properties are used as final decision criteria.

The steps described in the CDE and CDO workflow are followed through the combined use of a parametric modelling tool (Grasshopper) and a multidisciplinary design optimization platform (modeFRONTIER). Post-processing tools are adopted to help the identification of interaction effects of the variables on the performance targets. By a series of data visualizations and sensitivity analyses, it is determined whether the final optimal selected design configurations improve the visual and thermal performances.

The most important identified trends and variables are used as main inputs to produce a more structured and integrated computational workflow. The final proposed workflow is meant to be a versatile method to assist the designer in the decision making process, yet maintaining his/her autonomy of judgement.

Future research is needed to prove the validity and effectiveness of the proposed workflow. The integration of other design variables and performances objectives could lead to an holistic method, suitable for every kind of multi-objective design problem.

# TABLE OF CONTENTS

<b>INTRODUCTION</b>	<b>15</b>
<b>1.1 CONTEXT</b>	<b>1</b>
1.1.1 Energy Consumption	1
1.1.2 Performance oriented design	2
1.1.3 Integrative design process	2
1.1.4 Large span roof	4
<b>1.2 PROBLEM STATEMENT</b>	<b>4</b>
<b>1.3 RESEARCH QUESTIONS</b>	<b>6</b>
<b>1.4 OBJECTIVES</b>	<b>7</b>
<b>1.5 FUTURE DEVELOPMENT</b>	<b>8</b>
<b>1.6 METHODOLOGY</b>	<b>9</b>
<b>KNOWLEDGE PHASE</b>	<b>15</b>
<b>2.1 COMPUTATIONAL DESIGN</b>	<b>17</b>
2.1.1 Computer Aided conceptual Design	17
2.1.2 Performance-based design	17
2.1.3 Building performance optimization	19
<b>2.2 OPTIMIZATION TOOLS</b>	<b>20</b>
2.2.1 Optimization tools for GH	21
<b>2.3 DAYLIGHT</b>	<b>28</b>
2.3.1 Introduction	28
2.3.2 Daylight performance	31
2.3.3 Basic daylight principles	33
<b>2.4 LIGHTING DESIGN</b>	<b>36</b>
2.4.1 Lighting Indices	38
2.4.2 Amount of light	39
2.4.3 Distribution of light	44
2.4.4 Glare	46
2.4.5 Quality and benefits of light	50
<b>2.5 THERMAL COMFORT</b>	<b>55</b>

2.5.1	The Building envelope	55
2.6	SHADING SYSTEMS	56
2.6.1	Fenestration	56
2.6.2	Shading Devices	59
2.7	PRECEDENTS ROOF SHADING SYSTEMS	60
<b>COMPUTATIONAL WORKFLOW</b>		<b>67</b>
3.1	COMPUTATIONAL TOOLS	69
3.1.1	Tools requirements	69
3.2	INITIAL WORKFLOW ALTERNATIVE	71
3.2.1	GH and MF combination	71
3.2.2	Introduction to the workflow	72
3.3	OVERALL COMPUTATIONAL WORKFLOW	74
3.3.1	Computational design	75
<b>COMPUTATIONAL DESIGN EXPLORATION</b>		<b>81</b>
4.1	COMPUTATIONAL DESIGN EXPLORATION	83
4.1.1	Alternative geometry	83
4.1.2	Alternative making	84
4.1.3	Hypothesis	88
4.1.4	Exploration of the design space	89
4.2	CDE WORKFLOW	95
4.3	CDE RESULTS	97
4.3.1	Alternative 1	104
4.3.2	Alternative 2	106
4.3.3	Alternative 3	109
4.4	ALTERNATIVES COMPARISON	112
<b>COMPUTATIONAL DESIGN OPTIMIZATION</b>		<b>119</b>
5.1	SCHIPHOL TERMINAL	120
5.1.1	Building features	120

5.1.2	Model for performance simulation	121
5.1.3	Roof lighting design	123
5.2	CDO WORKFLOW	125
5.3	CASE STUDY VARIATION 1	128
5.3.1	Current roof shading system	128
5.3.2	Roof shading optimization	140
5.4	CASE STUDY VARIATION 2	155
5.4.1	Current roof shading system	155
5.4.2	Roof shading optimization	159
5.5	COMPARISON	172
	<b>NEW WORKFLOW PROPOSAL</b>	<b>181</b>
6.1	ADOPTED WORKFLOW	182
6.2	NEW PROPOSED WORKFLOW	186
	<b>CONCLUSIONS</b>	<b>193</b>
7.1	CONCLUSIONS	195
7.2	FUTURE WORK	199
	<b>APPENDICES</b>	<b>203</b>
8.1	APPENDIX A	204
8.2	APPENDIX B	211
8.2.1	Saint-Gobain products	211
8.3	APPENDIX C	212
8.4	APPENDIX D	219
8.5	APPENDIX E	220
8.5.1	History charts 1.2	220
8.5.2	Bubble charts 1.2	221
8.5.3	Pearson correlation strength	222
8.6	REFERENCES	224

8.7	LIST OF FIGURES	230
8.8	LIST OF TABLES	237



01







## 1.1 CONTEXT

The building sector is making huge steps towards sustainability. However many improvements are needed to reduce the energy consumption. The future of the built environment will be characterized by energy-efficient constructions, which rely on passive solutions. A passive design tries to create a comfortable and pleasant indoor space by means of the natural resources, such as building orientation, shading and solar radiation.

Recently, computational design exploration and optimization are becoming progressively more popular due to their combined potential. The use of performance-driven approaches, applied from the conceptual design phase can significantly reduce the energy consumption and lead to comfortable, appealing buildings.

### 1.1.1 ENERGY CONSUMPTION

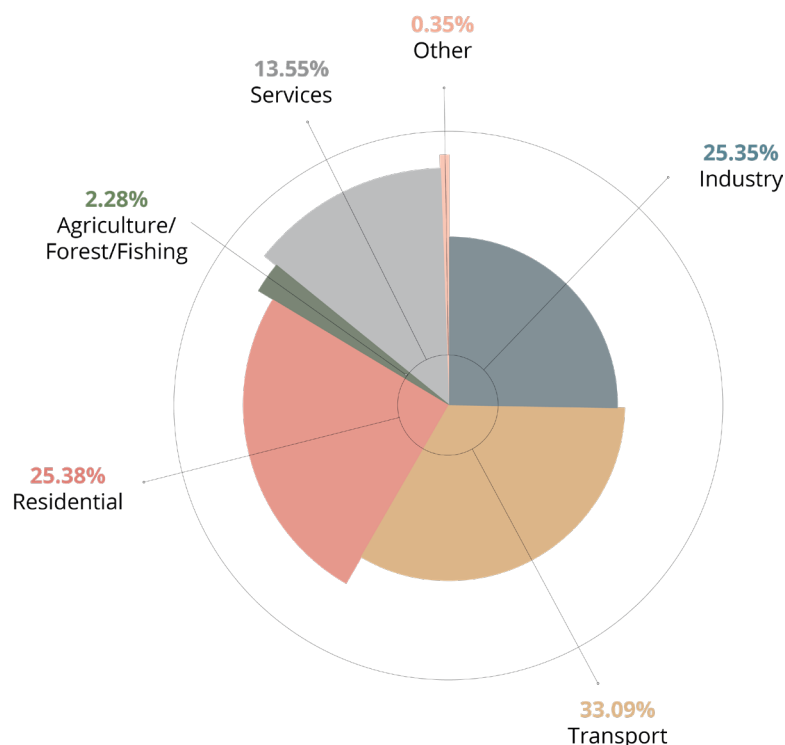


**Figure 1** Energy consumption per sector in the European Union in 2015. Source: Eurostat EU-28, 2015.

The energy consumption is mainly associated with four different sectors: transport, residential, industry and service sector. The awareness is growing in the building sector, especially considering that its energy consumption is

close to 25% of the total European energy consumption (see *Figure 1*) (Bertoldi, López Lorente, & Labanca, 2016) and second to the transport sector. Since sustainability is becoming a key goal, the building sector is promoting energy labels (e.g BREEAM, LEED, DGNB) to strive for green designs (Bertoldi, López Lorente, & Labanca, 2016). Reducing the energy consumption is becoming an essential requirement. The interrelation between form and performance should be taken into account from the start of the conceptual phase of a project (Turrin, Von Buelow, & Stouffs, 2011).

### 1.1.2 PERFORMANCE ORIENTED DESIGN

The architectural design process is complex and long and is divided in different phases in which the intentions are progressively defined and altered. The conceptual phase is usually limited to few alternatives and is driven by a set of assumptions regarding the consequences on the performances, such as energy and daylight. The shape and material properties are not considered in relation to the performance, despite they highly influence each other (Turrin, Von Buelow, & Stouffs, 2011). Design decisions can alter the energy behaviour of the

**Holistic Approach**  
To view the building and its environment as a whole and to examine all components when designing from the outside in

Green Building Illustrated

final solution, therefore it is necessary to aim for the adoption of an holistic approach. To achieve this, all involved members of a project need to work as a whole (Ching & Shapiro, 2014). The integration of engineering and architectural knowledge from the early design stages could facilitate the pursue of smart solutions (Turrin, 2014).

### 1.1.3 INTEGRATIVE DESIGN PROCESS

Traditional design is usually focused on later phases of the process. Modifying the design in these stages takes more effort and time compared to changes in an early phase. As Patrick MacLeamy (2010) said:

*“In today’s architects spend about 75% of their time on non-design tasks, practicing what I call defensive architecture. As a result design suffers from lack of attention. Not enough time is put into thoroughly vetting the design to be sure it absolutely suits the client’s purposes.”*

Traditionally, most of the effort is put into Construction Documents rather than the Design Phase. *Figure 2* shows how the ability to manage costs during time decreases until a point in which making changes and have an impact on the

performance of the building requires an extreme effort. Additionally, the more the design is documented, the harder it is to make changes. The trend of the cost of a project is so that the later a change in the design, the higher the effort and investment necessary.

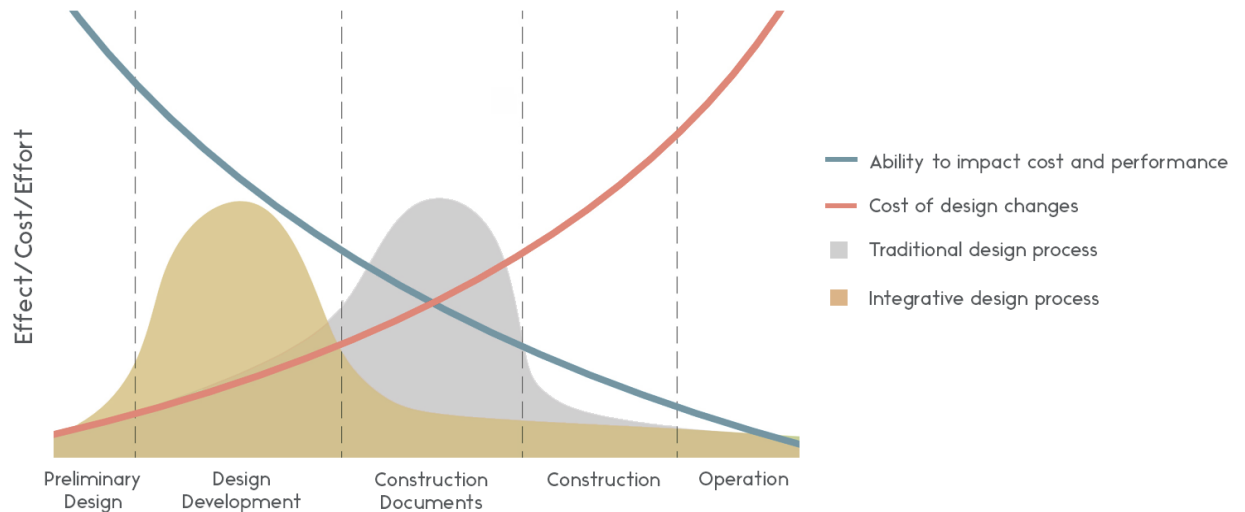


**Figure 2** The MacLeamy curve. Source: <http://danieloverbey.blogspot.com/2018/02/five-diagrams-every-design-team-should.html>

A new strategy of an integrative design process aims to “shift the effort” earlier in the timeline. Bragança, Vieira & Andrade (2014) emphasize the importance of approaching performance and cost problems during the early design phases, which have a higher impact on the final level of sustainability of the project.

The conventional design process consists in elaborating multiple designs which prioritize certain performance aspects and targets. After the model is ready, the designer carries out some simulations to assess the performance level. Finally, the optimization process aims to improve the solution and achieve better performance results (Shi, 2010). This is time-consuming and often results in a worthless optimization. The integrative design process operates with the combination of design exploration and optimization, supported by computational design methodologies, parametric models, simulation engines and optimization algorithms (Yang, Ren, Turrin, Sariyildiz & Sun, 2018). An holistic approach is necessary to obtain optimal solutions. Not only the projects can reach higher levels of sustainability, but also the design team effort and time during conceptual design are better repaid, leading to a smoother process (MacLeamy, 2010).

## 1.1.4 LARGE SPAN ROOF

The design of large open spaces is not a common practice in the building sector. Only few skilled and specialized architectural and engineering companies can deal with the complexity of these spaces and their envelopes. On the other hand, the request of big scale projects is increasing for applications in the public sector, such as train stations, urban spaces, museums, sport facilities, airport terminals, shopping malls, stadiums, etc. (Heinzelmann, 2018).

A roof is mainly constructed with the intentions of providing protection from all weather conditions, sound insulation from the inside to the outside and vice versa, thermal control for the underneath space and fire safety (Chudley & Greeno, 2014). Besides these common objectives, a large roof construction could function as source of natural daylight and artificial light (Turrin, Stouffs, & Sariyildiz, 2010).

## 1.2 PROBLEM STATEMENT

The design strategy for large span roof is generally based on the requirements of structural performance, aesthetic and budget. However, they represent a bigger challenge. The roof configuration has a major impact on the micro-climate of the space underneath it and on the surrounding area (Turrin, Stouffs, & Sariyildiz, 2010).

Performance-oriented design intentions can lead to an improvement in daylight, thermal comfort, energy performance, user experience and health. The features that an architectural work must contain are: Form, Function and Meaning (Sadeghi, Sani & Wang, 2015). That is why often a large structure has a high commercial and symbolic value. Often one of the design goals is to recreate a pleasant and open atmosphere for the user. This can be translated into lighting intentions (Tourre & Miguet, 2010).

In order to steer towards energy efficient solutions, it is necessary to integrate engineering and architectural knowledge. When the objective of a design is to achieve both an aesthetically pleasant and well performing solution, the final design often prioritizes one of the two aspects. This selection is due to the lack

of methods and techniques to fulfil multi-objective requirements. (Lin, 2014).



**Figure 3** Louvre Abu Dhabi. Source: Mohamed Somji © louvre abu dhabi

An important example of architectural work that encloses Form, Function and Meaning is given by the Louvre Abu Dhabi by Jean Nouvel showed in *Figure 3* and *Figure 4*. This building is the main inspiration for the topic of this thesis. The stunning dome of this museum is a masterpiece, it combines aesthetics with function, since the roof regulates the climate of the micro-city underneath it (Imbert et al, 2013).



**Figure 4** Interior spaces of Louvre Abu Dhabi; effect of 'rain of light'. Source: Roland Halbe © louvre abu dhabi

The dome is unique both on the outside and the inside (*Figure 4*), creating an effect of “rain of light”. Although the generated geometry appears to be completely random, the pattern is parametric and precisely controlled (Tourre & Miguet, 2010).

### 1.3 RESEARCH QUESTIONS

The main research question can be synthesized in the following:

“In which way can a work-flow, based on computational design exploration and optimization, be a supportive tool for the design decision making of customized large span roofs shading systems ”

Sub-research questions are:

- *Which CDE and CDO workflow can be applied for this research?*
- *Is it possible, using this workflow, to extract general rules and knowledge that can be applied for multiple case studies rather than a specific one only?*
- *Is it beneficial the use of the proposed workflow over the traditional computational design optimization (CDO) conducted in late stages of the project?*

## 1.4 OBJECTIVES

The aim of this thesis is to define an approach that can help the designer in the process of decision-making during the whole design process starting from the first phase. This method aims at obtaining daylighting-oriented roof design still respecting the ambition to conceive unique and customized solutions. The goal is to maintain the relation between art, architecture, engineering and sustainability through the use of parametric digital modelling. Furthermore, daylight cannot be considered separately from the energy consumption. The research addresses both daylight and energy performance.

The main objectives of this study are the following:

- What is computational design exploration (CDE) and computational design optimization (CDO)?
- Identify the Most relevant design variables
- Identify the most relevant performance objectives with daylight requirements as priority
- Investigating the lighting requirements for complex large spaces
- Set up multi-objective design optimization to identify the best geometrical features for the desired targets
- Propose a workflow implementing CDE and CDO that can be used as tool for a more informed decision making during the whole design process

## 1.5 FUTURE DEVELOPMENT

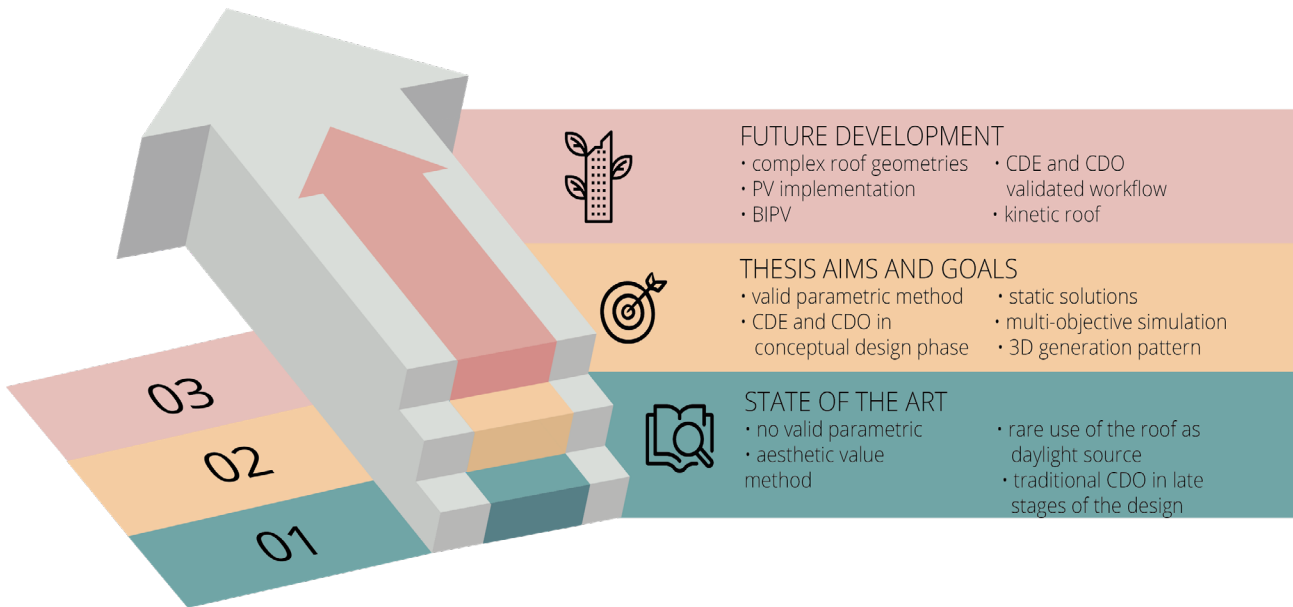


**Figure 5** Future development process

This study represent only a milestone in the whole development process. If the proposed method is developed until its full potential, it is possible to provide the designer with a tool able to handle complex problems. When the target of this research is reached, it is possible to move towards a more comprehensive method, integrating the study on complex shapes, embedded BIPV in the roof structure, relations with the internal materials, specific requirements for each space, implementation of users experience input through use of Virtual Reality etc. (see *Figure 5*).

## 1.6 METHODOLOGY

In order to answer these questions and reach the desired output, the structure of the research is divided in sections (*Figure 6*):

### Knowledge phase

The first part of the research is focused on parametric design and digital optimization, investigating the traditional and modern computational design exploration and optimization methods and tools. After this first part, knowledge on visual comfort, daylighting targets and indexes for a lighting design are provided. A chapter is fully dedicated to the effect of daylight on the energy performance of the building and basic information concerning static shading system are provided. Finally, a brief summary and analysis of the state of the art of large roof applications is presented.

### Practical research

This phase includes the method definition. The target is to generate a method which provides support to the designer and engineer to make performance driven decisions. This part is divided in four phases.

The **Parametric Design phase** aims to create parametric models of the possible patterns for the roof and building envelope. The software used is Grasshopper with relative plug-ins for daylight simulations, Diva, and for energy simulations, Archsim, using energyPlus. The variables of the model are set up, such as geometry, location and material performances. At the end of this stage, multiple design alternatives are formulated and modelled.

Following, the **Simulation phase** takes place. The parametric model is implemented with a set of variables related to geometry of the roof shading system, such as depth of the module, the opening ratio and inclination of the module. The user can execute several daylight and energy performance analyses. All the variables derived from the previous literature study and it is necessary to finalise this process by exploring and evaluating the parameters which highly influence the

daylight and energy performance simulations and produce realistic output.

The third phase is the **Computational Design Exploration (CDE)**, which aims in finding the optimal alternative between the proposed ones. The iterative exploration process weighs the design alternatives and allows data and knowledge extraction. Through statistical analysis, the most promising design features are identified. At this point it is possible to refine or create a new optimal concept alternative, based on the best performing features detected.

The fourth step is the **Optimization phase**. The optimization works through the use of multi-objective genetic algorithms, using the design variables and performance targets reformulated at the end of the previous step. The components that are needed for the correct operation of the algorithms are: design variables, constraints and objective functions (Wang et al, 2005).

## Case Study

The fourth step is the CDO, computational design optimization. With the support of ABT, one case study has been chosen: the New Schiphol Airport Terminal. To prove the effectiveness and adaptability of the proposed workflow, two variations of this case study are used. The first one with three curtain walls and the second one composed of only opaque façades. First, the performance simulation output of the current design variations are calculated and stored. Secondly, the case study variations are modified and the current roof system is changed with the previous refined alternative. The alternative is optimized following a proposed CDO workflow, after the daylighting targets and geometry variables are set. Finally, the results from the various performance simulations are compared and the best solution for each case study is identified.

## Conclusions

In this phase the overall conclusions are drawn and space is given for recommendations of future research.

OPTIMIZATION DESIGN WORKFLOW FOR  
LARGE ROOF SHADING SYSTEMS

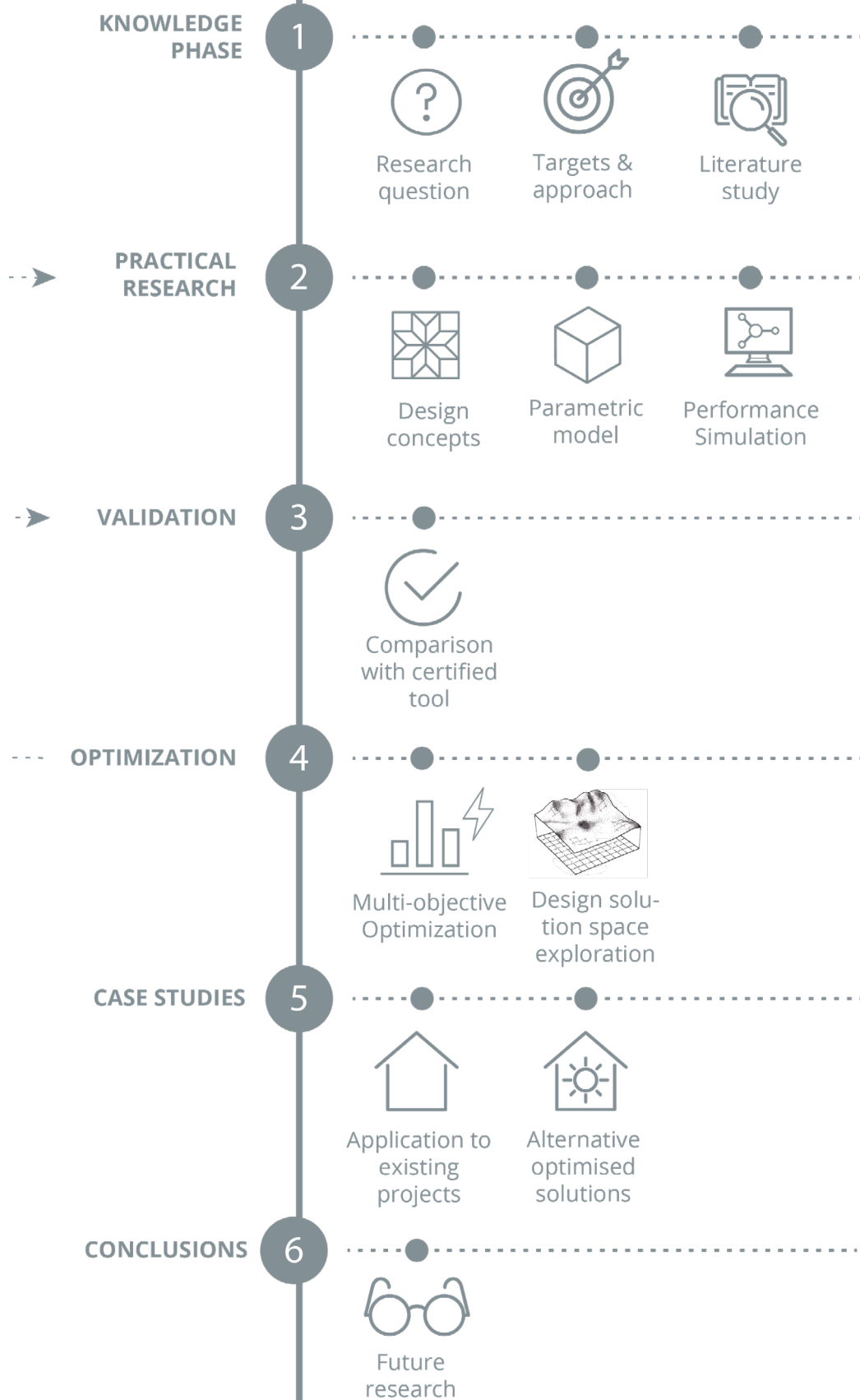


Figure 6 Research approach







02







## 2.1 COMPUTATIONAL DESIGN

### 2.1.1 COMPUTER AIDED CONCEPTUAL DESIGN

The conceptual design is defined from Pahl, Beitz, Feldhusen, and Grote (2007) as the part of the process through which is possible to define the design problems and requirements and obtain principle solutions. As stated from Wang (2002) the selection of poor alternatives can lead to a loss of 75% of the life-cycle cost and it is hardly possible to improve this projects in later design phases. Today, it is always more common practice to explore the alternatives using modern methods, which allows a more informed decision process. The CACD (Computer Aided Conceptual Design) methods support the form-exploration during the first phases of the design. These new techniques can revolutionize the way decision-making of conceptual solutions is carried out, introducing a more aware approach, which tends to base the selection on performance assessments.

### 2.1.2 PERFORMANCE-BASED DESIGN

Referring to the architectural process, the most common association is of geometrical complexity and aesthetic. Nevertheless, the design complexity is not exclusively linked to shape, but spreads in multiple branches (Michela Turrin et al, 2011). As Bernard Tschumi (1995) states: 'Architecture is not about conditions of design, but about the design of conditions'. The architectural system is an intricate mosaic created by interrelations and interdependencies between all the fragments.

There is consensus among design experts that the integration of energy considerations already from early stages enhances the exploration of performance solutions (Wang, Zmeureanu, & Rivard, 2005). Often the energy performing optimization is narrowed to few specific criteria (façade system, HVA, air flow etc.) and these analysis are mainly realized in advanced phases of the design, where the form finding process is already been finalized. In this way many solutions, forms and properties are ruled out purely in accordance to architectural conditions and this results in limiting the number of conceptual alternatives (Schlueter & Thesseling, 2009). However, the dependency between geometrical, material and environment properties are significant and require to be explored through the whole design process. According to Turrin (2013), the geometry is responsible in large scale for the performance output of the

building. It would be rather more efficient the use of an 'automated design cycle' (Schlueter and Thesseling 2009) which operates from the early conceptual design phases.

The architectural process is complex and in continuous transformation. The design is iterative and the geometry, the requirements and methodology keep changing. Often the architectural prerequisites during the conceptual stage are limited to budget, aesthetic and functionality (Michela Turrin et al, 2011). Designers rely on the availability of software that perform environmental analyses in late stages of the design, using criteria translated in numerical values. The decision-making process is based on assumptions dictated by personal experience rather than tested. The flourishing world of parametric design and computational modelling can change this mechanism (Tedeschi, 2014).

As Kolarevic (2003) points out, the future of the building design is the performative architecture, in which building performance is the key driving principle, integrated and assessed already from the conceptual phase. Performance is a wide term and refers to series of criteria from different fields like architectural, engineering, economic, social and environmental. The interrelation between all these disciplines increases the complexity of the design process and adds challenge in the assessment of the performance targets. However, it is possible to investigate the building model based on parametric study through the exploitation of new finding-form plug-ins and identify performance-based solutions. Through these software is possible to create dependencies between fixed parameters, variables and targets in order to realize performance simulations and optimizations of the design alternatives.

Various studies have assessed the efficacy of this new promising design method, which can lead to a conscious decision making process, with particular interest in the early design phases, when the chance to steer to energy-performance alternatives is higher (Bogenstätter, 2000). Tedeschi (2014) talking about form-finding parametric software combined with environmental analyses writes: 'These techniques, supported by a deep understanding of data, can lead to environmental-conscious designs'. The use of measurable criteria during the early stages of the design enables to drive the design through performance considerations and to aspire to more sustainable solutions.

### 2.1.3 BUILDING PERFORMANCE OPTIMIZATION

With the advent of new digital trends in the architectural design, the interest in computational modelling is growing. Through the use of computational tools, the designer is able to actively follow the dynamic design process and make decision in real-time. Engineering and architecture are starting to replace the old analytical calculation methods with more modern, fast and accurate computer systems. Generally these methods are experimental and are based on mathematical relations.

The use of optimization methods can influence the decision making significantly and are therefore an important aspect within the design process. The designer is able to investigate the different alternatives and understand the correlation between model variables and performance output. Indeed, through the use of Performance computational methods during the architectural shape exploration, it is possible to steer for good engineering choices (Riccobono, 2013).

The use of optimization algorithms is an approach which seek the optimal or sub-optimal solution to the problem of interest (Koziel & Yang, 2011). Pardalos and Resende (2002) state that “in mathematics, optimization is the discipline concerned with finding inputs of a function that minimize or maximize its value, which may be subjected to constraints”. The interest in optimization is mainly focused on cost, energy or environmental impacts, however the area of application fields is extremely vast.

Optimization in Mathematics

In mathematics, optimization is the discipline concerned with finding inputs of a function that minimize or maximize its value, which may be subjected to constraints

Pardalos & Resende (2002)

In the architectural field the term used is BPO. This acronym stands for building performance optimization. The intent of using this method is to solve performance design problems with algorithms that enable to find the best or sub-optimal solution. Using building performance simulations (BPS) to analyse the available alternatives and defining optimization targets and design variables it is possible to obtain the optimum or near-optimum design alternative (Athienitis & O’Brien, 2015). The optimization process necessitates a step in which the optimization criteria are translated in mathematical functions.

Optimizing does not necessarily mean to pick the best solution; this is due to the fact that in real-life there is always a part of unpredictable event and uncertainties. Furthermore, the research of one singular optimal solution based on a balance between different aspects can lead to sub-optimal solutions for one aspect at a time. Most of the time we aim for sub-optimal solutions, which are both fulfilling up to certain limits the desired performance requirements and are robust enough, engineering speaking (Koziel & Yang, 2011).

In computational design optimization, the computer is active in finding the optimal solutions based on the defined targets. Depending on the targets, the optimization method is different and can be either shape or topological optimization. In both cases it is important to define two main elements: the objective function, which is the guide for the optimization process and needs to be minimized or maximized, and the variables linked to the objective function (Tedeschi, 2014). The optimization solvers, as explained by Tedeschi (2014) can be divided in two groups and the user needs to be aware on which one is the best to use:

- **Exact solvers** - for simple problems it is possible to find the most efficient solution using exact solvers. The result is a single solution.
- **Heuristic solvers** - for more complex problem the heuristic evolutionary method is applied. This does not lead to a unique solution but to acceptable alternatives. The output is a 'population of candidate solutions'.

## 2.2 OPTIMIZATION TOOLS

This chapter has the intention of briefly comparing the various optimization tools available for the Architectural Design Optimization (ADO), in order to determine which one is the best to use for the specific goal of this thesis.

First of all, it is important to mention that the lack of available free tools and the scarcity of user-friendly interfaces, leave the adoption of the optimization process to a narrow circle of skilled designers and that is the reason why the popularity of ADO is limited and less diffused and accepted than what is commonly believed (Wortmann, 2018). Furthermore, there are some very well

known external tools that building designers use for the optimization process, like Matlab and GenOpt. However, these tools are very complex and require a wide skills in programming, which are not common in architects or engineers (Nguyen, Reiter & Rigo, 2014). Since these methods require too big of experience to be used for this research, it was decide to not take them into account.

Regarding the adoption of design tools, the choice was made in base of public available tools, personal knowledge and skills, and intention to gain experience in the use of the tool. The tools that are open-source and both capable of perform simulations and optimizations are essentially three: Grasshopper, Dynamo Studio and DesignBuilder.

Despite all of them are valid tools, Grasshopper includes more possibilities of integration with the numerous available plug-ins and interfaces made available from third-parties, who freely share their work. The reason behind its completeness lies in the wide and very involved community, which constantly keeps update and take care of improving this open source tool. Through the use of Grasshopper it is possible to carry out simulations of all the kinds: structural, energetic, acoustic, daylight etc. (Wortmann, 2018).

DynamoStudio and DesignBuilder are less flexible and offer less possibilities by using only the Pareto-front method of optimization, while with Grasshopper is possible to choose between different algorithms, depending on the aim of the optimization.

### **2.2.1 OPTIMIZATION TOOLS FOR GH**

Since the parametric tool chosen is Grasshopper, the investigation on optimization tool is restricted on the one that can be integrated in Grasshopper and some previous selection has been done accordingly to the optimization desired for this research.

## Galapagos

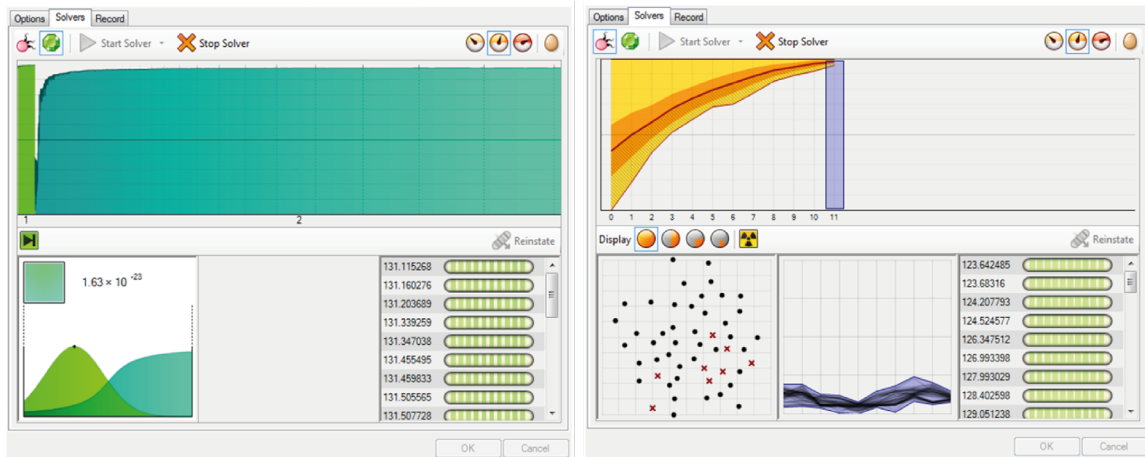


**Figure 7** Galapagos SA and GA interface. Source: Vierlinger, 2015

Galapagos is a plug-in designed by David Rutten, a graduate from TU Delft and currently working with the company ROBERT McNeel & Associates (RMN) (see interface in *Figure 7*). Galapagos is a tool that carries out optimization by means of two solvers: genetic algorithm (GA) and simulated annealing algorithm (SA). Rutten (2013) defines a phase space as a multi-dimensional landscape representing all the distinct possible solutions deriving from the combination of variables. Though, the number of solution can be exceptionally high, that is why it must be defined a fitness function, delineating the desired state.

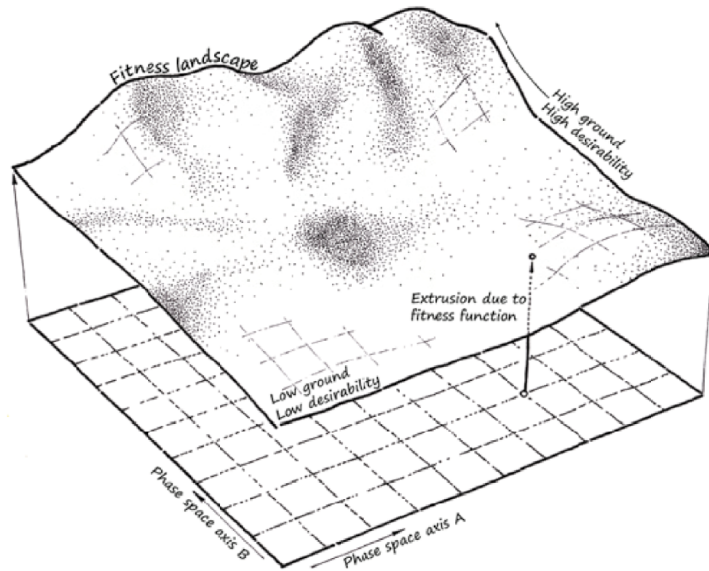


**Figure 8** Conceptual 2D phase space and relative 3D fitness landscape. Source: Rutten, 2013

The **simulated annealing algorithm** acts at first jumping from one state to the other, with the intent of finding good ground in the phase space or, as defined by Rutten (2013), the high peaks in the landscape, which represent high

desirability (*Figure 8*). The solver moves randomly by big steps until it finds a good space and then it starts to evaluate with smaller steps more confined areas. This process continues as far as a the highest peak or best solution is detected. *Figure 9* is a conceptual representation of the behaviour of a simulated annealing solver.

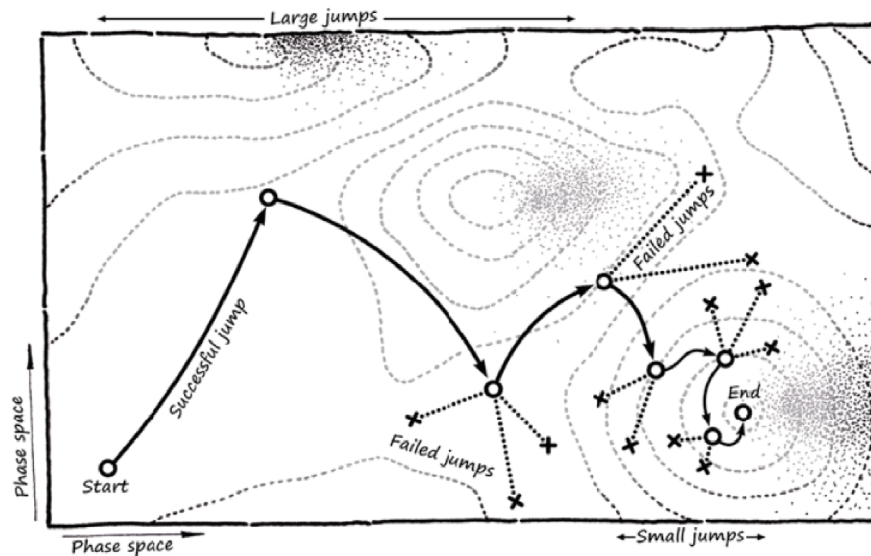


**Figure 9** Simulated annealing solver progression. Source: Rutten, 2013

Genetic algorithm is a category of evolutionary algorithm. The solver starts to investigate the whole landscape and slowly constrict the landscape with higher altitudes with population of individuals (*Figure 10*). This method does not imply that the better solution will be find. Each time that the evolutionary solver runs, the output can be different. The idea behind this method is to find a good-fitting solution instead of the best one.

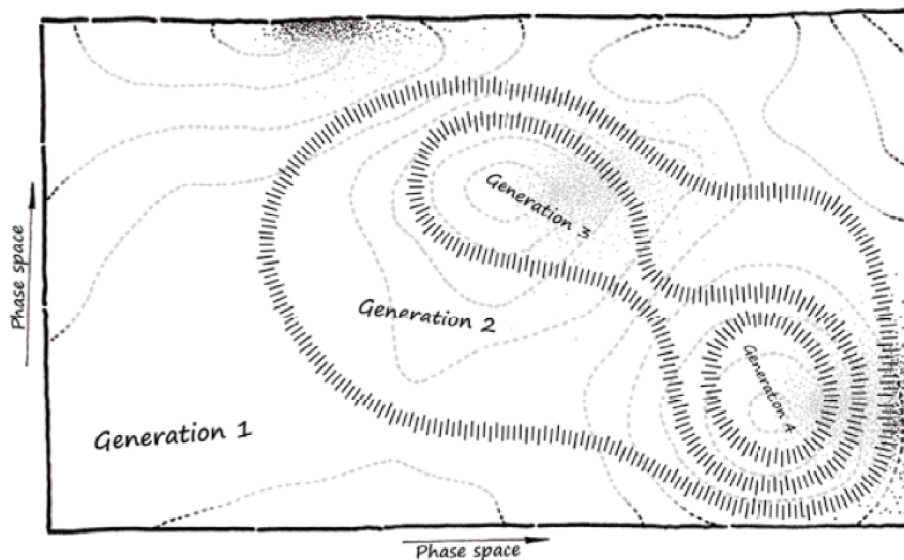


**Figure 10** Evolutionary solver progression. Source: Rutten, 2013

Rutten (2013) concludes:

‘Both solvers have their benefits and drawbacks. Annealing is better at navigating rough landscapes. Evolution is better at finding reliable intermediate solutions early on’.

### Goat

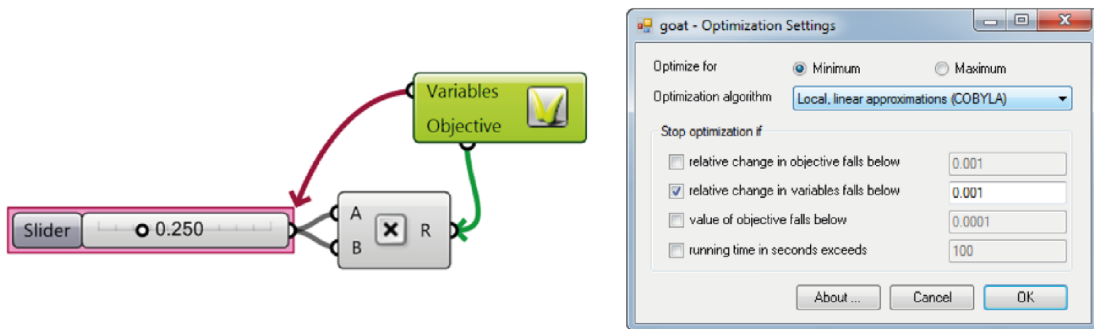


Figure 11 Goat's component and graphical user interface. Source: Vierlinger, 2015

Goat is an exact solver, which means that the output is one and no matter the number of time the solver runs the optimization, the solution will always be the same. Goat interface can be seen in *Figure 11*. Goat use a deterministic approach and has origins from Galapagos, using the same kind of workflow with components and parametric relations. It provides five different algorithms through which is possible to carry the optimization (Vierlinger, 2015). It is also possible to combine the potential of both Galapagos and Goat, by first exploit the potential of Galapagos to restrict the number the population of investigated solutions and carry out the final optimization with Goat (Flöry, Schmiedhofer & Reis, 2012).

### Octopus

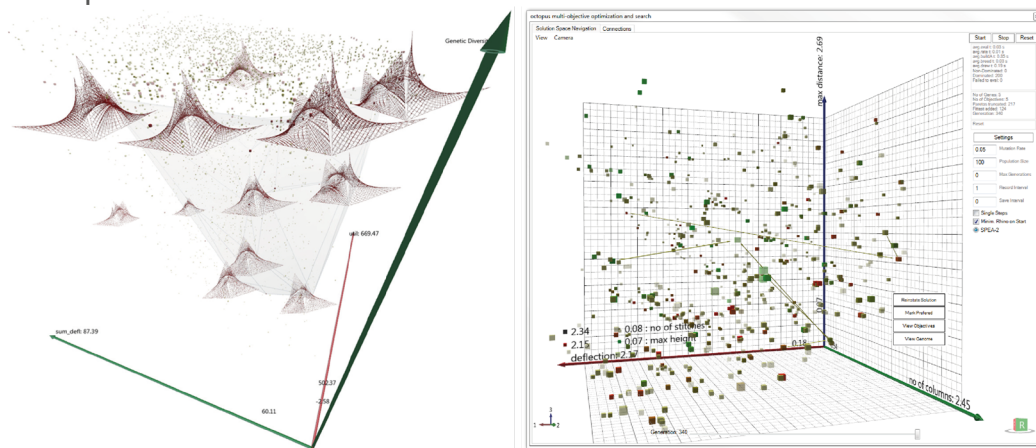
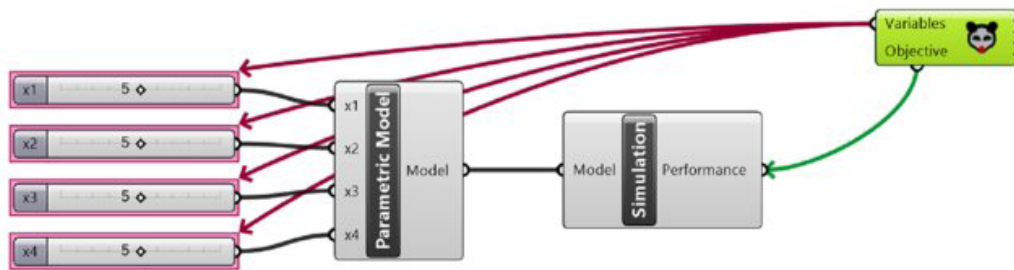


Figure 12 Octopus different visualization of trade-off space. Source: <https://www.grasshopper3d.com/group/octopus>

Octopus is a tool developed by Vierlinger (2013) allows to perform multi-objective optimization (*Figure 12*). Octopus is based on a meta-heuristic approach, which means that the solver uses algorithms that are not problem-specific (Bianchi, Dorigo, Gambardella & Gutjahr, 2009). The algorithm adopted is evolutionary and aims at finding a sufficiently satisfying solution, which is not a promise of being the optimal solution, but near-optimal solutions. The user is actively involved and can take decision based on the visualization of the possibilities. The research is not only restricted to the Pareto-front designs, but also external candidates. Together with Galapagos, Octopus represent one of the most diffused and used tools in the architectural optimization field. The reason behind this propagation lies behind the direct link with Grasshopper and the contribution that the user can make by actively participating to the decision-process (Wortmann, 2018).

### Opossum



**Figure 13** Opossum components in Grasshopper. Source: Thomas Wortmann

Opossum (*Figure 13*) (Optimization Solver with Surrogate Models) is a model-based optimization tool, one (if not the only one) user-friendly with a graphical user interface (GUI), which does not require programming knowledge (*Figure 14*). Wortmann is the developer of this free tool, which use a global-search algorithm, thus the final solutions found is among the global number of candidates.

Opossum connect to an open source library of RBFOpt, which enable the optimization of the model exploiting the potential of machine-learning for the morphology of the fitness landscape. The continuous fitness landscape data acquired are contemporaneously manipulated to narrow the amount of design candidates (Wortmann, 2018).

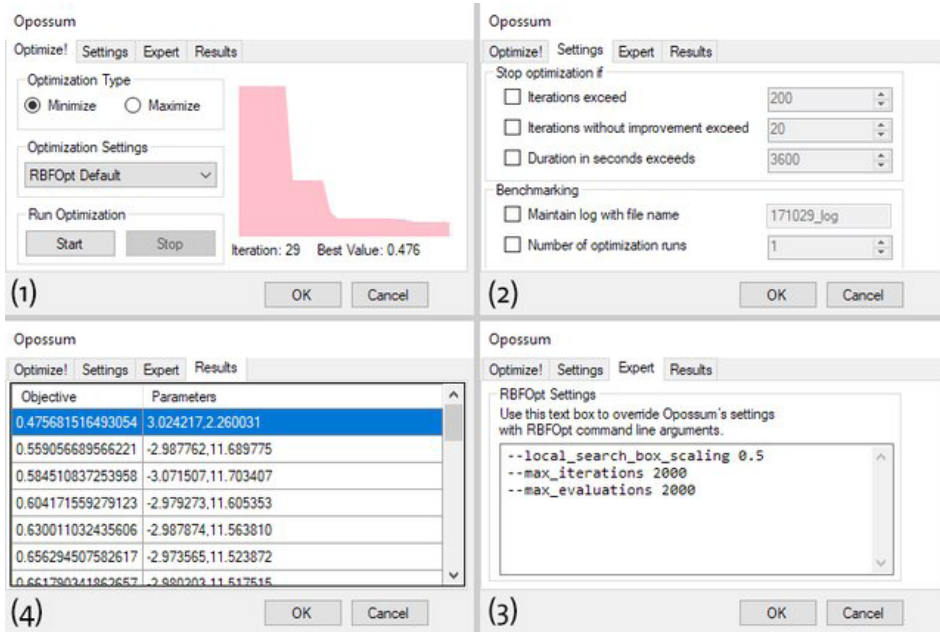


Figure 14 Opossum graphical user interface. Source: Thomas Worthmann

## Design Space Exploration

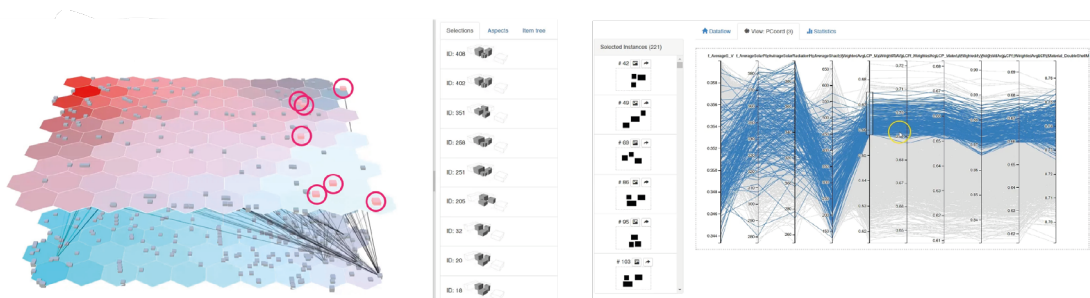
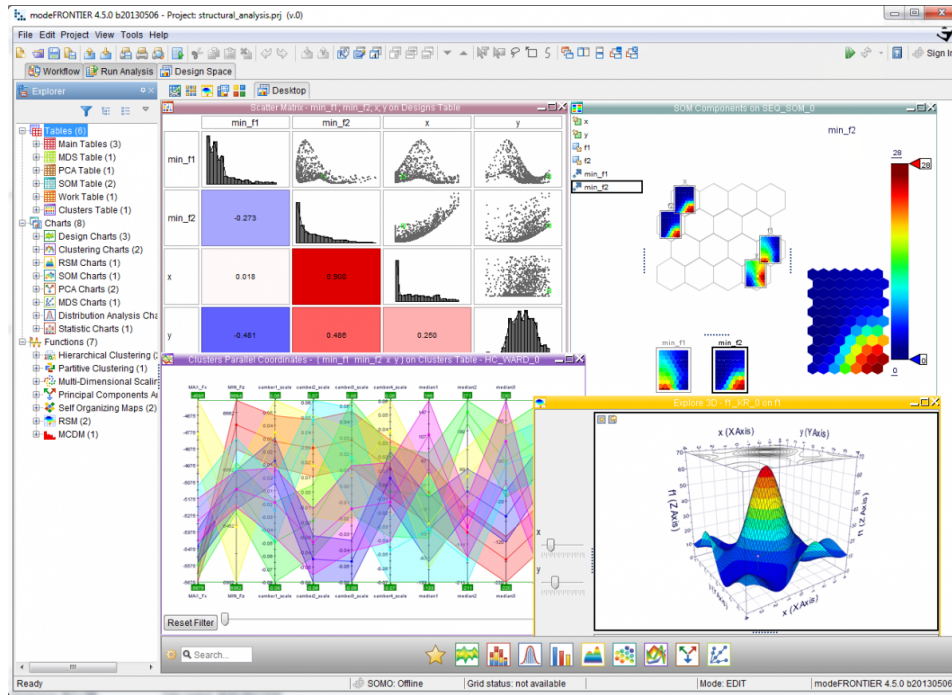


Figure 15 Design Space Exploration framework. Source: Reinhard Koenig

Design Space Exploration (DSE) is an optimization tool that supports a large number of different analysis methods. It was developed in 2015 by Digital Structures at MIT. The tool enables a priori and a posteriori optimizations and includes the possibility for the user to interact and actively prioritize certain targets over others (Figure 15).

Using Design Space Exploration it is possible to perform multi-objective optimization and it connects to Stormcloud which allows an interactive optimization. During the process the designer can select between the first optimization two parents, which are the starting point for the next evolutionary generation. DSE combines both quantitative and qualitative variables, integrating performance optimization and design preferences.

## modeFrontier



**Figure 16** modeFrontier visualization of the candidates. Source: [https://www.esteco.com/sites/default/files/design\\_space45.png](https://www.esteco.com/sites/default/files/design_space45.png)

In 2000 ESTECO SpA released a first commercial version of modeFRONTIER, a Multidisciplinary Design Optimization (MDO) software using multivariate analysis algorithms. Some of these algorithms are: Self-Organizing Maps, hierarchical clustering, Parallel Coordinates etc. modeFrontier enables the user to visualize the different designs and to actively participate to the optimization process (Figure 16). The tool works with mathematical optimization of the defined targets and it takes into account the designer personal preferences, integrating quantitative and qualitative elements. In this way, not only the performance aspect is taken in consideration, but the user has a large influence in the selection and breeding process of the design solutions.

This kind of interactive evolutionary optimization process includes the investigation of optimal and sub-optimal alternatives, so the designer can evaluate the fitting of the solution in the context, architectural intentions and the aesthetic aspect. The software can be linked to the Grasshopper environment through myNODE, a tool which makes possible the visualization and exploration of the morphologies and the relative data. myNODE creates the graphical user interface (GUI) to examine the phase space, however, it is not possible to defined it as a user-friendly interface for Design Space Exploration (DSE).

## 2.3 DAYLIGHT

### 2.3.1 INTRODUCTION

Daylight has a pivotal role in energy saving. The relation between building envelope and external environment could be exploited in order to obtain efficient solutions in the building sector. Previous research has established that natural light controlled properly can diminish the energy requests for the building in terms of heating, cooling and lighting (Chi, Moreno, & Navarro, 2017). Furthermore, it is important to consider daylight in the lighting design already in the early design phases. The proper incorporation of daylight is crucial for a wide range of aspects, some of them listed below.

- **Energy savings** - a proper lighting system with integrated daylight can allow the reduction of electricity
- **Health** - it has been proven that exposure to natural light stimulates our nervous system and modifies physiological functions and produce positive feelings. The body's natural clock can be maintained by proper connection with the external environment
- **Visual comfort** - depending on the person and activity, the lighting conditions can be different, visual comfort is essential to perceive a space as pleasant. Moreover, a proper lighting design induce an increment in productivity
- **Thermal comfort** - to allow natural light in a space can also create side effects, like absorption of solar energy with excessive increasing of the temperature
- **Safety** - additionally to the previous aspects, safety issues need to be addressed to ensure a proper visibility. This matter is particularly important when referring to train stations, airport terminals and sport centres.

Furthermore, one of the key aspects emphasized in building energy labels is the amount of light allowed inside the building. Therefore to obtain an higher sustainable certification it is meaningful to focus on the daylighting levels (Erlendsson, 2014).

## Goals

Light is an important element in terms of building energy performance. Much of the shading devices research has focused on identifying and evaluating their effects with application on building façades. However, there is little published data on their relevance on roofs. Previous studies have explored and established the importance of the relationships between building envelope and external environment and how this can be exploited in order to obtain efficient solutions. When natural light is controlled in a proper way, the final solution allows to reduce the energy demand for lighting, heating and cooling (Chi, Moreno, & Navarro, 2017). However light is not only related with energy, it is primarily an element that plays an important role for the health, comfort, security and productivity of the user.

## The sun path

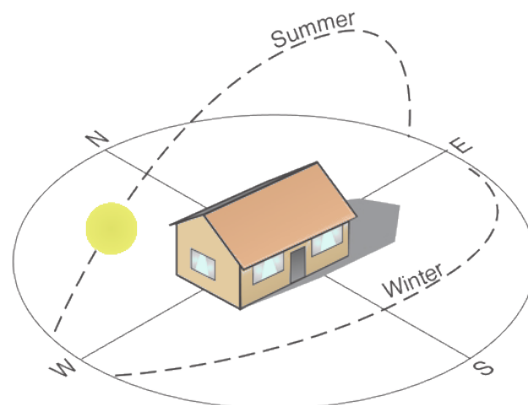


**Figure 17** Sun Path In North Hemisphere. Source: <https://www.nachi.org/building-orientation-optimum-energy.htm>

Daylight is a dynamic phenomenon due to the movement of the earth around the sun. The greatest source of natural light is the sun, that is why it is important

\*One type of house seems appropriate for Egypt, another for Spain ... one still different for Rome... This is because one part of the earth is directly under the sun's course, another is far away from it, while another lies midway between the two ... It is obvious that designs for homes ought to conform to the diversities of climate\*

Vitruvius (Morgan, 1960)

to determine the sun path (Figure 17). Present-day techniques allow to actively track and represent the sun path related to the earth. The fluctuation of the amount of daylight are dependent from the Earth's axial rotation around the Sun. The cyclical repetition of day and night and of the seasons of the year can be registered and the amount of daylight entering a building can be easily calculated.

As already stated by Vitruvius in the Roman society during the first century BC, the architectural design is in need of taking into account the sun path (Baker & Steemers, 2014). The building orientation is crucial to take advantage from the Sun to maximize the energy benefits.

### Health and physical needs

A good lighting design is beneficial for the health, comfort and productivity of human beings. The architectural integration of a lighting design is not only a matter of aesthetic, indeed it has a significant role in the human psychological responses. The lighting design needs to consider multiple aspects including the lighting level, the colour and the direction of light, which deeply affect the emotional sphere.

The way light strikes an object, get reflected or diffuse in the space can produce different feelings and affect people’s mood. The emotional quality is directly dependent from the light level and colour. Blue lights produce a cold feeling and incentive productivity, on the opposite the sensation of warmth is stimulated by yellow and red scale colours, finally a person can feel more calm surrounded by green tint (van Bommel & Rouhana, 2016).

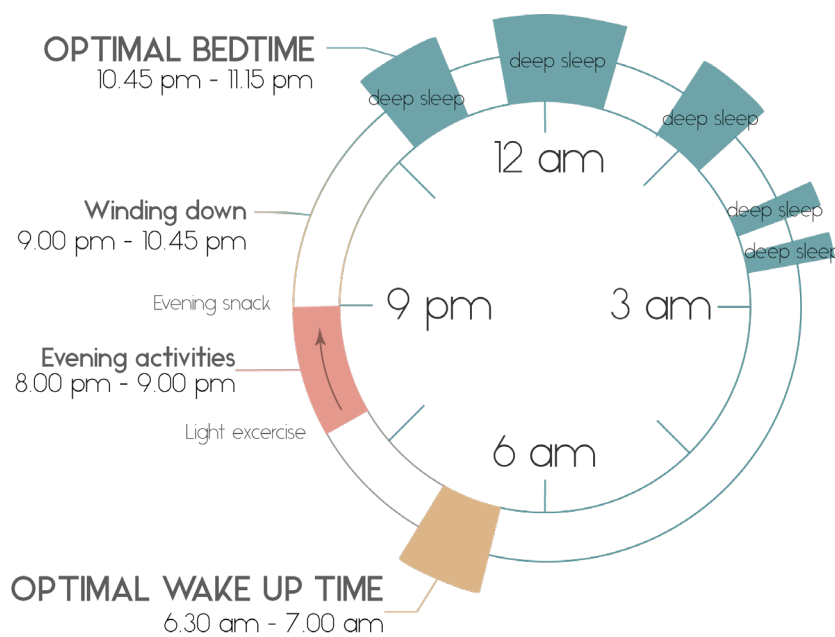


**Figure 18** Circadian rhythm. Source: <https://ouraring.com/find-your-own-circadian-rhythm/>

The life on Earth results on a continuous alternating of day and night, this cycle

creates an adjustment of our body, regulating our “internal biological clock”. The Circadian rhythms is a terms related to the dynamic nature of daylight (*Figure 18*). The master clock regulates the human biological system, which consists in a series of important functions like hormones production, body temperature and blood pressure. The physical and psychological response of the human body to the light and night circle is unquestionable, this certainty push engineers and architects to lead a more precise and detailed investigation on the lighting design. A well designed lighting system and solar control allows natural light to reach the internal ambient, positively affecting the living atmosphere. According to Figueiro (2013), the lighting system needs to follow the natural daylight levels, facilitating sleep during the night with the release of melatonin and inducing a higher production of cortisol during the day to increase productivity and alertness.

### **2.3.2 DAYLIGHT PERFORMANCE**

Daylight is a dynamic phenomenon and its availability depends on location, orientation, weather conditions, surrounding and shape of the building (Heinzelmann, 2018). Daylight can be manipulated as source of natural and free energy. A building properly designed according to daylight driven performance can exploit the conditions of natural light to illuminate and heat up the internal spaces in order to reduce the energy demands regarding lighting, heating and/or cooling. In some cases, especially during summer, the goal is to minimize the cooling load. Solar energy is the only responsible for solar gain and it represents a problem, especially in southern climates, however it is still desirable to let daylight in. On the contrary, during winter is wished a reduction in the heating demands, trying to exploit the sun energy to keep the ambient warm (Baker & Steemers, 2014).

In short, the general aim is to efficiently regulate the space temperature in order to maintain a comfortable environment, with minimum help from the cooling and heating system, to optimize the reflection and/or absorption of heat gain and providing enough light energy inside the building. Energy saving is possible by finding solutions that allow to minimize the cooling and heat load and cutting down the artificial lighting needs for the building.

## Solar Radiation

Daylight is the result of direct and indirect sunlight. Sunlight or daylight can be described as the combination of three components: ultraviolet (UV), visible light (VL) and infrared (IR) (*Figure 19*). The portion of visible light received from the earth is only 45%, the rest consists of ultraviolet (5%) and solar infrared radiation (50%). The portion of the spectrum from 310 to 380nm is the UV, the range from 380 to 780 nm represents the visible light and the infrared are from 780 to 2500 nm.

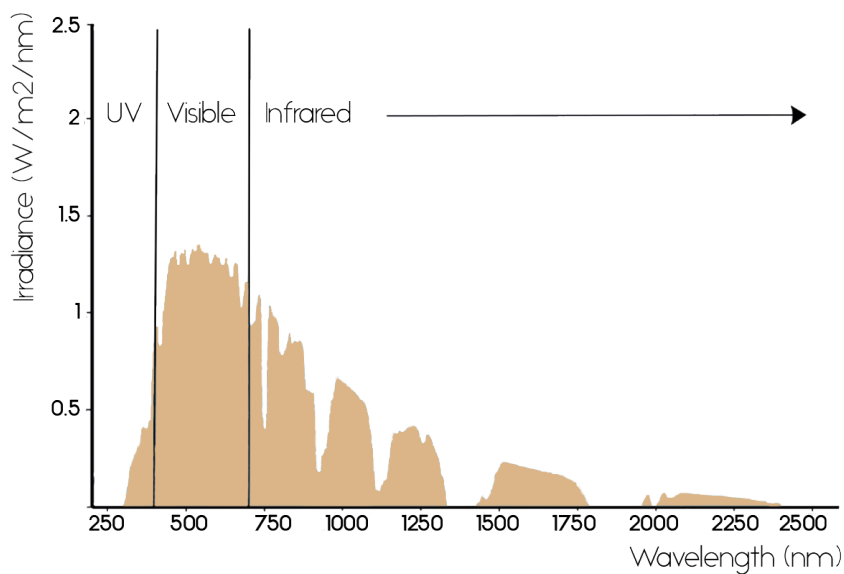


**Figure 19** Solar spectrum. UV, Visible and Infrared wavelengths. Source: Lechner, 2015

The greenhouse effect (*Figure 20*) is responsible for the solar heat gain. 98% of the solar energy derives from visible and infrared light. The interior spaces heat up due to long-wave radiation, also called near infrared, which represents the light between 700 and 2500 nm, not visible to the human eyes.

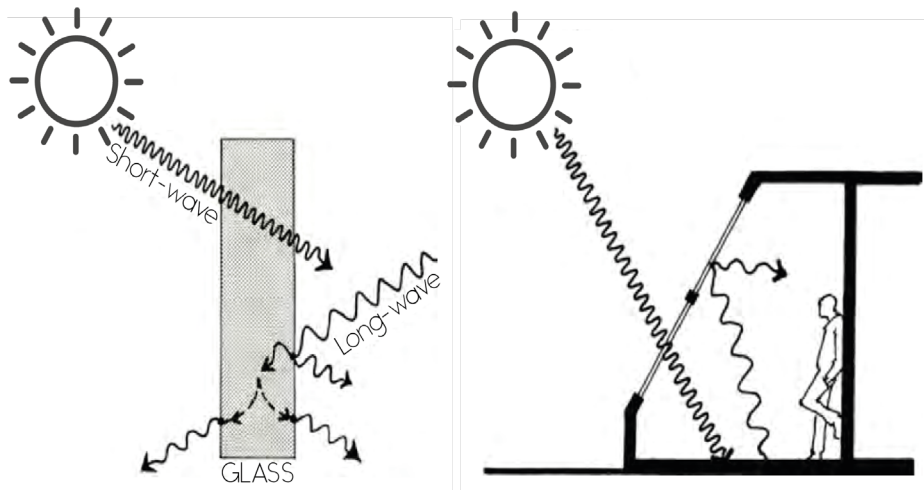


**Figure 20** The greenhouse effect. Source: Lechner, 2015

As showed in *Figure 23*, the phenomenon starts when the solar radiation passes through the glass, enters the room/building and hits the interior objects. The objects heats up and consequently release long-wave radiation. Glass acts as a transparent material associated with short-wave radiation, while it acts as a barrier when associated with long-wave radiation. Therefore, after the light enters, it is transformed in long-wave radiation, trapped by the glazing and the room temperature starts to increase (Lechner 2015).

### 2.3.3 BASIC DAYLIGHT PRINCIPLES

Light has a double personality which can be explained by De Broglie's theory (1924) which combines the wave hypothesis of Maxwell and the quantum theory of Planck. According to this theory either one or the other nature of light prevails depending from the wavelength (Kamsteeg, 2016). The visible portion of the electromagnetic spectrum with wavelengths between 380 to 780 nm is the one defined as 'light' (van der Linden et. al, 2016) (*Figure 21*).

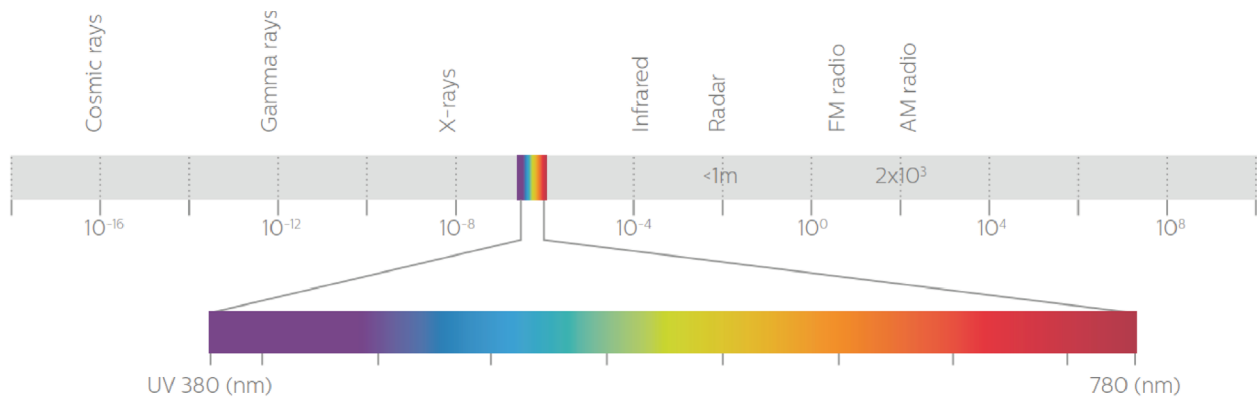


**Figure 21** Electromagnetic spectrum. Source: van Bommel & Rouhana, 2016

The electromagnetic spectrum can be divided in bands, each band produces a different perception to the human eye, which is translated in different colours of the light, this effect is called 'colour sensation' (Kamsteeg, 2016).

## Sources

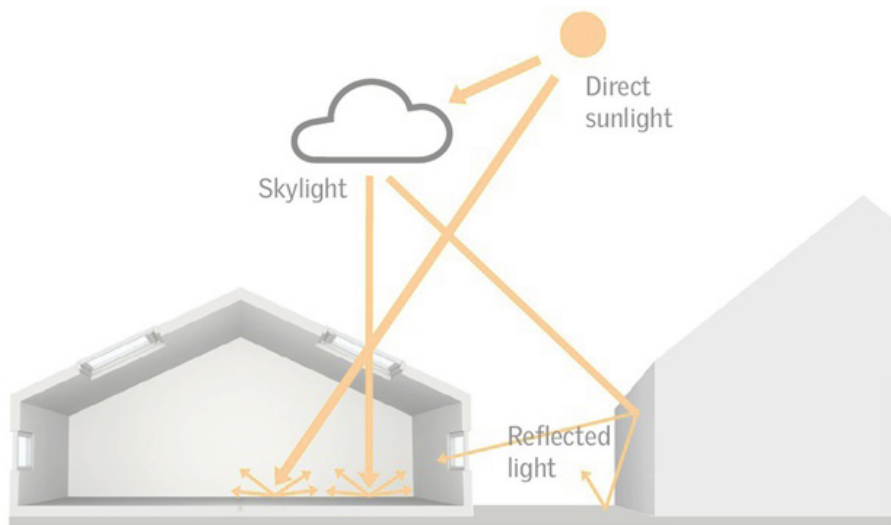


**Figure 22** Daylight sources. Source: <https://www.velux.com/deic/daylight/daylighting>

Daylight sources can be divided in two groups: direct and indirect (*Figure 22*). The first category refers to sunlight, the sun radiation reaching the surfaces in case of clear sky, while the second is referred to diffuse skylight, deriving from the scattering phenomenon, which is due to absorption from elements from the earth's atmosphere in case of a cloudy sky, and the components that are reflected from the ground and other obstructions (Samant, 2011).

## Light behaviour

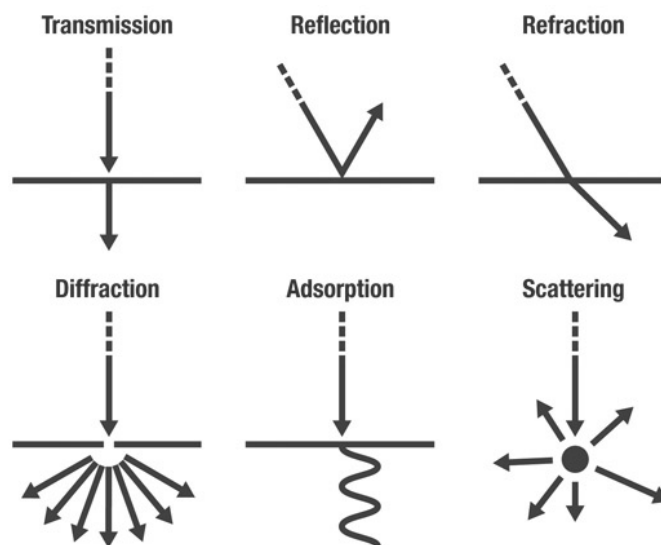


**Figure 23** Light behaviour. Source: <http://weeklisciencequiz.blogspot.com/2011/09/when-light-meets-matter.html>

Light propagates in the vacuum as electromagnetic wave with speed of around 300,000 km/s (Kamsteeg, 2016). When light strikes a medium (solid or liquid), its behaviour changes and different phenomena can occur: transmission, reflection and adsorption (*Figure 23*). It is possible to define the incident radiation or incident radiant flux  $\Phi(\lambda)$  as sum of reflected radiant flux  $\Phi_{\rho}(\lambda)$ , absorbed radiation  $\Phi_{\alpha}(\lambda)$  and transmitted radiant flux  $\Phi_{\tau}(\lambda)$  (Pinterić, 2017):

$$\Phi_{\rho}(\lambda) + \Phi_{\alpha}(\lambda) + \Phi_{\tau}(\lambda) = \Phi(\lambda)$$

- **Transmission** - in this case the light passes through the material unaltered and maintains its route unchanged. The transmission coefficient or transmittance  $\tau(\lambda)$  can be defined as followed:

$$\tau(\lambda) = \frac{\Phi_{\tau}(\lambda)}{\Phi(\lambda)}$$

- **Reflection** - when light meets a mirrored surface the effect is the reflection of the incident radiation. The ratio of reflected radiation and total incident energy is defined as reflectance  $\rho(\lambda)$ :

$$\rho(\lambda) = \frac{\Phi_{\rho}(\lambda)}{\Phi(\lambda)}$$

- **Absorption** - when light hits a material, part of it is absorbed and transformed into energy, represented by the acceleration in the vibration of the atoms composing the substance, which is translated into radiated heat. The absorptance  $\alpha(\lambda)$  is defined as:

$$\alpha(\lambda) = \frac{\Phi_{\alpha}(\lambda)}{\Phi(\lambda)}$$

Because of the energy conservation principle, the sum of this coefficient is equal to the unity:

$$\rho(\lambda) + \alpha(\lambda) + \tau(\lambda) = 1$$

In *Figure 24 Light behaviour for non-transparent (left) and transparent material (right)*. Source: Pinterić, 2017 the left image shows how light behave when radiation strikes a non-transparent object. The incident radiation ( $\Phi$ ) is in part reflected ( $\Phi_{\rho}$ ) and in part absorbed ( $\Phi_{\alpha}$ ). The right image illustrates the behaviour of the radiant flux when hitting a transparent object. The main fraction of the

incident flux is transmitted ( $\Phi_{\tau}$ ), another fraction is reflected ( $\Phi_{\rho}$ ) and the remaining flux is absorbed by the material ( $\Phi_{\alpha}$ ).

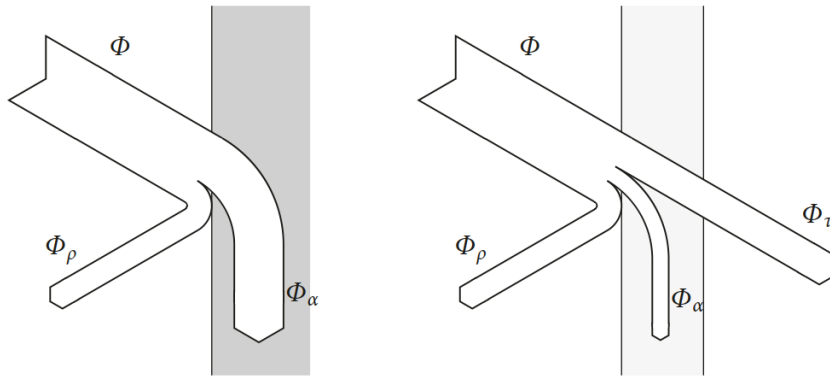


**Figure 24** Light behaviour for non-transparent (left) and transparent material (right). Source: Pinterić, 2017

For an ideal black body the light is only transmitted and absorbed, while the reflectance coefficient would be 0. For a perfectly white surface the reflectance would be 1. A perfectly transparent material would have transmission index equal to 1, while the opaque material transmittance is 0 (Figure 24 Light behaviour for non-transparent (left) and transparent material (right). Source: Pinterić, 2017). More about refraction, diffraction and duality nature of the light can be found in "Appendix A".

## 2.4 LIGHTING DESIGN

In order to accomplish a good lighting design it is necessary to take in consideration both quantitative and qualitative requirements. The central driving demand is the fulfilment of three main criteria (NEN-EN 12464-1, 2011):

- **Visual comfort** - the well-being related to lighting conditions is relatively hard to classify since it can not be categorized as perceptible sensation, but more as a feeling that can be conscious or unconscious. The user mainly realize when the illumination produces an uncomfortable sensation (Baker & Steemers, 2014)
- **Visual performance** - it is important to comply with the requirements that allows to perform usual tasks and colour perception related to our sight. A good illuminated space enables to perform our

duty in a precise and productive way (Baker & Steemers, 2014)

- **Safety** - a well-designed lighting system provides a safe and protected environment

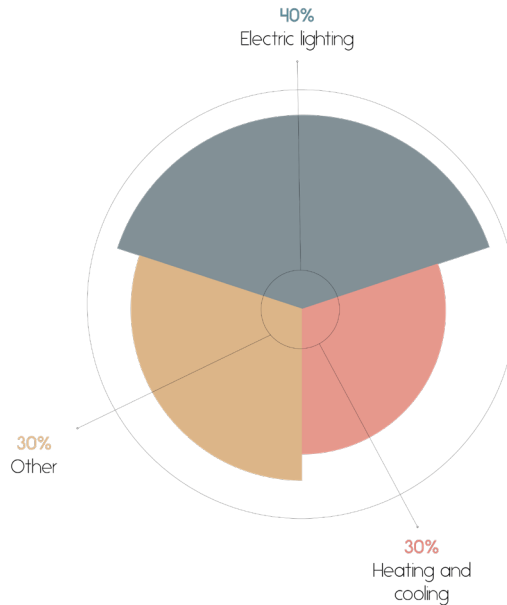


**Figure 25** Energy use distribution for generic buildings. Source: Norbert, 2015

Besides these important aspects, lighting represents a big portion of the electricity needed for the building sector, more than the 30% (Nelson, 2016), for offices this percentage is higher than 40% (**Figure 25**) (Todd, 2011). According to Lechner (2015), daylighting has a big potential in the reduction of electric lights consumption. A window of 0.9 x 1.5 meters produce the same amount of light as 100 lamps, each of 60 W power (**Figure 26**).

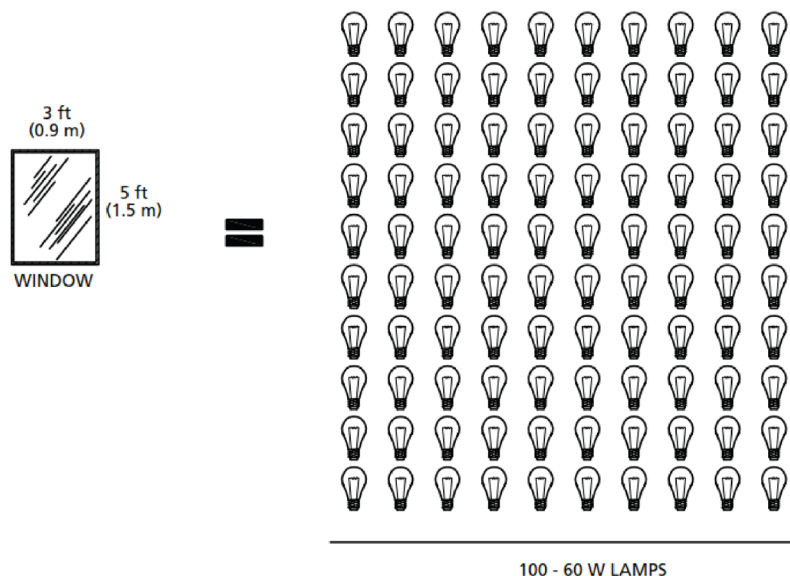


**Figure 26** Indication of the energy and electrical demand savings possible with daylighting. Source: Norbert, 2015

It may arise the concern regarding the strict correlation between daylight and heat production. In some situation, like summer time or warm climates, it is important to limit passive solar heating. Shading devices are used to obstruct the light from the outside to the inside. However, the need of reducing solar gain can be in contrast with the aim of intensify the natural light. A well-designed system can overcome this problem, the temperature can be controlled and the daylighting properly regulated. In this way both energy and money savings can be maximized (Lechner, 2015).

The Dutch normative NEN-EN 12464-1 “Light and lighting - Lighting of work places - Part 1: Indoor work places” clarifies that the European standard does not provide requirements so to fulfil the safety and health demands for people, but rather requirements in terms of daylight quantity and quality, however without restrictions on the typology of the solution. The standard does not restrict the design freedom, technological innovation and alternative designs are valid solutions that the designer is free to explore and apply.

### 2.4.1 LIGHTING INDICES

Light indexes						
Visual comfort metric	Scope of the index	Light source	Space discretization	Time discretization	Acceptability criterion	Presence of a comfort treshold
Illuminance ( $E_v$ )	Amount of light	Natural Artificial	Local	Short-term	One-tailed	Yes
Luminance (L)	Glare	Natural Artificial	Local	Short-term	One-tailed	Yes
Luminance ratio	Glare	Natural Artificial	Local	Short-term	One-tailed	Yes
Daylight Factor (DF)	Amount of light	Natural	Local Zonal	Short-term	One-tailed	Yes
Illuminance Uniformity ( $U_o$ )	Light distribution	Natural Artificial	Zonal	Short-term	Not applicable	Yes
CIE Glare Index (CGI)	Glare	Natural Artificial	Local	Short-term	One-tailed	Yes
Daylight Autonomy (DA)	Amount of light	Natural	Local	Long-term	One-tailed	No
Discomfort Glare Probability (DGP)	Glare	Natural Artificial	Local	Short-term	One-tailed	Yes
Useful Daylight Illuminance (UDI)	Amount of light	Natural	Local	Long-term	Two-tailed	No
Frequency of Visual Comfort (FVC)	Amount of light	Natural	Zonal	Long-term	Two-tailed	Yes
Intensity of Visual Discomfort (IVD)	Amount of light	Natural	Zonal	Long-term	Two-tailed	Yes
Spatial Daylight Autonomy (sDA)	Amount of light	Natural	Zonal	Long-term	One-tailed	No

**Table 1** Daylight comfort indexes. Source: Carlucci, Causone, De Rosa, & Pagliano, 2015

The lighting indices have been conceived to provide a tool to evaluate the lighting quality and quantity. Through these indices it is possible to assess the amount of light, the light quality, the glare, the light distribution etc. of a specific area. To determine which indices was appropriate to consider for this study, it was necessary to determine which parameters are related to a natural source of light.

The table used for this analysis is the one reported from Carlucci, Causone, De Rosa, & Pagliano (2015) (see *Table 1*), which shows the comparison of visual comfort indices features. These indexes, internationally recognized, could be used as optimization target functions for the building design. Since the research aimed to adequately illuminate a large space with an appropriate roof shading system by allowing natural daylight to enter the building, the indexes studied are the ones generated by natural sources. In *Table 2* the indexes considered are framed by an ocher-colored rectangle. In the following paragraphs the lighting design criteria derived from the NEN-EN 12464-1 and the indexes listed above are described.

A basic framework of the terms and definitions can be found in "*Appendix B*". The following paragraphs aim to investigate the indexes and values specified by the European Standard. Afterwards, a selection of the indexes is conducted, in order to restrict the number of functions that is used as optimization target for the design of the shading devices. Finally, during the practical research, it is evaluated the influence and effect that the indexes have on the final geometry of the shading system and it is realized a final formulation of the objective functions.

## 2.4.2 AMOUNT OF LIGHT

An appropriate premise is necessary when dealing with daylight measurements. The amount, direction, quality and uniformity of daylight is not constant and is directly influenced by the daylight available in the outdoor environment. The indoor illumination differs, depending on the weather conditions, season of the year, month and time of the day. This is why most of the daylight indexes provide values that are not absolute, instead are time-dependent.

## Illuminance $E_v$

The first target of a daylighting design is to ensure a good illuminance distribution and that in the space is provided enough amount of light. The illuminance is defined as the quantity of luminous flux reaching a surface and its unit is the lux ( $lm/m^2$ ). The illuminance requirements are dependent on the space typology (Table 2). Each indoor situation demands different level of illumination and, therefore, of illuminance values. The level of illuminance depends on the task area and considers different aspects like the psychological and physiological element, the visual performance, the risk of errors, economic factors and sociocultural considerations (Szokolay, 2014).

Examples of activities/interiors appropriate for each maintained illuminance*		
Standard maintained illuminance (lux)	Characteristics of activity/interior	Representative activities/interiors
50	Interiors used rarely with visual tasks confined to movement and casual seeing without perception of detail	Cable tunnels, indoor storage tanks, walkways
100	Interior used occasionally with visual tasks confined to movement and casual seeing calling for only limited perception of detail	Corridors, changing rooms, bulk stores, auditoria
150	Interiors used occasionally with visual tasks requiring some perception of detail or involving some risk to people, plant or product	Loading bays, medical stores switch-rooms, plant rooms
200	Continuously occupied interiors, visual tasks not requiring perception or detail	Foyers and entrances monitoring automatic processes, casting concrete, turbine halls, dining rooms
300	Continuously occupied interiors, visual tasks moderately easy, i.e. large details >10 min arc or high contrast	Libraries, sports and assembly halls, teaching spaces, lecture theaters, packing
500	Visual tasks moderately difficult, i.e. details to be seen are of moderate size (5-10 min arc) and may be of low contrast. Also colour judgment may be required	General offices, engine assembly, painting and spraying, kitchens, laboratories, retail shops
750	Visual tasks difficult, i.e. details to be seen are small (3-5 min arc) and of low contrast, also good colour judgment may be required	Drawing offices, ceramic decoration, meat inspection, chain stores
1000	Visual tasks very difficult, i.e. details to be seen are very small (2-3 min arc) and can be of low contrast. Also accurate colour judgment may be required	General inspection, electronic assembly, gauge and tool rooms, retouching paint-work, cabinet making, supermarkets
1500	Visual tasks extremely difficult, i.e. details to be seen extremely small (1-2 min arc) and of low contrast. Visual aids and local lighting may be of advantage	Fine work and inspection, hand tailoring, precision assembly
2000	Visual tasks exceptionally difficult, i.e. details to be seen exceptionally small (<1 min arc) with very low contrasts. Visual aids and local lighting will be of advantage	Assembly of minute mechanisms, finished fabric inspection

\* Maintained illuminance is defined as the average illuminance over the reference surface at the time maintenance has to be carried out by replacing lamps and/or cleaning the equipment and room surfaces

**Table 2** Illuminance average values. Source: *Lighting at work Health and Safety Guidance HSG38* (Sudbury: HSE Books) (1998)

The European standard provides a table with the illuminance values for each particular case (interior area, task or activity) (NEN-EN 12464-1, 2011). As an

example, in the Health and Safety Executive Guide (HSE), *Lighting at work* specify average illuminance level for different visual tasks. The area on the immediate surrounding needs to maintain a level of illuminance lower than the one of the task area, in this way it is possible to avoid discomfort and create an appropriate visual environment.

## Daylight factor DF

The daylight factor (DF) is an important index, which gives information about the effectiveness of the daylighting design. The only way to have data about the quality and quantity of daylight is through measurements using physical models. However, it is not possible to have accurate information, since it would require an indication of the lowest illuminance levels inside the model during the worst day, which is consider to be reliable. Though, it is highly improbable that this test would ever be possible. The daylight factor brings a resolution to this issue, calculating the percentage of illumination outdoor that is able to enter the indoor space during an overcast sky.

The DF is the ratio between indoor illuminance and outdoor illuminance, when this factor is above 5% the space receive a good amount of daylight from the outside, which means that is needed not a lot or not artificial lighting sources at all for the specific visual tasks. Realizing this experiment at different altitudes, the daylight factor changes and is lower in northern part of the world, where the available natural light is less. With this knowledge it is possible to apply reduction factors, estimate the DF at every latitude and finally obtain the indoor illuminance (Lechner, 2015).

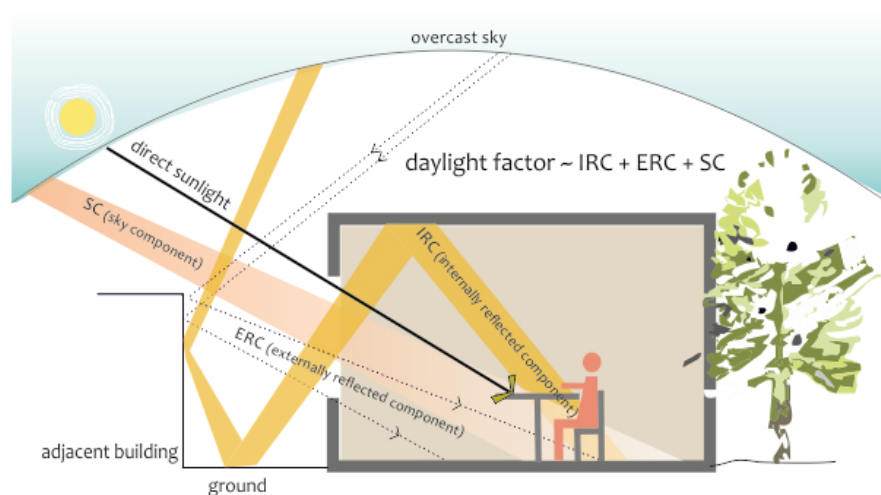


**Figure 27** Daylight factor. Source: <http://www.nzeb.in/knowledge-centre/passive-design/daylighting/>

The daylight entering the indoor environment can derive from three type of sources: sky component (SC), externally reflected component (ERC) and the internally reflected component (IRC) (*Figure 27*). The daylight factor is the sum of these three fractions (Szokolay, 2014).

$$DF = SC + ERC + IRC$$

The quantity and quality of daylight entering the room depends on the amount, dimension and position of the openings. There are smart strategies to integrate natural and artificial lighting to increase the energy efficiency of the building, maintain comfortable thermal properties of the space and create a pleasant environment.

The DF depends on (Mardaljevic, Andersen, Roy, & Christoffersen, 2012):

- The location, orientation, dimensions of the building
- The physical properties of the roof and façades openings
- The outline of the interior space and the furniture disposition
- The reflectivity of interior and exterior materials and surfaces
- The obstructions of adjacent objects (e.g. trees, structures, buildings)

### **Daylight autonomy DA and Spatial daylight autonomy sDA**

The daylight autonomy factor (DA) indicates the percentage of time in which a minimum illuminance threshold is reached. The illuminance level considered is the one only derived from natural sources (daylight). For instance, a minimum illuminance level setted at 400 lux for a threshold of 50% implies that 50% of the time of the year, the illuminance level is required to be equal or higher than 300 lux.

The DA is a long-term indication of the daylight available in a space, in order to give an indication of how much electrical lighting is needed during the year. However, this important index, if considered by itself, exposes the daylighting

design to some risks because is a one tailed factor and does not take into account that some illuminance levels above the threshold could be cause of distress and displeasure; at the same time, some levels below the threshold could be well accepted from the occupants and this could reduce the usage of artificial illumination (Carlucci et al, 2015).

Another factor that can be used is the Spatial Daylight Autonomy (sDA) which describes the daylight autonomy per surface, meaning that the calculation is performed according to an area grid and for each area of a grid point is determined whether the illuminance level is above the target minimum level. The final sDA factor is given by the combination of all the acceptable values, which increases its final value (IES, 2012).

### Useful daylight illuminance UDI - Frequency of visual comfort FVC

The UDI or useful daylight illuminance is a two-tailed factor indicating the percentage of time during the year when the illuminance at a point is included in the target range of values (Carlucci et al, 2015) (*Table 3*). The two values are selected as reference for a discomfort situation. The lower illuminance value in the range represents the circumstance in which the natural light is so low to not ensure a visually safe and comfortable environment; the greatest value represents the time in which the lighting level is exceeded so as to create discomfort.

UDI illuminance limit values		
Source	Lower illuminance limit (lx)	Upper illuminance limit (lx)
Nabil and Mardaljevic	100	2000
Mardaljevic, Hescong	100	2500
Olbina and Beliveau	500	2000
David, Donn	300	8000

**Table 3** UDI illuminance limit values. Source: Carlucci et al., 2015

Finally, the average of the two value is the level considered the opportune one, at which the right amount of natural light is supplied. Despite this factor is very precise and gives important information, it is quite difficult to collect an

overall interpretation of the results, since the output is a set of three values for each point of the selected grid. Another constraint is the non-existence of fixed illuminance values ranges, but the limit values change depending on the author (Mardaljevic et al, 2012).

The frequency of visual comfort (FVC) is a two-tailed indicator of the percentage of time in which visual comfort is ensured. The alternative of UDI and FVC are very similar and both rely on two extreme illuminance levels. However, the FVC is more narrowed than the UDI, in order to ensure visual comfort and avoid optical distress, i.e. glare, too low values. Despite this, both UDI and FVC are indexes that evaluate daylight and do not rely on the artificial lighting system (Sicurella, 2011).

### 2.4.3 DISTRIBUTION OF LIGHT

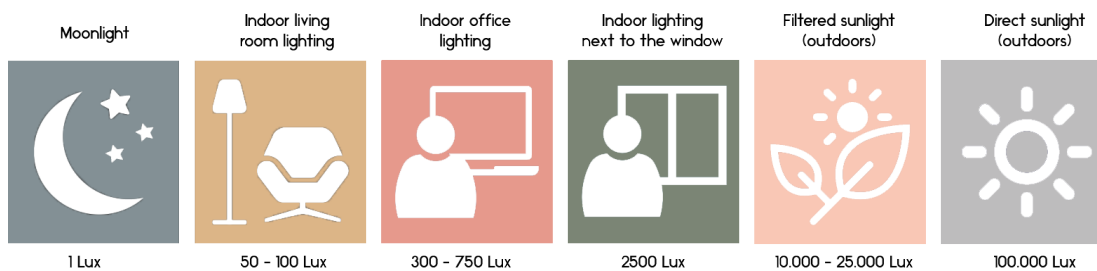


**Figure 28** Range of lighting levels. Source: van Bommel & Rouhana, 2016

The amount of daylight entering a building is not enough to ensure a well-designed and comfortable visual environment. It is also necessary to pay attention to its distribution. A well designed luminance distribution is necessary to create an adequate environment for the visual tasks (**Figure 28**). The control of the light distribution allows to help the normal ophthalmic functioning, to avoid the visual fatigue due to continual accommodation and adaptation of the sight and to promote a stimulating and productive environment. Whenever the lighting level is not uniform in the space, both visual comfort and performance can be affected and reduced.

## Illuminance uniformity $U_0$

Illuminance Uniformity recommended in standards for indoor spaces, reproduced from Slater & Boyce, 1990	
Source	Illuminance uniformity over task
AS 1680	$U_{O,average} > 0.67$
DIN 5035	$U_{O,average} > 0.67$
NSVV	$U_{O,average} > 0.7$
CIBSE	$U_{O,average} > 0.8$
BS 8206-1	$U_{O,average} > 0.8$
CIE 29.2	$U_{O,max} > 0.7$
	$U_{O,average} > 0.8$

**Table 4** Illuminance Uniformity recommended in standards for indoor spaces. Source: Slater & Boyce, 1990

An important element to consider when talking about visual comfort, is the illuminance uniformity  $U_0$ . The quantity of light is not enough by itself, indeed it is also necessary to consider how the daylight is distributed in the space. The  $U_0$  index points out the minimum illuminance required (or luminance) level compared to the average illuminance (or luminance) level on a surface.

The ratio between these two measurements should not be greater than a certain  $U_0 = E_{min}/\bar{E}_m = L_{min}/L_m$ . The  $U_0$  might change depending on the reference source, as showed in **Table 4**. When the space is homogeneously illuminated, the eye fatigue is prevented and the eye is not obliged to continuously re-adapt to the different light levels (Van Bommel & Rouhana, 2016).

## Reflectance of surfaces

To ensure illuminance uniformity, the lighting designer is invited to follow some general precautions, like opportune reflectance and illuminance values. The following ranges of values are the one expected for interior surfaces reflectance (NEN-EN 12464-1, 2011):

- **Ceiling:** from 0.7 to 0.9
- **Walls:** from 0.5 to 0.8

### Reflectance $\rho$ :

For incident radiation of given spectral composition, polarization and geometrical distribution) ratio of the reflected radiant or luminous flux to the incident flux in the given conditions

Source: IEC 60050-845:1987 845-04-58 /  
CIE S 017:2011: 17-1058

- **Floor:** from 0.2 to 0.4.

### Illuminance on surfaces

Regarding the illuminance level on a surface, the following restrictions need to be applied (NEN-EN 12464-1, 2011):

- $\bar{E}_m > 50 \text{ lx}$  and  $U_o$  on the walls needs to be equal or higher than 0,10
- $\bar{E}_m > 30 \text{ lx}$  and  $U_o$  on the ceiling needs to be equal or higher than 0,10

## 2.4.4 GLARE

Glare is a discomfort sensation due to excessive level of luminance, to which the human eye is not used to. The lighting source can be either natural or artificial. Glare can be created by excessive amount of light or too much contrast (Pinterić, 2017). Glare is dependent from parameters like the type of source, its direction, colour and intensity. Glare deriving from natural sources is mainly due to direct sunlight, however there are many other parameters like the reflection caused by interior materials and also the way some shading devices creates illuminance peak (i.e. venetian blinds) (Wienold and Christoffersen 2006, Weinold 2014). An additional important factor is the background luminance, because the glare level is strictly dependent on its relative brightness compared to the background luminance. This is the main reason why the ceiling coating is usually white (Lechner, 2015).

There are two glare typologies depending on its intensity: discomfort glare and disability glare (Van Bommel & Rouhana, 2016). The situation in which the source produces distress and visual discomfort is called **discomfort glare**, while **disability glare** takes place when the brightness of the source or the contrast is so high to reduce the visual performance or even produce a temporary loss of sight (Carlucci et al, 2015). Glare can also be categorized in **direct** and **indirect** glare depending if the cause is the light source itself or if its due to reflection from other objects (Szokolay, 2014). While disability glare can be easily identified, the

classification of the discomfort glare can be more complex. Numerous indexes has been developed to predict the severity of glare, considering the luminance levels and distribution and the human perception of the phenomenon (Carlucci et al, 2015).

## Glare index G

Discomfort glare represents a complicated phenomenon to measure and assess. The glare index G correlates different factors: the luminance of the source and of the background, the source direction relatively to the field of view and the position of the source in relation with the observer's eye (Wienold and Christoffersen, 2006). Following the equation of the glare index G Carlucci et al, 2015):

$$G = \left( \frac{L_s^e \cdot \omega_s^f}{L_b^g \cdot f(P)} \right)$$

Where:

- $L_s$  is the luminance emitted by the glare source [cd/m<sup>2</sup>]
- $\omega_s$  is the solid angle subtended by the source [sr]
- $L_b$  is the luminance in background [cd/m<sup>2</sup>]
- $P$  is the position index, represents the glare source position relatively to the field of view [-]
- **e, f and g** are exponents that introduce a weight to each of the factors and vary depending on the specific glare conditions

Other important indexes try to measure the glare degree of discomfort based on subjective perception of unpleasant situations. Despite the large number of indexes, there is consensus among experts that does not yet exist an holistic method to judge and prevent distress due to glare (Osterhaus, 2005).

## Luminance L

Luminance is a parameter expressing the human eye perception of brightness and its unit is cd/m<sup>2</sup> or nit. Given a point in the space, the luminance is the quantity per unit of luminous intensity radiated by a source in the direction of the

point (Zumtobel, 2018). The easier way to evaluate the discomfort in a specific point of the space is using absolute threshold luminance values. However, as stated from Suk, Schiler and Kensek (2013) the selection of absolute luminance thresholds is the most critical aspect in the definition of a glare index. Thus, it is necessary to further research and set fixed values for the evaluation of the glare intensity (Suk et al, 2013). The assessment of glare is also related to the luminance contrast ratio between the source and the background.

### Luminance ratio CR

Relative glare factors, which are the proportion between the luminance of the visual task and the surrounding luminance, can be very useful in the evaluation of the glare level of distress. Depending on the author, the luminance ratio calculation can change and the claimed contrast thresholds can vary. For instance, the Illuminating Engineering Society of North America (IESNA) and NUTEK selected a ratio of 1:3 between surrounding luminance and visual task area, while Osterhaus (2005) claims that the luminance ratio depends on the area of the visual field and he pinpoints three different zones: the **central zone**, which is the region strictly limited to the visual task; the **adjacent zone**, representing the zone confined within the visual activity, is the space enclosed in the solid angle of 60°, and finally the far-off surfaces, enclosed by the cone of 120° and named **non-adjacent zone**.

According to Osterhaus (2009), for the central zone it is required a luminance ratio of 1:3, in the adjacent zone is recommended a luminance ratio of 1:10 and for the non-adjacent zone is prescribed a ratio of 1:20. The nature and quality of the light source has a significant influence on the visual perception, for instance natural light sources are better accepted from the user than artificial lighting systems. The setting of the room and the user position are other important factors related to the glare subjective rating (Carlucci et al, 2015).

### CIE Glare index CGI

The CGI or CIE glare index is the index that allows to translate the perception of glare and define its degree. It is suitable for calculation related to both natural and artificial sources and takes into consideration both direct and indirect light. Suk et al (2013) suggest a division in three level of glare discomfort depending

on the value of the CGI index: **imperceptible** if  $CGI < 13$ , **perceptible** if the value is between 13 and 22, **disturbing** when  $22 < CGI < 28$  and **intolerable** if CGI is greater than 28.

### Discomfort glare probability DGP

DGP is the other important factor assessing the discomfort glare probability for natural and artificial light sources. As noted by Suk et al (2013), DGP would represents the most pertinent way of conducting an analysis on the glare level of discomfort, considering that this index is not only a measure of the luminance ratio and does not only take into account the contrast between the glare source and the background ("Table 5" on page 49).

Comparison of a number of glare discomfort indices on a four-point glare sensation scale		
Degree of glare sensation	CGI	DGP
Intolerable	>28	>0.45
Disturbing	22-28	0.35-0.45
Perceptible	13-22	0.3-0.35
Imperceptible	<13	<0.3

**Table 5** Comparison of CGI and DGP indexes. Source: Jakubiek & Reinhart, 2012

DGP includes the term  $E_v$ , the vertical illuminance generated by the light source, calculated at eye level. Hence, this index looks at the user's perception of glare, which makes this index the most appropriate for glare assessment (Wienold and Christoffersen, 2006). However, this kind of calculation requires a long computation time, that can be the reason for choosing another prediction method. **Table 5** shows the comparison between the values of the CGI and DGP indexes.

## 2.4.5 QUALITY AND BENEFITS OF LIGHT

The positive effects of daylight on a psychological and physical level are well known and proven by many studies (Ott, 1982; Brody, 1981; Wurtman, 1975; Kotzsch, 1988). The benefits of daylight can be divided in two typologies: the ones effecting the neural system and the ones depending on the skin exposition to the sun. It is demonstrate that when our body is in contact with the natural light, our health improves.

\*When we speak about health, balance, and physiological regulation, we are referring to the function of the body's major health keepers: the nervous system and the endocrine system. These major control centers of the body are directly stimulated and regulated by light, to an extent far beyond what modern science... has been willing to accept.\*

Dr. Liberman (1994)

Daylight is, like food and water, a biological necessary elements for our metabolic processes. The human being necessitates to maintain a connection with the natural environment and daylight provides this contact (Robbins, 1986). Light can reduces stress and anxiety, can improve the mood and the body immune system. In office buildings, light is an essential factor to improve productivity, reduce eyestrain and it is important for the worker circadian rhythm, which can be aligned to the flow of the usual working hours. Furthermore, if daylight is controlled and used in a proper way, it can improve the retail environment in order to attract more costumers and increase the sales (Edwards & Torcellini, 2002).

### Circadian rhythm

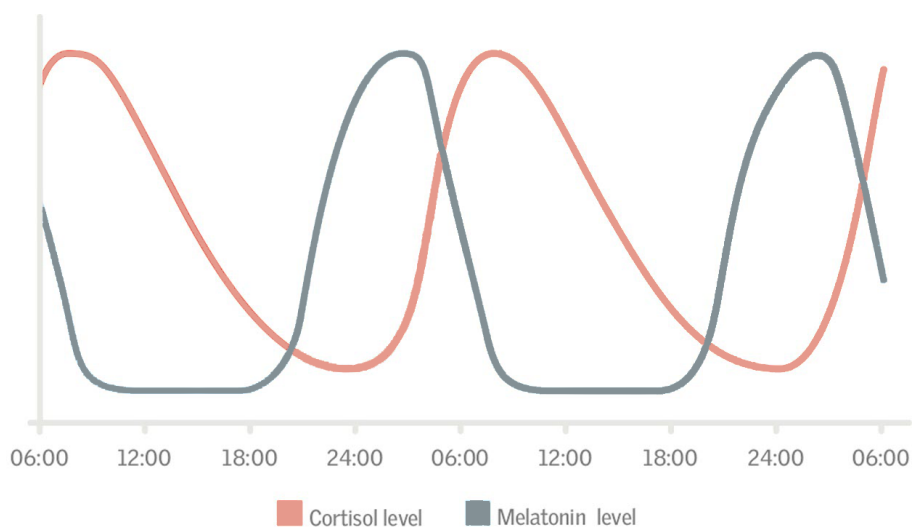


**Figure 29** Hormones production related to the circadian rhythm. Source: Brainard, 2002

The body production of hormones like cortisol and melatonin has a significant impact on the neurological and physiological functions. The 24 hours cycles of daylight is the responsible for the regulation of our hormones production and, as a consequence, many aspects like mood, sleep and health are affected (Edwards & Torcellini, 2002) (*Figure 29*).

The levels of melatonin in our body is responsible for the regulation of the grade of alertness. Low quantities of melatonin hormone in our body results in an alert and vigilant state, while, in absence of light, the melatonin level drops down producing sleepiness and reducing the energy (Ott, 1997). Cortisol is another relevant hormone influenced from the light rhythm, its secretion follows the one of melatonin. Cortisol has a big role in the stress levels, metabolism, blood pressure, reducing inflammation and many other aspects.

### Light colours

Daylight quality can be altered by the colour of a light source. The type of colour of a white light source can be described using a factor called correlated colour temperature (CCT). White colours are the product of a combination of range of colours, and each kind of white is different depending on the spectral colours composition. The colour temperature of artificial lighting can vary depending on the proportion of red and blue.

Lamps with higher amount of red results in producing a warmer white colour than the ones with high percentage of blue. Natural daylight has a high colour temperature, when a source has high colour temperature it seems warmer; vice versa if the colour temperature is low, the light appears warmer (van Bommel & Rouhana, 2016).

The following image shows the spectral energy distribution of an incandescent lamp (*Figure 30 Spectral energy distribution of an incandescent lamp (2800 K). Source: van Bommel & Rouhana, 2016*):

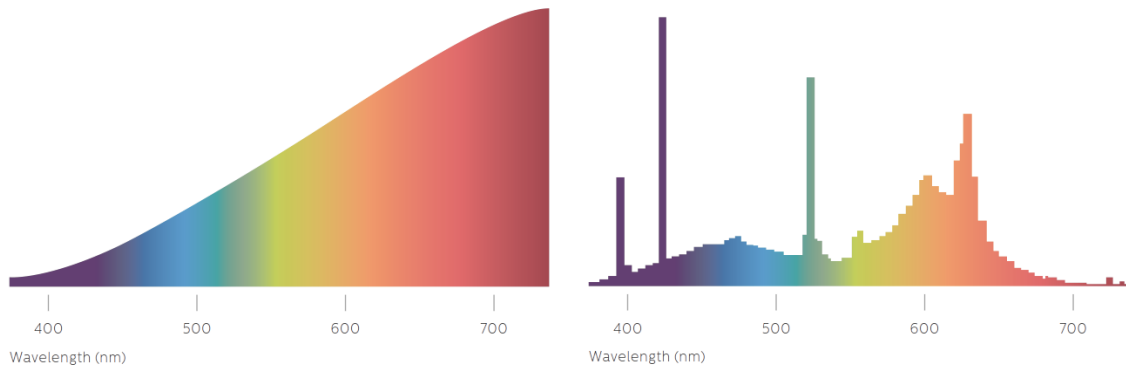


**Figure 30** Spectral energy distribution of an incandescent lamp (2800 K). Source: van Bommel & Rouhana, 2016

Below the spectrum of daylight (*Figure 31*):

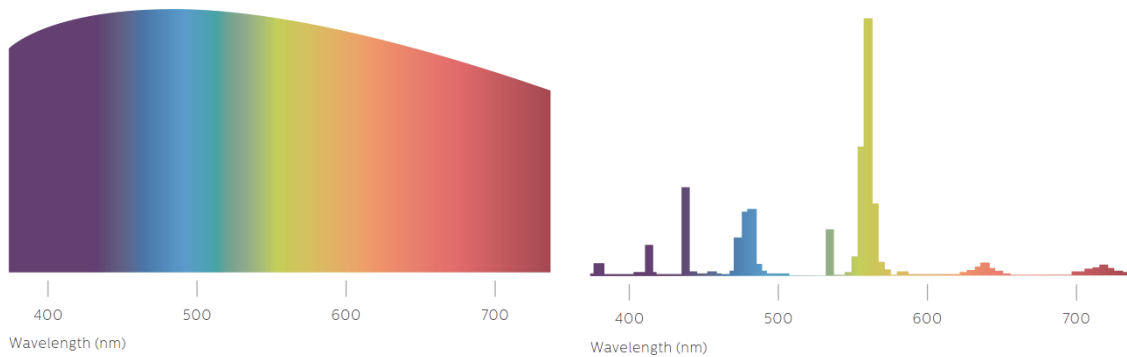


**Figure 31** Spectral energy distribution of daylight (5000 K). Source: van Bommel & Rouhana, 2016

The three main properties of light that can affect its colour are brightness, saturation and Hue.

- **Brightness** corresponds to the quantity of luminous flux (lux) produced by the source. Lower brightness creates a more rational environment in which people are able to keep more under control the emotions, while in brighter illuminated spaces the perception of feelings can be altered and stronger
- **Saturation** expresses the vibrancy and pigmentation of a

colour, this can also be applied for light. The more the saturation, the less the intensity of the colour, the stronger the perception of emotions. When a colour is not saturated, it is less easily associated with an emotion

- Hue represents the colour itself and, specifically, its shade. As already mentioned in *2.3.1 Introduction* in section *Health and physical needs*, light has a direct influence on emotions and feelings

Below (*Figure 32*) an explanation of the impact that a colour can have on human perception.

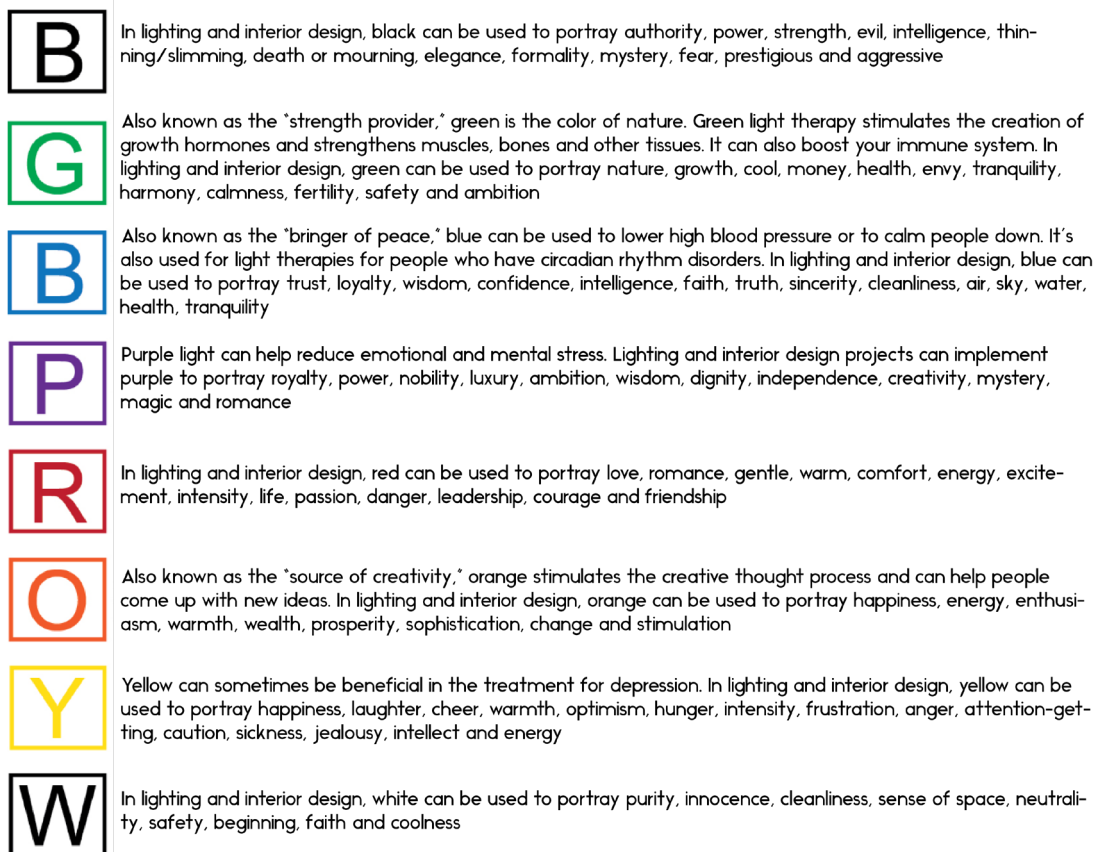


**Figure 32** Impact of colours. Source: <https://www.tcpi.com/psychological-impact-light-color/>

In 1941 Aries Anders Kruithof studied the dependency of mood with the illuminance levels and colour temperature and defined a graph showing the comfort zone. The study is an analysis of the psychophysical effects of various lighting sources at different illuminance levels on human beings. The Kruithof curve (*Figure 33*) predicts three areas: a white area, representing the pleasant zone and an upper and lower area, in which the feeling is of unpleasantness.

Kruithof concludes that:

“Below the lowest curve the illumination is ‘dim’ (at low colour temperature) or ‘cold’ (at high colour temperature). Above the highest curve the unnatural colour reproduction was unpleasant.”

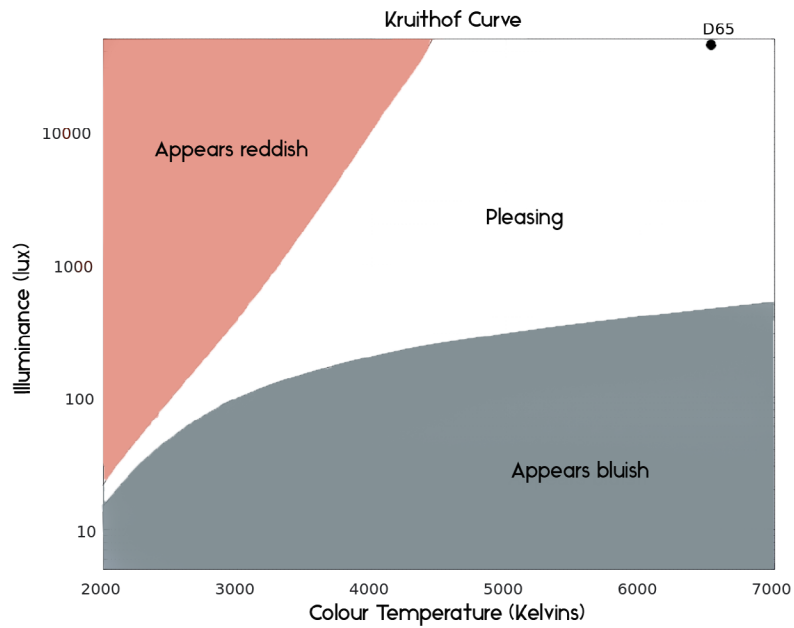


**Figure 33** Kruithof curve, modern version. Source: Wikipedia

## 2.5 THERMAL COMFORT

### 2.5.1 THE BUILDING ENVELOPE

The envelope of a building is a multifunctional element, protecting from external agents, creating a division between indoor and outdoor spaces and has a significant impact on the micro-climate of the building. The skin of a building has three major functions: support, finish and control (Straube, 2005). Depending from the geometry and materials, the building envelope has a different impact on the thermal comfort and daylight inside the building. Beside its importance regarding the comfort aspect, the envelope is also responsible for a big part of the energy performance of the entire structure. Therefore, a properly designed building skin means also higher energy efficiency. The connection that the building envelope creates between inside and outside space is dynamic and knowing how this relation acts, gives the ability to control it and design the building in order to fulfil the stakeholders requirements (Hansen, 2012). Balancing the exchange of energy between the two environments can be able to assess thermal comfort and sustainability targets in the internal micro-climate.

In the design of the building envelope it is important to be aware of the variable and factors that are responsible for the sustainability level. To properly address an envelope design it is important to be sure that it regulates the thermal conditions. Balaras (1995) identifies the following features as the primary causes affecting the thermal mass:

- **Material properties** - the building's materials can change their temperature during time. The choice of a material needs to be accurate, depending on the need of release and store of the heat
- **Location** - the location of the building is essential. To each location corresponds different weather conditions. Depending on the solar radiation and the external temperature, the building envelope behaves differently. Furthermore, the orientation of the building affect the way direct radiation hits the building envelopes and how the thermal gain get absorbed by it
- **Insulation and mass** - the choice and distribution of the insulation material are relevant for the system. Depending on the primary concern, in locations with warm climates it is important to select the thermal insulation to easily let the heat dissipate to the

outside. While, in climates where the heating is the main issue, the heat dissipation must be delayed as much as possible

- **Air ventilation** - the ventilation system can be mechanical, natural or a mixed system. A proper control of the convective heat loss through air-conditioning can considerably reduce the energy consumption
- **Occupancy behaviour** - when considering a building, people's behaviour highly effects the energy consumption. The occupancy schedule, the equipment usage and the various utilities are all variables that increase the heat gain of the internal space

Considering a roof shading system design, other essential properties to examine are:

- **Glazing opening ratio** - generally, in façade designs, the optimal wall to glazing ratio to refer to is around 50% (Raji, Tenpierik & Dobbelsteen, 2016)
- **Material** - together with the opening ratio, the glass typology represent an important aspect. The goal is to achieve thermal comfort and energy savings both during summer and winter periods. The system must be able to reduce the heat losses during cold weathers and the heat gain during warm external conditions
- **Shading system position** - not only the selection of the typology of shading system is essential, but also its relative position. Solar shading can be installed externally to the envelope, internally or mid-pane. Considering thermal efficiency, the outside solution is mostly more effective then the other three installation options

## 2.6 SHADING SYSTEMS

### 2.6.1 FENESTRATION

A conscious design of the apertures in a space, combined with many other technical measures, can lead to a sustainable solution and reduce the energy consumption by increasing the amount of natural light entering the building. However, it is important to pay particular attention to the solar heat gain that could derive from it. The best approach is the integration of daylighting

intentions from early stages of the design, so that the strategy can be studied and developed through the whole process (Ruck & Aschehoug, 2000). People behaviour is one of the first factors to have impact on the improper use of energy in buildings. However, it is very hard to induce people to modify their habits, so it is important to create daylighting-conscious design through the application of innovative technologies and systems in the architectural design. With the integration of more sustainable solutions it is possible to create more awareness of the ecological impact of building, and it might be possible to intrigue and promote the passage towards NZEB (Net Zero Energy Buildings) (Drozdowski, 2011).

### Glazing selection

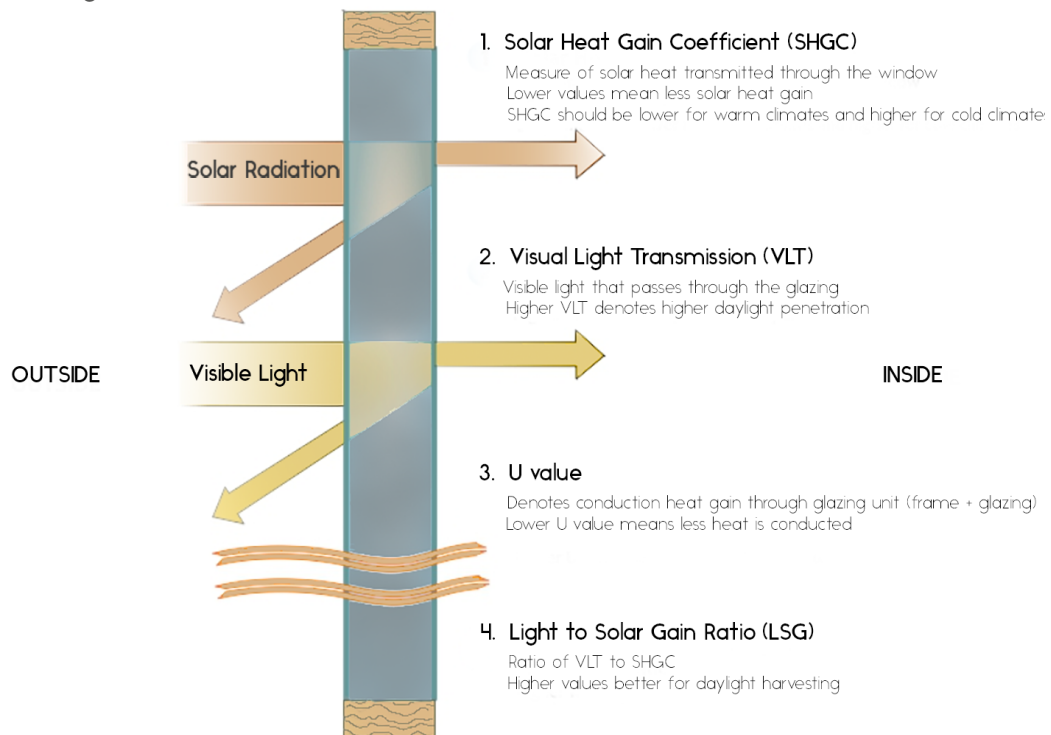


**Figure 34** Glass properties. Source: <http://www.nzeb.in/knowledge-centre/passive-design/fenestration/>

The glazing typology used has a major impact on the quantity and quality of light allowed to enter the interior space. In **Figure 34** are indicated the three main properties of glass when referring to daylighting and thermal comfort (Leftheriotis & Yianoulis, 2012):

- SHGC or Solar Heat Gain Coefficient is a dimensionless quantity that can vary between 0 and 1 and represents the amount of heat admitted to the inside from the glazing. The higher the SHGC, the higher the heat transmitted. For colder climates it is desired a higher SHGC, in order to heat up the interior ambient; on the way

around, for warm climates it is preferred a lower SHGC

- VLT or Visual Light Transmission is the portion of the visible light (380-780 nm) reaching the fenestration that can pass through the glazing system. Normally, the required VLT is higher than 30%
- U-value represents the insulation potential of the glazing system, thus the heat transmitted from the material. It is an intrinsic characteristic of the material. When considering a window, the U-value is affected by the whole window composition (glass, coating, frame, spacers). Generally lower U-values are preferred, the lower the U-factor, the higher its insulation power. When aiming at energy efficient products the window should have both low U-value and SHGC factor (for cold climates it is better to look for greater SHGC). The U-value can be reduced using double or triple glazing that have an U-factor that can reach respectively 0.30 and 0.15.

Coatings and coloured glass have the effect of reducing or changing the transmittance of visible light. However, Besides, it is important to notice that the “whole product” U-factor and SHGC are different than the same values considering only one part of the system (like the only glass). The “whole-product” factors can be worse by 10 to 40% than the “only-glass” coefficients. Finally, the ratio VLT to SHGC is referred as LSG (Light to Solar Gain Ratio) and it can be an useful criteria for daylight harvesting. The greater the LSG, the better the natural light penetration.

### **Orientation, layers and coatings**

The orientation of fenestrations has large impact on the quality and quantity of daylight entering the building. The west, east and south orientations provides mainly direct light with large levels fluctuations , while a window located on the north hemisphere transmit for the majority diffuse and steady light. When dealing with horizontal (skylights) or low pitched window systems, the main problem to deal with is glare, since this typology of openings are subject to direct sunlight. Particular interest is the exploitation of this system to efficiently bring natural light in a space avoiding visual discomfort. Lastly, the dimensions of an opening are an important aspect for the design decision of a window system (IEA SHC Task 21/ ECBCS, 2000).

## 2.6.2 SHADING DEVICES

The selection of the fenestration system is an important step in the daylighting design, though it is not the only way to achieve an efficient solution. A good daylighting system regulates the amount and quality of daylight coming inside, creating the right environment for the illumination tasks, contributes to a proper thermal control to ensure comfort and finally it drastically reduces the risk of glaring. The combination of shading system with a good fenestration can contribute to diminish the need of cooling and heating in moderate climates by 8 to 17% and by 12 to 26% in hot climate, while the choice of an efficient material by itself can reduce the energy consumption for heating and cooling by 6-11% in moderate climates and 8-12% in hot climates (NZEB, 2019).

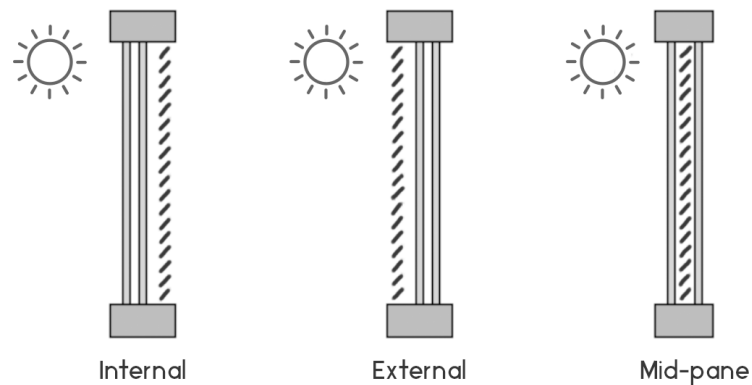


**Figure 35** Position of shading device. Source: [https://designbuilder.co.uk/helpv1/Content/\\_Window\\_shading\\_internal\\_1.htm](https://designbuilder.co.uk/helpv1/Content/_Window_shading_internal_1.htm)

Shading systems are essential for regulating the thermal and visual comfort and thus have a pivotal role in the NZEB strategies. As showed in *Figure 35*, shading devices solutions can be internal, external or integrated. The central difference between interior and exterior shading device is that an external shading system is also able to regulate the solar gain transmitted, contrarily interior systems have a lower impact since they act after the heat has already reached the internal space. The systems integrated inside the window glazing has the advantage of requiring less cleaning, from the moment that they are protect from dust from the glazing layers. Despite the cleaning aspect, the maintenance of a mid-pane system could be demanding, especially if the system is kinetic.

## 2.7 PRECEDENTS ROOF SHADING SYSTEMS

In the following pages is presented a list of existing buildings with large roof shading systems. Each system is analysed and quickly compared. The results from the analysis are summarized in *Table 6*.

OPTIMIZATION DESIGN WORKFLOW FOR  
LARGE ROOF SHADING SYSTEMS

CASE STUDY	SHADING TYPOLOGY	MATERIAL/S	POSITION	DYNAMIC OR STATIC	TPOLOGY OF MOVEMENT	FACTOR OF ADAPTIVITY	CONTROL PURPOSE	LIGHT CONTROL	STRUCTURE TYPOLOGY	DESIGN FREEDOM	COST	TYPE OF CONTROL
1. Abu Dhabi Louvre	metal cladding	•stainless steel nodes •aluminium bars •aluminium modules	•horizontal •layered on the inner and outer surfaces of the dome structure	static	-	-	•lighting •solar shading •thermal	•block-filter light •light pattern •glare control	part of the self-bearing structure	high	total cost: high •design process •installation	-
2. Shenzhen Airport	perforated double skin envelope	•stainless steel frames - opaque •glass panels - translucent	•horizontal and vertical •double-skin envelope with structure integrated in between	static	-	-	•lighting •solar shading •thermal	•block-filter light •light pattern •glare control	double skin envelope on the structural frame	high	total cost: high •design process •installation	-
3. Landscape canopy	metal grid/sort of horizontal eggcrate	•metal	•horizontal •canopy	static	-	-	•lighting •privacy	•allow light	cantilevered from the buildings next to it	medium	?	-
4. Roof Mshereb Heart of Doha	retractable frame modules	•aluminium profiles covered by white colored PVDF •steel structural cables	•horizontal •roof on open square	kinetic	sliding and folding	-	•lighting •solar shading •thermal	•filter light	lay on structural cables connected to lateral buildings	medium	•installation	•schedule •wind speed constraints
5. Simons Center	framed layers of perforated metal	•stainless steel	•vertical •mid-pane/integrated	kinetic	sliding	•solar radiation or •light levels	•lighting •thermal •privacy •solar shading	•allow-filter light •thermal •redirect light •glare control	•integrated •non load bearing	high	•materials •production	•solar radiation sensor •light level sensor
6. KAPSARC	hexagonal double-skin membrane cells	•semi-translucent •membrane cells-glass PTFE fabric •steel	•horizontal •connection canopy	static	-	-	•solar shading •ventilation •lighting	•block-filter light •solar shading	•supported by steel columns	medium	total cost: high	-
7. Institute du monde Arabe	metallic brise soleil, diaphragms	•steel diaphragms	•vertical •façades •mid-pane/in between	kinetic	rotating	•light levels	•lighting •thermal	•glare control •redirect light •light pattern	•integrated •non load bearing	low	•maintenance •failures of system	•light level sensors
8. Al Bahr Towers	triangular screens creating an hexagonal structure	•PTFE (polytetrafluoroethylene) panels •fiberglass coating	•vertical •external	kinetic	folding	•solar shading	•lighting •solar shading •thermal	•block light •glare control	•non integrated •independent frame	high	•installation	•schedule pre-calculated •solar radiation sensor
9. Cneteca Nacional Siglo XXI	panels with triangular perforations	composite aluminium panels: •aluminium •polyethylene •gloss aluminium finish	•horizontal •double skin envelope with structure integrated in between	static	-	-	•solar shading •thermal	•block light	double skin with structural steel space frame	high	?	-
10. Kiefer technic showroom	micro-perforated screen shutters	•aluminium posts and transoms •EFS-panels	•vertical •external	kinetic	folding	•solar radiation	•lighting •solar shading •thermal	•glare control	•non-load bearing •external aluminium frame connected to the façade	medium	•materials •maintenance	•solar radiation sensor •user preference
11. ThyssenKrupp quarter - head office	triangular panels made of horizontal lamellas	•stainless steel coated with zinc and magnesium	•vertical •external	kinetic	rotating	•solar radiation	•solar shading	•redirect light •glare control	•outer building skin •attached to horizontal fixed louvres with vertical system	medium	•maintenance	•automated •solar radiation •weather station on the roof
12. Burton Barr Central Library	north and south façades with vertical fins	•translucent Teflon-coated acrylic fabric	•vertical •external	static	-	-	•solar shading •thermal	•filter light •glare control	•fixed vertical fins •non load bearing	medium	•maintenance	-

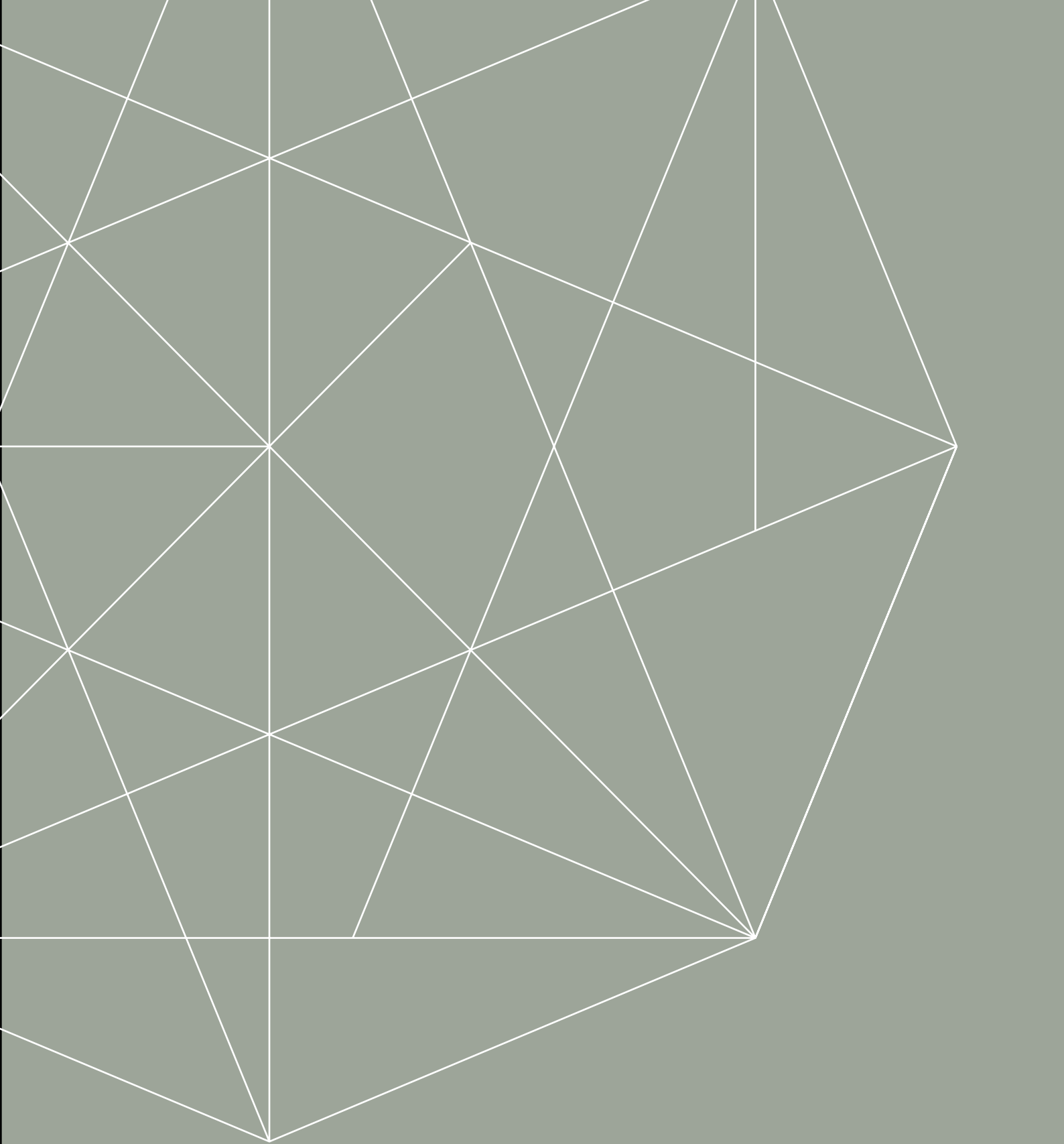
Table 6 Table summarizing the features of precedent buildings with large roof shading systems

CASE STUDY	SHADING TYPOLOGY	MATERIAL/S	POSITION	DYNAMIC OR STATIC	TYPOLGY OF MOVEMENT	FACTOR OF ADAPTIVITY	CONTROL PURPOSE	LIGHT CONTROL	STRUCTURE TYPOLOGY	DESIGN FREEDOM	COST	TYPE OF CONTROL
13. Esplanade	curved cladding pyramids	•aluminium	external	static	-	-	•solar shading	•glare control	non structural/grass	medium	•maintenance	-
14. The Broad	eggcrate, non-eycomb	glass fiber reinforced concrete (GFRc)	•horizontal and vertical •external	static	-	-	•solar shading •thermal	•allow-filter light	supported at three points with beams steel girders roof cantilever system	medium	•material	-
15. L'Hermistère	large shelter made of awnings	steel glass	integrated with the structure	dynamic	folding	•external/internal solar radiation •external/internal temperature •air exchange	•lighting •thermal •natural ventilation	allow light	integrated	low	•maintenance	sensors
16. CH2 Melbourne City Council House 2	vertical louvers	•timber louvres •aluminium frame	vertical external	dynamic	rotating	solar radiation	•lighting •thermal •solar shading	•glare control •filter light	external	low	•low •maintenance	•solar radiation sensor
17. National Aquatics Center - Water Cube	layers of ETFE cladding	fritted translucent ETFE	vertical and horizontal entire façade	static	-	-	•lighting •thermal	•glare control •filter light	• steel structure housed in the cavity in between the cladding • cladding frame in steel connected to the structure cavity	medium	installation	-
19.POLA Ginza Building Façade	shutters	acrylic sheet	mid-pane between double skin facade vertical	dynamic	folding	solar radiation	•lighting •thermal	•allow-filter light	non-structural in between double skin facade	medium	production	solar radiation sensor
20. One Ocean	moveable lamellas	glass-fiber-reinforced polymers (GFRP)	vertical external	dynamic	twisting (elastic bending and side rotation)	solar radiation	•lighting	•light pattern	top and bottom edge by fixed supports on one corner and extendable actuators on the other corner	high	installation maintenance	solar radiation sensors
21. SDU Campus Kolding	triangular perforated panels	steel	vertical external	dynamic	rotating	solar radiation	solar shading thermal lighting	•filter light	non structural	medium	material maintenance	•solar radiation sensor •light level sensor
22. Headquarters for Swatch and Omega	free form shell	ETFE glass timber or polycarbonate	cold bended polycarbonate as an internal layer of the ETFE	static	-	-	solar shading thermal lighting	•block - filter light	curved timber framing	high	installation	-
23. Burj Doha Tower	four layers pattern of different scales	aluminium elements reflective glass for inner facade	external vertical	static	-	-	solar shading thermal	•light pattern	non structural connected to the inner facade through walkway	high	material installation	-









03





## 3.1 COMPUTATIONAL TOOLS

### 3.1.1 TOOLS REQUIREMENTS

The first step was to define the tools to use in order to obtain consistent results in a quick and flexible way. There was a need to rely on software that could allow to easily revise and correct the parametric model used. Furthermore, another requirement was the freedom of expression, to be able to give form and visualize the alternatives conceived. These tools have been chosen for their design freedom, their ability to adapt to different simulations and the possibility to interlink, facilitating the exchange of data and information and allowing interoperability. The choice of the tools is the result of various considerations, including some desirable requirements:

- **Parametric** – the first essential prerequisite is the parametric interface which can describe and build the model using a set of variables linked through parametric relations and constraints.
- **Shared knowledge and availability of information** – the presence of open community and/or web-support is an important factor since it represents the possibility for the user of taking advantage of the continuous assistance throughout the whole design process.
- **Popularity** - The popularity of the tools, in terms of use and exploitation of the possibilities, is an important aspect. It ensure a continuous development of the interface and components.
- **Flexibility** – to fulfil the various purposes of this research is necessary to have the flexibility of programming without requiring extremely advanced skills.
- **Visualization** – the visualization of the design solutions and simulation results enable the user to quickly analyse and gain control over the design space.
- **Interoperability** – the straightforward exchange of information between tools facilitate the simulation and optimization activity.
- **Scientific reliability and consistency** - it is very important that the tools produce reliable results and that they are universally accepted and built on validated engines to ensure strong results

## Grasshopper

The construction of the model of the building and the shading device system of the roof is realized using Grasshopper. As already widely explained previously, this is an open source parametric tool, which uses graphical components to generate the model. The contribution of every user of the community creates a network of shared information and discussion forums that provide guidance for the use of this tool and the wide range of plug-ins developed. Harnessing the power of multiple plug-ins, the daylighting simulations are performed without the need of external programs. Diva and Archsim are widely used and they use Radiance as engine to run daylight simulations. Radiance is a validated tool that use ray tracing method to run the analyses on a selected scene. Specifically, the calculation is based on the materials' reflection properties and on the way daylight rays hits the surfaces and bounce inside a space.

## DIVA and ARCHSIM

Diva is a validated plug-in available for Rhinoceros and Grasshopper, distributed by Solemma LLC. All daylighting simulations were performed using this plug-in. The results from the daylight calculations were implemented in the energy calculations, using lighting schedules. The plug-in used for the energy simulations is Archsim, which can easily communicate with Diva. Diva is based on Radiance, Daysim and EnergyPlus and allows annual radiation analysis, thermal comfort and multi-zone energy simulations.

## modeFRONTIER

modeFRONTIER is a desktop platform and is "the comprehensive solution for process automation and optimization in the engineering design process". It is possible to search for optimal or sub-optimal solutions by creating the logical workflow behind the desired optimization. The workflow expresses the logical links between inputs and outputs, the constraints and the targets towards which the solver has to work. The solver tries to find the local or global best solution through the selected algorithm. modeFRONTIER has been chosen among other optimization tools for its wide variety of algorithms and design exploration possibilities. It can be used to improve the architectural and engineering practice by providing the means for an optimization-driven design

process. Furthermore, TUDelft was involved in the realization of a component that enables the integration of Grasshopper and makes the communication between the two software possible. The optimization workflow follows the one described by modeFRONTIER and the user-defined Grasshopper script carries out the performance simulation. Finally, modeFRONTIER collects all the outputs and enables the design space exploration. However, modeFRONTIER presents the drawback of being a commercial software, which requires the purchase of a license and consequently makes its use restricted.

### 3.2 INITIAL WORKFLOW ALTERNATIVE

#### 3.2.1 GH AND MF COMBINATION

The communication between Grasshopper and modeFrontier has been made possible thanks to the collaboration between TUDelft and Esteco, and it is obtained through a plug-in which allows the interaction of the two software and the interchange of data. The plug-in allows MF to send the input variables and directions to GH, which runs the simulations and send back the output to MF. MF collects the data and stores them in an accessible database, from which is possible to explore the solution space.

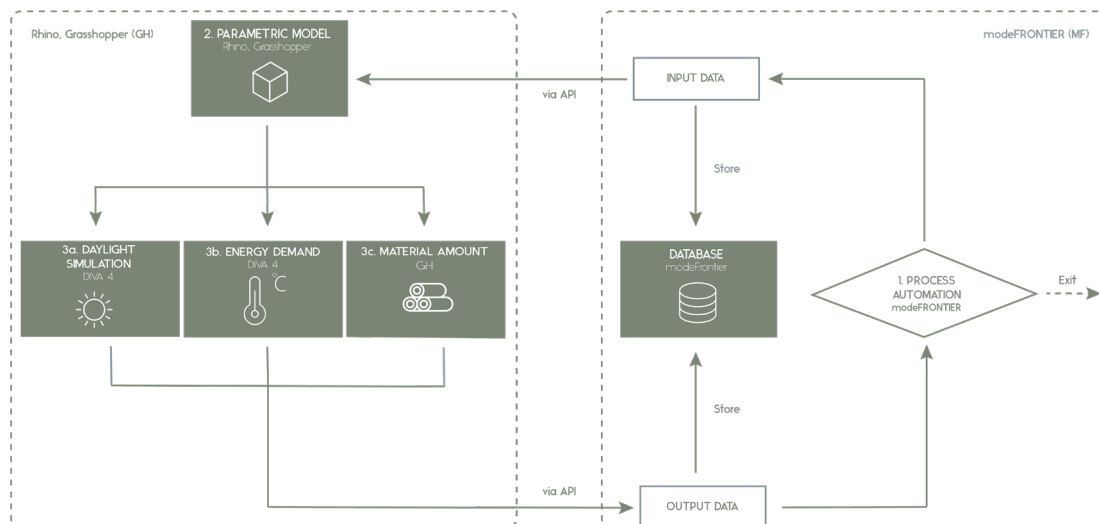


**Figure 36** Grasshopper and modeFRONTIER workflow. Adapted from: Yang, Ren, Turrin, Sariyildiz & Sun, 2018

To understand how the integration of the two tools works, a good representation is provided by the workflow from Yang, Ren, Turrin, Sariyildiz & Sun, 2018, showed in *Figure 36*. The first step is the realization of the parametric model

in Grasshopper, which also uses plug-ins that can perform daylight and energy simulations, and provides values for the performance of the model (in this specific case: daylight, glare, heat load). modeFrontier directs the values for the input variables in the Grasshopper model and starts the performance simulations, at the end of which modeFrontier acts as a database and stores the output data. The end of the iterative process is also ruled by MF. In conclusion, modeFrontier act as director, determining when to start and stop the simulations, and decides the data samples, while Grasshopper is the engine that runs the simulations and produces results.

### 3.2.2 INTRODUCTION TO THE WORKFLOW

One of the goal of this research is to prove how effective the combined use of design exploration and optimization tools can leads the designer to a more informed and better solution. Traditionally, the optimization phase is carried out only after the main conceptual design has been chosen and the CDO (computational design optimization) focus on aspects that do not have a big impact on the performance and can only slightly change the solution(*Figure 37*). The reason behind this choice is the idea that the parametric modelling and performance driven design could somehow restrict the freedom of the designer, limiting the creativity and exploratory thinking. However, the risk of an optimization process applied in later stages of the design, is to focus the attention and the effort on a sub-optimal design, which, no matter the effort spent on the optimization process, would never lead to an optimal performing solution. So it is possible, to introduce boundaries in the design exploration with the possibility of reducing the chances of achieving the best solution.

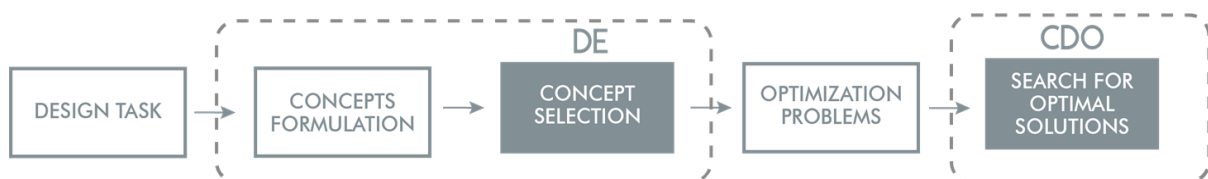


**Figure 37** Conventional design process. Adapted from Yang, Ren, Turrin, Sariyildiz & Sun, 2018

As explained, optimization problem solving (OPS) is an approach mainly used in advanced stages of the design, when a number of important assumptions have been made regarding the design performances. These assumptions lead the design towards a alternative considered “the optimal one”. However, these choices are simply based on experience rather than being informed decision found on knowledge extraction. The latter can be possible when the statistical

analyses are conducted during the computational design exploration. The idea is to be able to change the optimization problem formulation (OPF) using first a computational design exploration (CDE), which allows to broaden the dimensions of the design space.

Yang, Ren, Turrin, Sariyildiz & Sun (2018) points out that OPF is often “ill-structured”, referring to the low attention spent on formulating the optimization problem in a proper, knowledge-supported way. This is proven to be true especially in the preliminary phase, when not a lot of knowledge has been yet acquired and the freedom level is high. As disadvantage of the lack of the problem definition, the optimized solutions might be meaningless or even misleading.

The best way to proceed is to apply an iterative process of CDE, which makes clear how to properly choose variables and objectives, with relative constraints (Figure 38).

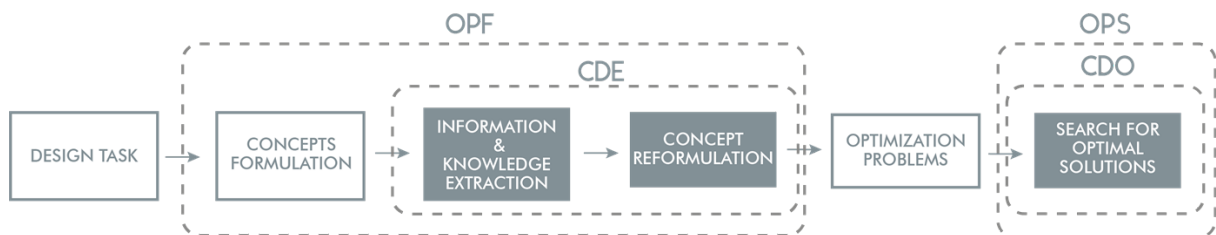


**Figure 38** Relation between design exploration and optimization phases. Source: Yang, Ren, Turrin, Sariyildiz & Sun, 2018

It has already been proven (Yang, Sun, di Stefano, & Turrin, 2017) how a computational approach, by means of parametric modelling and optimization algorithms, through the whole design phase can improve the final outcome and increment the dimensions of design solutions space.

Working with a parametric modelling tool (GH) combined with plug-ins that allows performance simulations, together with a design exploration and optimization software, gives the possibility to discard and select alternatives in a more informed way. The multi-objective optimization represents the next step, through which is possible to analyse all the collected data and redefine scopes and variables. The step of optimization problem formulation is often underestimated, though a good definition of the problem with the selection

of input variables and performance targets is equally, if not more important than the OPS (optimization problem solving) in order to achieve the objectives delineated.

### 3.3 OVERALL COMPUTATIONAL WORKFLOW

The study carried out requires various passages of complexity. To achieve the desired result, the methodology applied consists in starting from the consideration of simple alternatives and slowly introducing complexity in the model, in the simulation and in the optimization. Another essential step taken into consideration is the validation of the results from the simulations built in the parametric model. The approach followed for the design exploration is inspired by the one presented by Yang, Sun, di Stefano, & Turrin, in the paper “A computational design exploration platform supporting the formulation of design alternatives” (2017).

The methodology of this computational design exploration process consists of three stages: 1. Alternative making, 2. Computational Design Exploration, 3. Refinement of alternatives. This whole procedure has been applied for two alternatives, which are the one to be tested to refine and find the best performing geometrical solution

#### 1 Alternatives making

- Formulation of multiple alternatives
- Formulation of the problem and description of the system in a systematic way, with variables and constraints
- Definition of the simulations targets of the simulations

#### 2 Computational exploration of the design space, this step represents the main learning process phase

- This phase is the central point for knowledge extraction and is the main decision support system
- This is an iterative phase that helps the results to converge and supports the identification of the best alternative and variables

- It is important to :
- Define the working process
- Run performance simulations
- Collect data and statistical analysis
- Weigh alternatives and first recognition of the best performing idea

### 3 Refinement of the alternative

- The acquired knowledge from the previous steps is useful to readjust the alternatives and/or create new ones, so it is important to redefine:
  - Design variables of the system
  - Objectives of the performance simulations

#### 3.3.1 COMPUTATIONAL DESIGN

##### Computational Design Exploration (CDE)

The computational design exploration (*Figure 39*) is divided into two parts, each made up of 3 main steps. These three steps are those already described in paragraph 3.3 on page 74:

- Alternatives making
- Computational exploration of the design space
- Refinement of the alternative.

The first step is the formulation of the three alternatives (alternative1, 2, 3) all belonging to the same family of geometries, but all different from each other. Although there may be an initial knowledge based on experience that can guide the choice of the alternative variation among the three proposed, following intuition can lead to a misguided decision. Therefore, after the formulation of the alternative alternatives, the second phase consists of carrying out a computational exploration of the alternatives. This can start after the formulation of the design variables and performance targets. From the CDE it

is possible to extract useful data and knowledge. The information acquired makes possible to understand whether a alternative works better for some targets rather than others, and which geometrical properties allow the best performances. In this way we can identify the most promising alternative and create a refined, optimal solution based on the best performing features of alternative 4.

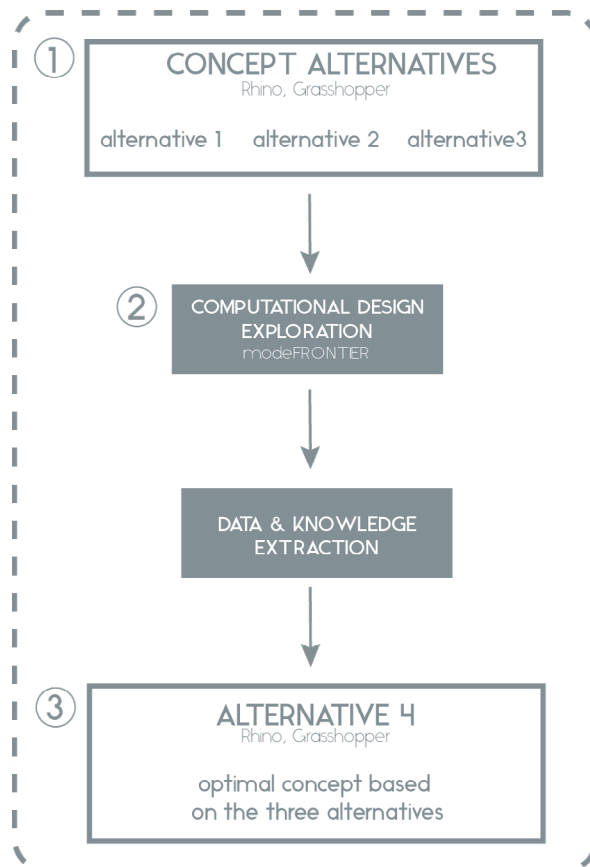


**Figure 39** Computational Design Exploration

At the end of the CDE, the question to be asked is how well the alternative obtained (alternative 4) responds to the desired performance targets. Whether the overall targets are unbalanced, the next step would be the formulation of other alternatives that “learn” from alternative 4, and try to correct the issues and improve the performances.

The importance of this kind of computational design exploration is that, contrary from the automated optimization, it keeps intact the user decision power. The role of the design is still ensured and the design environment used in this research acts as a decision guideline, from which the user can learn and can take advantages.

## Computational Design optimization (CDO)

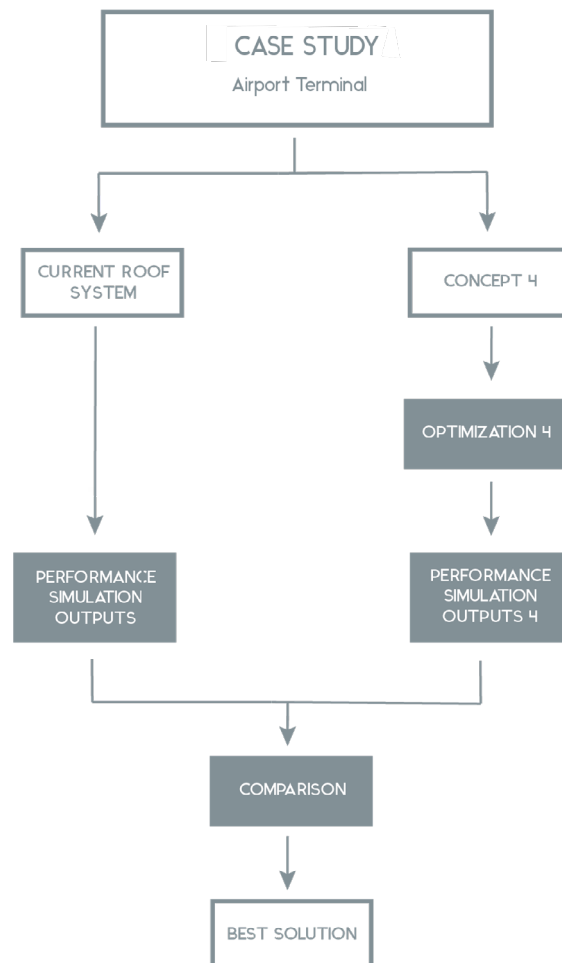
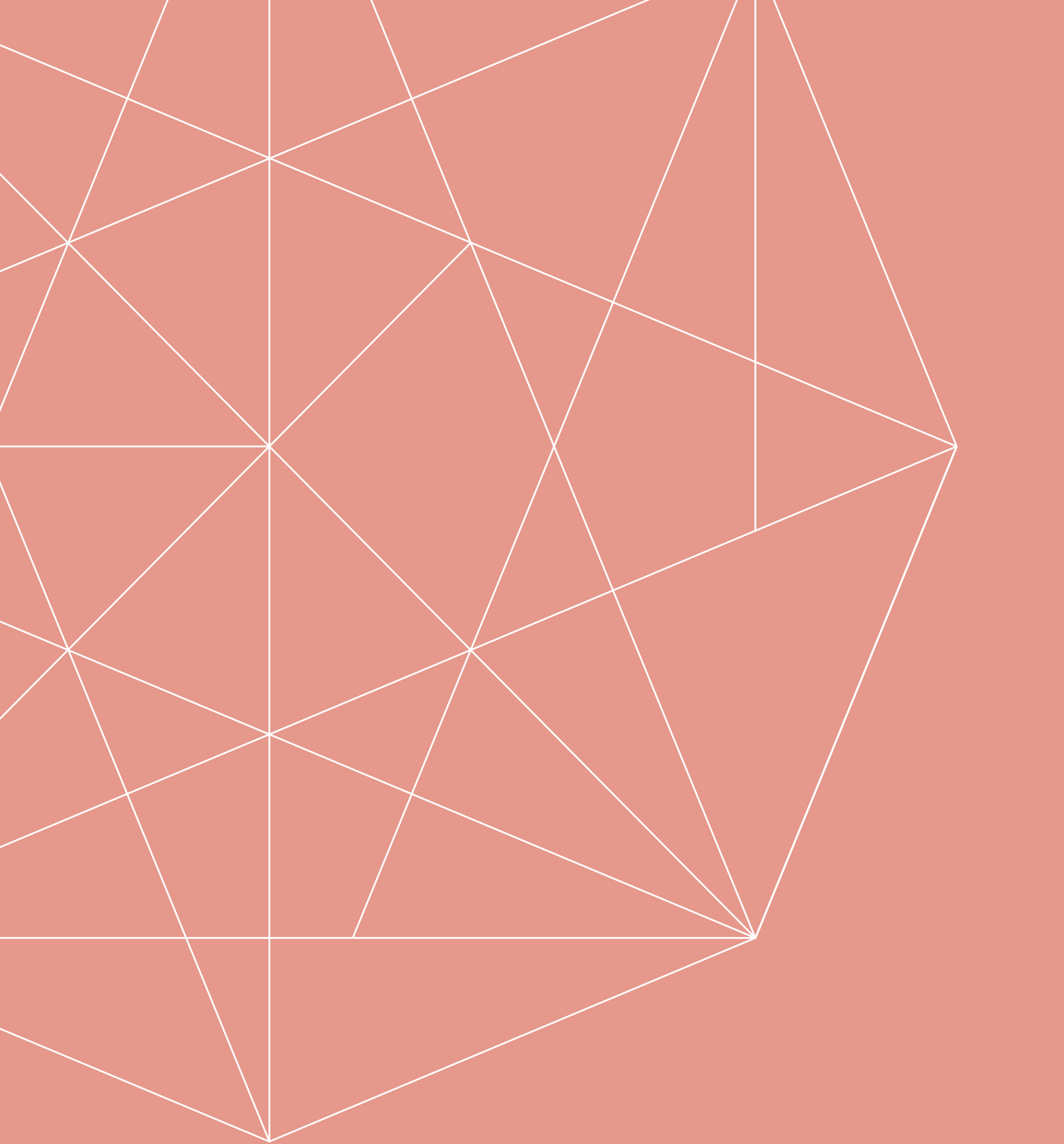


**Figure 40** Computational Design Optimization workflow

The computational design optimization process showed in *Figure 40*, starts with the selection of one case study, which is the New Schiphol Airport Terminal located in Amsterdam, Netherlands. The case study is analysed with the current roof system and the performance simulation outputs are computed. Afterwards, the current roof is replaced with the final design (alternative 4). The design variables and performance objectives are selected and it is defined the optimization strategy. Hence, alternative 4 is optimized for the specific objectives of the case study and the performance outputs can be collected. Finally, the all gathered performance data are compared and the best solution is recognized.







04





## 4.1 COMPUTATIONAL DESIGN EXPLORATION

### 4.1.1 ALTERNATIVE GEOMETRY

The reasons of choosing a triangular extrusion instead of any other shape, are many. In first place, the triangular shape is easy to assemble and in general it ensures stability and allows the weight to be uniformly distributed. Furthermore, using the triangulation of a curved surface it is always possible to be discretized in flat triangular surfaces. (Henriksson & Hult, 2015) (*Figure 41*).

Some examples are the Great Court of the British Museum in London, the New Milan Trade Fair and the Dali Museum of St. Petersburg in Florida. Another reference is made to the research about existing shading system and take inspiration from many projects. The main reasons behind this shape is the ability of act as a shield against unwanted heat gain, still providing a good illumination in the space underneath with a playful effect of light.

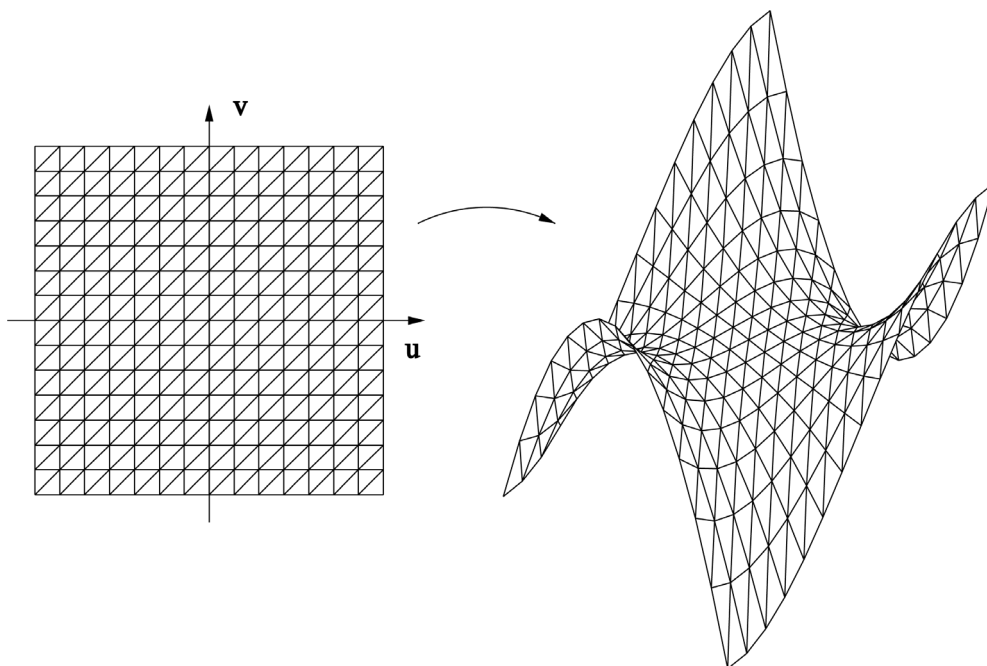


**Figure 41** Parametric surface triangulation (Monkey Saddle). Source: CC BY-SA 4.0 (<https://creativecommons.org/licenses/by-sa/4.0>)

In this specific case the building is treated as single zone. The important thing is to be very precise about input parameters and schedules, like the occupancy schedule. Another important schedule is the lighting schedule which is the

results of the daylight simulations which run through DIVA 4. While the heating, cooling and lighting energy use ARCHSIM, that uses EnergyPlus as engine. The period in which the energy calculation is set is hourly for the entire year. When the simulations are complete, it is possible to analyse whether the results are valid or not. The model is modified as well as the geometry until we got the desired working model. At this point it is possible to run the optimization.

The heat considered is the one coming from the sun through windows, through people, equipment, lighting fixtures. The cooling system turns on in the moment when the temperature inside is over the set point. The heat losses are due to air infiltration, through material conduction. When the temperature is too low the heating system turns on.

### 4.1.2 ALTERNATIVE MAKING

#### 1 Alternatives making

The alternative variations are three and they consist of three-dimensional triangular extruded modules (*Figure 42, Figure 43 and Figure 44*).

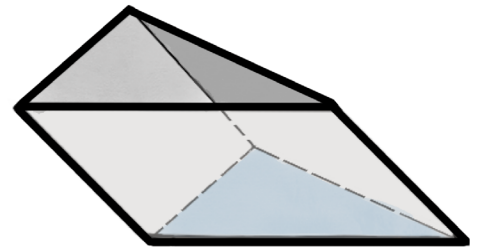
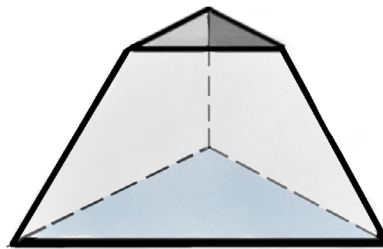
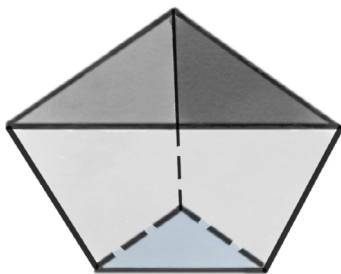
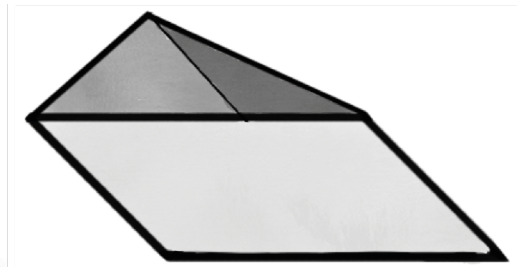
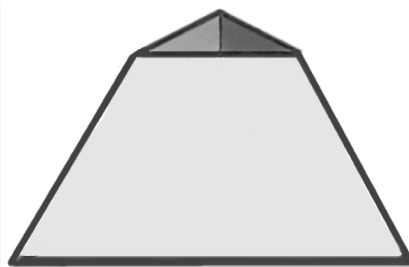
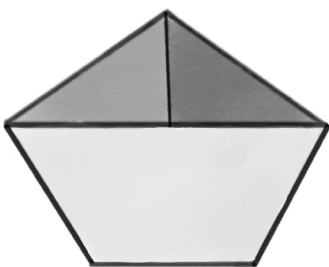


**Figure 42** *Concept alternative 1*

**Figure 43** *Concept alternative 2*

**Figure 44** *Concept alternative 3*



The principle of this concept is the redirection and reflection of light, so that the direct light is blocked and the glare is reduced (*Figure 45*).

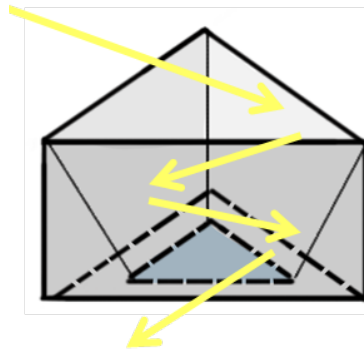


**Figure 45** Principle of concepts of group 1

The whole shading system is the result of the planar tessellation of singular modules in both x and y directions. The concept takes inspiration from various projects, as the Cineteca Nacional Siglo XXI from Rojkind Arquitectos (2014), from Shenzhen Bao'an International Airport, Terminal 3, from the architect Massimiliano Fuksas (2013) and for the triangular shaped elements is inspired from the Esplanade, Theatres on the Bay from DP Architects, Michael Wilford & Partners (2002).

The final shading system is meant to be positioned on the outside, as a cladding shading system covering a glass structure. Each element is based on a triangular shape, which is extruded in different ways and directions. The three different alternatives (1, 2, 3) are variations of the same geometrical alternative and they are explored and compared to determine the most appropriate features that the shading system should have to meet the set targets and requirements.

Generally, the decision on the geometrical shape of the single element of the roof shading system, is taken based on general knowledge and based on experience, however this approach could be misleading and does not take into consideration the analysing each feature of the modules. Thus, after the formulation of the performance targets and the design variables, the computational design process (CDP) comes next; the results and data obtained from the design exploration provides enough information to identify the most promising features of the system that improve the overall daylighting performance of the building.

Alternative 1 consists of a triangular base, which is scaled down at the same level. Then the larger triangle is projected at a certain height (h). Finally, the

edges of the three triangles are connected by planar surfaces. The alternative 2 follows exactly the same geometrical construction, but it is overturned (*Figure 46*).

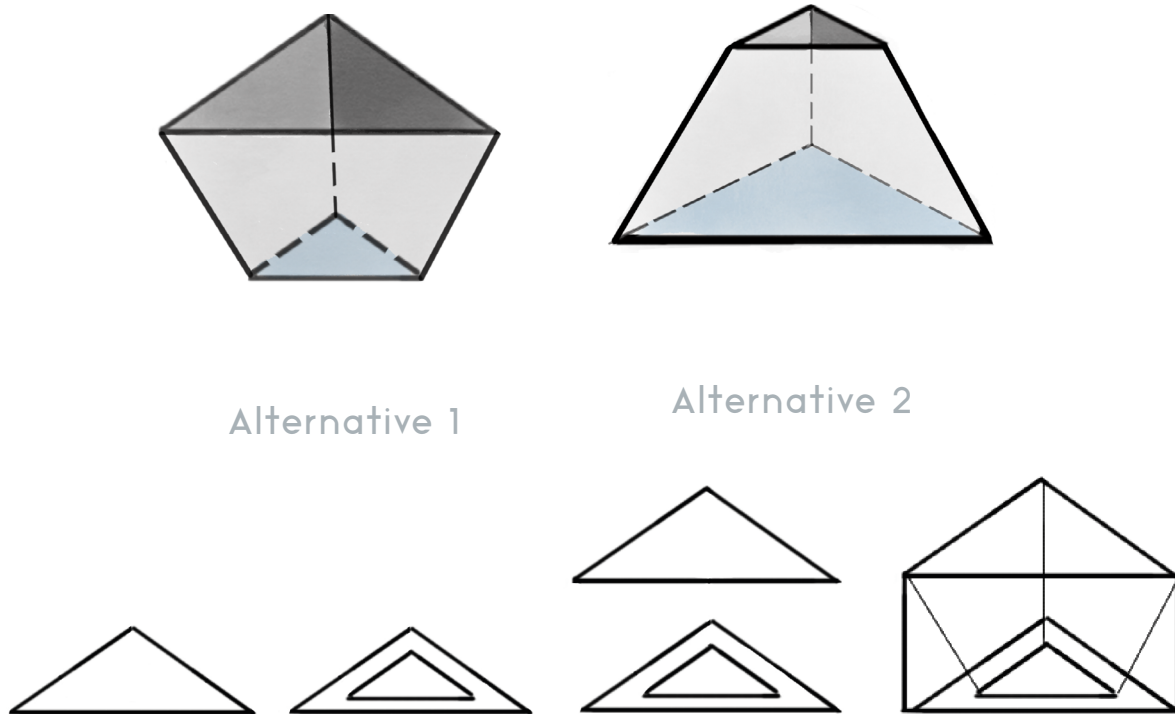


**Figure 46** Logical and geometrical construction of alternative 1 and 2

The third variation (alternative 3) consists in the only projection of the triangular base and its translation in the x-y direction (*Figure 47*).

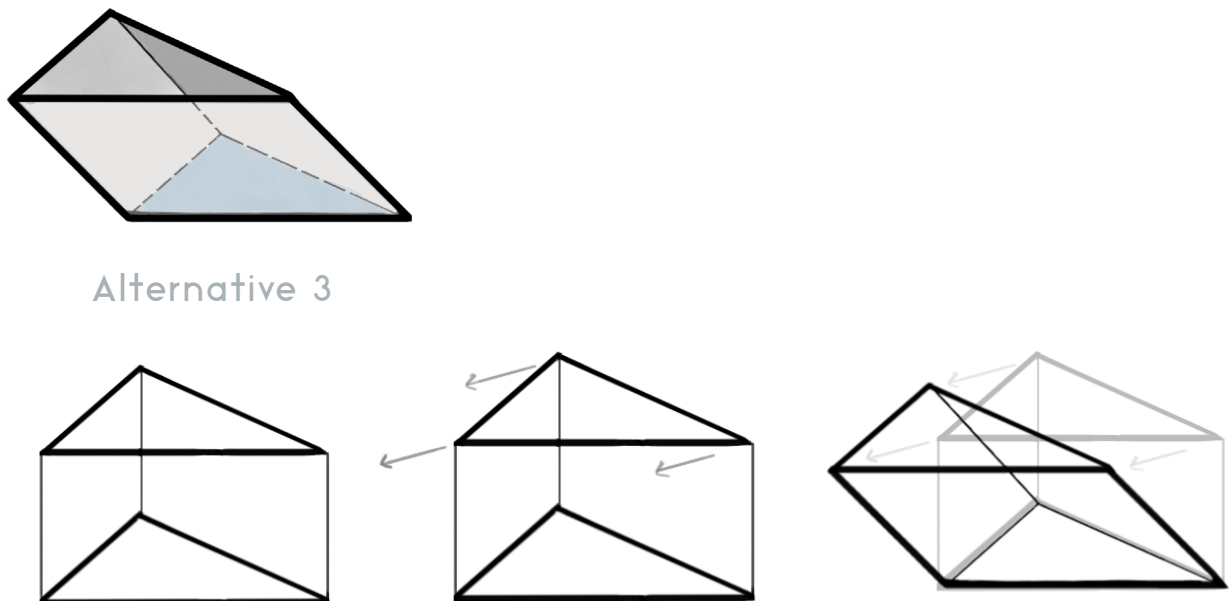


**Figure 47** Logical and geometrical construction of alternative 3

The model construction of a full shading system follows the showed steps(*Figure 48*):

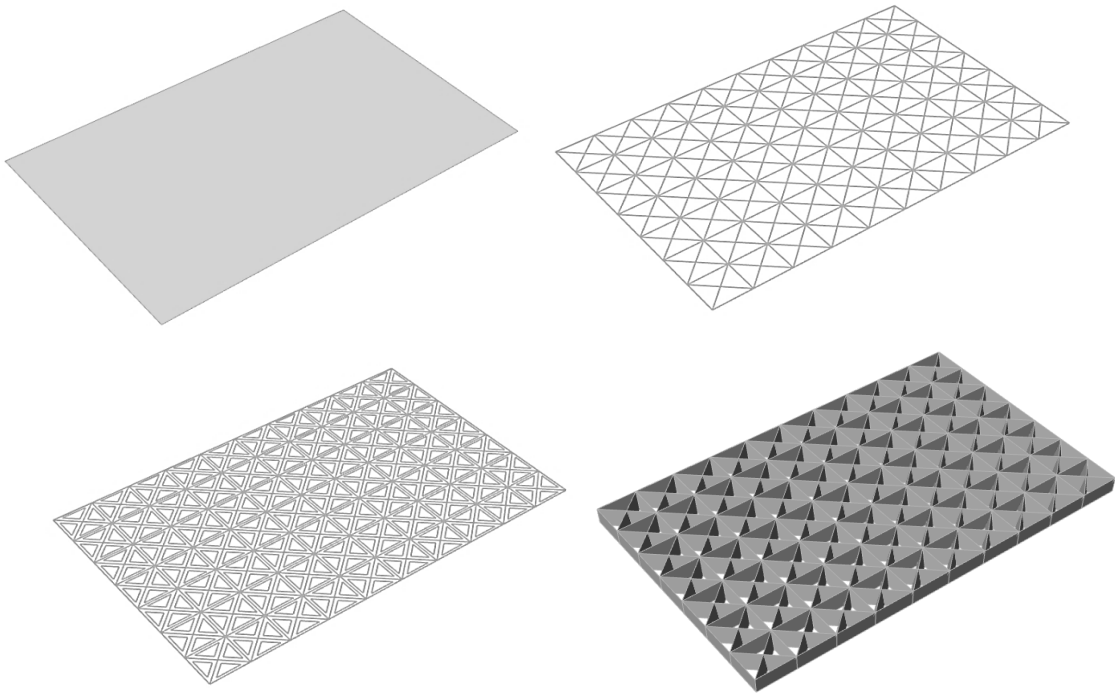


**Figure 48** Example of logical and geometrical construction of a full shading system

Following it is possible to observe some images of the three concept alternatives applied to a reference building (*Figure 49*).

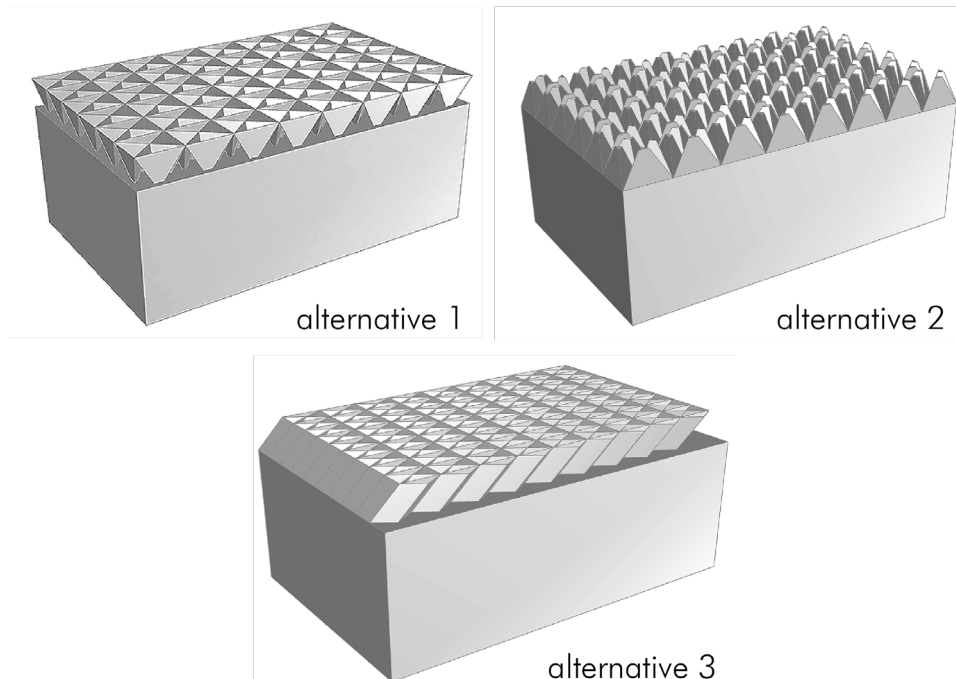


**Figure 49** Examples of concept alternatives applied to reference building.

### 4.1.3 HYPOTHESIS

The creation of these three different design alternatives derives from the idea on their features and performance behaviour relatively to different targets.

- Alternative 1 performs allowing a large amount of daylight from all the directions and reflecting it on the indoor space. At the same time, since the geometry is more open to the outside, the heat can dissipate more easily. It is expected that alternative one performs well in terms of daylight performances due to the widest opening facing the outside. This can take in more sun rays from different angles.
- Alternative 2 is more likely to trap the heat in the shading module. The heating energy needed is expected to be relatively lower compared to alternative 1. On the other side, the daylight entering from the small opening of alternative two, is likely to be less than for alternative 1, so that the natural light reaching the inner space is blocked from the shading beforehand.
- Both Alternative 1 and 2 are symmetrically constructed creating a more uniform distribution of the illuminance and solar radiation, Alternative 3 is conceived with the different purpose of blocking only certain direction of daylight. The shape and inclination in both x and y direction gives the possibility to direct the three-dimensional shape so that the inclined faces of the modules obstruct the direct light and the stronger solar radiations. The directionality of this alternative can create a more complex distribution of the daylight. The idea behind it is the reduction of the highest illuminance levels ( $UDI > 2000lx$ ).

The initial hypotheses might seem quite immediate and “obvious”, on the other hand, the number of variables considered in the Design Exploration and Design Optimization are many and considering how changing these parameters can vary the performances of each alternative might be pretty difficult and not so evident. Accepting the assumptions made a priori about the three designs could lead to a wrong selection reducing the opportunities of reaching high shading performances of building daylight and energy.

In this specific scenario, according to my little experience, without deeper

analysis, the choice would fall on Alternative 2. Since the location in which the study is based is Amsterdam, the heating energy might be the most concerning aspect in terms of building energy required to meet the thermal comfort targets. Alternative 2 seems the most promising in terms of heating energy reduction. Also looking at daylight performances, alternative 2 might be able to block a range of light, avoiding the risk of glare, but still meeting a good daylight autonomy.

These personal, first hypotheses need to be verified and the Computational Design Exploration is the process through which is possible to carry out in-depths studies and draw better conclusions.

#### 4.1.4 EXPLORATION OF THE DESIGN SPACE

This phase is essential to give insights of the design exploration, so that is possible to refine the alternatives and come up with a better, more performing solution, which is optimized during the CDO. The simulations are executed in GH through the use of DIVA 4 and ARCHSIM. The engines that they work with are Radiance and Energyplus. Both use weather files as source for the climate, sun-path and radiation data.

##### Alternative inputs

The building used as reference for the computational design exploration is located in Amsterdam. It is an arbitrary space with dimensions 10 x 6.25 m and 3.5 m height (excluding the shading system). The shading system alternative is conceived to be applied on top of the building fixed height.



**Figure 50** Reference building orientation

The building orientation is as showed in *Figure 50*. The y-axis represents also the north direction and for this reference case the width of the building is on the x direction and is smaller than the length.

The input data, showed in *Table 8* are divided in fixed and variables. The inputs are inserted to execute the daylight and energy simulations.

The initial building design is kept simple and aims to question the efficacy of the designed shading alternatives and how these affects the daylighting performance of the building. The dimension of the reference building are 10\*6.25\*3.5 m. The dimensions are scaled down in order to reduce the computational time. There are no horizontal openings, so to be able to fully analyse the effect of the roof shading system on the space. The closed space does not have horizontal windows, in this way it is possible to focus on the performance effect of the shading system alone.

The model is built so that the design exploration is possible between alternatives. A slider can switch from alternative 1, 2 and 3 and investigate the impact of the choose module on the performance targets. The three alternatives have some variables in common and other that do not affect the other designs, but only one. modeFRONTIER controls the selection of the values of each variable. For each simulation, MF select a set of values and starts Grasshopper to run the performance simulation. At the end of each step of the computational exploration, MF collects the data obtained from GH and initiate the next simulation.

The variables of the modules chosen (*Figure 51*) are eight and are listed in the following table (*Table 7*):

INPUTS NAME	LOWER BOUND	UPPER BOUND	STEP	CONCEPT VARIATION
depth_triangle	0.1	2.6	0.1	
material_glass	0	2	1	
alternative	1	3	1	Valid for concept 1, 2, 3
x_division_panels	3	10	1	
y_division_panels	3	10	1	
scaling_factor	0.1	0.9	0.1	Valid for concept 1 and 2
inclin_y	0	1	0.1	
inclin_x	0	1	0.1	Valid for concept 3 only

**Table 7** Input variables of reference building for CDE

INPUT DATA		
location	Amsterdam, Netherlands	fixed
BUILDING GEOMETRIES		
length (a)	10 m	fixed
width (b)	6.5 m	fixed
height (c)	3.5 m	fixed
DIVA 4 - DAYLIGHT SIMULATIONS		
floor	GenericFloor_20, 20% reflectance	fixed
walls	GenericInteriorWall_50, 50 % reflectance	fixed
curtain walls	Terminal_curtainwall , 60% transmittance	
roof/ceiling	SheetMetal, 90% reflectance	fixed
skylights	0 - SGG PLANITHERM ONE, 70% transmittance	variable
	1 - SGG COOL-LITE SKN 154, 50% transmittance	
	2 - SGG COOL-LITE KNT 140, 37% transmittance	
ENERGYPLUS		
Loads		
people	0.15 [p/m2]	fixed
schedule	weekdays, 8.00 - 18.00	fixed
equipment	5 w/m2	fixed
schedule	weekdays, 8.00 - 18.00	fixed
lights	5 w/m2	fixed
target	300 lux	fixed
dimming	continuous	fixed
lighting schedule	depending on daylight simulation	variable
Conditioning		
heating setpoint	21°C	fixed
heating setback	18°C	fixed
cooling setpoint	23°C	fixed
cooling setback	30°C	fixed
humidity control	OFF	fixed
mechanical ventilation	OFF	fixed
Ventilation		
infiltration	0.2 ACH	fixed
natural ventilation	OFF	fixed
Construction		
roof	120 mm insulation 200mm concrete $U_{value} = 0.26 \text{ W/m}^2\text{K}$	fixed
floor	120mm insulation 200 mm concrete - adiabatic, $U_{value} = 0.26 \text{ W/m}^2\text{K}$	fixed
façade	120mm insulation 200 mm concrete, $U_{value} = 0.26 \text{ W/m}^2\text{K}$	fixed
skylights	0 - SGG PLANITHERM ONE	variable
	1 - SGG COOL-LITE SKN 154	
	2 - SGG COOL-LITE KNT 140	

**Table 8** Input settings in Grasshopper for the CDE

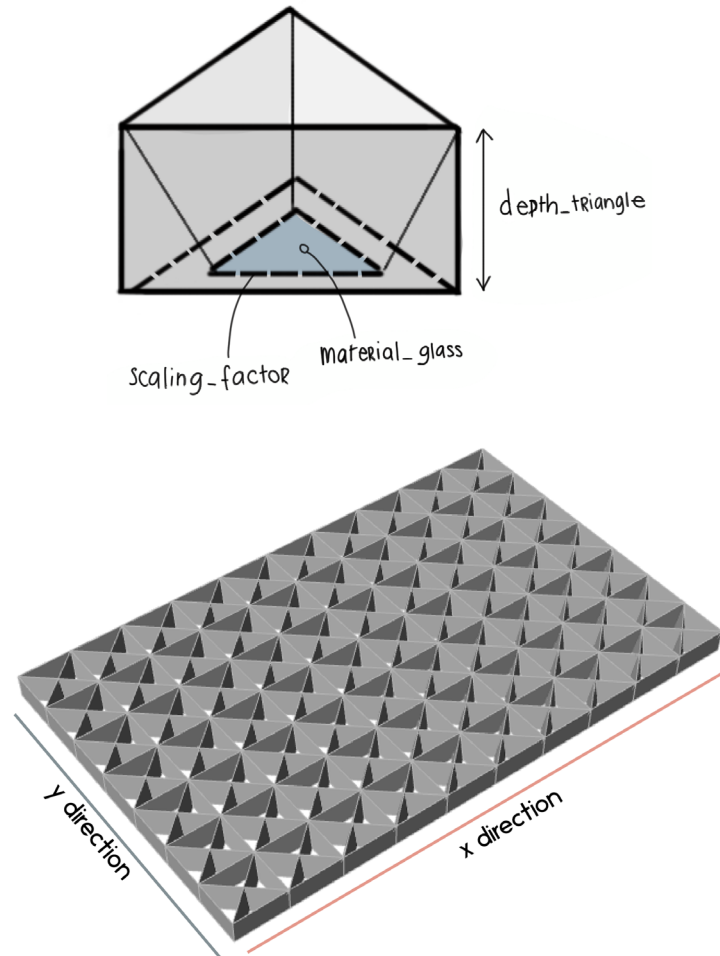


**Figure 51** Input variables displayed

The inclination of the modules in the x and y directions (variables *inclin\_x*, *inclin\_y*) is valid only for Alternative 3 (Figure 52). Parameter *inclin\_x* is intended as the translation of the upper triangle on the direction of the x-axis, so the metal shading element protrudes towards the west or east direction. When the *inclin\_y* value changes, the top triangle is moving on the y-axis, the module opening stretches towards the south or north direction (Table 9).

VARIABLE	VALUE	PROTUSION DIRECTION
inclin_x	0.0	maximum inclination towards West (W)
	0.5	perpendicular to the x-axis
	1.0	maximum inclination towards East (E)
inclin_y	0.0	maximum inclination towards South (S)
	0.5	perpendicular to the y-axis
	1.0	maximum inclination towards North (N)

**Table 9** Variables inclination\_x and inclination\_y explained

The maximum inclination both in the x- and y-axis depends on the geometric features of the shading unit modelled for each value of the input parameters. Each combination of input variables creates a different geometry, thus the

inclination of the protruding roof shading element has different upper and lower bounds.

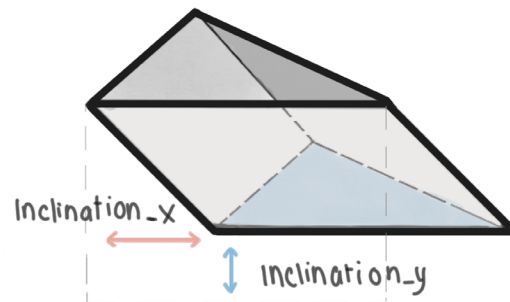


**Figure 52** Input variables inclination x and y for concept alternative 3

The maximum inclination is limited to the ability of the upper geometry to slide laterally until the edge of the geometry below.

For depth\_triangle is intended the height of the module. For material\_glass, as reference materials have been chosen three glass with different properties, in order to evaluate which one gives a better performance (see “8.2 Appendix B” on page 211).

The three glass materials for the skylights are chosen from the Saint-Gobain glass (2013) and are listed in *Table 10*.

ID	PRODUCTS	light transmittance LT (%)	solar Factor g-value	Shading Coefficient SC	U-value (EN 673) W/(m <sup>2</sup> K)
	Average values given according to the standards ISO 9050 m) and EN 673 <b>High light transmission low-E glass (DGU 6 + 12 + 6 mm)</b>				16 mm argon
0	SGG PLANITHERM ONE	70	0.48	0.56	1.0
	Average performance values of DGU(6+12+6 mm) with coating on surface #2, according to the standards ISO 9050 m) and EN 673 <b>Neutral</b>				
1	SGG COOL-LITE SKN 154	50	0.27	0.31	1.0
2	SGG COOL-LITE KNT 140	37	0.28	0.33	1.3

**Table 10** Reference glass products. Source: Saint-Gobain Glass, 2013

Each glazing material has different light transmittance factor to evaluate the best one performing for daylighting conditions. The U-value is the same for glazing 0 and 1 (U-value=1.0) while the SGG COOL-LITE KNT 140 has a U-value of 1.3 W/(m<sup>2</sup>K), allowing more rate of thermal transmission.

## 4.2 CDE WORKFLOW

The Computational Design Exploration workflow is set in MODEfrontier (see *Figure 53*). The communication between the two software is through a MF plug-in that allows MF to send instruction to Grasshopper. Grasshopper run the simulations and the performance outputs are collected and stored in MF. This iterative loop in Design Exploration run without an algorithm and it is user controlled. The process stops whenever the designer decides that the number of data is enough to extrapolate some informations and extract knowledge.

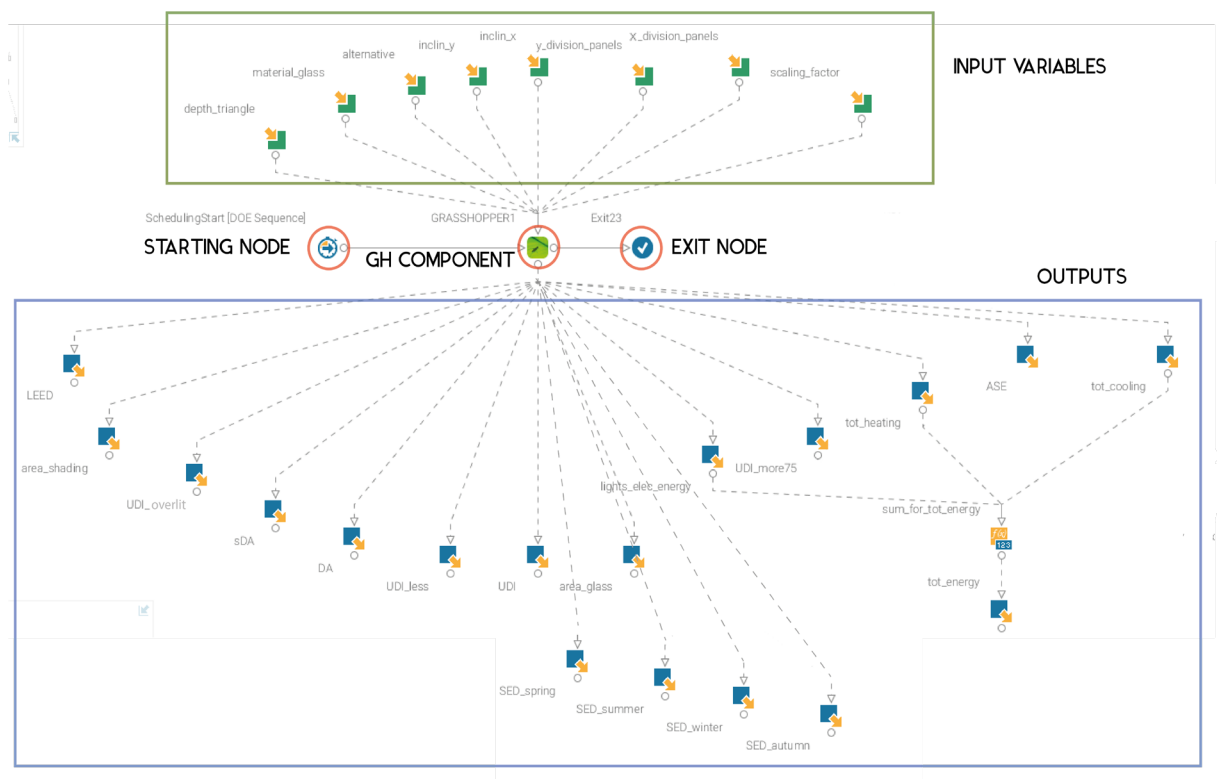


**Figure 53** Computational Design Exploration workflow constructed and used with modeFRONTIER

The upper green box encloses the input variables for the Grasshopper model. The bottom blue contain the outputs from the simulations run from the Grasshopper engines. The Grasshopper node allows to connect the GH model and choose the parameter to use as input and output variables. The starting node contains the setting for the DOE (Design of Exploration) and/or the optimization algorithm. In this case the DOE uses the Uniform Latin Hypercube algorithm. This is a stochastic algorithm which originate a number of samples with uniform distribution, so that each variable has the same probability of been selected. For this specific DOE the number of designs is set to 200.

The Grasshopper Algorithm used for the construction of the Parametric model and for the visual and thermal performance simulation can be found in **8.3 Appendix C**.

The outputs calculated are the following:

### DAYLIGHT PERFORMANCES

- sDA
- DA
- ASE
- UDI
- UDI,underlit percentage
- UDI,overlit
- UDI,75

### SHADING MATERIAL

- area\_glass
- area\_shading

### ENERGY PERFORMANCE

- lights\_elec\_energy
- tot\_cooling
- tot\_heating
- tot\_energy (tot\_cooling+tot\_heating)

## 4.3 CDE RESULTS

In order to analyse the results in a more systematic way, first the three alternatives are compared and then explored separately.

### ALTERNATIVES COMPARISON

From a first general evaluation of heating, cooling and total energy is clear how the biggest impact on the total energy is given by the heating portion. Thus, most of the observation on the energy aspect, are more focused on the heating energy rather than cooling. This is mainly due to the fact that the building is a closed box to which is applied a roof shading system and it is located in Amsterdam with a temperate maritime climate. Furthermore, the selection of the material properties have high influence on the energy demand.

In this case the construction materials of the reference building are chosen as standard material, however they represent a typology of quite low insulating construction materials, with high U-values. This material choice, together with the building context, induces the heating load to be higher than the cooling load.

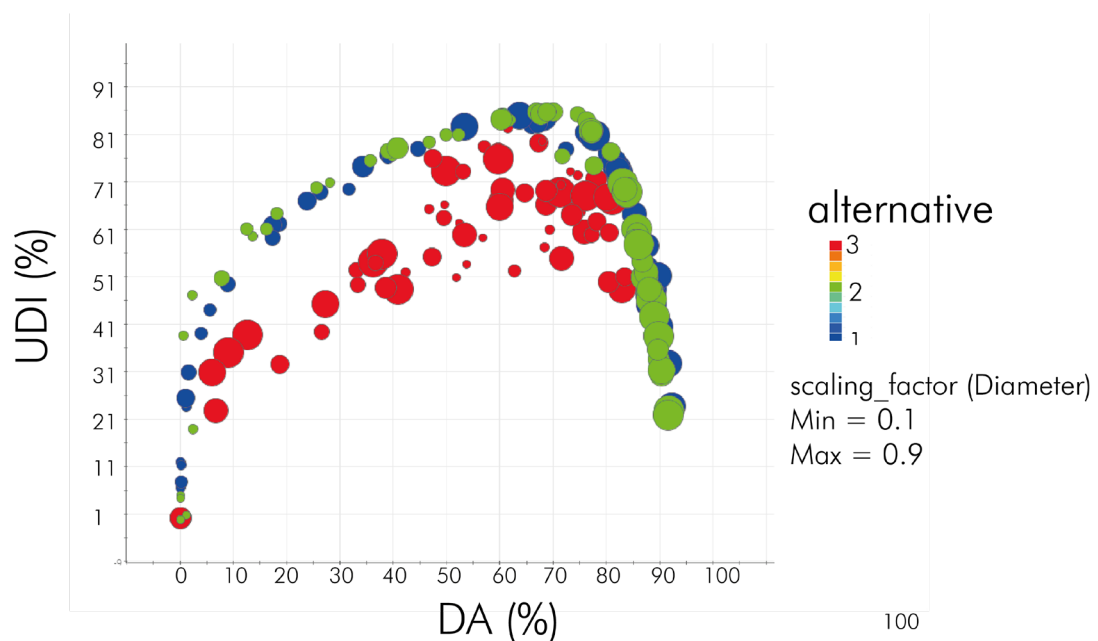


**Figure 54** 4D bubble chart of all the three concept alternatives. Relation DA, UDI, alternative (colour) and scaling\_factor (diameter)

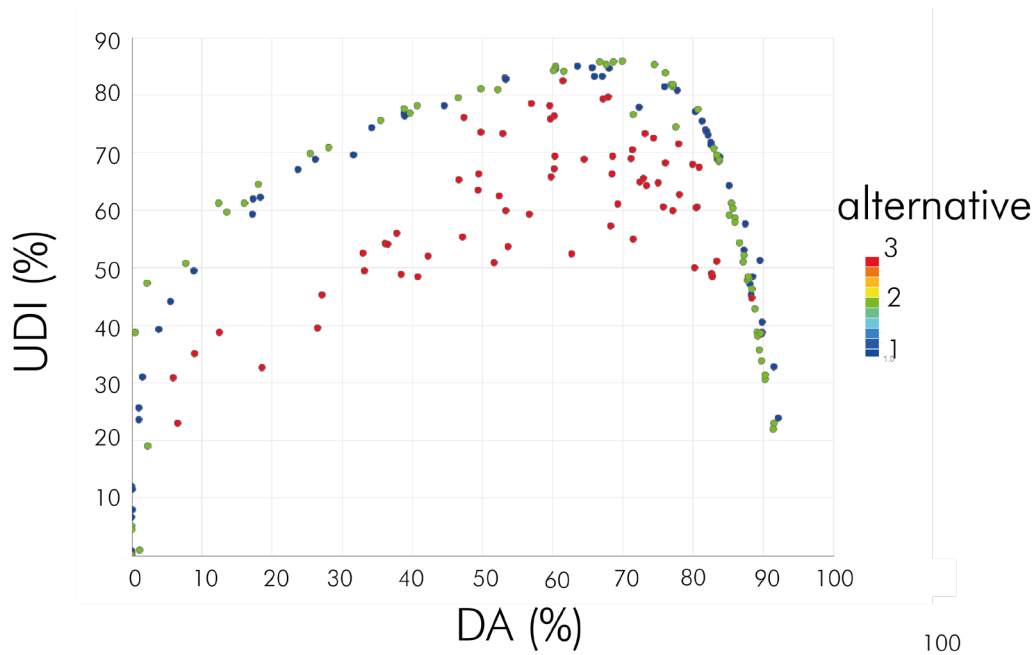


**Figure 55** Bubble chart of all the three concept alternatives. Relation DA, UDI and alternative (colour)

From the graphs above (*Figure 54 and Figure 55*) show the clear trend of the DA-UDI. When the daylight autonomy is low the UDI is also low, since the daylight conditions of the space are mainly underlit (<100lux). With the DA growing, also the UDI grows until a point in which the higher the DA, the higher the overlit percentage and UDI starts again to drop. Almost the same trend is followed by the scaling\_factor which seems to have almost a linear influence on the UDI, while it is almost linear considering the DA.

The distinction between the three alternatives is made by the different colours. As visible alternative 3 seems to have a less accentuate curve, reaching slightly lower values of UDI. However, looking at the graph above, the intensity of the samples of alternative 1 at high levels are sporadic, while alternative 2 and 3 can reach high UDI with a major number of samples.

What can be clearly seen from the bubble charts below (*Figure 56 and Figure 57*) is the linear dependency between the heating energy and the total energy demand. The alternatives are recognizable from the three different colours chosen by modeFRONTIER:

- Alternative 1 - blue
- Alternative 2 - green
- Alternative 3 - red

Alternative 2 has on average the highest heating demand and therefore energy consumption, while alternative 1 seems to be the best performing in terms of energy demands.

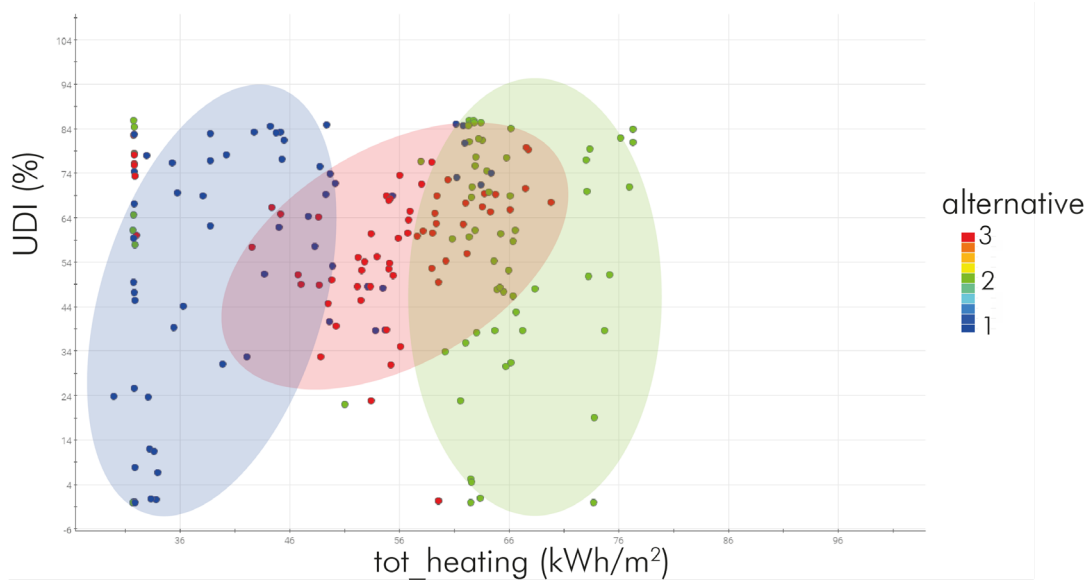


**Figure 56** CDE Bubble chart \_ alternatives behavior regarding heating energy demand and UDI

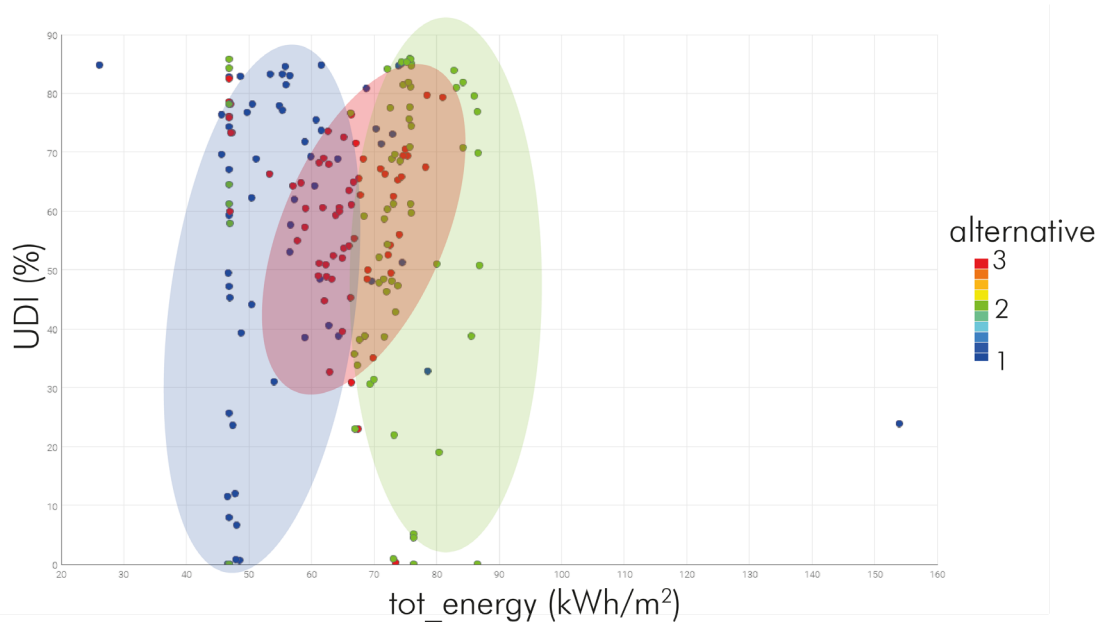


**Figure 57** CDE Bubble chart \_ alternatives behavior regarding tot energy demand and UDI

What also stands out is that all the alternatives, except variation 3, fluctuate in a wider UDI range, while samples of concept 3 are more concentrated in the UDI range between 25 and 75%.

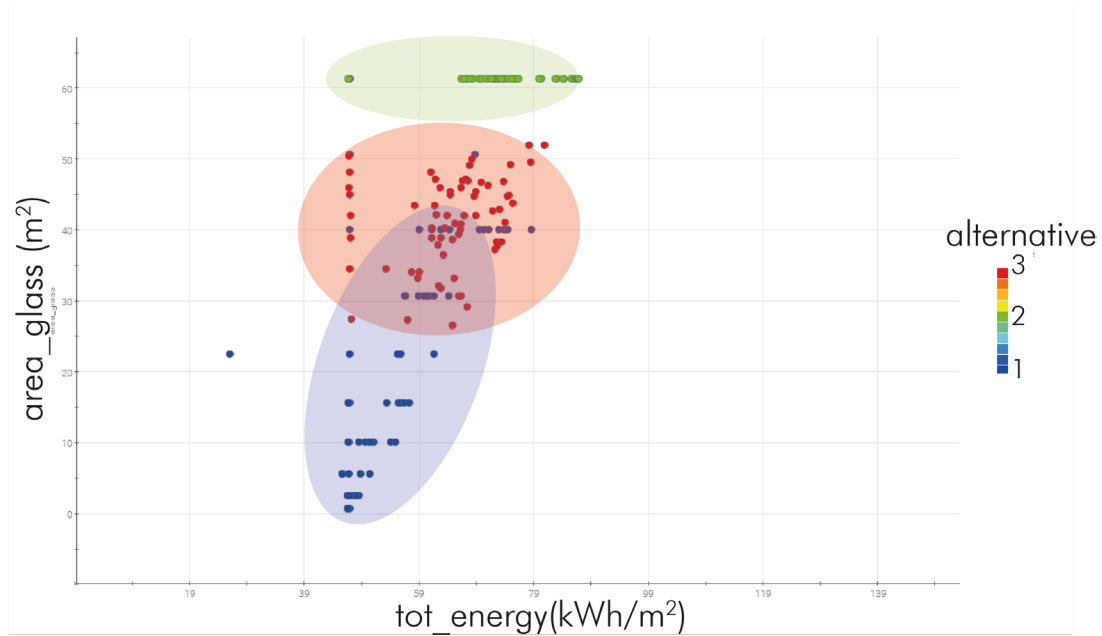


Figure 58 CDE \_ Bubble chart alternatives comparison \_ relation between energy demand and glass area

The total energy of all the three concept alternatives is strictly related to the area of the glass (Figure 58). Respectively each concepts differs in the percentage of glazing area. Alternative 2 does not vary the amount of glass, since the glass is at the bottom, which is not affected by any variables. The opening ratio acts exclusively on the top triangle.

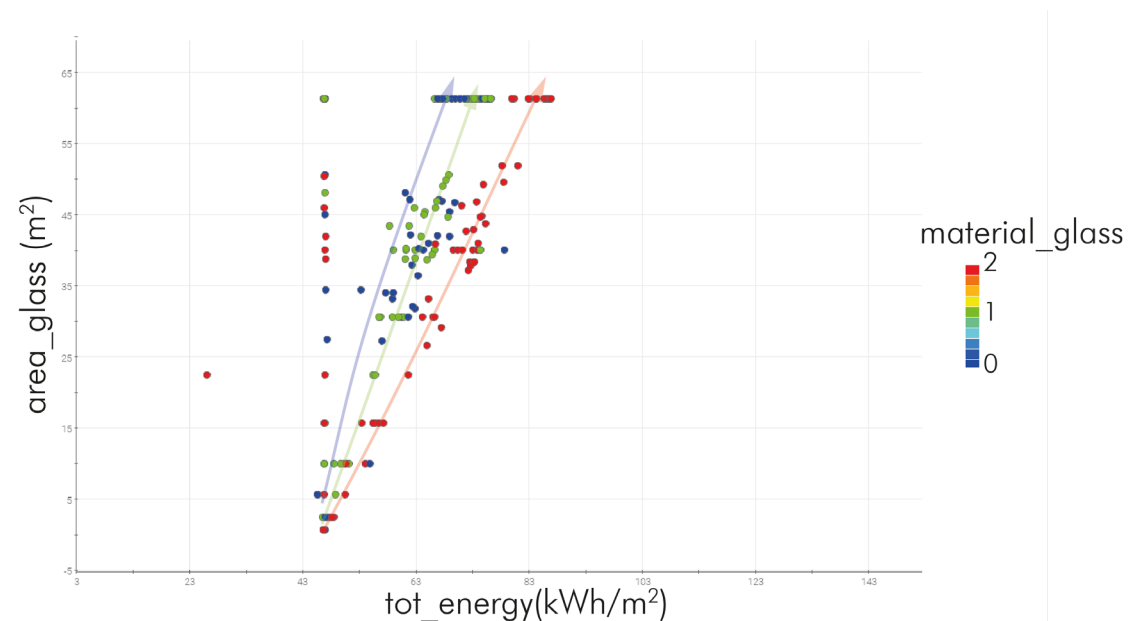
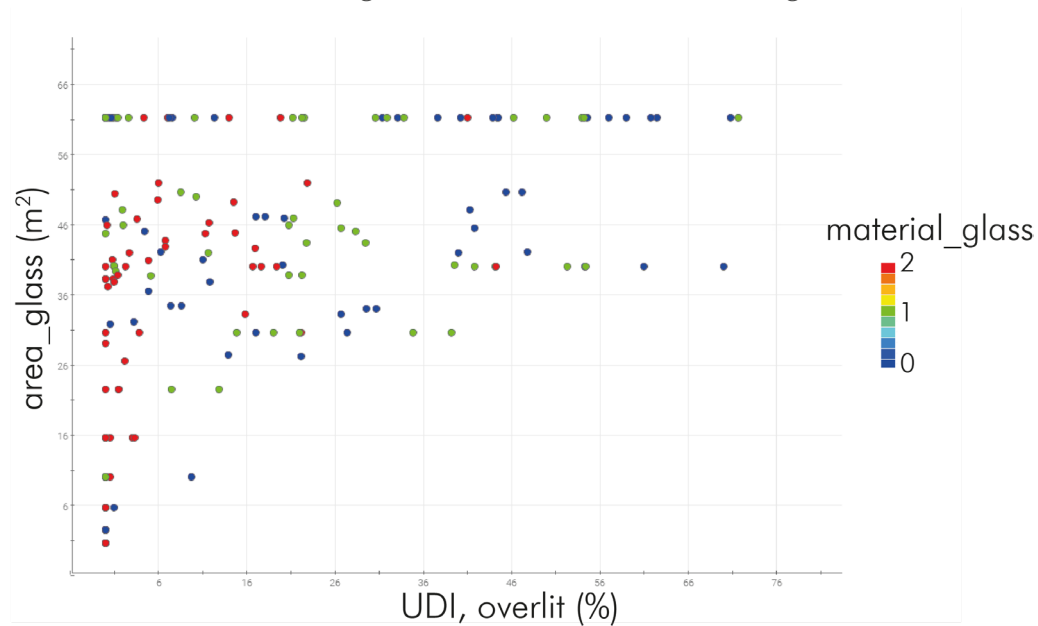


Figure 59 CDE \_ Bubble chart alternative comparison \_ relation between energy demand, glass area and glass material

The total energy consumption is not only related to the amount of glass. Other factors determine the energy performance of the building. The bubble chart in *Figure 59* highlights the dependency from the material glass. The bigger the glazing area, the higher the U-value the more the heat losses which results in higher heating demands.

The dependency from the type of glass is not solely correlated to the U-value. Other important properties of the glazing affecting the thermal load as well as the visual comfort are the Light Transmittance (%) and the g-value.



**Figure 60** Bubble chart showing the relation between the UDI,overlit, the area of glass and the glazing material

The light transmittance, which indicates the percentage of visible light transmitted through the glass, plays a role in determining the effects of the visual and thermal comfort. Bigger LT values, as for glass material 0 (LT=70%) increase the Daylight Autonomy. However, this may also bring to a higher chance of glare, whether the shading system is not properly designed (see *Figure 60*).

Higher light transmittances reduce the need of artificial illumination, thus the lighting electrical demand. As consequence, in order to reach the thermal comfort, the heating load results higher during winter and the cooling load smaller during the warm season (*Figure 61*).

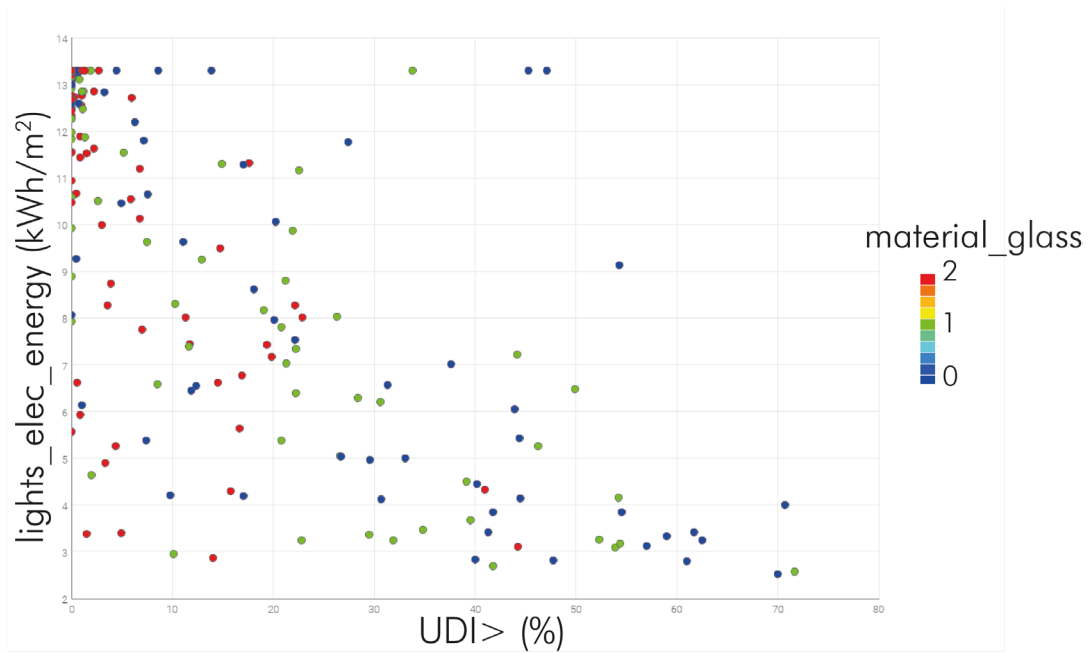


Figure 61 Bubble chart showing relation between UDI, overlit, lights energy and glass material

The Shading Coefficient represents the thermal performance of a glazing system. The lower the SC value, the greater the shading effect of the glazing. This factor is important especially when the direct solar exposure is high. While SC indicates the amount of total solar radiation, the g-value is specify the heat gain penetrating through a material. Higher g-value, like for material 0 (g-value = 0.48) produce more solar heat gain and as final effect, the heating load is reduced.

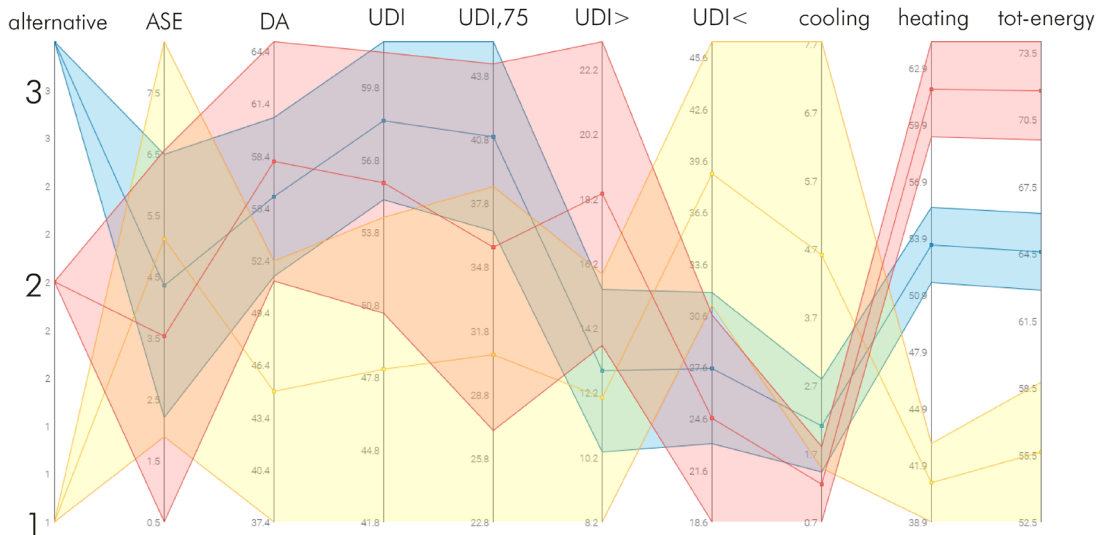


Figure 62 Clusters parallel coordinates chart\_ hierarchical clustering of the three concept alternatives

The above parallel chart (Figure 62) is filter using hierarchical clustering. The chart shows the distribution of the variables selected and it is meaningful when looking at input-output relations. The graph is created with a confidence level of 0.9, meaning that there is a probability of 90% that the values fall in the band

interval. The mid-line represent the mean value. In this specific case each band represent one of the alternatives:

- Alternative 1 - yellow
- Alternative 2 - red
- Alternative 3 - blue

Looking at each output and objective separately it is possible to extract important information. Each alternative is analysed more in details in the following paragraphs.

### 4.3.1 ALTERNATIVE 1

To sum up the main performances of alternative 1 (Figure 63):

- Performs very well in reducing the Overlit percentage, in achieving the less amount of Glazing, reducing the heating and therefore the energy demand.
- Performs relatively bad in sDA, ASE, UDI and UDI,75. As well as area of the shading system and cooling demands
- Performs very bad in DA, Underlit and lights electric energy, due to the low quality of daylight that can bring to the space

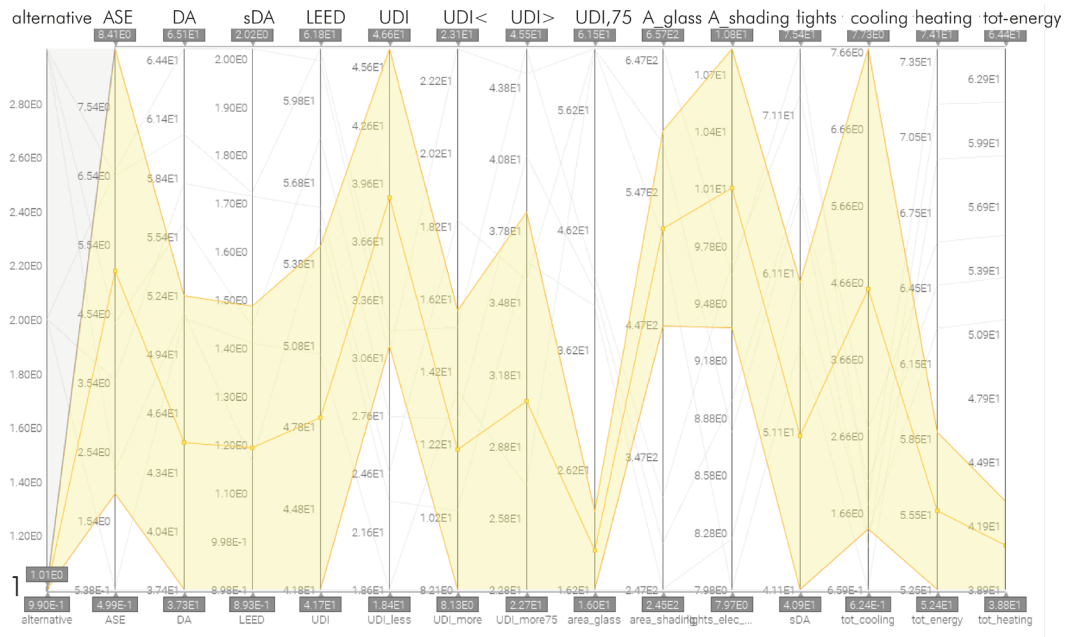


Figure 63 Cluster parallel chart filtering only concept alternative 1

### DAYLIGHT PERFORMANCES

The overlit conditions (high UDI,overlit values) occur whenever the scaling factor is high and it is combined with a low depth of the shading system. On the other hand, when the shading system depth is bigger and the scaling factor smaller, the percentage of UDI underlit raises. The best conditions occur when the scaling factor is bigger than 0.4 and the shading system depth is bigger than 60 cm up to 2.6 m. The underlit conditions are not very present in this case, since the main opening is on the outside, top part, more light from multiple angles

can reach the shading and get bounced to the inside without too much direct radiation (low ASE).

## ENERGY PERFORMANCES

Results indicate that the cooling demand of the building is relatively higher with the application of alternative 1 compared to the other alternatives. Alternative 1 become wider going upwards. This shape facilitates the indoor space to receive the solar radiation from multiple directions. This is a key factor in increasing the cooling demand.

The graph below (*Figure 64*) indicates that the opening ratio and depth of the shading module have a major influence on the heating demand. For small scaling factors, the depth of the shading does not cause any change in the energy consumption, since the heat losses and heat gain are very small. At the point that the whole building acts almost as a closed box.

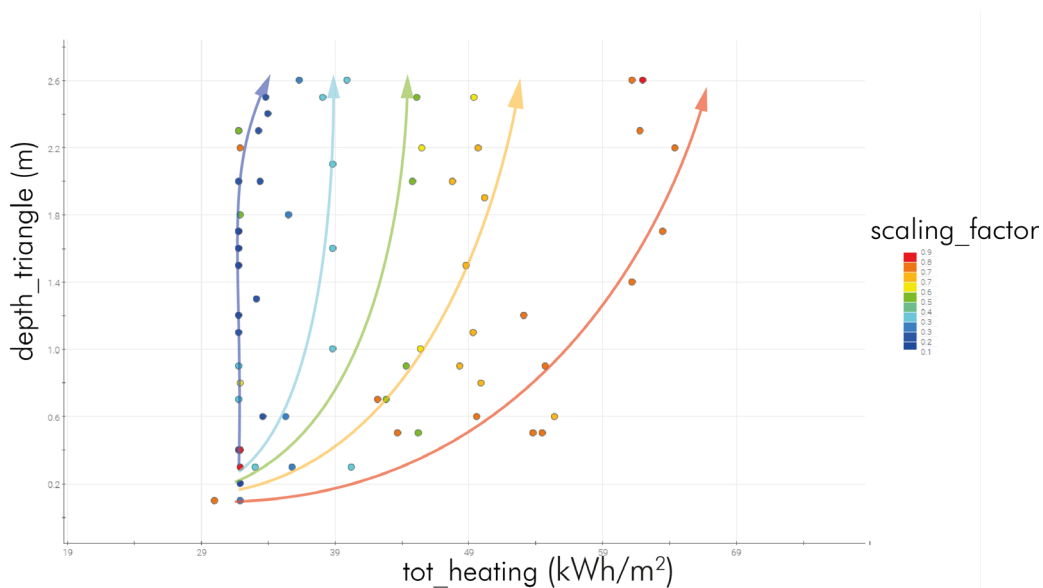


**Figure 64** CDE \_ Bubble chart alternative 1 \_ relation between energy demand, module depth and scaling factor

However, when the scaling factor is bigger and consequently the percentage of glass higher, the depth has a significant impact on the final heating energy consumption. Large opening ratios are likely to show more heat losses through the glass. Though, a small depth enables sufficient heat gain to keep the total heating demand low. While, a higher depth creates more shading reducing the heat gains and therefore increasing the heating energy consumption.

### 4.3.2 ALTERNATIVE 2

To sum up the main performances of alternative 2 (Figure 65):

- Performs very well in sDA, DA, ASE, underlit percentage. In reducing the light energy and the cooling energy
- Performs relatively good in UDI and UDI,75
- Performs relatively bad in UDI\_overlit
- Performs very bad in reducing the glazing and shading area, and in reducing the heating and total energy

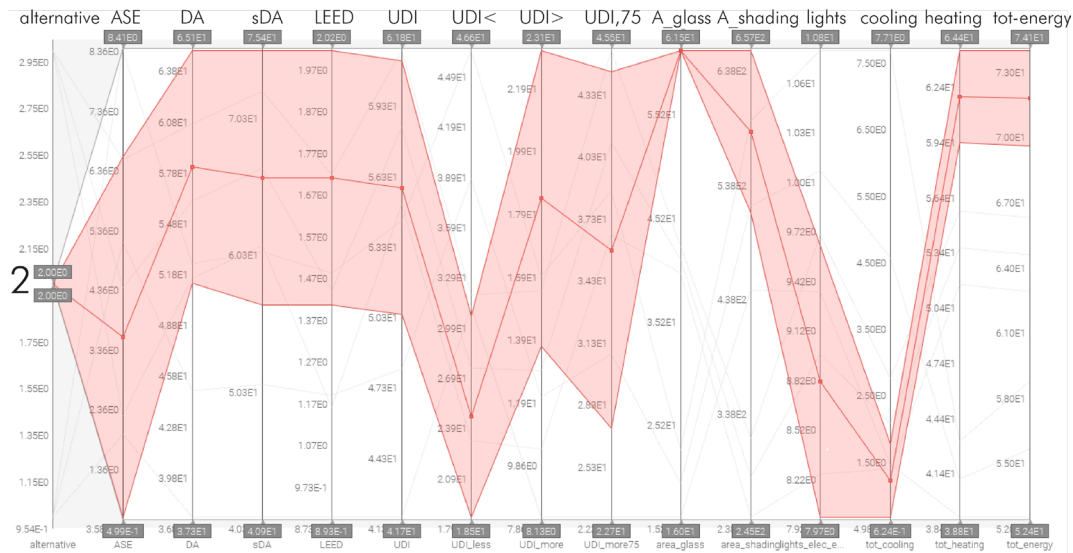
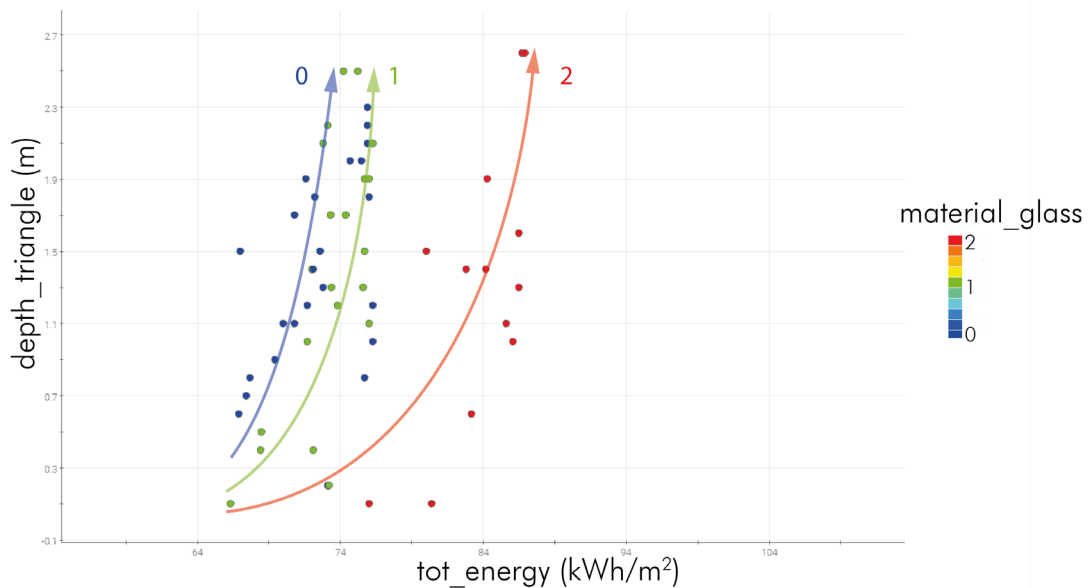


Figure 65 Cluster parallel chart filtering only concept alternative 2

#### DAYLIGHT PERFORMANCES

When the inputs variables of alternative 2 are set to a medium scaling factor, alternative 2 allows to reach highest UDI values in the building. This configuration enable the reduction of the percentage of area during the year with insufficient amount of daylight. However, glare can be an issue if the geometrical properties are not properly chosen. In fact more direct light is allowed in the indoor space. While for alternative 1 the sun rays entering skylights are in large part reflected from the internal surfaces of the shading modules, for alternative 2 the light entering the alcove is mainly not reflected from the lateral surfaces, reaching in a more direct way the bottom glass and producing overlit conditions.

## ENERGY PERFORMANCES



**Figure 66** CDE \_ Bubble chart alternative 2 \_ relation between energy demand, shading module depth and glass material

The glass material and depth of alternative 2 are important driving factors of the final energy consumption. Alternative 2, is characterized by a smaller opening area on the top part, which blocks most of the direct radiation to enter the roof shading system and reach the indoor space. Moreover, the lateral surfaces create a self-shading structure reducing the heat load inside the building. Consequently, the heating energy demand needed is higher compared to Alternative 1 and 3. What is striking in the bubble chart of **Figure 66** is the slow growth of energy demand with the growing of the shading system depth.

The area of glazing in alternative 2 does not vary, since the scaling factor operates on the top triangle and not on the alcove base. Therefore, the typology of glass adopted for the skylights plays an important role in the final energy. What is striking in the bubble chart in **Figure 60** is the variability of the energy performance caused by the different glass typologies. Glazing with higher U-values are expected to perform better during summer, while during winter the heat losses are high. The building is located in the Netherlands, therefore the cold seasons are predominant and the heating results more determinant for the final energy consumption. In this specific building configuration a low U-value (1.0 W/m²K) is preferred, reducing the heat losses during the winter months.



### 4.3.3 ALTERNATIVE 3

To sum up the main performances of alternative 3 (*Figure 67*):

- Performs very well in UDI, UDI,75 and area shading
- Performs relatively good in sDA, DA, in reducing ASE, in underlit and overlit percentage, in reducing the light energy needed and the cooling load
- Performs relatively bad in reducing the glazing area, the heating and total energy demand

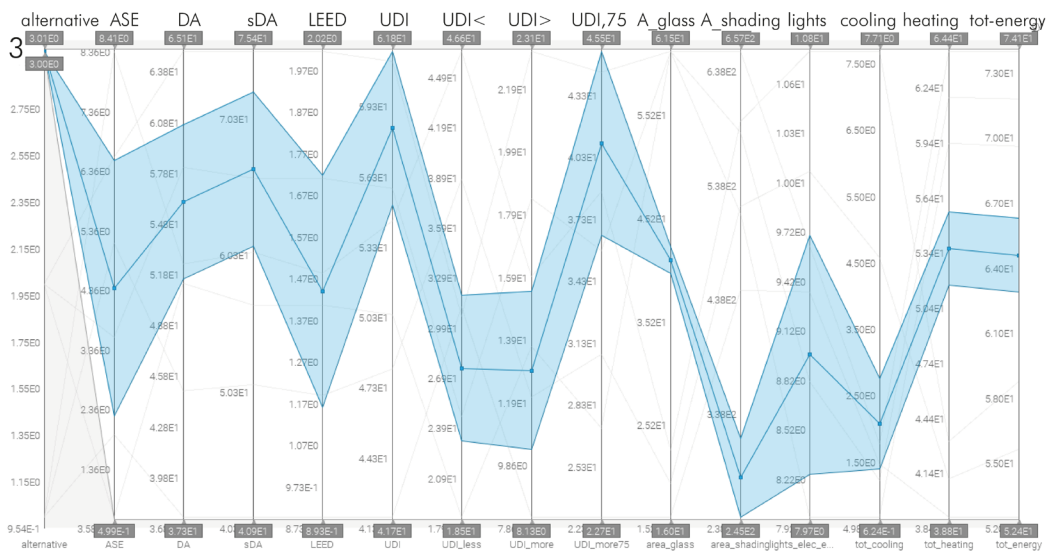


**Figure 67** Cluster parallel chart filtering only concept alternative 3

### DAYLIGHT PERFORMANCES

Alternative 3 can be directed and inclined as wished, therefore it is possible to shield the direct light and reduce glare probability. Hence, it is also possible to maximize the UDI. Alternative 3 has potential if the right setting is used:

From the CDE it is quite hard to read a clear trend, however more settings are showed to lead to good UDI performances:

- South, slightly inclined towards east, combined with high depths of the shading system and small opening ratios: this inclination receives sun rays from more directions, however this can lead to high

levels of Overlit area, especially if the shading depth is low and the opening ratio very big. High shading and small opening mainly create a self-shading system, providing a better daylight control

- Almost vertical shading combined with Medium to high shading depths and medium to small opening ratio: in this case to avoid the direct summer radiations is desired a deep shading system and small opening ratio
- North- slightly west inclination, low depth and big opening ratio: this inclination blocks direct rays and they bounce inside the alcoves. Yet, a lot of daylight is still allowed inside the building by cause of the big openings and small depths.

What stands out is that the optimal solutions, in terms of visual comfort, are never completely facing the East direction, possibly to avoid the low angles of the morning lights and the deriving glare risk. ( $0.2 < \text{inclin}_x < 0.6$ ).

### ENERGY PERFORMANCES

Alternative 3 performs relatively worse regarding heating and total energy consumption compared to alternative 1, while relatively better than alternative 2.

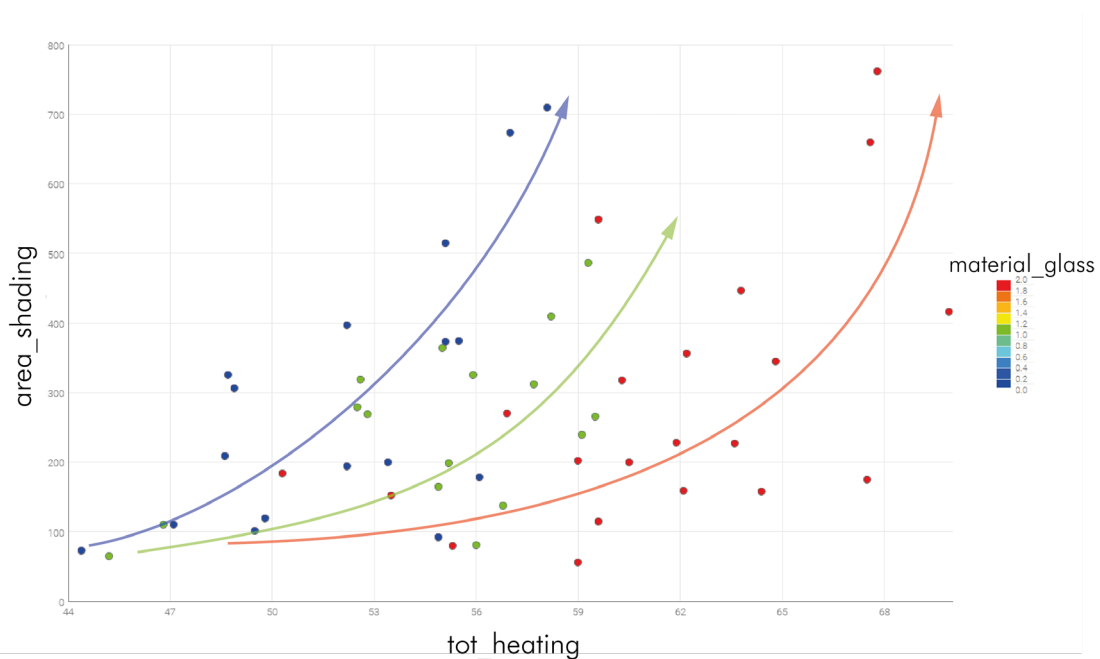


**Figure 68** CDE \_ Bubble chart alternative 3 \_ relation between heating energy, shading area and glass material

The shading area, glazing area and the glass material affect the rate of the energy needed for the thermal comfort of the building. The highest the depth of the modules, the bigger the shading area. **Figure 68** reveals that there has been a gradual increase of the heating demand with the rise of the shading area. This is due to the fact that bigger alcoves surfaces can give rise to low heat gains, which leads to higher heating energy consumption. Low heating demand are also a consequence of smaller opening ratios, reducing the heat losses through the skylights (see **Figure 69**).

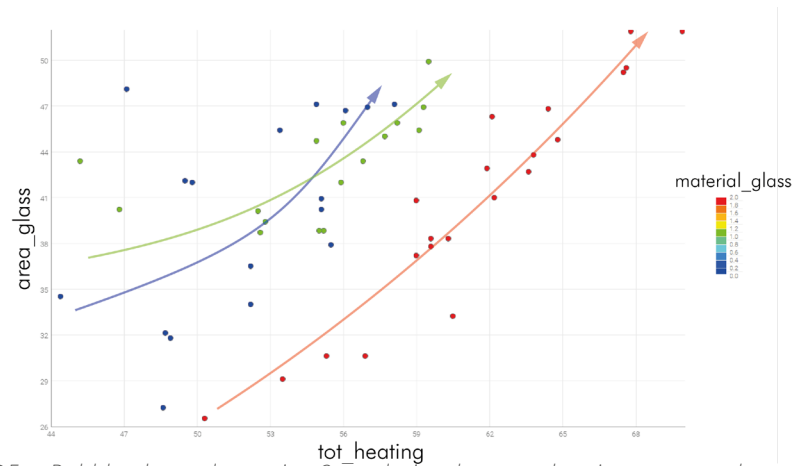


**Figure 69** CDE \_ Bubble chart alternative 3 \_ relation between heating energy, glass area and glass material

## 4.4 ALTERNATIVES COMPARISON

A multi-criteria analysis was adopted to evaluate each alternative and support the decision-making (*Table 11*). To assess each criteria based on the desired outcomes, a grading system has been created in which scores are in the range from 4 to 1:

- 4 circles represents a very good performance level (4 points)
- 3 circle a good performance level (3 pt)
- 2 circle a relatively good performance level (2 pt)
- 1 circle a relatively bad performance level (1 pt)

WEIGHTED PARTIAL SCORES		ALTERNATIVE 1	ALTERNATIVE 2	ALTERNATIVE 3	WEIGHT
DAYLIGHT PERFORMANCE	DA	3	12	9	3
	ASE	6	12	9	3
	UDI	6	9	12	3
	UDI_less	1	4	3	1
	UDI_overlit	8	4	6	2
	UDI_more75	6	9	12	3
MATERIAL AMOUNT	area_glass	4	1	2	1
	area_shading	2	1	4	1
ENERGY PERFORMANCE	lights_elec_energy	1	4	3	1
	tot_cooling	4	8	6	2
	tot_heating	12	3	6	3
	tot_energy	12	3	6	3

**Table 11** Multi-criteria analysis table with weighted scores for each criteria

No negative scores have been assigned since all the concept alternatives improves all the performance targets.

To take into account the importance of each objective, a weighting scale was established with range from 3 to 1. The weighted total score are showed in *Table 11* and indicates the overall best option, which leads to more balanced performances. The underweight score are listed in *Table 52* in “Appendix E”. The weights are assigned depending on the relevance of each criteria. In this specific

case weight 3 has been assigned to the targets of the design exploration, which are mainly focused on visual and thermal comfort. The main objectives of this CDE are for daylight: DA, UDI, UDI<sub>overlit</sub>, ASE and UDI<sub>75</sub>. While in terms of thermal comfort the highest weight has been assigned to heating and total energy, since from the simulations has been observed that the heating demand is the one overall mainly effecting the building total energy consumption.

It is important to consider that the weights have been assigned according to this specific case. The weighting scale can change based on the objectives. Giving more priority and importance to different criteria, the outcome can change, influencing the final concept selection.

Finally, the sum of the total points reveal which alternatives is the best performing and which alternative performs better in the different field (*Table 12*):

WEIGHTED SCORES	weighted tot score	weighted daylight score	weighted material/cost score	weighted energy score
alternative 1	65	30	6	29
alternative 2	70	50	2	18
alternative 3	78	51	6	21

**Table 12** Weighted scores total score for each alternative and partial for each performance

As a conclusion it is possible to interpret the scores and summarize the relative performances.

In general alternative 1 performs very well in the energy demands, reducing the consumption and very good in terms of cost, reducing the amount most expensive material, the glazing of the skylights. It reaches good efficiency reducing the overlit percentage and so the glare probability. However, its performances are relatively bad in terms of daylight quality and visual comfort.

Alternative 2 performs very well achieving high daylighting targets, accordingly the lights energy need is very low. On the other hand, it does perform relatively bad reducing the overlit percentage and extremely bad in reducing the heat losses, and therefore the total amount of energy demand.

In general alternative 3 performs on average on all the three sectors (daylight performance, material amount and energy performance). Slightly better in daylight and slightly worse in heating and total energy reduction.

Based on the knowledge extracted, the new alternative 4 is the combination of the best performing features of alternative 1 and 2 (Figure 70 and Figure 71). Contrary to the hypothesis, alternative 1 was expected to perform better in the daylight aspect. From the result, alternative 1 performs very good reducing the energy demands. This is probably due to the smaller percentage of glass achievable with a small bottom open ratio. So the roof is subject to less heat losses. While Alternative 3 is chosen for its performances in terms of daylight performances and for the capability of reducing the materials amount, which also mean more possibilities to control the final cost of the shading system. As performing feature the inclination on the x and y direction is chosen for the influence in controlling the quantity and quality of light entering the building. The resulting concept alternative 4 is a three-dimensional triangular alcove with a double inclination on the u and v directions, with the triangular base that can be scaled down, reducing the opening ratio.

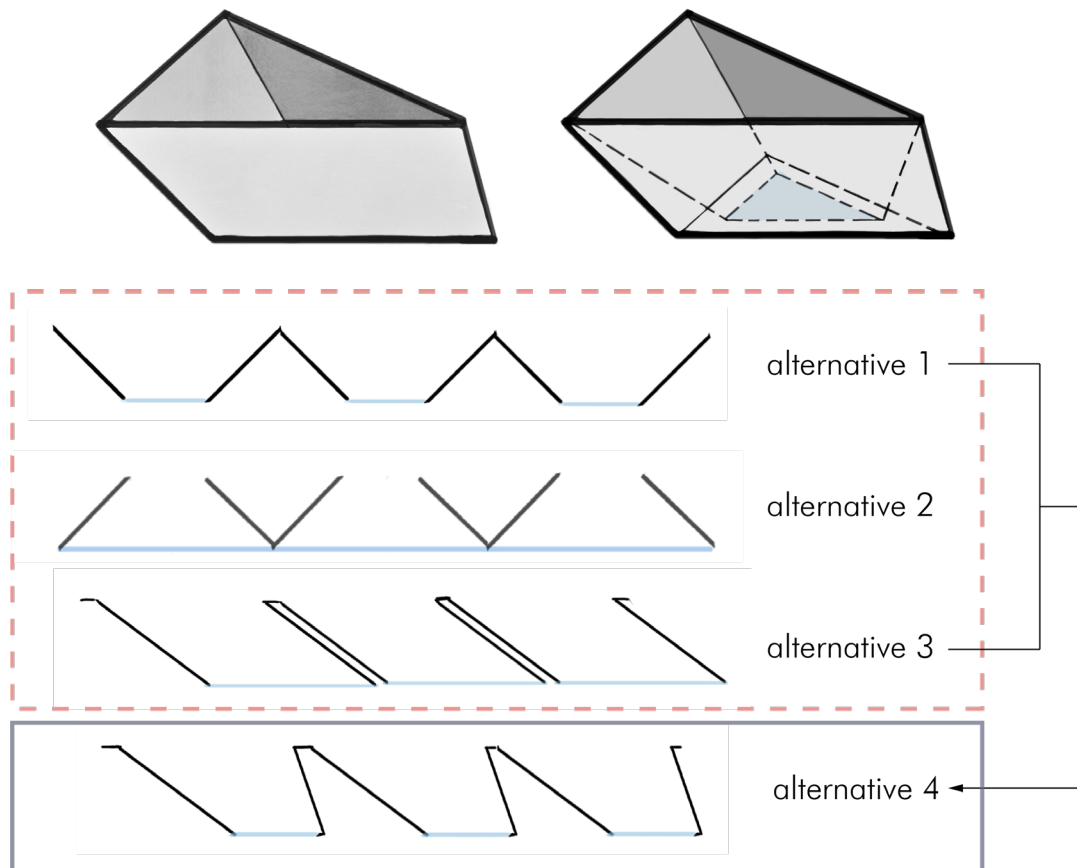


**Figure 70** Section view of the three initial concept alternatives for CDE (1-3) and final optimal alternative concept 4

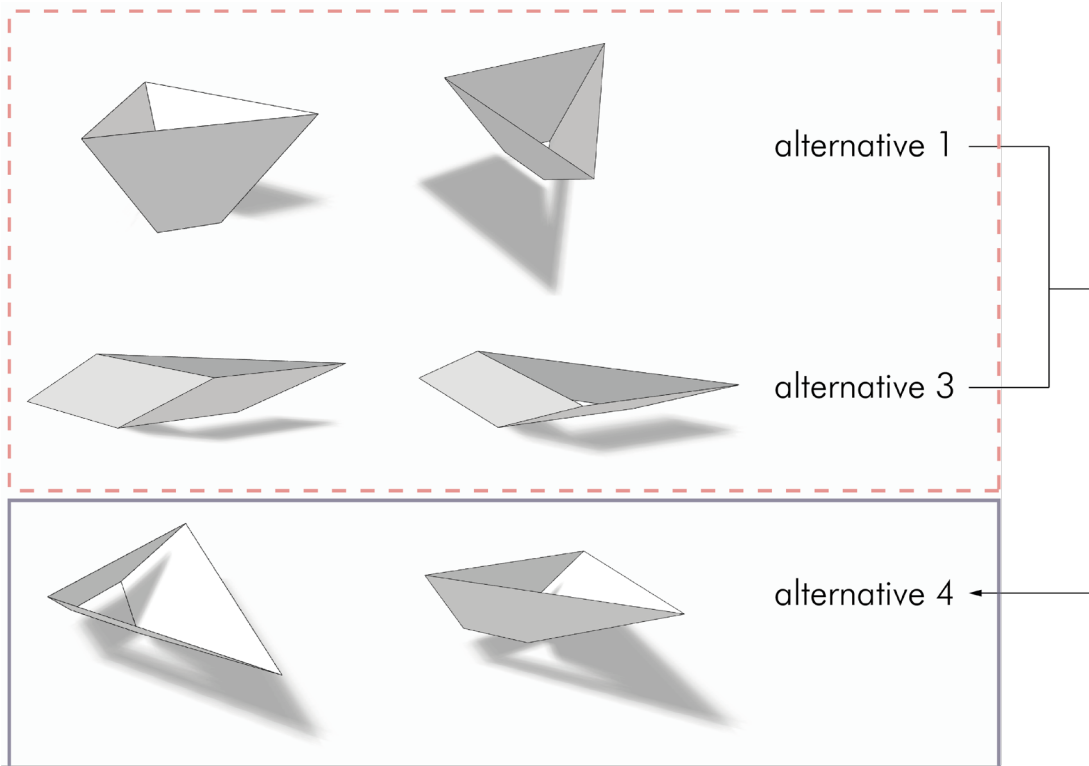


**Figure 71** 3D view of the three initial concept alternatives for CDE (1-3) and final optimal concept alternative 4







05

---



## 5.1 SCHIPHOL TERMINAL

### 5.1.1 BUILDING FEATURES

The case study for this research is the new Amsterdam Airport Schiphol Terminal (*Figure 72*), which is a project led by KL AIR, which is the collaboration between KAAAN Architecten, Estudio Lamela, ABT and Ineco, with the partnerships of Arnout Meijer Studio, DGMR and Planeground. The location of the building is Jan Dellaert Square (*Figure 73*), on the south side of Schiphol Plaza. The new Terminal project is still ongoing. It started in 2017 and will be completed in 2023.



**Figure 72** Render of the Terminal, front view. Source: ©KAAAN Architecten

The new Amsterdam Schiphol Airport is used as case study for this research. Schiphol Airport New Terminal is conceived to be a large space with a significant and engaging long span roof. The building will represent an example of minimalistic architecture, consists of a single open space zone, with a transparent facade about 20 meters high, held up by steel structures. The large span roof consists of modular skylights, with a three dimensional trapezoidal shape. Thanks to the roof openings together with the lateral curtain walls, the passenger has both view to the outside space and to the Dutch sky.

This project has been chosen not only as example of large space, but also because it represents an interesting case study in this research as it already integrates a roof shading system. The roof alcoves add an extreme value to the building. The lighting alternative is developed from A. Meijer with the purpose of

recreate the perception when standing under the Dutch sky.

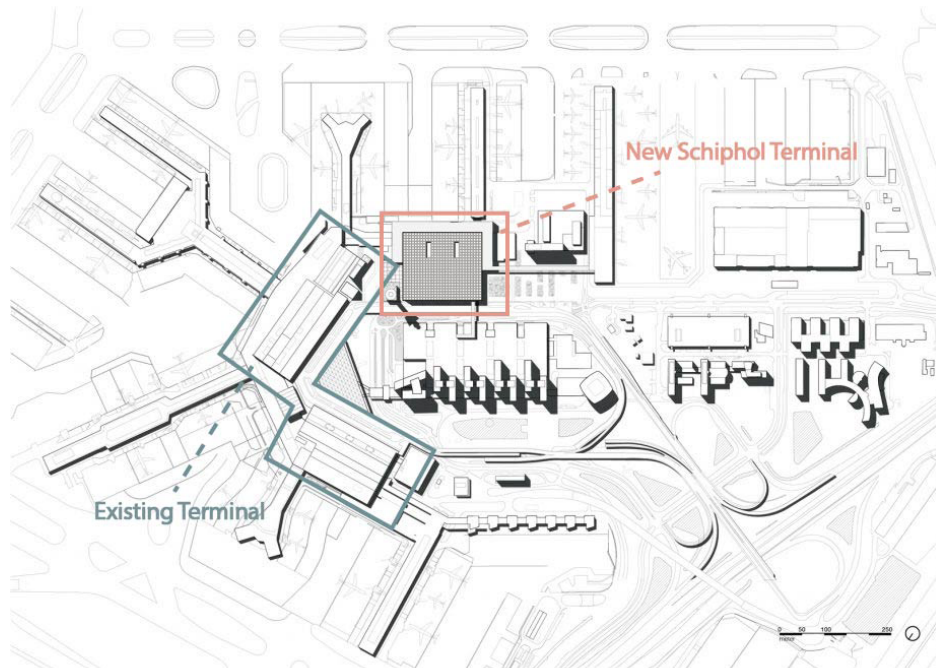


**Figure 73** Top view of the New Schiphol Terminal. Source: ©KAAN Architecten

## 5.1.2 MODEL FOR PERFORMANCE SIMULATION

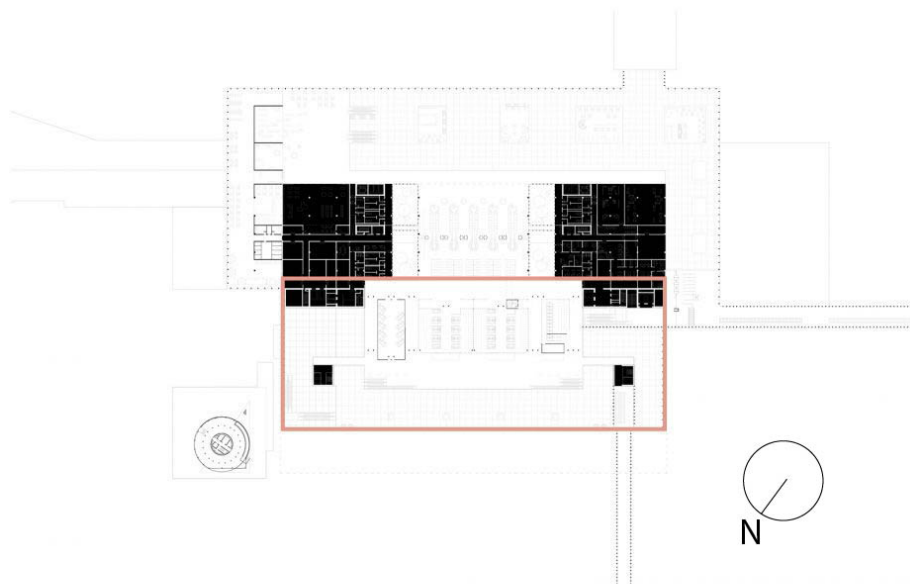


**Figure 74** Terminal floor plan with highlight of the space considered for the simulation. Source: ©KAAN Architecten

In order to reduce the complexity of the calculation without too many differentiations between the numerous spaces of the project, the zone

considered is the area including check-in and departure, which is the one showed in *Figure 74* and *Figure 75*.

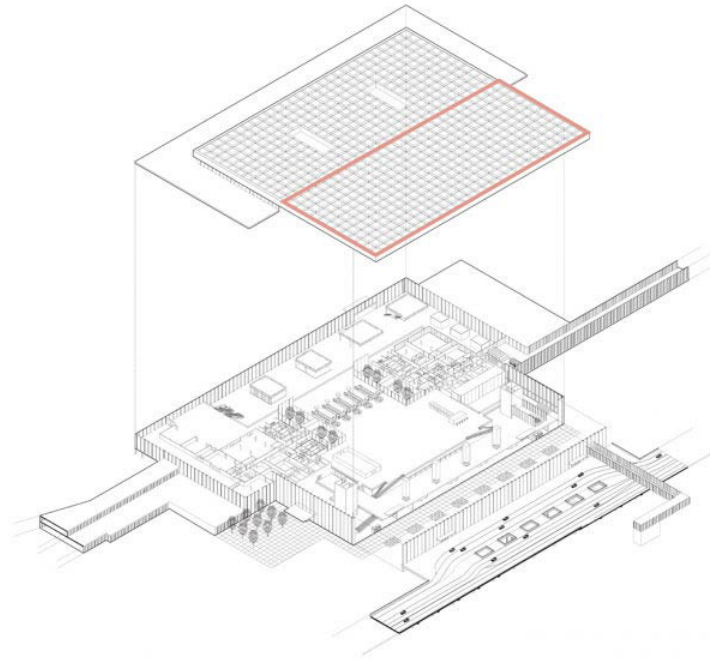


**Figure 75** Exploded view of the Terminal and highlight of the space considered for the optimization.  
Source: ©KAAN Architecten

The lighting design is interrupted in the middle area. The building has been simplified in order to obtain a simple thermal zone and to have more clear results. The portion of the space considered has dimensions  $63.2 \times 111 \times 20$  m, as displayed in *Figure 76*.

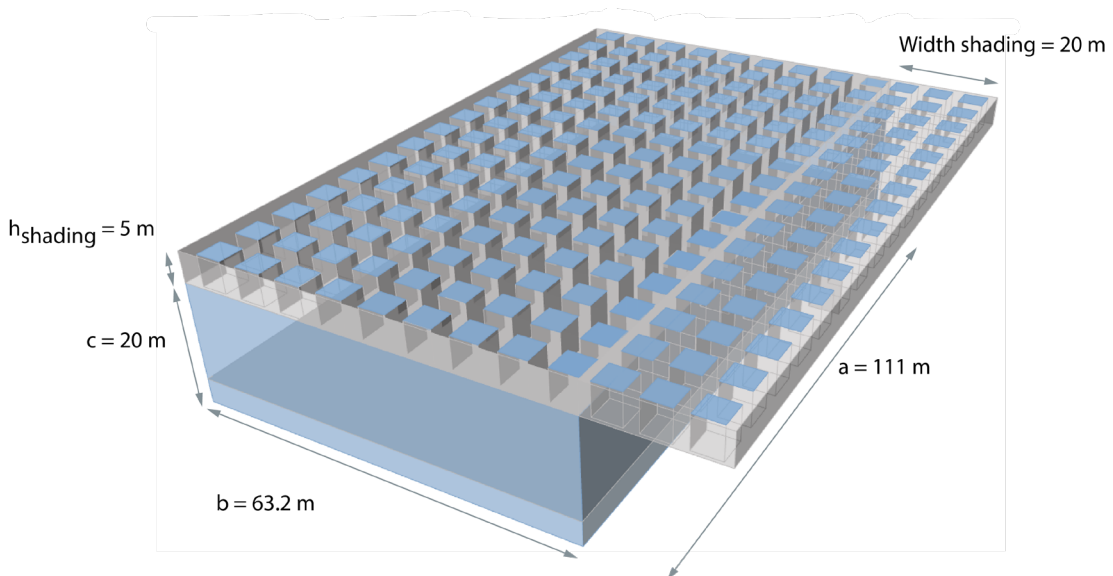


**Figure 76** Dimensions of the analysed space

To reduce the computational time, the model is scaled down by a factor of four, resulting with the dimensions presented in *Figure 77*.

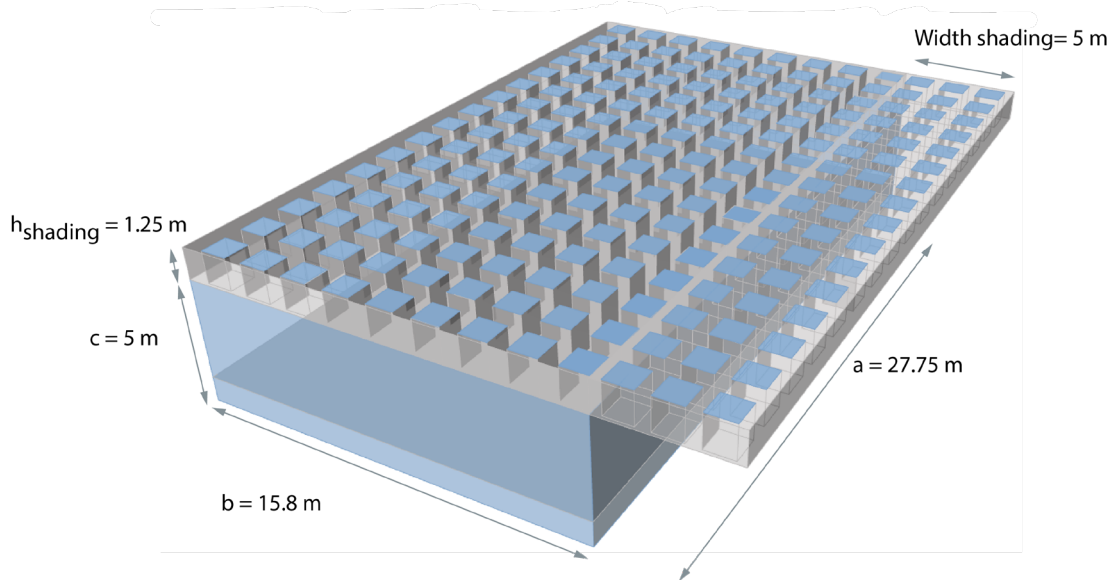


**Figure 77** Dimension of the area considered scaled down four times. Model used for computational workflow.

### 5.1.3 ROOF LIGHTING DESIGN



**Figure 78** Render of the main entrance of the Terminal. Source: ©KAAN Architecten

The roof of the model used for the computational optimization is based on the real project (*Figure 78*). It is a modular system characterized by 12\*16 assembled elements, with a total of 192 alcoves. Each skylight is represented in and has a height of 5 meters (scaled down to 1.25m) and a squared base of 4.2 \* 4.2 meters (scaled down to 1.05\*1.05 m) (*Figure 79*). Moreover, each area of the building has an assigned function and consequently specific daylighting targets.

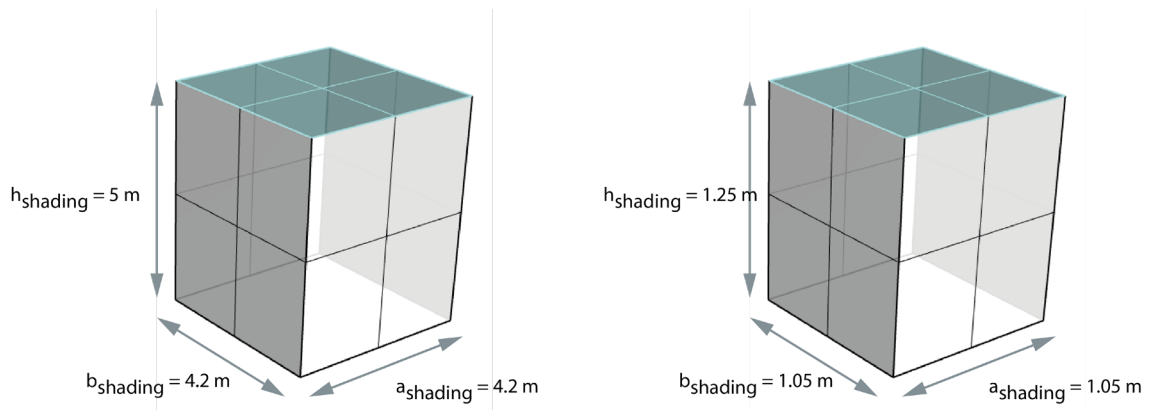


**Figure 79** Original and scaled dimensions of the roof shading module

Since the project is still in the early design stage, building materials are not yet fully defined. Furthermore, many aspects are still confidential. The materials used for the daylight simulation are a white ceiling panels, as finishing material of the shading module, and a skylight glazing with average total transmittance equal to 0.6.

## 5.2 CDO WORKFLOW

The established Computational Design Optimization for the case study is divided into two sections, which represent different optimizations. Two variations are chosen to ensure the effectiveness of the workflow. The purpose of having two variations is to show how the optimization process operates and how for each case the outcome is different. An overview of the workflow for the variations is presented in *Figure 80* and *Figure 81*.

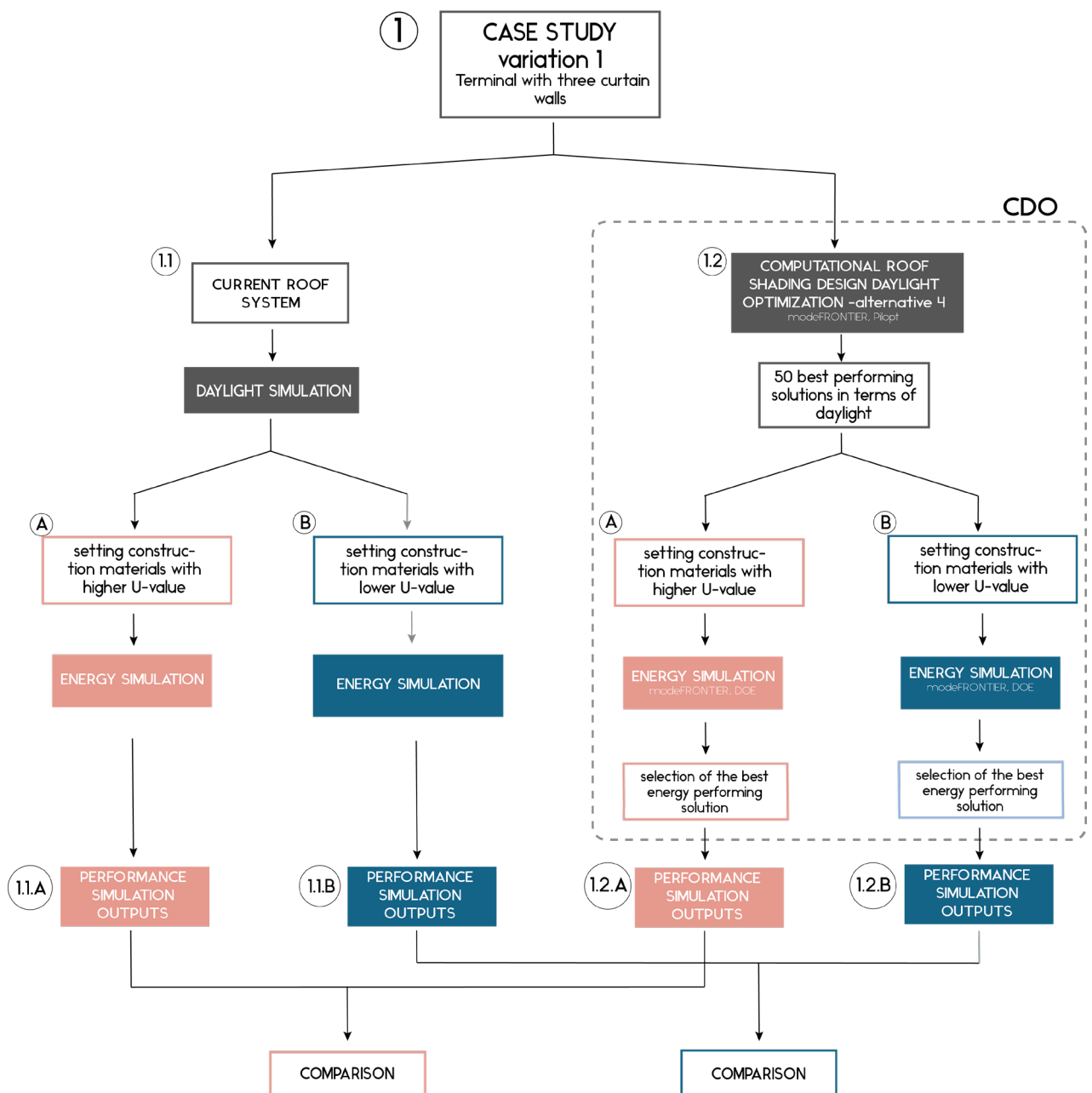


**Figure 80** Workflow part 1 - case study variation 1 \_ three curtain walls

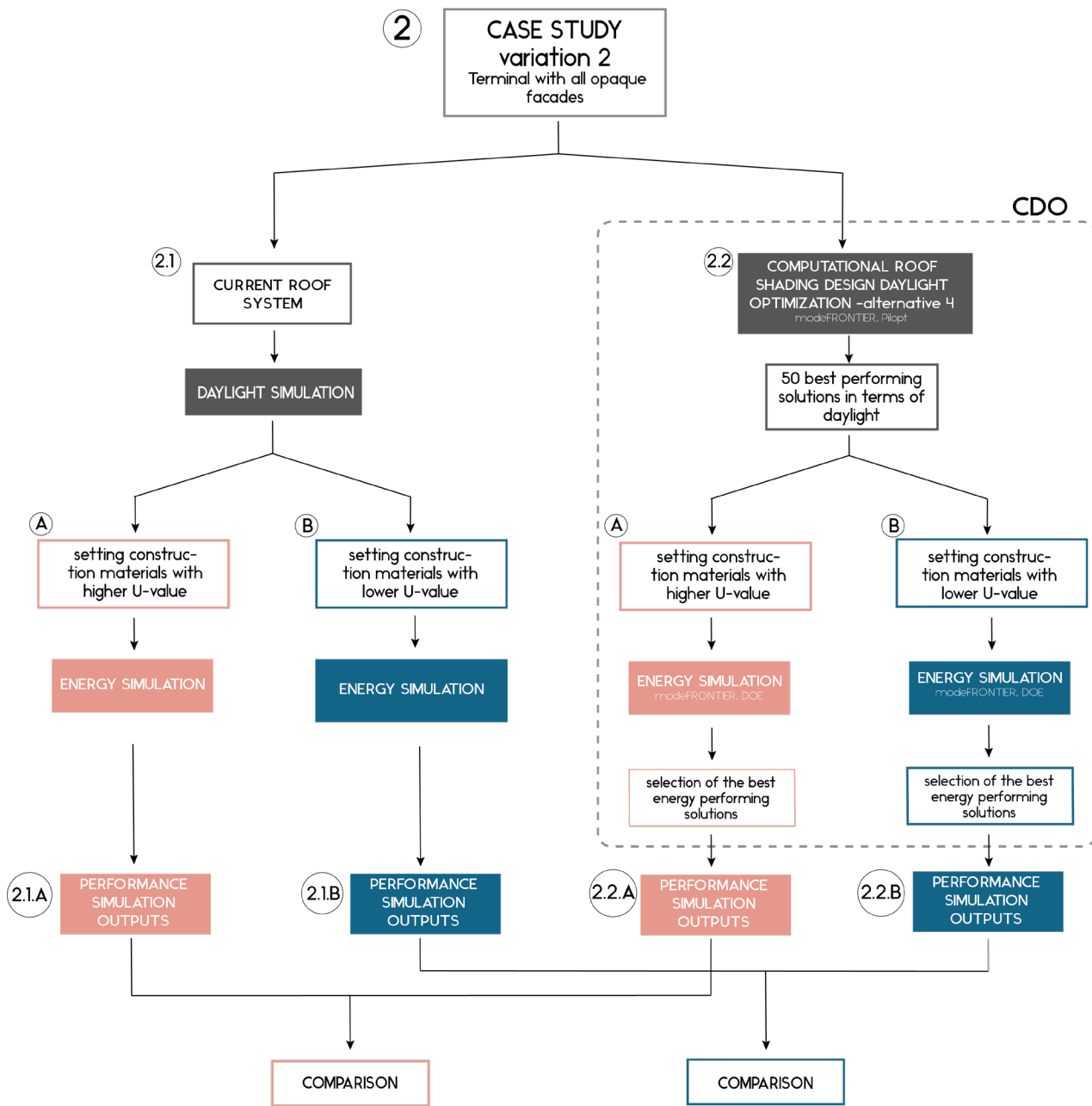
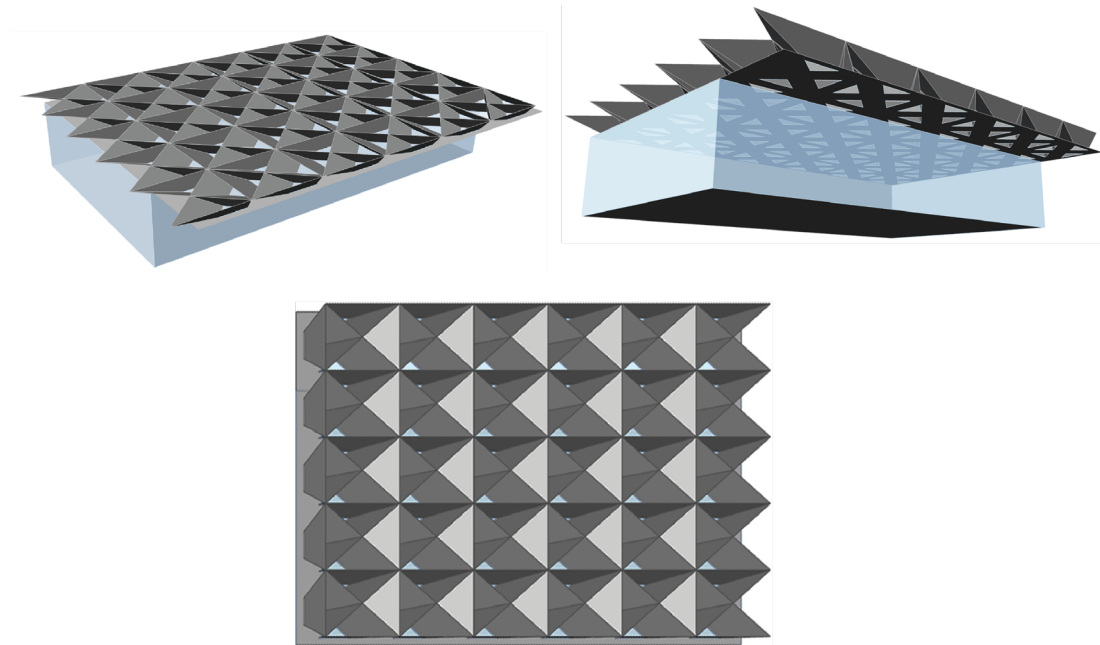


Figure 81 Workflow part 2 - case study variation 2 \_ opaque walls

The versatility is also the strength of this computational process. The aim is to find a method which is adaptable to various situations and performance problems.

Variation 1 of the Case Study evaluates the building with 3 curtain walls and one opaque facade. For variation 2 of the case study, the New Schiphol Terminal design is assessed with all four façades opaque, substituting the curtain walls with fully opaque construction materials.

Both variations are evaluated with the current roof system (1.1, 2.1) (see *Figure 80*) and with the 50 best performing solutions in terms of daylight, that resulted from the roof computational design optimization of the roof shading system composed by the arrangement of alternative 4 as an array of modules (1.2, 2.2) (see *Figure 81*).



**Figure 82** Example of alternative concept 4 applied to New Schiphol Terminal. Prospective views and top view

For both variations and roof systems, building materials with lower (*A*) and higher U-values are modelled (*B*) and plotted. After, the energy simulations are performed. The outcomes of the current roof system are compared with the outcomes of the best solutions in terms of energy performance for both variations of the case study. An example of alternative concept 4 applied to the building is showed in *Figure 82*.

The approach of slicing the process in two parts made possible to show the potential of the optimization process developed, and how it enables to seek for an optimal solution by plotting different input data.

The scope of this exploration is mainly focused on shape optimization, however it is essential to keep into consideration how the output varies from case to case and many other external settings influence the outcome. A complete study would require an holistic approach considering both shape and material optimization.

### 5.3 CASE STUDY VARIATION 1

Figure 80 shows the first workflow application, which adopts the New Schiphol Terminal with one opaque wall and three curtain walls, an approximation of the real design.

#### 5.3.1 CURRENT ROOF SHADING SYSTEM

The first part of the workflow consists in performing the daylight and energy performances of the building as it is in the real design. The New Schiphol Terminal is modelled as displayed in Figure 83.

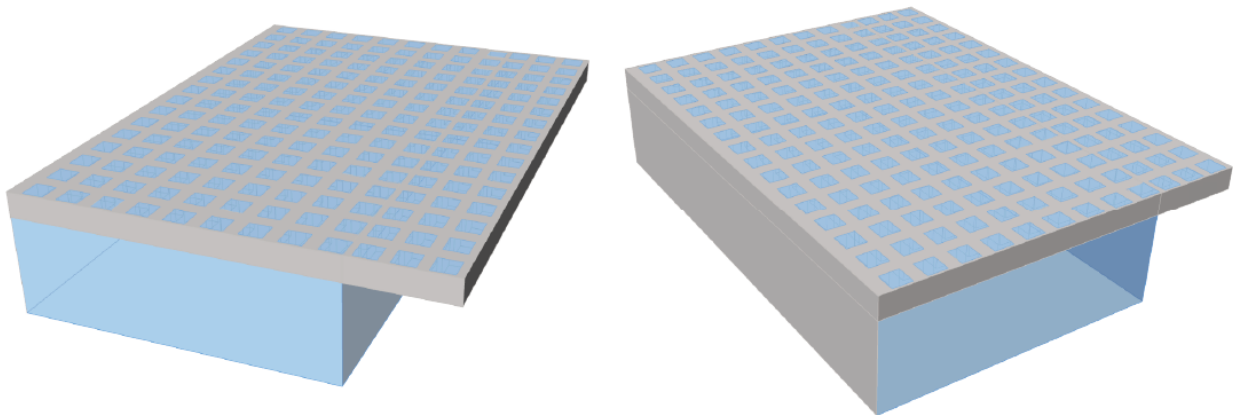


Figure 83 Perspective views of the model of the Terminal - variation 1

The current roof system has the following material amounts (Table 13):

glazing_area (m2)	441.0
shading_area (m2)	1492.9

Table 13 Material areas of the current roof shading system

#### DAYLIGHT SIMULATION 1.1

- INPUTS daylight simulation 1.1

As said before, the materials choice is not yet fully completed. For the analysis, materials are based on some preliminary energy simulations carried out from ABT. The reflectance values of the interior materials, used as input for the daylight

simulation, are the lowest limit of the values suggested the recommendations from the NEN -EN 12646-1 (2011), except for the ceiling, which has a white panel used as finishing material.

To facilitate the multi-objective optimization the requirements for the area considered have been standardized and set up as recommended. The NEN-EN 12646-1 (2011) gives specific lighting requirements for the different zones of terminal airports. In the case of this research the area considered is the check-in and departure, thus the required maintained illuminance  $\bar{E}_m$  on the reference surface. Looking at the requirement for the arrival and departure hall (*Table 14*), the required  $\bar{E}_m$  is equal to 200 lux, while for the check in area is 500 lux. The target has been set at 350 lux, which is the average value between the two different task spaces.

**Table 5.52 – Transportation areas – Airports**

Ref. no.	Type of area, task or activity	$\bar{E}_m$ lx	UGRL –	$U_0$ –	$R_a$ –	Specific requirements
5.52.1	Arrival and departure halls, baggage claim areas	200 lux	22	0.40	80	
5.52.2	Connecting areas	150 lux	22	0.40	80	
5.52.3	Information desks, check-in desks	500 lux	19	0.70	80	DSE-work, see 4.9.
5.52.4	Customs and passport control desks	500 lux	19	0.70	80	Facial recognition has to be provided.

**Table 14** Lighting requirements for interior airports transportation areas. Source: NEN-EN 12464-1:2011 en

For this study, the lighting system considered, is composed mainly by LED lamps. The lighting loads is determined to be around 5 W/m<sup>2</sup>.

The daylighting analysis grid is created by elevating the floor surface at 1 meter height. The grid is subdivided in areas with spacing 1 meter from each other. To each sub-area of the grid is assigned a sensor. In total the daylighting analysis grid is composed by 60 sensor points.

The summary of the settings for the daylight simulation of the Terminal - variation 1 are listed in *Table 15*.

INPUT DAYLIGHT SIMULATION variation 1		
location	Amsterdam, Netherlands	fixed
BUILDING GEOMETRIES		
length (a)	27.75 m	fixed
width (b)	15.8 m	fixed
height (c)	5 m	fixed
skylight module height	1.25 m	fixed
DIVA 4 - DAYLIGHT SIMULATIONS		
floor	GenericFloor_20, 20% reflectance	fixed
walls	GenericInteriorWall_50, 50 % reflectance	fixed
curtain wall	Terminal_curtainwall , 60% transmittance	fixed
roof/ceiling	White_ceiling_panels, 89% reflectance	fixed
skylights	Terminal_s skylights, 60% transmittance	fixed

**Table 15** Input daylight simulation \_ step 1.1 of the workflow Case Study variation 1

• **OUTPUTS daylight simulation 1.1**

The results of the daylighting simulation are summarized in *Table 16*. What stands out is the sufficient illuminance levels in the space. It is possible to notice how the *DA* is above the percentage limit of 50% and significant values of *ASE* and *UDI*> emphasize a high percentage of overlit area during the year, with consequent elevated risk of glare.

OUTPUT DAYLIGHT SIMULATION variation 1	
sDA	100%
ASE	42.40%
DA	87.24%
UDI	44.02%
UDI<	6.70%
UDI>	47.77%
UDI,75	0.67%

**Table 16** Output values daylight simulation \_ step 1.1 of the workflow Case Study variation 1

In order to identify the main cause behind these results, the case study was tested by applying a completely closed roof, without any source of daylight coming through the ceiling (see *Figure 84*).

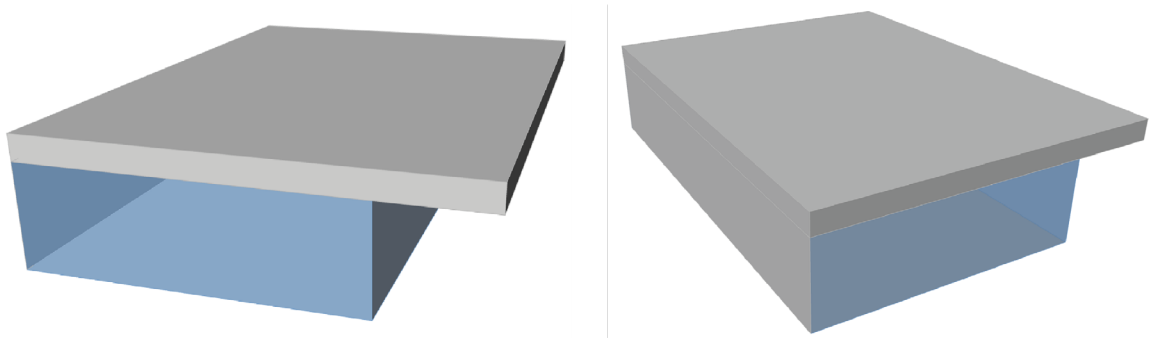


**Figure 84** Perspective views of the model of the case study with three curtain walls and completely opaque roof

From the table below (*Table 17*) we can see that limiting the natural light sources to the curtain walls, the *DA* level decreases from 87% to 79%. The daylight autonomy results to be still quite good. While, there is a significant drop in the percentage of overlit area during the year (*UDI>*), going from almost 48% to 23%.

OUTPUT DAYLIGHT SIMULATION Terminal with closed roof	
sDA	100%
ASE	32.6%
DA	79.57%
UDI	65.81%
UDI<	9.72%
UDI>	22.97%
UDI,75	52.46%

**Table 17** Output values of daylight simulation from Terminal with closed roof

These results revealed how the illuminance allowed inside the space through the curtain walls is by itself already sufficient to ensure good daylighting conditions. The implementation of roof openings improve the daylight autonomy, though with the downside of increasing the exposition to excessive illuminance level, creating uncomfortable visual circumstances.

Hence, it could conceivably be hypothesised that the optimal shape solution for maximizing the indoor visual comfort will lead to a peculiar configuration. It is possible, therefore, that the pareto-front of the daylight optimization for Case Study variation 1 will show relatively small opening ratio and/or rather high shading module depth. The main objective is to attempt to improve the Useful Daylight Illuminance of the space, yet trying to prevent the increase of glare probability.

The model with the three curtain walls is expected to present sub-optimal solutions striving towards a closed roof, because the façades provide already sufficient daylight penetration.

## ENERGY SIMULATIONS

In order to understand how the materials affect the energy demand in building and how this influence the decision-making of the final optimal alternative, a series simulations was performed. The energy simulation typology A consists of the application of less insulating materials (construction materials with higher U-values), on the other hand typology B adopts structural components with lower thermal transmittances (lower U-values).

### ENERGY SIMULATION 1.1.A

- **INPUTS energy simulation 1.1.A**

The energy simulation 1.1.A (see *Figure 80*) of the alternative variation 1 were performed using the following settings (*Table 18*):

INPUT ENERGY SIMULATION		
1.1.A		
ENERGYPLUS		
<b>Loads</b>		
people	0.25 p/m2	fixed
schedule	occ-Terminal	fixed
equipment	5 w/m2	fixed
schedule	occ-Terminal	fixed
lights	4 w/m2	fixed
target	350 lux	fixed
dimming	continuous	fixed
lighting schedule	depends on the daylight simulation	fixed
<b>Conditioning</b>		
heating setpoint	19°C	fixed
heating setback	18°C	fixed
cooling setpoint	24°C	fixed
cooling setback	30°C	fixed
humidity control	OFF	fixed
<b>Conditioning</b>		
Fresh Air	7 L/s/person	fixed
Fresh Air	0.3 L/s/zone area m2	fixed
Schedule	occ-Terminal	fixed
Heat recovery	Sensible	fixed
Sensible recovery ratio	0.7	fixed
Latent recovery ratio	0.65	fixed
Economizer	No Economizer	fixed
<b>Scheduled Ventilation</b>		
Set point	18°C	fixed
Hourly Air Change	0.6 ACH	fixed
Schedule	occ Terminal	fixed
Infiltration	0.2 ACH	fixed
infiltration	0.2 ACH	fixed
natural ventilation	OFF	fixed
<b>Construction</b>		
roof	Roof Terminal - U <sub>value</sub> = 0.27 W/m2K	fixed
floor	Floor Terminal - U <sub>value</sub> = 0.18 W/m2K	fixed
façade	External wall terminal - U <sub>value</sub> = 0.36 W/m2K	fixed
curtain wall	Curtain wall terminal - U <sub>value</sub> = 1.7, SHGF = 0.4, T <sub>vis</sub> = 0.76	fixed
skylights	Skylights terminal - U <sub>value</sub> = 3.37, SGHF = 0.49, T <sub>vis</sub> = 0.76	fixed

**Table 18** Input values energy simulation\_step 1.1.A of the workflow Case Study variation 1. Based on data of the project provided by ABT

• OUTPUTS energy simulation 1.1.A

OUTPUT ENERGY SIMULATION 1.1.A	
people heating	118.20 kWh/m2
lights electric energy	1.41 kWh/m2
infiltration tot heat loss	49.42 kWh/m2
infiltration tot heat gain	0.065 kWh/m2
ideal tot heating energy	173.13 kWh/m2
ideal tot cooling	113.79 kWh/m2
tot energy	288.33 kWh/m2

**Table 19** Output energy simulation \_ step 1.1.A of the workflow Case Study variation 1

Table 19 provides the results of the energy simulation of point 1.1.A (see Figure 80). The total energy consumption appears to be very high and this is mainly due to the elevated heating load. Using materials with greater U-values means a construction less effective as insulator. The heat is transmitted faster from the inside to the outside and vice versa, flowing from a warmer to colder space.

Month	heating 1.1.A [kWh/m2/month]	cooling 1.1.A [kWh/m2/month]
January	33.911111	1.152028
February	27.669167	1.129833
March	21.041944	3.585278
April	10.646111	7.130833
May	4.549722	18.524444
June	1.428639	22.609722
July	0.311556	25.354722
August	0.596333	20.182778
September	3.409167	8.579722
October	11.476944	3.068056
November	24.737222	1.354222
December	33.363889	1.115083
kWh/m2/year	173.14	113.79

**Table 20** Monthly values of energy demand \_ step 1.1.A of the workflow Case Study variation 1

The U-values of setting A lead to better thermal performances during the summer period. This is because during winter the direction of the heat flow is unique and goes from the indoor to the outdoor space. While, during summer

the heat flow fluctuates in both directions (values shown in *Table 20*. As highlighted from the chart below (see *Figure 85*), the total heat loss is greater than the heat gain.

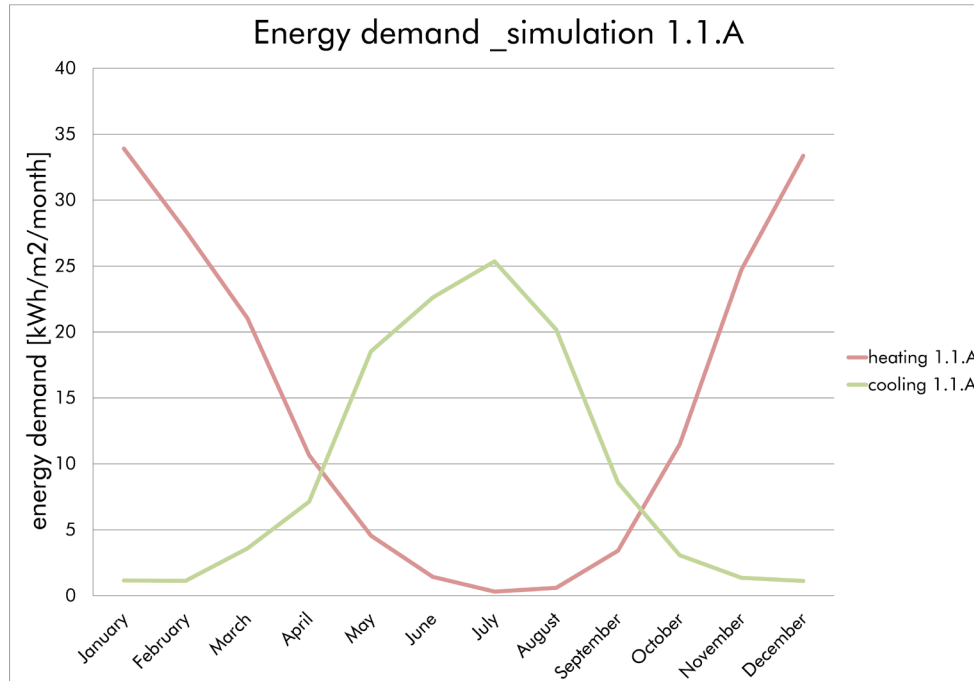


**Figure 85** Line graph of monthly values of energy demand \_ step 1.1.A of the workflow Case Study variation 1

The higher heating energy consumption indicates the need of reducing the heating load. After the computational design daylight optimization the selection of the optimal solution is driven by the aim of reducing the energy consumption. With the use of materials of setting A, with high U-value, this target corresponds mainly to the reduction of the heating energy. However, when the same simulation is carried out, but with more insulating materials (setting B), the heating energy is expected to be lower than the cooling. In this case, when looking into energy consumption it is mainly important to focus on the reduction of the cooling load.

ENERGY SIMULATION 1.1.B

• INPUTS energy simulation 1.1.B

The energy simulation 1.1.B (see *Table 21*) of the alternative variation 1 were performed using the following settings:

INPUT ENERGY SIMULATION 1.1.B		
ENERGYPLUS		
<b>Loads</b>		
people	0.25 p/m2	fixed
schedule	occ-Terminal	fixed
equipment	5 w/m2	fixed
schedule	occ-Terminal	fixed
lights	4 w/m2	fixed
target	350 lux	fixed
dimming	continuous	fixed
lighting schedule	depends on the daylight simulation	fixed
<b>Conditioning</b>		
heating setpoint	19°C	fixed
heating setback	18°C	fixed
cooling setpoint	24°C	fixed
cooling setback	30°C	fixed
humidity control	OFF	fixed
<b>Conditioning</b>		
Fresh Air	7 L/s/person	fixed
Fresh Air	0.3 L/s/zone area m2	fixed
Schedule	occ-Terminal	fixed
Heat recovery	Sensible	fixed
Sensible recovery ratio	0.7	fixed
Latent recovery ratio	0.65	fixed
Economizer	No Economizer	fixed
<b>Scheduled Ventilation</b>		
Set point	18°C	fixed
Hourly Air Change	0.6 ACH	fixed
Schedule	occ Terminal	fixed
Infiltration	0.2 ACH	fixed
infiltration	0.2 ACH	fixed
natural ventilation	OFF	fixed
<b>Construction</b>		
roof	Roof Terminal - $U_{value} = 0.16$ W/m2K	fixed
floor	Floor Terminal - adiabatic - $U_{value} = 0.18$ W/m2K	fixed
façade	External wall terminal - $U_{value} = 0.21$ W/m2K	fixed
curtain wall	Curtain wall terminal - $U_{value} = 1.0$ , SHGF = 0.34, $T_{vis} = 0.6$	fixed
skylights	Skylights terminal - $U_{value} = 1.0$ , SHGF = 0.34, $T_{vis} = 0.6$	fixed

**Table 21** Input values energy simulation \_ step 1.1.B of the workflow Case Study variation 1. Based on data of the project provided by ABT

• OUTPUTS energy simulation 1.1.B

OUTPUT ENERGY SIMULATION 1.1.B	
people heating	118.20 kWh/m <sup>2</sup>
lights electric energy	1.46 kWh/m <sup>2</sup>
infiltration tot heat loss	53.05 kWh/m <sup>2</sup>
infiltration tot heat gain	0.062 kWh/m <sup>2</sup>
ideal tot heating energy	57.05 kWh/m <sup>2</sup>
ideal tot cooling	124.69 kWh/m <sup>2</sup>
tot energy	183.20 kWh/m <sup>2</sup>

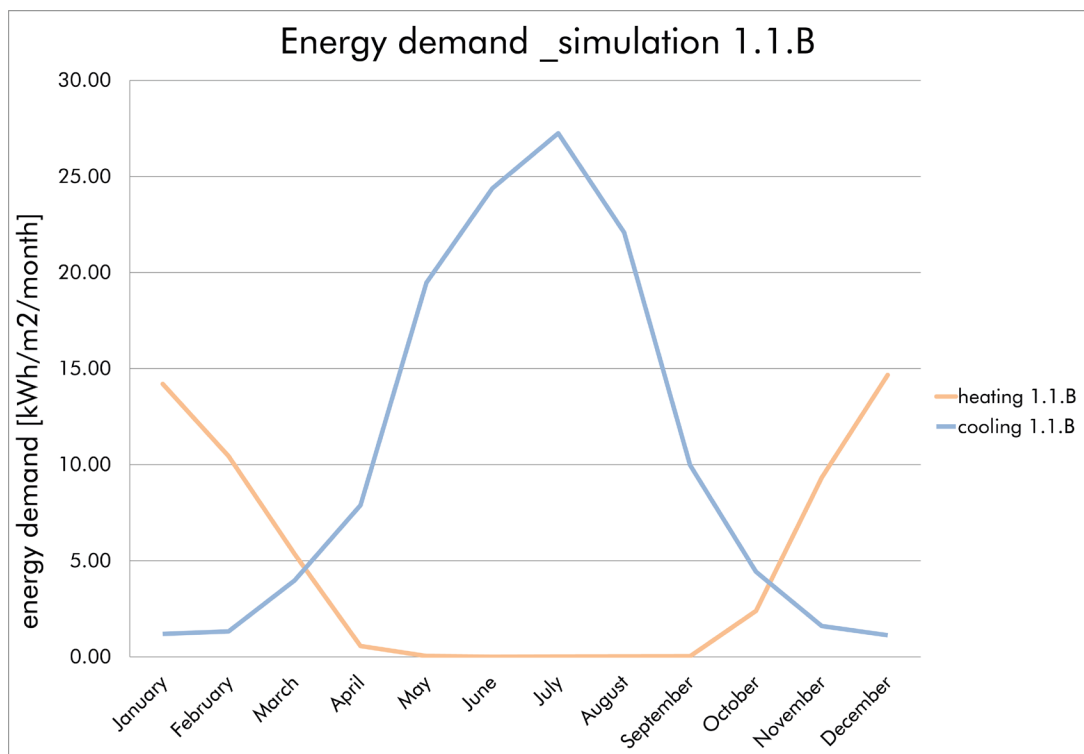
**Table 22** Output values energy simulation \_ step 1.1.B of the workflow Case Study variation 1

Table 22 provides the results of the energy simulation of point 1.1.B (see *Figure 80*). The total energy consumption is relatively lower to the output simulation 1.1.A. Using materials with lower U-values means a construction more effective as insulator. The heat is transmitted slower from the inside to the outside (*Table 23*).

Month	heating 1.1.B [kWh/m <sup>2</sup> /month]	cooling 1.1.B [kWh/m <sup>2</sup> /month]
January	14.20	1.19
February	10.44	1.33
March	5.36	3.97
April	0.56	7.89
May	0.04	19.47
June	0.00	24.38
July	0.01	27.25
August	0.02	22.08
September	0.03	9.98
October	2.39	4.43
November	9.33	1.60
December	14.66	1.12
kWh/m <sup>2</sup> /year	57.05	124.68

**Table 23** Monthly values of energy demand \_ step 1.1.B of the workflow Case Study variation 1

In case of alternative variation 1, composed of a high percentage of glazing, due to the presence of three curtain walls, the adoption of better insulating material (setting *B*) leads to greater cooling demand rather than heating. In fact the amount of heating load is reduced due to the lower U-values of the construction materials. From the data of *Table 23*, we can see that the output of energy simulation 1.1.B resulted in a heating demand about three times lower than the one with setting A. On the other hand, it can be detected a slight increase in the cooling consumption.



**Figure 86** Line graph of monthly values of energy demand \_ step 1.1.B of the workflow Case Study variation 1

As showed in graph *Figure 86*, the summer period is the season in which most energy is consumed, due the high glazing area and the good insulating performances of the construction materials. As mentioned previously, the heat during the warm periods fluctuates in both directions, from the inside to the outside and vice versa. Therefore, it is expected similar performance during the summer period for both settings A and B, while different outcomes during the cold season can be predicted. As opposite to the setting A (see *Figure 87*), this means that when looking at the energy goal, after performing the daylight computational optimization, the reduction of the total energy demand corresponds mainly to the reduction of the cooling energy.

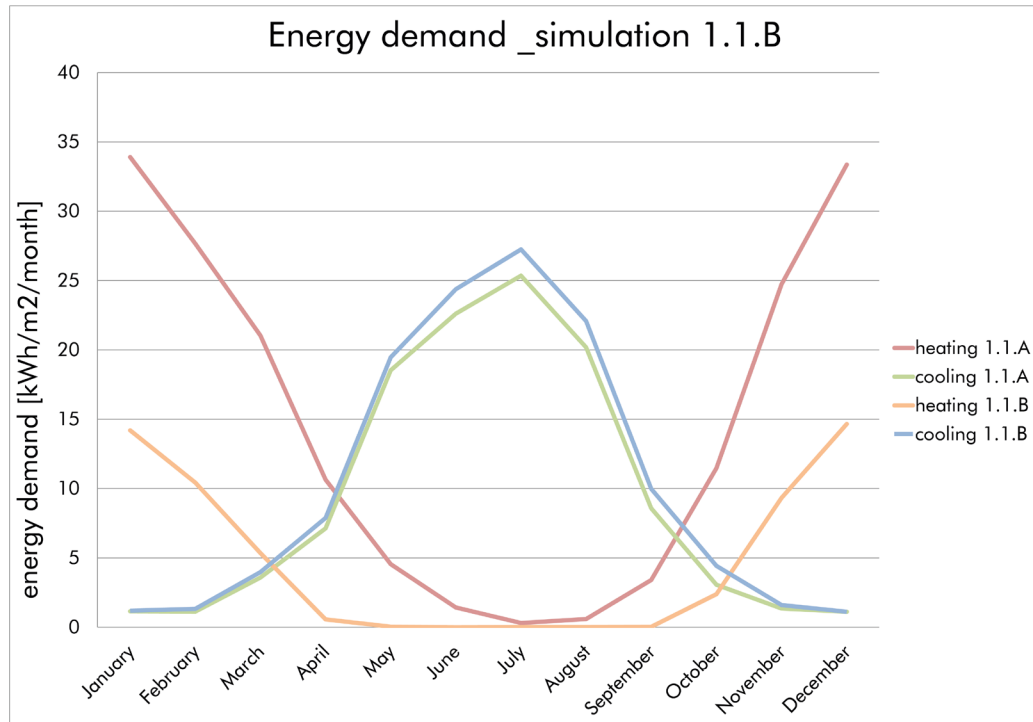


**Figure 87** Line graph of monthly values of energy demand \_ step 1.1.A and 1.1.B of the workflow Case Study variation 1

## 5.3.2 ROOF SHADING OPTIMIZATION

### DAYLIGHT OPTIMIZATION 1.2

- INPUTS daylight optimization 1.2

The settings of the daylight optimization of Case Study variation 1 (with three curtain walls) are listed in *Table 24*.

INPUT DAYLIGHT computational design optimization 1.2		
location	Amsterdam, Netherlands	fixed
BUILDING GEOMETRIES		
length (a)	27.75 m	fixed
width (b)	15.8 m	fixed
height (c)	5 m	fixed
skylight module height	0.6-1.5m	variable
DIVA 4 - DAYLIGHT SIMULATIONS		
floor	GenericFloor_20, 20% reflectance	fixed
walls	GenericInteriorWall_50, 50 % reflectance	fixed
curtain wall	Terminal_curtainwall , 60% transmittance	fixed
roof/ceiling	White_ceiling_panels, 89% reflectance	fixed
skylights	0 - SGG PLANITHERM ONE, 70% transmittance	variable
	1 - SGG COOL-LITE SKN 154, 50% transmittance	
	2 - SGG COOL-LITE KNT 140, 37% transmittance	

**Table 24** Settings for computational design optimization \_ step 1.2 of the workflow Case Study variation 1

The optimization is performed through modeFRONTIER, creating a logical workflow and connecting the Grasshopper file through a specific plug-in (see "modeFRONTIER" in paragraph "2.2.1 Optimization tools for GH" on page 21). modeFRONTIER provides numerous optimization methods and possibilities. The algorithm choice highly depends on the computational problem to solve.

In this case pilOPT is chosen as multi-strategy algorithm. The potential of pilOPT is the self-learning and adapting properties. Furthermore, this solver considers the available evaluation time and adapts the process to efficiently find the

optimal solutions. piLOPT use both global and local search and smartly combines real and virtual (RSM-based) optimization (modeFRONTIER, n.d). It is possible to either set a DOE or run the self-initializing mode. For this specific case the latter is selected and the number of simulation is set to 400.

The output performances calculated and stored in modeFRONTIER are the one presented in *Table 25*. *Table 26* presents the optimization targets of the computational design optimization of Case Study variation 1.

OUTPUTS	TARGETS
sDA	
DA	constraint <span style="color: green;">↑</span> 50%
UDI	
UDI,75	maximize <span style="color: red;">↑</span>
UDI,underlit	
UDI,overlit	
ASE	minimize <span style="color: blue;">↓</span>
glazing_area	
shading_area	
SED	

**Table 25** Outputs and target CDO\_ step 1.2 of the workflow of Case Study variation 1

TARGETS	
DA	constraint <span style="color: green;">↑</span> 50%
UDI,75	maximize <span style="color: red;">↑</span>
ASE	minimize <span style="color: blue;">↓</span>

**Table 26** Targets of the CDO\_ step 1.2 of the workflow of Case Study variation 1

For the purpose of this research, more attention is given to the daylighting design goals. The CDO targets chosen are two, UDI,75 and ASE, with the addition of a constraint, DA. The scope behind this optimization objectives is to maximize the Useful daylight autonomy (UDI,75) and minimize the Annual Sun Exposure, which is an indicator of the percentage of space receiving too much light. To be sure that the analysis surface receives sufficient daylight during the year, the minimum Daylight Autonomy threshold has been set to 50%.

In this way, it is possible to reach visual comfort in the space, with the reduction of both underlit and overlit conditions, reducing the risk of glare.

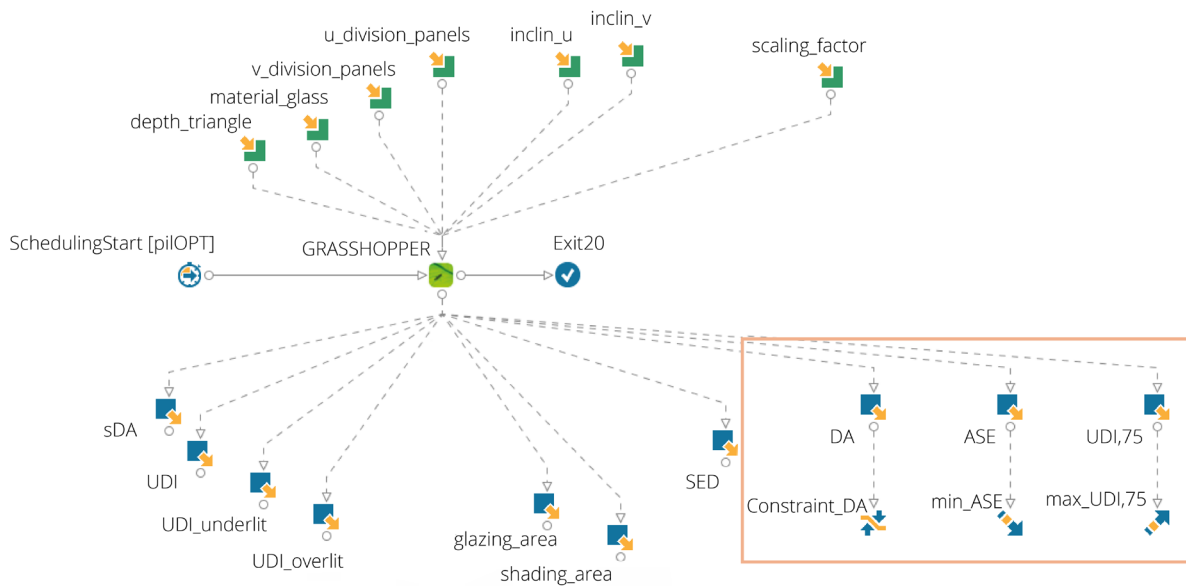


**Figure 88** modeFRONTIER logical computational optimization workflow \_ step 1.2 of the workflow Case Study variation 1

The logical optimization workflow built in modeFRONTIER is presented in **Figure 88**. The objectives with the relative targets are enclosed in a rectangular shape. The input variables are showed in green on the top part of the process and are listed in table below (**Table 27**).

INPUT VARIABLE NAME	LOWER BOUND scaled	UPPER BOUND scaled	STEP	REAL VALUES
depth_triangle	0.6	1.5	0.05	2.4 - 6 m, step 0.2 m
material_glass	0	2	1	
u_division_panels	3	10	1	
v_division_panels	3	15	1	
scaling_factor	0.1	0.9	0.1	
inclin_x	0	1	0.1	
inclin_y	0	1	0.1	

**Table 27** Input variables of the CDO \_ step 1.2 of the workflow of Case Study variation 1

In *Table 28* and *Figure 89* it is explained and displayed the meaning of the *inclination\_x* and *inclination\_y* variables.

VARIABLE	VALUE	PROTUSION DIRECTION
inclin_x	0.0	maximum inclination towards West (W)
	0.5	perpendicular to the x-axis = W-E axis
	1.0	maximum inclination towards East (E)
inclin_y	0.0	maximum inclination towards South (S)
	0.5	perpendicular to the y-axis
	1.0	maximum inclination towards North (N)

**Table 28** Input variables inclination in x and y direction

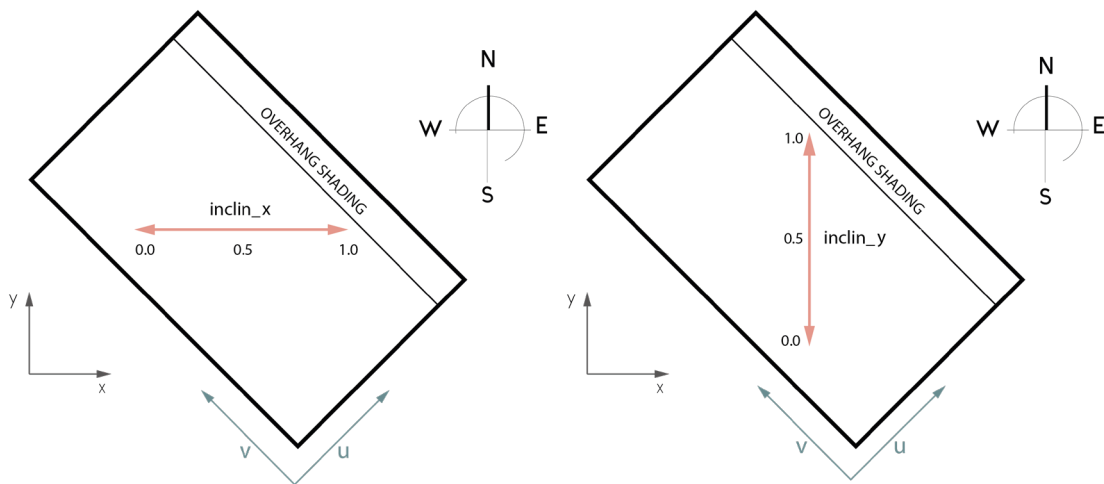


**Figure 89** Case Study orientation and direction of the inclination in x and y direction

• **OUTPUTS daylight optimization 1.2**

modeFRONTIER provides multiple analysis and visualization methods to carry out the design exploration after the computational design optimization. In this way it is possible to determine the best design configurations and interpret the results.

From the 400 samples evaluated, 72 (18%) produced a real-error during the simulation run (*Figure 90*). The remaining designs are all feasible, meaning that they all meet the DA constraint. This finding is consistent with data obtained in the daylight simulation performed on the Terminal with the closed roof. As a matter of fact, *Table 17* on paragraph “5.3.1 Current roof shading system” on page 128 shows that the value of DA was already significantly greater than the

50% threshold applied as constraint, reaching the value of 79.57%. Inserting in the roof a system of openings, can only creates an increment of this value.

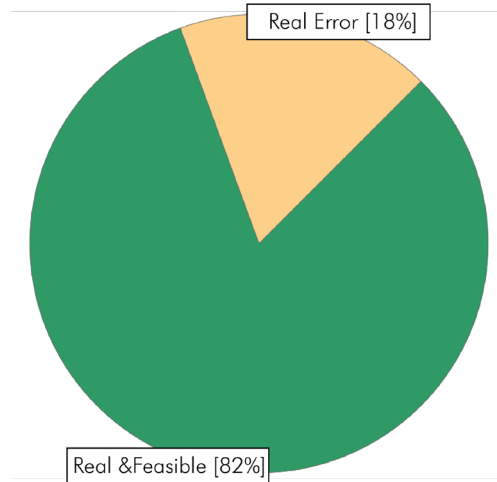


Figure 90 Pie chart design summary \_ optimization step 1.2

The graph below (Figure 91) is an history chart and shows the convergence of the design alternatives to meet the target of the minimization of ASE. The same graph is realized for the other optimization target (UDI,75) and for the constraint (DA) (see 8.5 Appendix E). The number of design are plotted sequentially following their generation. The higher the design ID number, the later the stage of the optimization process. With the growing of the Design ID it is possible to notice the convergence of the design samples to the same ASE level, which indicates the convergence of the algorithm to the optimal design distributed on the Pareto front.

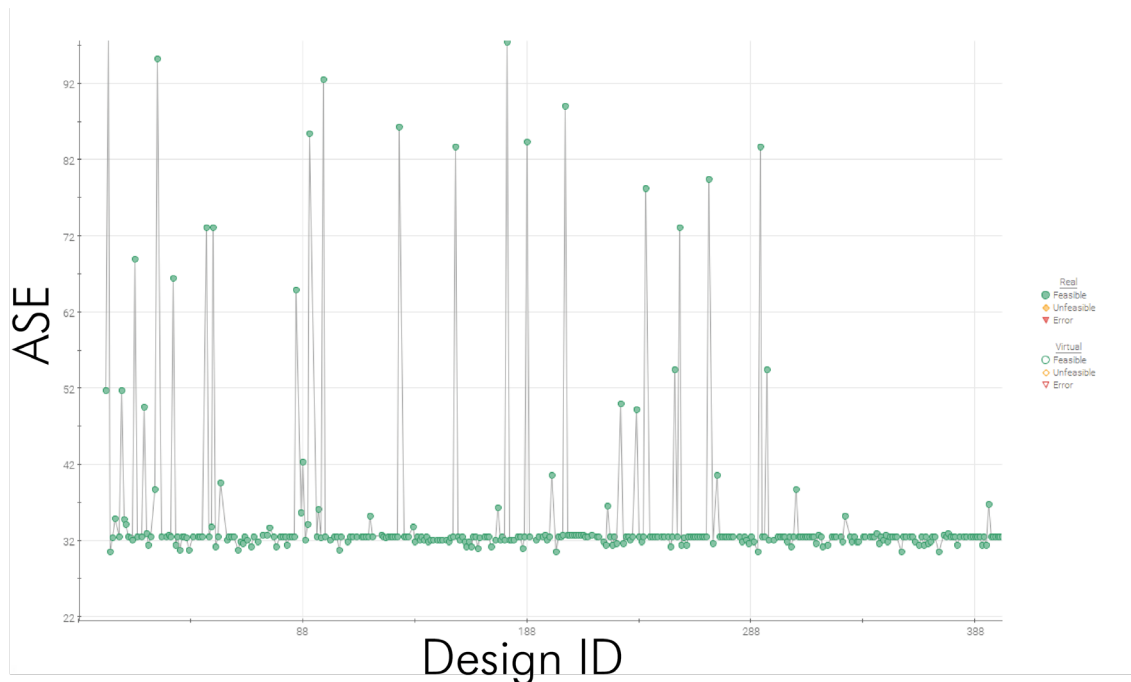
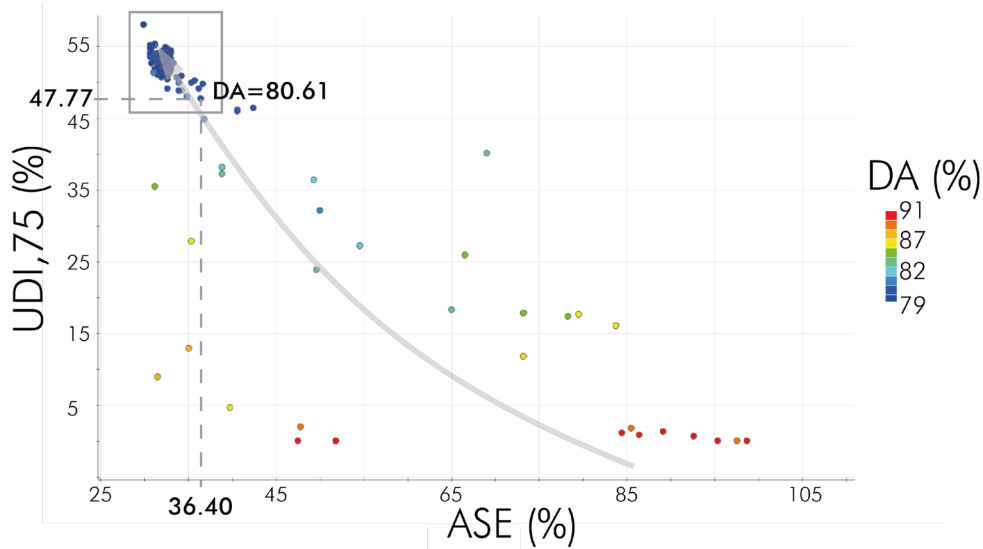


Figure 91 History chart of the optimization algorithm converging to minimize ASE

In *Figure 92* can be clearly seen the continual growth of UDI,75 in correspondence with the decrease of ASE. In the same way that ASE decrease, DA diminish. With the targets of minimizing the Annual Sun Exposure, the DA converges to values slightly higher then the 50% threshold. As a matter of fact, the increase in the Daylight Autonomy would affect negatively the optimization.



**Figure 92** Bubble chart with designs converging to the optimization targets \_step 1.2 of the workflow of Case Study variation 1

*Figure 93* represents a parallel chart of the feasible design of the CDO. The user is able to control and filter the information in order to meet the objectives and reveal which design options are the most appropriate and wanted for the scope of the optimization. In this specific case, a number of 50 designs are filtered in order to further evaluate them from an energy point of view. ASE varies in a range between 32 and 30%, UDI,75 has acceptable levels (50-55%) and the DA is always grater than the threshold setted.

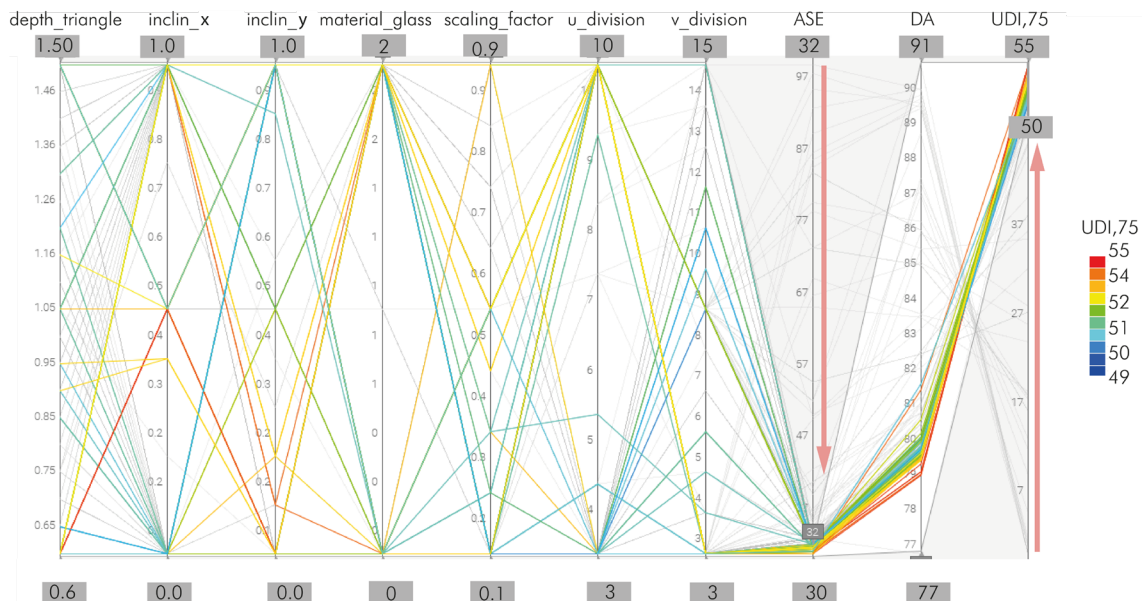


**Figure 93** Parallel chart of feasible designs from optimization 1.2, filtered to meet the daylight targets

Comparing the results in the bubble chart (*Figure 92*) with the output values of the daylight performance simulation of case study variation 1 in *Table 16*, it is possible to observe that the optimization process can only slightly improve the visual comfort levels.

*Table 29* presents the daylight output from daylight optimization of the optimal 50 filtered. The results reveal how the output of simulation can be slightly improved, but without achieving extremely positive visual comfort levels. To reduce the overlit conditions as well as the annual sun exposure, the DA constraint is always met and the DA value is slightly reduced with almost a steady 80% for all the converging designs. The UDI is higher as the UDI,75 with higher values than 47%.

OUTPUT DAYLIGHT OPTIMIZATION concept variation 1 50 optimal design		
	lower value	higher value
ASE	30.6%	36.0%
DA	78.8%	81.4%
UDI	65.7%	68.3%
UDI<	9.0%	10.0%
UDI>	20.2%	23.3%
UDI,75	50.7%	55.1%

**Table 29** Summary of the output from daylight optimization of the best 50 designs \_ step 1.2

*Table 30* presents five of the filtered designs of the Pareto front after the optimization is completed. What is striking from the five designs is that the optimal designs in terms of daylight tend all to have a roof configuration which allows only a small amount of indirect daylight to reach the analysis grid.

	Design no	1	2	3	4	5
INPUT VARIABLES	depth_triangle	0.6	0.6	1.5	0.6	0.6
	inclin_x	0.5	0.5	0.5	0.5	1
	inclin_y	0	0	0.1	1	0.1
	material_glass	0	2	2	0	2
	scaling_factor	0.1	0.1	0.9	0.1	0.1
	u_division_panels	10	10	10	3	10
	v_division_panels	3	3	3	3	3
TARGETS	ASE (%)	31.2	31.2	30.6	31	30.8
	UDI,75 (%)	55.1	55.1	54.9	55.1	54.9
	DA (%)	78.9	78.9	81.3	79.2	78.9
OUTPUTS	UDI (%)	67.8	67.8	67.8	67.3	67.7
	UDI,underlit (%)	10.0	10.0	9.1	9.9	10.0
	UDI_overlit (%)	20.7	20.7	21.6	21.4	20.9
	glazing_area (m2)	4.3	4.3	352.0	4.8	4.9
	shading_area (m2)	3107.5	3107.5	4996.1	1618.5	1942.4

**Table 30** Five best designs from the computational optimization\_ step 1.2 of the workflow of Case Study variation 1

The observations on the optimal designs obtained support the hypothesis made previously that the addition of an opening system in the roof of this particular case study would have created some challenges (see **5.3.1 Current roof shading system**). The solver tries to reduce the introduction of more direct daylight to avoid overlit conditions. This is achieved by either reducing the scaling opening ratio to the minimum value and with very high inclinations of the shading system toward the east side, or by increasing the shading height, incrementing the scaling factor (0.9) and with a deep inclination of the modules toward the east direction (**Figure 94**).

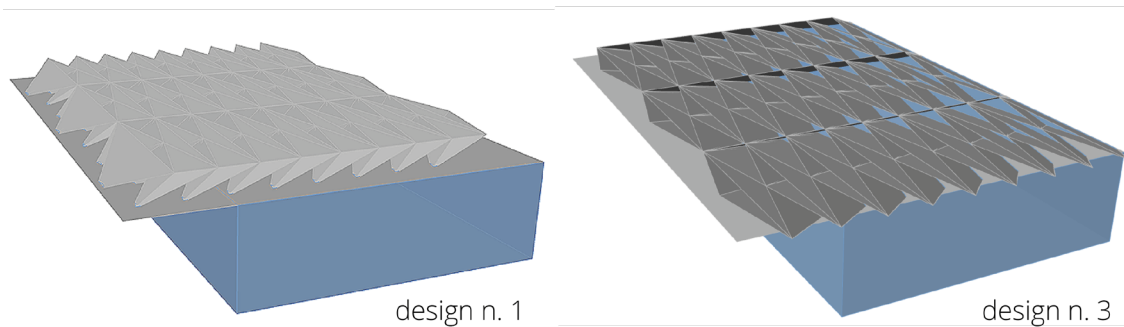


**Figure 94** Perspective view of design no.1 and no.3

## ENERGY SIMULATION 1.2.A

With this second step of evaluating the energy performance of the 50 filtered optimal design configurations from the computational design optimization. After the optimization of the roof system to solve the multi-objective daylight problem, it is possible to introduce the energy performance as decision criteria post-optimization. Following the selection of the final design based on the energy performance using construction material less (A) and more insulating (B).

- **INPUTS energy simulation 1.2.A**

The 50 optimal designs selected are plotted as DOE to implement an energy evaluation of the best solutions. In this way the choice of the final configuration between the sub-optimal designs is driven by their thermal performances. The input settings for the energy simulation 1.2.A are the ones of *"Table 18" on page 133*.

- **OUTPUTS energy simulation 1.2.A**

The outputs from the energy simulation of the optimal design configurations from the optimization process 1.2, are processed and analysed to determine the final proposed solution which is selected based on the lowest energy consumption.

The graph below (*Figure 95*) presents the Pearson correlation coefficients between the selected variables. The guideline showing the strength of a correlation can be found in *"Appendix E" paragraph "8.5.3 Pearson correlation strength"*. Darker colours represent a stronger correlation, which is also indicated with a number between -1 and 1. -1 represent a perfectly negative correlation, which means that the correlation is linear and the growing of one value corresponds to the decrease of the other one. While 1 represent a perfectly positive correlation, which signifies the linear growth of both variables (modeFRONTIER, n.d.).

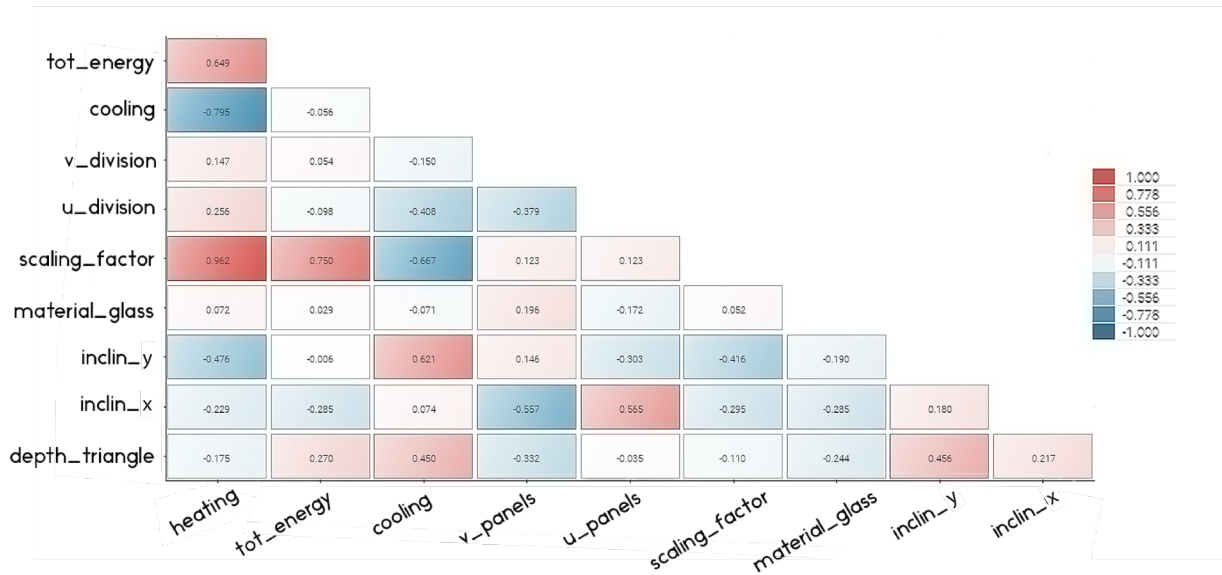


**Figure 95** Correlation matrix chart displaying Pearson correlation coefficients between the selected variables\_ step 1.2.A

In this specific design exploration it is possible to observe some input-output correlations. The impact of the *scaling\_factor* on the *heating energy* is almost a perfect correspondence (0.962). The *scaling\_factor* has also a high influence on the total energy demand. The energy load is in fact determined by both heating and cooling load as well as lighting load. The heating load is negatively affected by *inclin\_y*. This means that the more the shading system is facing the north direction, the greater the heating demand. What stands out is the strong positive correlation between *tot energy* and *heating load* (0.649), compared to the very low strength of association between the total energy and the cooling load (-0.056).

This indicates that the heating is the main component that needs to be reduce in order to minimize the total energy consumption and find the best energetically performing solution between the optimal selected designs.

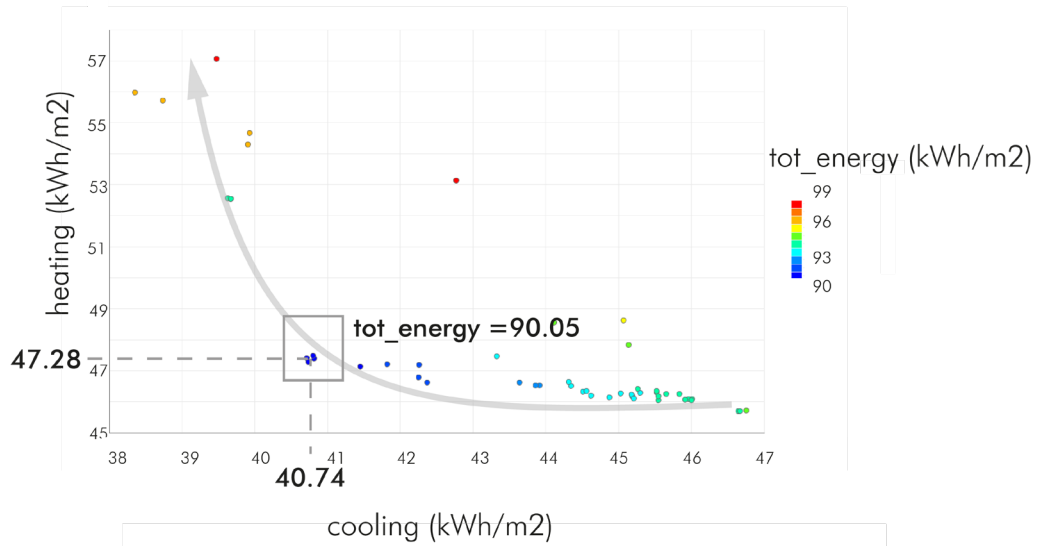


**Figure 96** Bubble chart showing relation between cooling, heating and total energy demand of the 50 selected designs \_ step 1.2.A

The bubble chart above (*Figure 96*) provides an overview of the energy demand of each of the 50 configurations. The heating demand increases with the reduction of the cooling load. The total energy is lower in the bottom left corner, in the situation in which both total cooling and heating are low.

The best energetically performing solution is selected by identification of the lowest energy demand and presents the following geometrical properties (see *Table 31*) :

depth_triangle	0.6
inclin_x	1
inclin_y	0.1
material_glass	0
scaling_factor	0.1
u_division_panels	10
v_division_panels	3

**Table 31** Input settings for best energy performing solution \_ step 1.2.A of the workflow Case Study 1

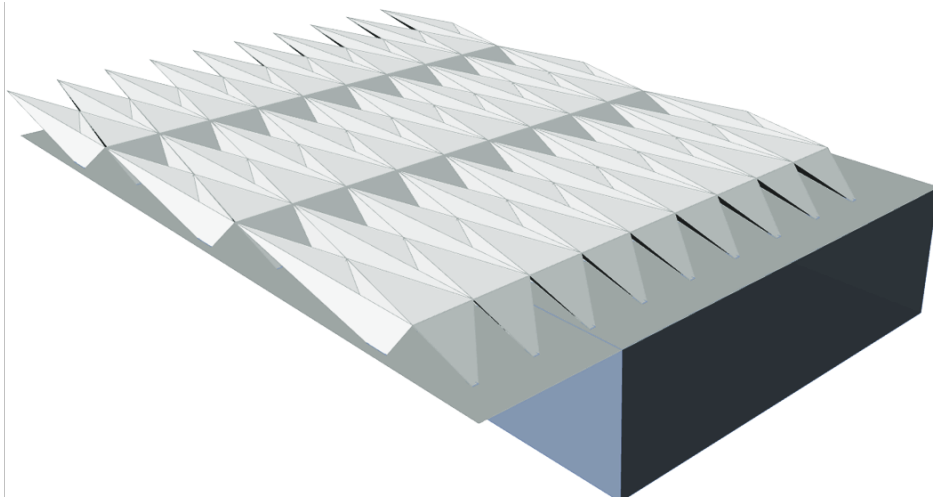


**Figure 97** Perspective view of the final selected design \_ step 1.2.A

The modules are inclined towards South-East to minimize the heating load (*Figure 97*). The daylight performances and material amount of the final selected design are listed in *Table 32*. While in *Table 33* are presented the energy performances.

ASE (%)	30.8
DA (%)	78.88
UDI (%)	67.69
UDI,75 (%)	54.91
UDI,underlit (%)	10.01
UDI overlit (%)	20.89

glazing_area (m2)	4.87
shading_area (m2)	1942.37

**Table 32** Daylight performances and material amount of the final selected design \_ step 1.2.A

tot_cooling (kWh/m2)	40.74
tot_heating (kWh/m2)	47.28
tot_energy (kWh/m2)	90.05
lights_elec_energy (kWh/m2)	2.02
people_heat_gain (kWh/m2)	118.20
max_operat_temp (kWh/m2)	22.93
min_operat temp (kWh/m2)	17.92

**Table 33** Energy performances of the final selected design \_ step 1.2.A

## ENERGY SIMULATION 1.2.B

- INPUTS energy simulation 1.2.B

The input settings for the energy simulation 1.2.B are the ones of "Table 21" on page 136.

- OUTPUTS energy simulation 1.2.B

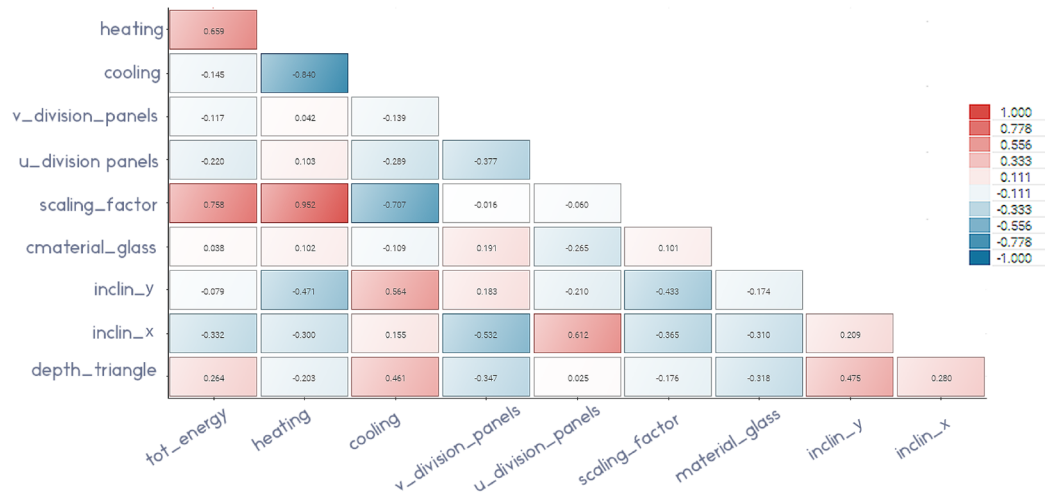


Figure 98 Correlation matrix chart displaying Pearson correlation coefficients between the selected variables \_ step 1.2.B

The Pearson chart above (Figure 98) is very similar to the one obtain from the design exploration 1.2.A, however in this case it is striking a slightly higher dependency of the total energy demand not only from the heating (0.659) but also from the cooling load.

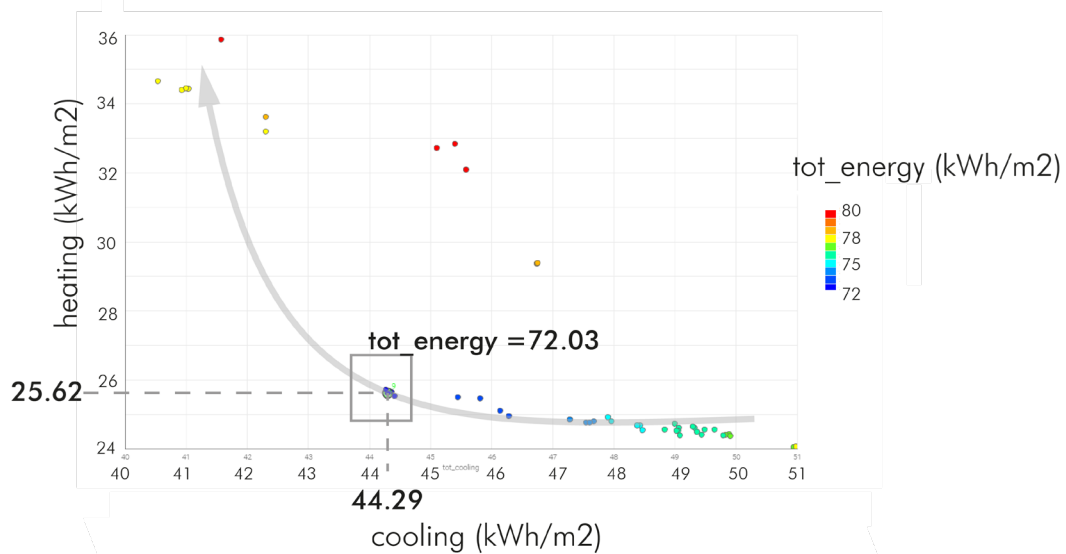


Figure 99 Bubble chart showing relation between cooling, heating and total energy demand of the 50 selected designs \_ step 1.2.B

The best energetically performing solution is selected by identification of the lowest energy demand and presents the following geometrical properties (see *Table 34*) :

depth_triangle	0.6
inclin_x	0.5
inclin_y	0
material_glass	0
scaling_factor	0.1
u_division_panels	10
v_division_panels	3

**Table 34** *Input settings for best energy performing solution \_ step 1.2.B of the workflow Case Study variation 1*

The selected design is very similar to the one chosen from the design exploration 1.2.A, with the difference in the inclination. In this case the shading modules are completely oriented to face South, with the same scope of introducing in the building as much radiation as possible to minimize the heating load, and so the total energy demand.

The daylight performances and material amount of the final selected design are listed in *Table 35*. While in *Table 36* are presented the energy performances.

ASE (%)	31.2
DA (%)	78.94
UDI (%)	67.84
UDI,75 (%)	55.13
UDI,underlit (%)	9.99
UDI,overlit (%)	20.74

glazing_area (m2)	4.35
shading_area (m2)	3107.47

**Table 35** *Daylight performances and material amount of the final selected design \_ step 1.2.B*

tot_cooling (kWh/m <sup>2</sup> )	44.29
tot_heating (kWh/m <sup>2</sup> )	25.62
tot_energy (kWh/m <sup>2</sup> )	72.03
lights_elec_energy (kWh/m <sup>2</sup> )	2.12
max_operat_temp (kWh/m <sup>2</sup> )	23.80
min_operat_temp (kWh/m <sup>2</sup> )	18.39

**Table 36** Energy performances of the final selected design \_ step 1.2.B

The difference from design 1.2.A and 1.2.B lays mainly into the heating demand. While the cooling is slightly higher, (from 40.74 kWh/m<sup>2</sup> of design 1.2.A to 44.29 kWh/m<sup>2</sup> for design 1.2.B) the heating consumption is almost half the one reached with the final design 1.2.A (from 47.28 to 25.62 kWh/m<sup>2</sup>). The minimization of the heating corresponds to lower the total energy value of 20% ca.

## 5.4 CASE STUDY VARIATION 2

*Figure 81* shows the first workflow application, which adopts the New Schiphol Terminal with all the four walls opaque (*Figure 100*). This is a less realistic simplification of the real design, compared to the Variation 1. However, this decision has been made to show how the computational design optimization adopted produces different outcomes if the context is different.

### 5.4.1 CURRENT ROOF SHADING SYSTEM

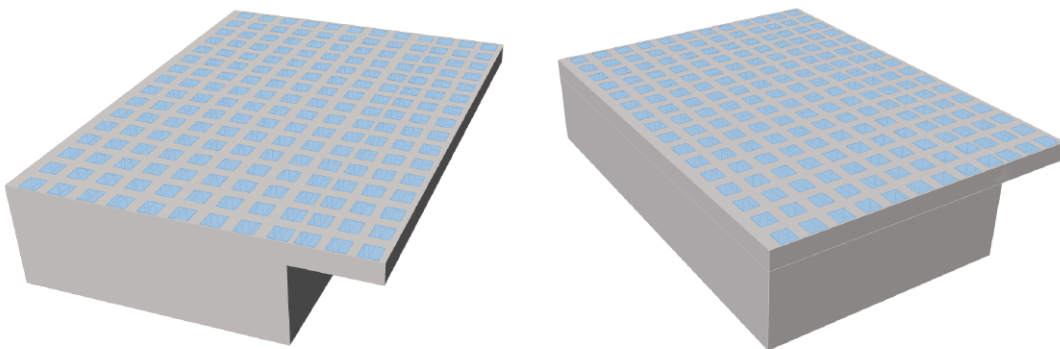


**Figure 100** Perspective views of the model of the Terminal - variation 2

#### DAYLIGHT SIMULATION 2.1

- INPUTS daylight simulation 2.1

The settings for the daylight simulation 2.1 are the same as the one of simulation 1.1 listed in *Table 15*, with the exception of the curtain walls material, which is not applied since concept 2 has no curtain walls, but four opaque façades.

- OUTPUTS daylight simulation 2.1

*Table 37* reveals an adequate daylight distribution in the space when the concept is adjusted and the curtain walls are switched with fully opaque façades. The illuminance levels deriving from simulation 2.1 are acceptable whereas the one from simulation 1.1 (see *Table 16*) appears to have an extreme value for the overlit area (47.77%). Case study variation 2 tends to perform well in UDI, reaching a percentage of 77%, compared to case study variation 1, which scores only the 44%.

OUTPUT DAYLIGHT SIMULATION concept variation 2	
sDA	99%
ASE	5.60%
DA	74.37%
UDI	76.93%
UDI<	10.79%
UDI>	10.81%
UDI,75	64.51%

**Table 37** Output values daylight simulation \_ step 2.1 of the workflow Case Study variation 2

## ENERGY SIMULATION 2.1.A

- INPUTS energy simulation 2.1.A

The inputs for the daylight simulation 2.1.A are the same as listed on *Table 18*, with the exception of the curtain walls material, which is not applied since concept 2 has no curtain walls, but four opaque façades. The U-values of the material are relatively high, with the effect of creating a less insulating construction.

- OUTPUTS energy simulation 2.1.A

OUTPUT ENERGY SIMULATION 2.1.A	
people heating	118.20 kWh/m <sup>2</sup>
lights electric energy	1.58 kWh/m <sup>2</sup>
infiltration tot heat loss	49.89 kWh/m <sup>2</sup>
infiltration tot heat gain	0.064 kWh/m <sup>2</sup>
ideal tot heating energy	143.17 kWh/m <sup>2</sup>
ideal tot cooling	122.41 kWh/m <sup>2</sup>
tot energy	267.15 kWh/m <sup>2</sup>

**Table 38** Output values energy simulation \_ step 2.1.A of the workflow Case Study variation 2

The final energy consumption is relatively elevated (*Table 38*). As predicted, the final total energy consumption is the effect of both elevated heating and cooling energy demand. Though, as for performance simulation 1.1.A, the heating load is the main cause of inflated consumption levels.

## ENERGY SIMULATION 2.1.B

- **INPUTS energy simulation 2.1.B**

The inputs for the daylight simulation 2.1.B are the same as listed on *Table 21*, with the exception of the curtain walls material, which is not applied since concept 2 has no curtain walls, but four opaque façades.

- **OUTPUTS energy simulation 2.1.B**

OUTPUT ENERGY SIMULATION 2.1.B	
people heating	118.20 kWh/m <sup>2</sup>
lights electric energy	1.46 kWh/m <sup>2</sup>
infiltration tot heat loss	53.83 kWh/m <sup>2</sup>
infiltration tot heat gain	0.062 kWh/m <sup>2</sup>
ideal tot heating energy	41.27 kWh/m <sup>2</sup>
ideal tot cooling	121.03 kWh/m <sup>2</sup>
tot energy	163.94 kWh/m <sup>2</sup>

**Table 39** Output values energy simulation \_ step 2.1.B of the workflow Case Study variation 2

The results of this analysis (*see Table 39*) show a significant reduction of the heating energy compared to 2.1.A, with a positive effect on the energy efficiency of the building, which decreases by about 39%.

From the daylight optimization of Case Study variation 1 it is possible to conclude how a more controlled use of the natural light sources would be possible by means of application of vertical shading systems on the curtain walls.

## 5.4.2 ROOF SHADING OPTIMIZATION

### DAYLIGHT OPTIMIZATION 2.2

- **INPUTS daylight optimization 2.2**

The settings of the daylight optimization of Case Study variation 1 (with three curtain walls) are listed in *"Table 24" on page 140*, with the exception of the curtain walls material, since Case Study variation 2 has fully opaque façades.

The optimization is carried out in the same way of optimization 1.2. pilOPT is the algorithm used, the modeFRONTIER logical workflow established is the same (see *"Figure 87" on page 139*) as well as the input variables (*"Table 27" on page 142*). However, for this optimization was created a DOE table of 20 designs using the Uniform Latin Hypercube algorithm, which tries to distribute the samples uniformly in the design exploration space over the variable range (modeFRONTIER User Guide, n.d.). In line with the time available, the number of evaluations has been set to 200.

- **OUTPUTS daylight optimization 2.2**

Numerous errors have been encountered during the process, however the optimization has been continued to the completion of the 200 simulations, excluding the real errors.

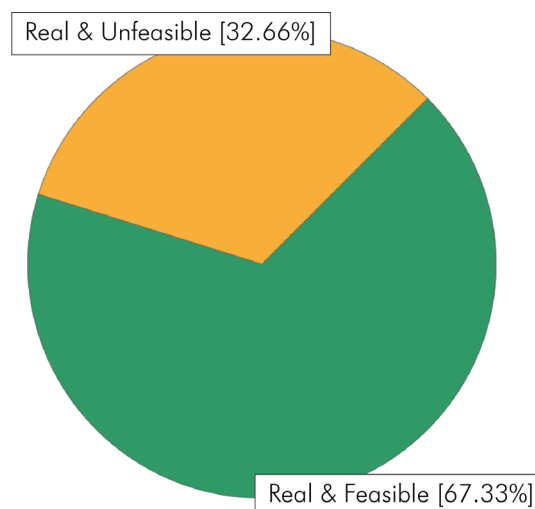


**Figure 101** Pie chart design summary \_ optimization step 2.2

The pie chart above (*Figure 101*) show the percentage of Real and Feasible designs (32.66% equal to 66 designs) and the Real and Unfeasible (67.33% equal to 134 designs), which represent all the configurations that do not meet the constraint of 50% DA.

The graphs below (*Figure 102*) show the relation between the three optimization targets (DA, UDI<sub>75</sub> and ASE). It can be observed that the UDI<sub>75</sub> is the highest in the central values of DA, when the overlit and underlit percentage is low. The ASE increases with the growth of the DA, generating more Annual Sun Exposure when the overlit levels are greater.

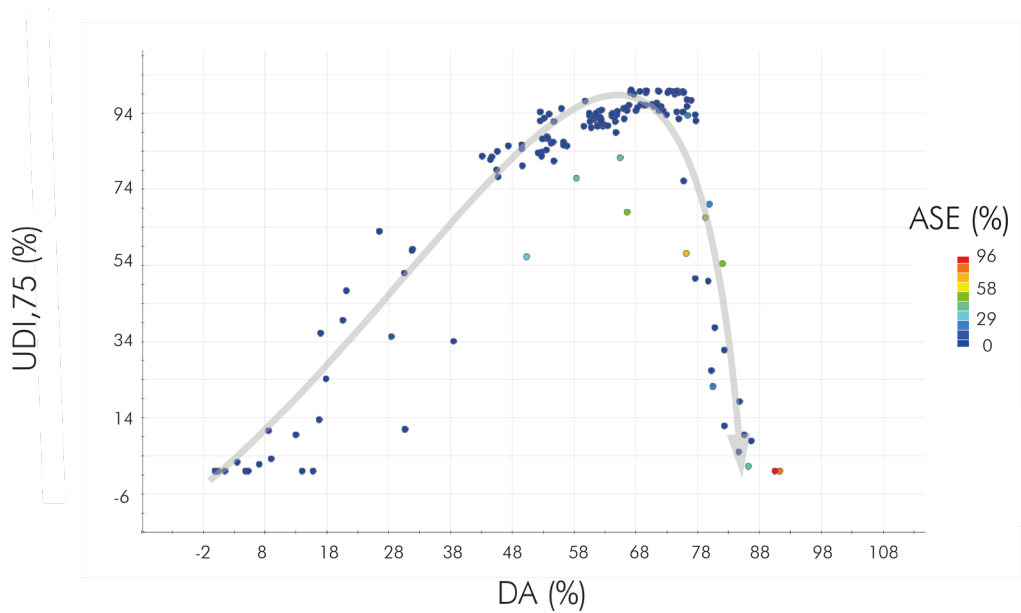


**Figure 102** Bubble chart showing relation between DA, UDI<sub>75</sub> and ASE \_ optimization step 2.2

The bubble chart in *Figure 103* displays the dependency of the UDI<sub>75</sub> and DA from the depth of the shading modules. The highest values of the UDI<sub>75</sub> are in

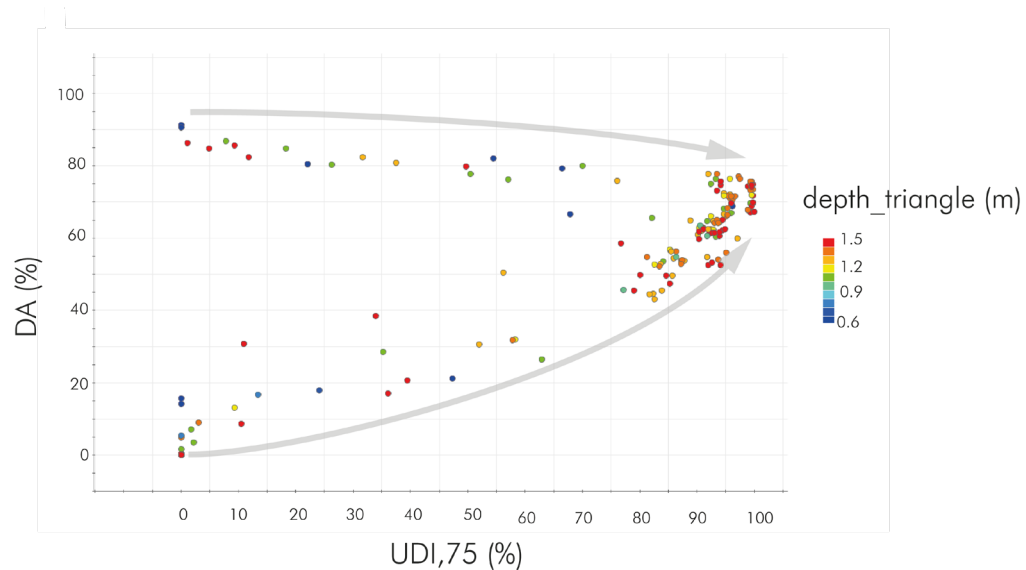


**Figure 103** Bubble chart showing relation between UDI<sub>75</sub>, DA and depth\_triangle\_ optimization step 2.2

correspondence with medium to high depth of the shading system. This observation can be explained with the ability of higher shading units to reduce the direct light entering the building.

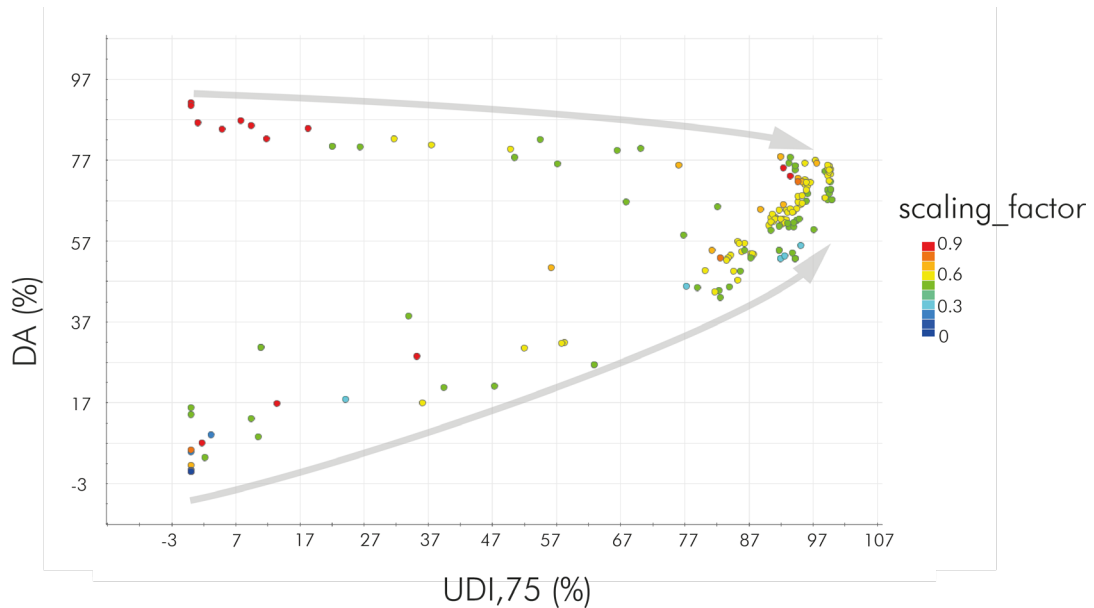


**Figure 104** Bubble chart showing relation between UDI,75, DA and scaling factor \_ optimization step 2.2

The best configuration to improve the UDI is by combining high shading depths to medium opening ratio (*Figure 104*). The goal is to allow as much indirect daylight as possible in the indoor space to improve the visual comfort.

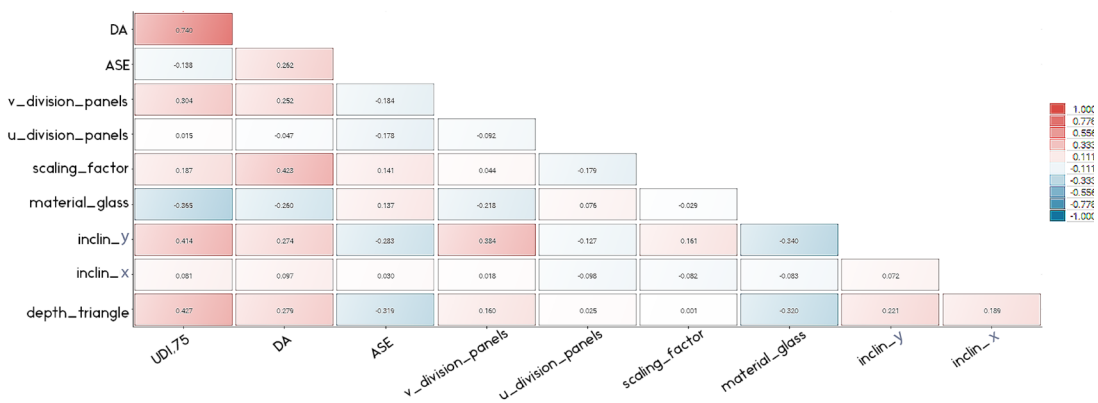


**Figure 105** Correlation matrix chart displaying Pearson correlation coefficients between the selected variables \_ step 2.2

The Pearson correlation chart above (*Figure 105*) shows that depth\_triangle and inclin\_Y are important driving factors of UDI,75. Furthermore, also the division of the panel in the v direction and the glass material have medium strength correlation with the UDI. The DA is strongly dependent from the value of the

scaling factor. The bigger the openings, the higher the daylight autonomy level.

Through the parallel chart it is possible filter the designs and observe which ones fulfil the optimization requirements (*Figure 106*).

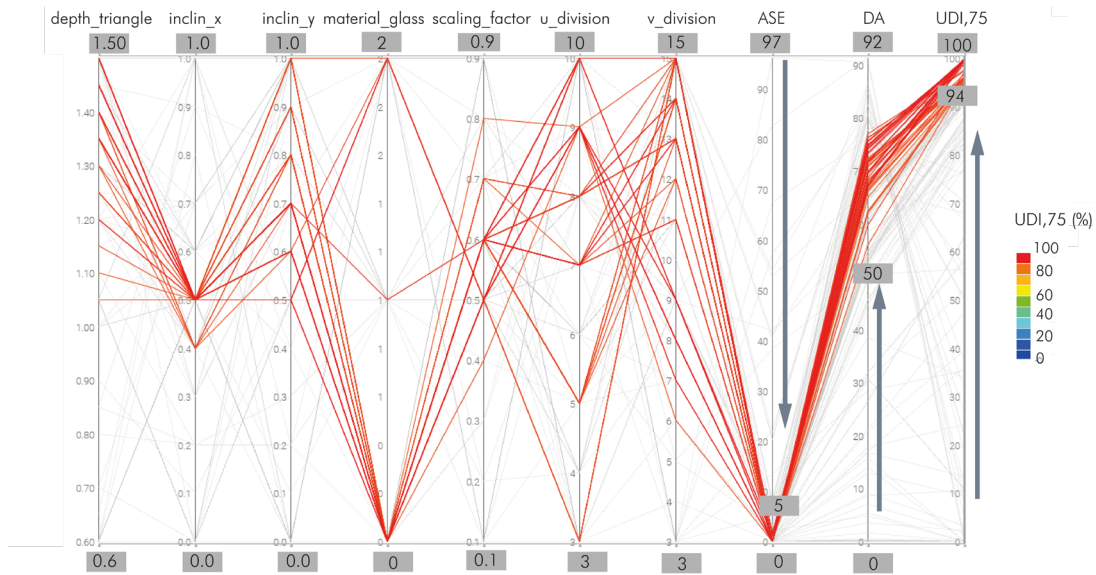


**Figure 106** Parallel chart of feasible designs from optimization 2.2, filtered to meet the daylight targets

The number of designs selected to be analysed in a second moment from an energetic point of view, are again 50 (same as for optimization 1.2). The daylight performances of these 50 designs are as follow (*Table 40*):

OUTPUT DAYLIGHT OPTIMIZATION concept variation 2 50 optimal design		
	lower value	higher value
ASE	0.0%	1.6%
DA	56.0%	77.0%
UDI	80.6%	85.8%
UDI<	9.4%	15.5%
UDI>	0.1%	8.2%
UDI,75	94.4%	100.0%

**Table 40** Summary of the output from daylight optimization of the best 50 designs \_ step 2.2

The results reveal positive performances in terms of visual targets. The DA value of the converging designs is in the range of 80%-86% and it is possible to

achieve extremely UDI<sub>75</sub> values (94%-100%). The glare can be almost completely reduced, reaching very low percentages of ASE.

Looking at *Figure 106*, the 50 selected designs are characterized by high depths of the shading alternative (1.05 to 1.50 m). The slope is almost absent or slightly towards the West direction (inclin\_x in the range of 0.4-0.5), and it is mainly facing North (inclin\_y between 0.5 and 1.0). The material that performs better in this case is the one with the highest Light Transmittance (material 0, LT = 70%), which enables the most visible radiation to reach the analysis grid. However, the glazing material 1 and 2 (with lower LT values) are also a possibility with the proper module configuration. The opening ratio creates a roof with skylights covering from 40 to 80% of the total surface (scaling factor 0.4-0.8). Finally, the number of panels is relatively high, creating a high number of modules. The number of modules in the v direction has more impact on the visual performance.

In *Table 41* are collected 5 Pareto-front designs. The best performing configuration seems to be characterized by high depths of the modules, a slight inclination towards North and vertical on the West-East axis and medium scaling factor. A possible explanation for this combination of values might be that the high shading system surfaces and the medium scaling factor combined together create a self-shading system so that mainly indirect light enters the construction, but still allowing a big amount of light to get reflected inside the building. The verticality of the modules enables the daylight to enter from wide angles and improve the UDI.

	Design no	1	2	3	4	5
INPUT VARIABLES	depth_triangle	1.4	1.4	1.45	1.45	1.5
	inclin_x	0.5	0.5	0.5	0.5	0.5
	inclin_y	0.7	0.6	0.6	0.6	0.5
	material_glass	0	0	0	0	0
	scaling_factor	0.6	0.6	0.5	0.5	0.5
	u_division_panels	8	10	9	9	10
	v_division_panels	13	15	8	7	9
TARGETS	ASE (%)	0	0	0	0	1.3
	UDI <sub>75</sub> (%)	99.8	99.8	99.8	99.8	100.0
	DA (%)	73.5	69.7	69.8	71.7	67.2
OUTPUTS	UDI (%)	84.5	84.8	85.2	84.5	82.9
	UDI <sub>underlit</sub> (%)	10.6	11.7	11.6	11.2	12.4
	UDI <sub>overlit</sub> (%)	3.6	2.2	1.9	2.9	3.2
	glazing_area (m2)	206.3	206.3	143.3	143.3	143.3
	shading_area (m2)	3111.7	3581.2	2705.6	2622.2	3010.7

**Table 41** Five best designs from the computational optimization \_ step 2.2 of the workflow of Case Study variation 2

In *Figure 107* and *Figure 108* are displayed the top and perspective view of design no. 1 and Design no. 5.

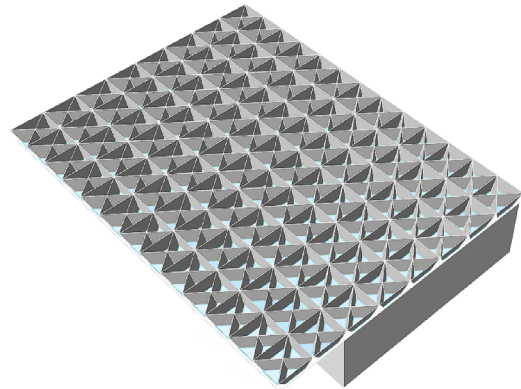
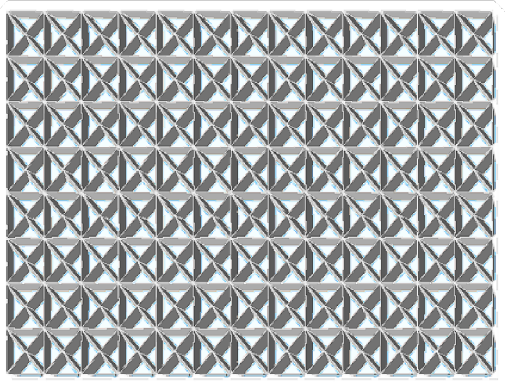


**Figure 107** Top and perspective view of design no. 1 \_ optimization 2.2

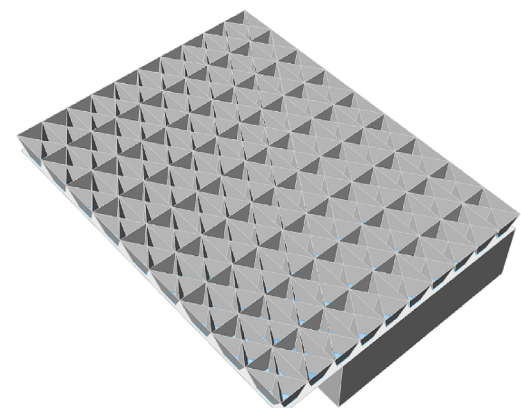
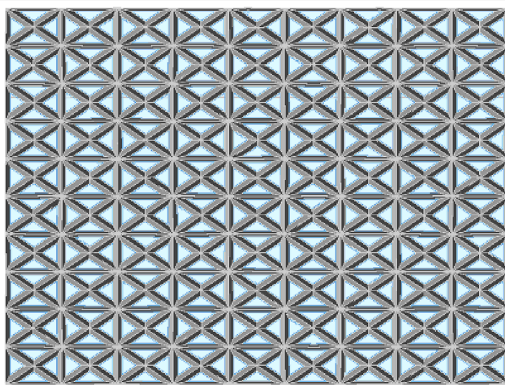


**Figure 108** Top and perspective view of design no. 5 \_ optimization 2.2

## ENERGY SIMULATION 2.2.A

As for the optimization 1.2, the same process has been follow for the final decision of the optimal concept of optimization 2.2. This second part consists of the evaluation of the 50 optimal designs from an energy point of you.

- **INPUTS energy simulation 2.2.A**

The input of simulation 2.2.A are the one of *“Table 18” on page 133* with the exception of the curtain walls which are not presents in Case Study variation 2. In this case the materials used are the ones of setting are, meaning less insulating materials, with relatively low U-values.

- **OUTPUTS energy simulation 2.2.A**

The Pearson correlation matrix in *Figure 109* shows the strong correlation between the total energy and heating. Cooling has also a very strong impact on the total amount of energy consumption.

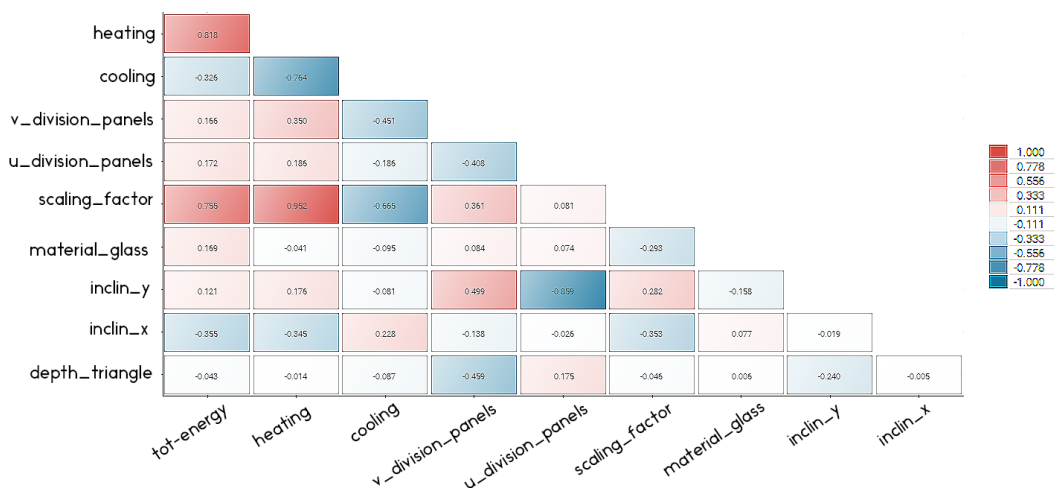


**Figure 109** Correlation matrix chart displaying Pearson correlation coefficients between the selected variables \_ step 2.2.A

The depth of the triangle is the factor with the main impact on the energy value (0.755), almost a perfectly positive correlation with the heating load (0.952) and a high negative influence on the cooling load. In this case the inclination on the x-axis (West-East) has more contribution in the energy performance, rather than inclin\_y.

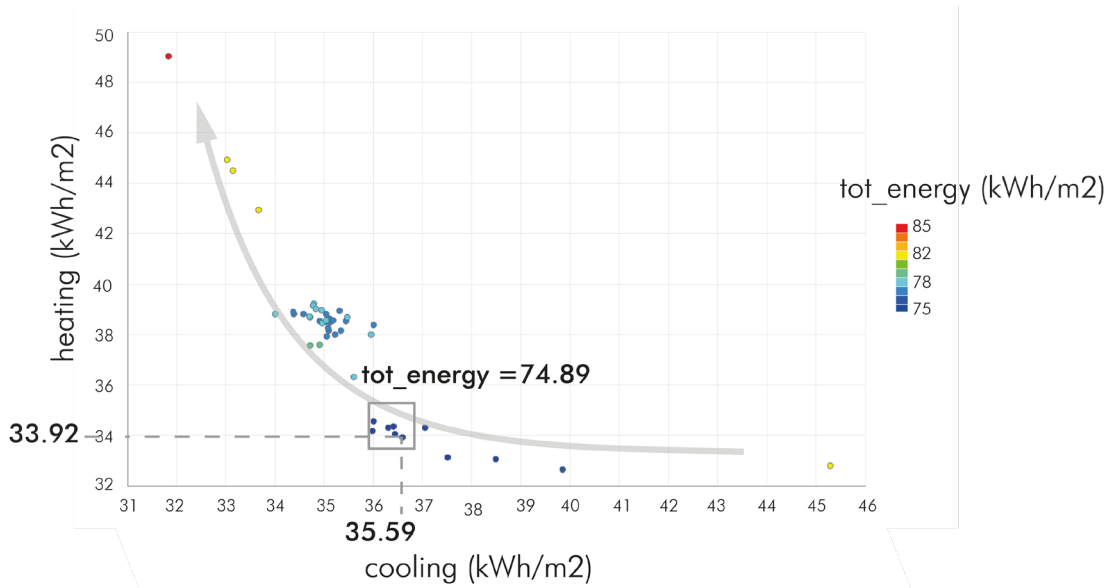


**Figure 110** Bubble chart showing relation between cooling, heating and total energy demand \_ optimization step 2.2.A

The bubble chart in *Figure 110* displays the trend of the cooling load, which decrease with the increase of the heating. The total energy is the lowest in the point in which both heating and cooling load are low. In this particular configuration, the cooling load is the key factor in the increment of energy consumption.

The best energy performing solution is selected by identification of the lowest energy demand and is characterized by the following properties:

depth_triangle	1.05
inclin_x	0.5
inclin_y	0.5
material_glass	0
scaling_factor	0.5
u_division_panels	10
v_division_panels	15

**Table 42** Input settings for best energy performing solution \_ step 2.2.A of the workflow Case Study variation 2

The final solution is displayed in *Figure 111*.

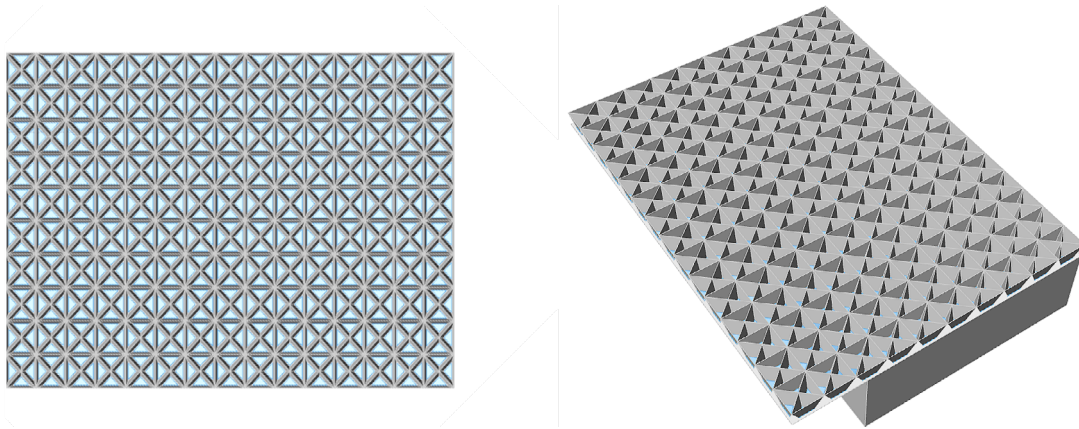


**Figure 111** Top and perspective view of the final selected design \_ step 2.2.A

The modules are perfectly perpendicular to the ceiling and the opening ratio is 0.5, which creates a glazing system that covers 50% of the roof surface.

The daylight performances and material amount are listed in *Table 43*, while in *Table 44* are presented the energy performance.

ASE (%)	1.6
DA (%)	69.60
UDI (%)	81.30
UDI,75 (%)	99.30
UDI,underlit (%)	11.90
UDI overlit (%)	5.40

glazing_area (m2)	143.30
shading_area (m2)	2707.20

**Table 43** Daylight performances and material amount of the final selected design \_ step 2.2.A

cooling (kWh/m2)	36.60
heating (kWh/m2)	33.90
tot_energy (kWh/m2)	74.90
lights_elec_energy (kWh/m2)	4.40
people_heat_gain (kWh/m2)	118.20
max_operat_temp (kWh/m2)	22.60
min_operat temp (kWh/m2)	18.30

**Table 44** Energy performance of the final selected design \_step 2.2.A

## ENERGY SIMULATION 2.2.B

- INPUTS energy simulation 2.2.B

The inputs for the daylight simulation 2.2.B are the same as listed on *Table 21*, with the exception of the curtain walls material, which is not applied since concept 2 has no curtain walls, but four opaque façades.

- OUTPUTS energy simulation 2.2.B

The Pearson correlation matrix in *Figure 112* shows the strong correlation between the total energy and heating (0.518). Cooling has also a medium impact on the total amount of energy consumption (0.241). This is due to the fact that the higher insulating materials reduces the heating demand and so the total energy consumption.

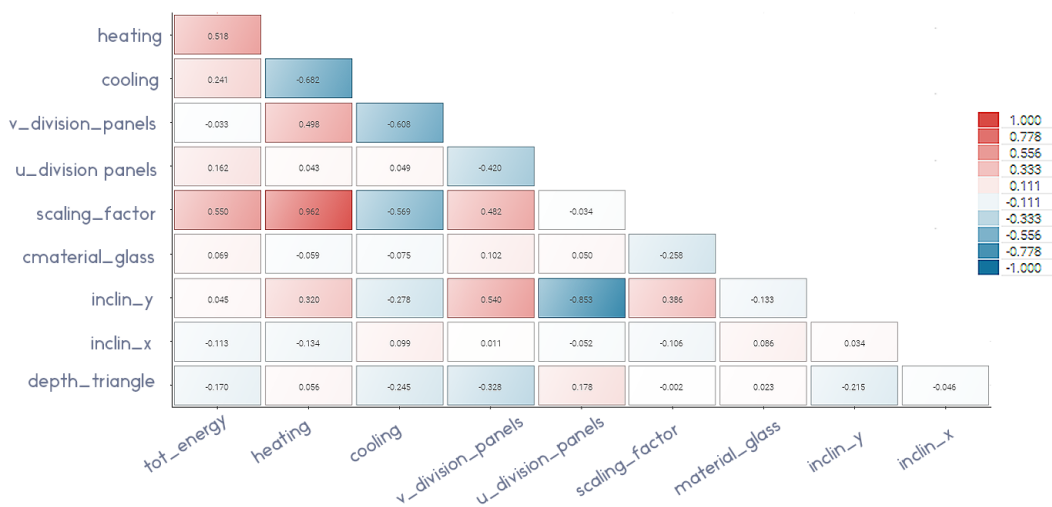


**Figure 112** Correlation matrix chart displaying Pearson correlation coefficients between the selected variables \_ step 2.2.A

The Pearson chart above is very similar to the one obtain from the design exploration 2.2.A, with the main difference that the cooling load has a positive influence on the heating energy (0.241), meaning that the higher the cooling, the higher the total energy demand. This is due to the fact that the insulating materials are able to reduce the heating load, but no the cooling, which is now the main component of the energy demand. Heating is still a key factor in the energy performance, as the heating increase the energy increase. This relation is more linear than the one with the cooling.

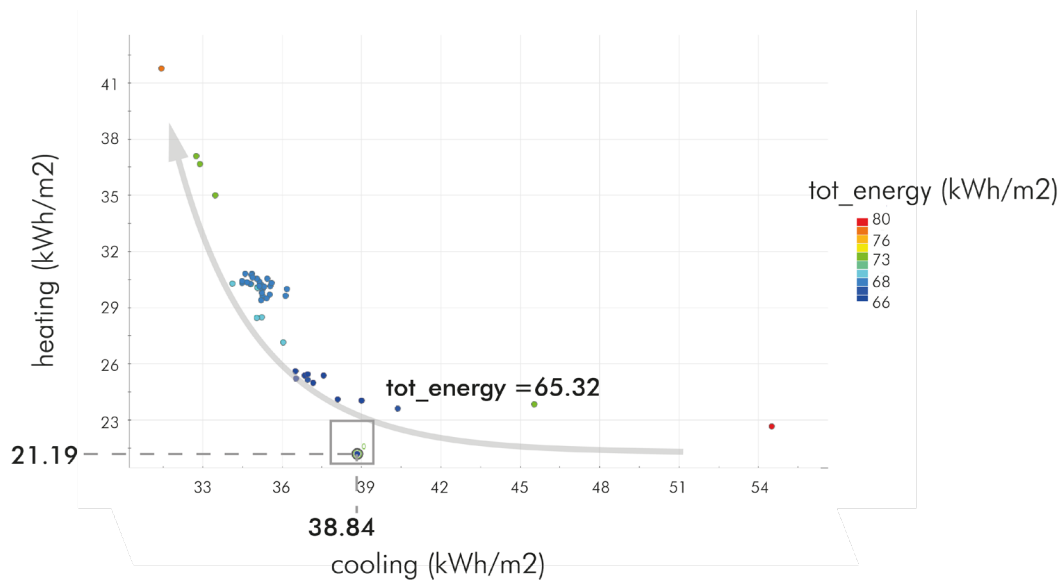


**Figure 113** Bubble chart showing relation between cooling, heating and total energy demand \_ optimization step 2.2.B

The best performing solution in terms of energy is chosen by identification of the lowest energy demand and is identified by the properties in **Table 45**.

depth_triangle	1.4
inclin_x	0.4
inclin_y	0.6
material_glass	0
scaling_factor	0.4
u_division_panels	9
v_division_panels	6

**Table 45** Input settings for best energy performing solution \_ step 2.2.B of the workflow Case Study variation 2

The solution is composed of high shading modules, slightly tilted on the North-West direction. The considerable depth of the shading units create a self-shading system, so the light is allowed inside the space, but without increasing too much the heat gain. This slight inclination has the main purpose to reduce the cooling load by avoiding the direct radiation to reach the indoor space. The openings represent 40% of the roof surface and the material selected is the one deriving from the daylight optimization, which has the highest VT value (70%).

In *Figure 114* it is displayed the final solution from top and perspective view.

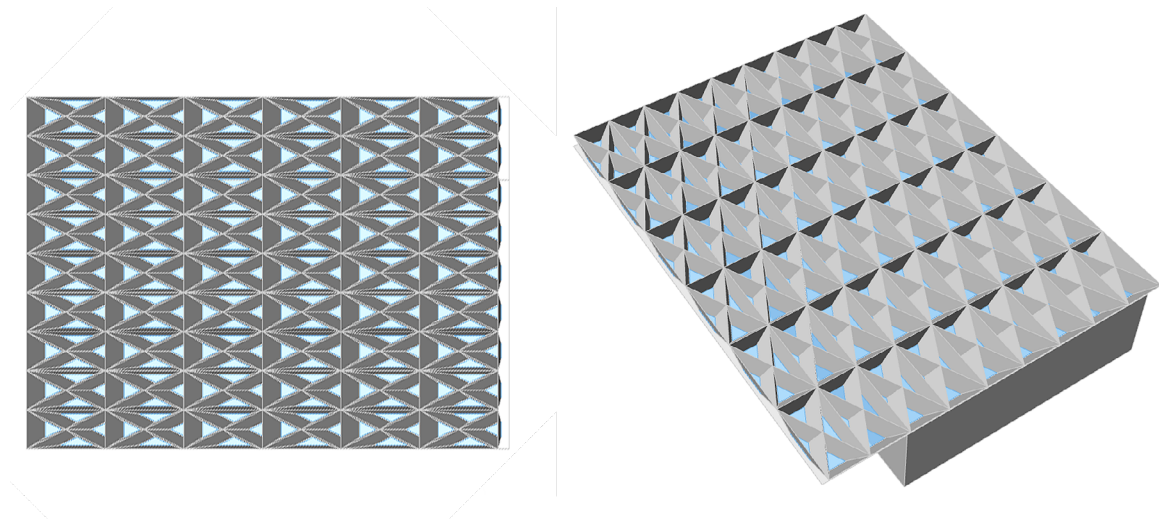


**Figure 114** Top and perspective view of the final selected design \_ step 2.2.B

The daylight performances of this selected final design are calculated and listed in *Table 46*, while the outcome form the energy performance are presented in *Table 47*.

ASE (%)	0
DA (%)	55.96
UDI (%)	83.14
UDI,75 (%)	95.09
UDI,underlit (%)	15.49
UDI overlit (%)	0.33

glazing_area (m2)	91.69
shading_area (m2)	2412.71

**Table 46** Daylight performances and material amount of the final selected design \_ step 2.2.B

cooling (kWh/m2)	38.84
heating (kWh/m2)	21.19
tot_energy (kWh/m2)	65.33
lights_elec_energy (kWh/m2)	5.30
people_heat_gain (kWh/m2)	118.20
max_operat_temp (kWh/m2)	23.22
min_operat temp (kWh/m2)	18.60

**Table 47** Energy performance of the final selected design \_step 2.2.B



## 5.5 COMPARISON

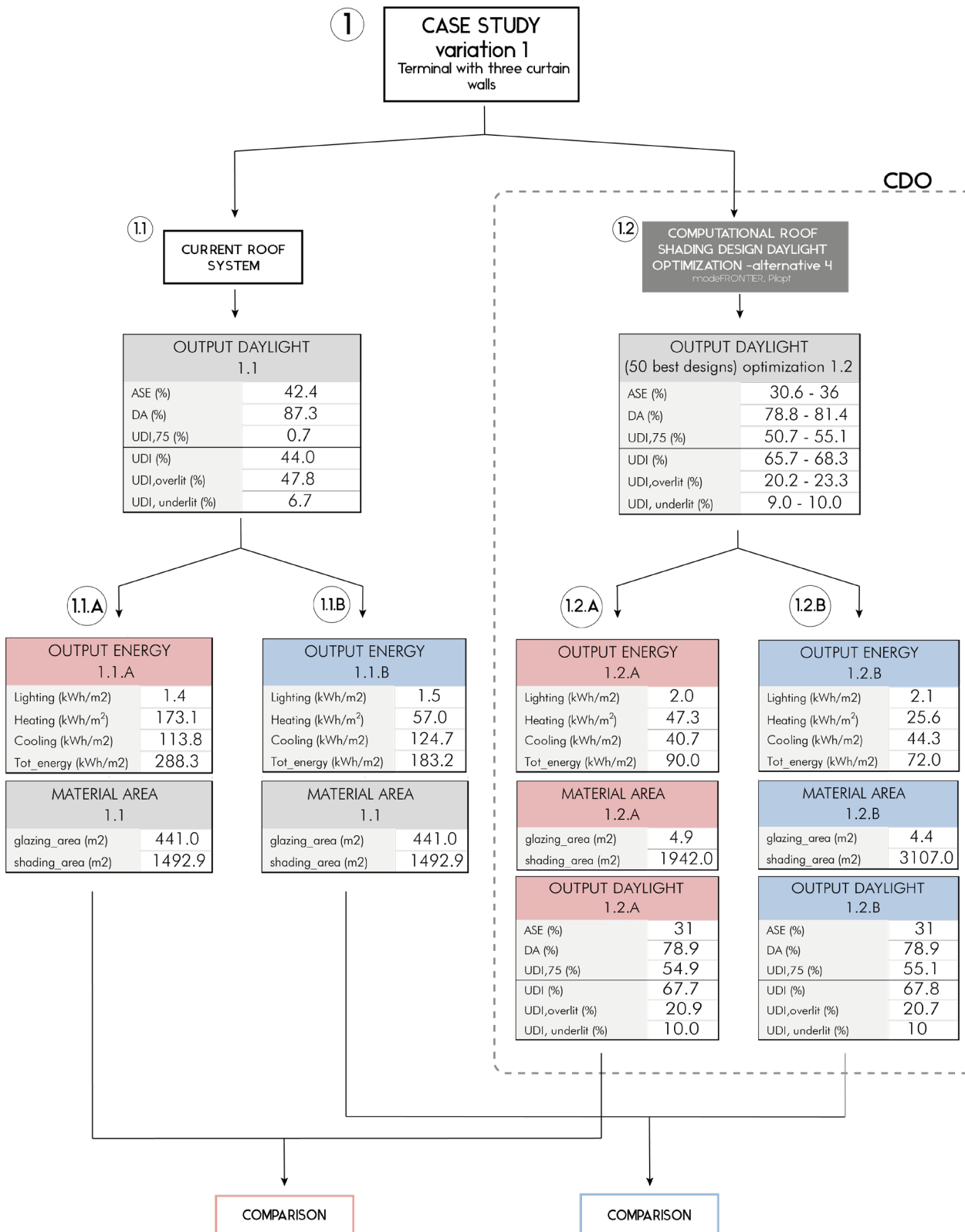


Figure 115 Workflow Case Study variation 1 \_ performance outputs comparison

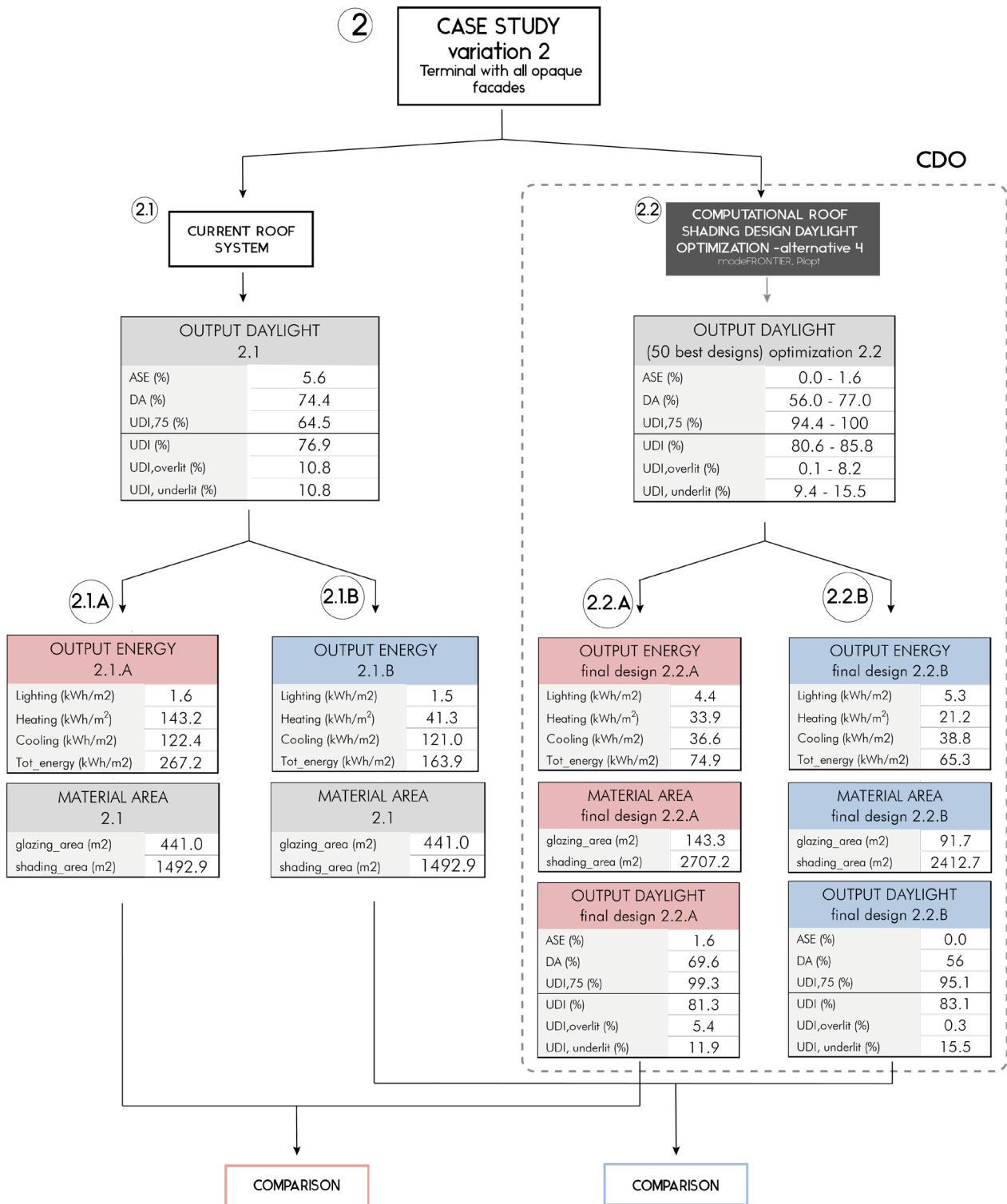


Figure 116 Workflow Case Study variation 2 \_ performance outputs comparison

The workflows above (*Figure 115* and *Figure 116*) are a visual summary of the results obtain from the optimizations of Case Study variation 1 and 2.

### Comparison 1.1 with 1.2

*Table 48* presents the daylight outputs from the selection of the best 50 performing designs in terms of visual requirements. The results reveal how the output of the daylight simulation can be slightly improved, but without achieving extremely positive visual comfort levels. To reduce the overlit conditions as well as the annual sun exposure, the DA constraint is always meet and the DA value is slightly reduced with almost a steady 80% for all the converging designs. The UDI is higher as the UDI,75 with greater values than 47%.

OUTPUT DAYLIGHT SIMULATION concept variation 1		OUTPUT OPTIMIZATION 1.2
ASE	42.40%	30.6 - 36.0%
DA	87.24%	78.8 - 81.4%
UDI	44.02%	65.7 - 68.3%
UDI<	6.70%	9.0 - 10.0%
UDI>	47.77%	20.2 - 23.3%
UDI,75	0.67%	50.7 - 55.1%

**Table 48** Comparison daylight output Case Study variation 1(step 1.1) and optimization 1.2

In chapter “5.3.1 Current roof shading system” section “*OUTPUTS daylight simulation 1.1*” was already proven through performance simulation on the New Schiphol Terminal, that the configuration with three curtain walls façades allows enough daylight to reach good illuminance values in the indoor space.

### Comparison 2.1 with 2.2

OUTPUT DAYLIGHT SIMULATION concept variation 2		OUTPUT OPTIMIZATION 2.2
ASE	5.60%	0.0 - 1.6%
DA	74.37%	56.0 - 77.0%
UDI	76.93%	80.6 - 85.8%
UDI<	10.79%	9.4 - 15.0%
UDI>	10.81%	0.1 - 8.2%
UDI,75	64.51%	94.4 - 100%

**Table 49** Comparison daylight output Case Study variation 2 (step 2.1) and optimization 2.2

For Case Study variation 2, with opaque facade walls, the optimal geometries improve the daylight comfort level by reducing the glare risk and improving the illuminance in the indoor space (*Table 49*). The skylights allow more daylight to enter the building, without allowing large amount of direct sun-rays. The self-shading system redirect the light avoiding overlit situations. The range of values of UDI,75 are extremely high, which indicates a good, uniform illuminance for the whole year.

### Comparison 1.1.A with 1.2.A

- Daylight

The daylight performances are improved by the adoption of the optimized concept 1.2.A. The ASE value is reduced and so the overlit percentage, the UDI,75 is significantly higher. The optimization process on Case Study variation 1 with daylight targets, delivers geometrical configurations that tend to minimize the opening ratio e maximize the shading system inclination. This kind of modules enable to slightly increase the visual targets. The downside of this optimal design is the higher percentage of UDI,underlit. The cause behind this reduction is the aim of the algorithm to avoid increase in the overlit conditions. Closing almost completely the skylights is the algorithm best found solution.

- Energy

The minimization of the roof openings brings to an increment in the lighting energy needed to illuminate the space when the daylight target is not met. On the other hand, the heating and cooling loads of the optimal design are about three times lower than the one of 1.1.A. This leads to a total energy reduction of 69%.

- Material

The final selected concept is composed by an extremely low amount of glass, but with the counter-effect of presenting a shading material area larger of 23% from the existing shading system.

### **Comparison 1.1.B with 1.2.B**

Almost the same observations made for the comparison of concept 1.1.A and 1.2.A. The main difference from setting A and B lays on the total energy demand which is mainly affected by the heating load for setting A, and by the cooling load for setting B. This behaviour is due to the differently insulating materials. The higher insulating material have a bigger impact on the heating energy, which is less dispersed on the outside. In this way the heating energy consumed is extremely lower, while the cooling energy is almost the same. Another difference is the amount of shading surface, which in case of geometry 1.2.B is almost doubled the one from 1.1.B.

### **Comparison 2.1.A with 2.2.A**

- Daylight

The daylight performances are improved by the adoption of the optimized concept 2.2.A. The ASE value is reduced and so the overlit percentage, the UDI<sub>75</sub> is significantly higher. The optimization process on Case Study variation 2 with daylight targets, delivers geometrical configurations mainly perpendicular to the ceiling surface. The opening ratio (scaling-factor) creates a glazing area covering 50% ca of the roof surface. This kind of modules enhance the visual targets.

- Energy

The Daylight Autonomy of design 2.2.A is lower by 4%, this creates an increment in the lighting energy demand. On the other hand, the total energy demand is exceptionally reduced by 72%. Both cooling and heating values are extremely lowered.

- Material

The final selected concept is composed by three times lower glazing area, but with the counter-effect of a shading system composed by a great material surface, almost two times the one of design 2.2.A.

### **Comparison 2.1.B with 2.2.B**

Almost the same observations made for the comparison of concept 2.1.A and 2.2.A. The main difference from setting A and B lays on the total energy demand which is affected by both heating load and cooling load for setting A, while for setting B the cooling load is highest percentage. As already explained before, this behaviour is due to the differently insulating materials. The higher insulating materials have a bigger impact on the heating energy, which is less dispersed on the outside. In this way the heating energy consumed is lowered, while the cooling energy is almost the same.





# 06



## 6.1 ADOPTED WORKFLOW

The adopted Computational Design Exploration (*Figure 117*) and Computational Design Optimization workflow (*Figure 118* and *Figure 119*) are intended as a tool to be used from the early stage of the design process. During the Conceptual Design, many geometrical and physical properties of the building are not yet defined. Therefore, it is very important to consider a wide range of settings when adopting the proposed workflow.

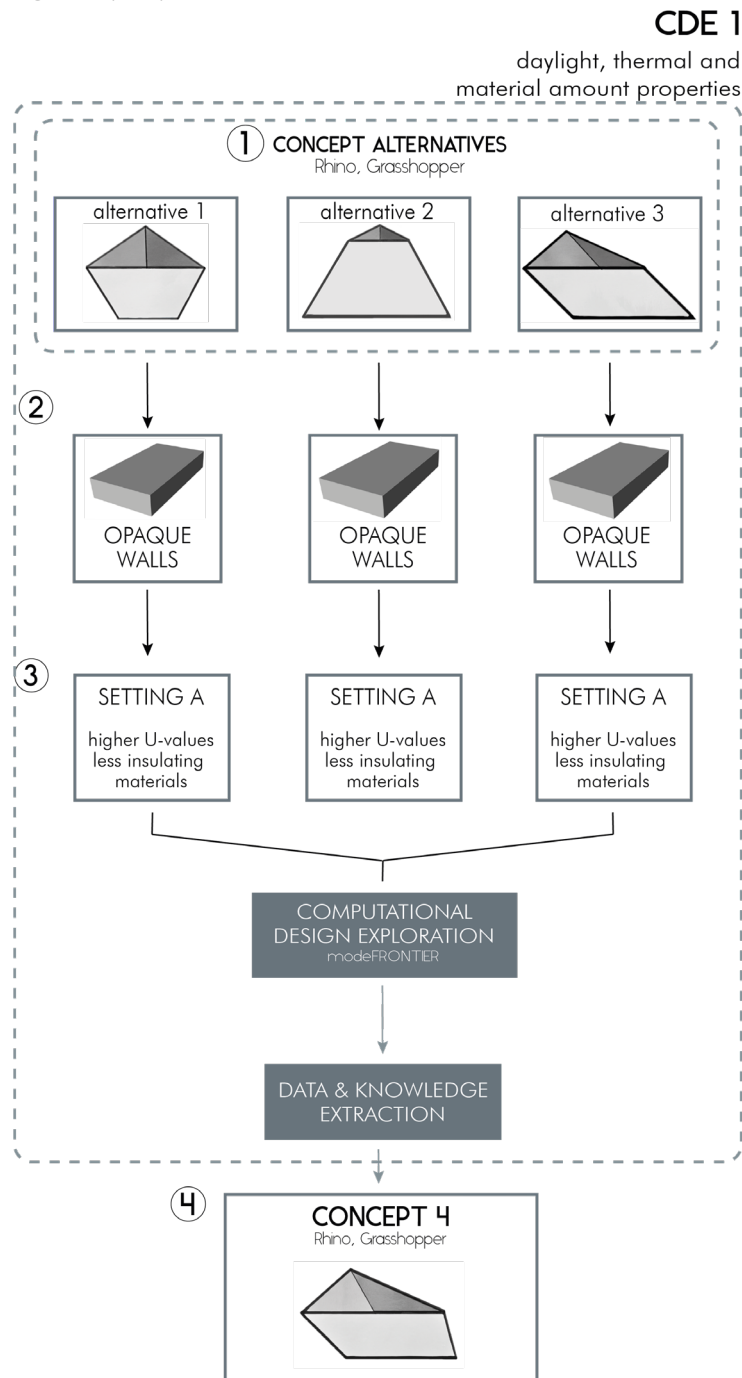


*Figure 117* First proposed and adopted CDE workflow

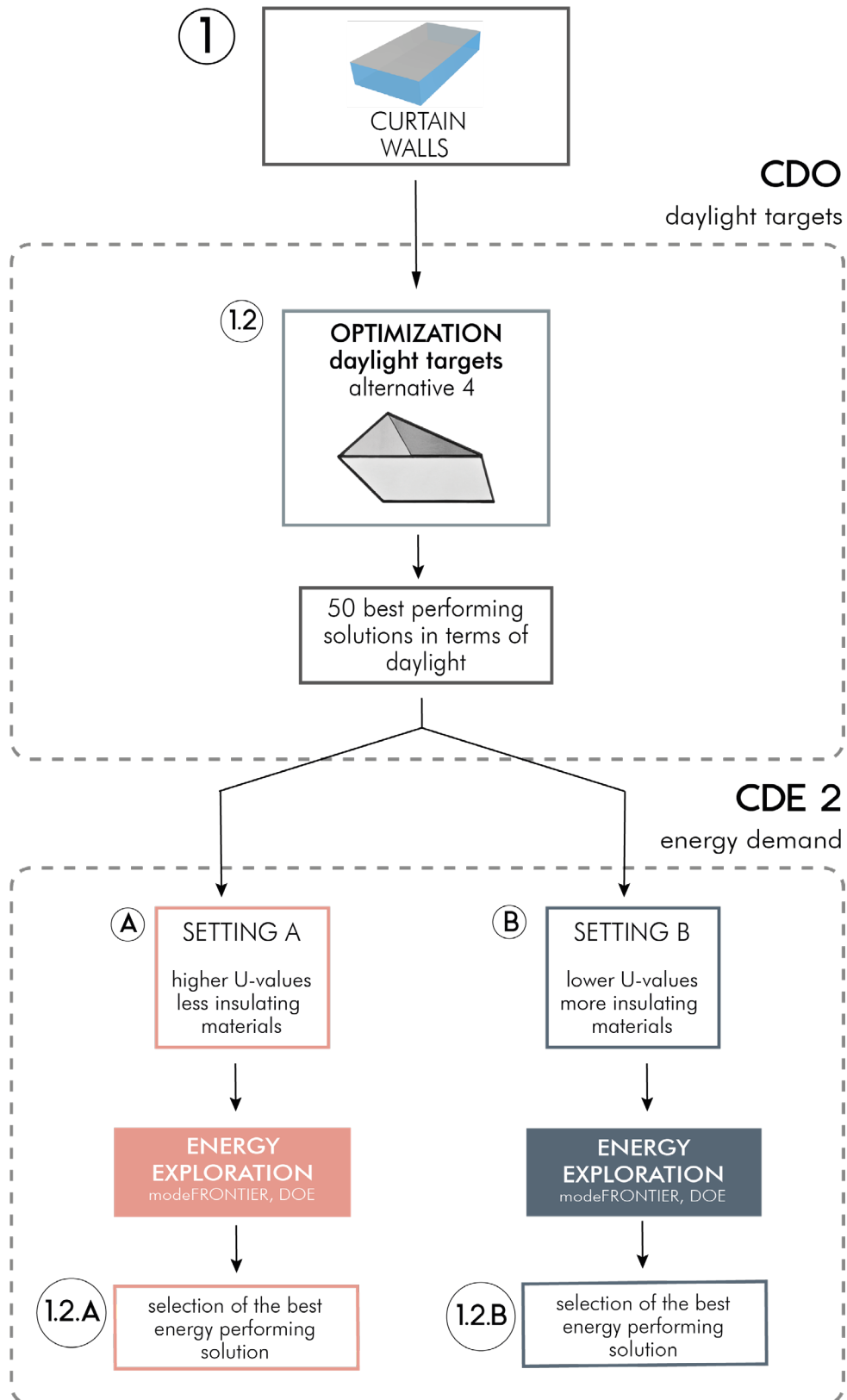


Figure 118 First proposed and adopted CDO workflow applied on Case Study variation 1

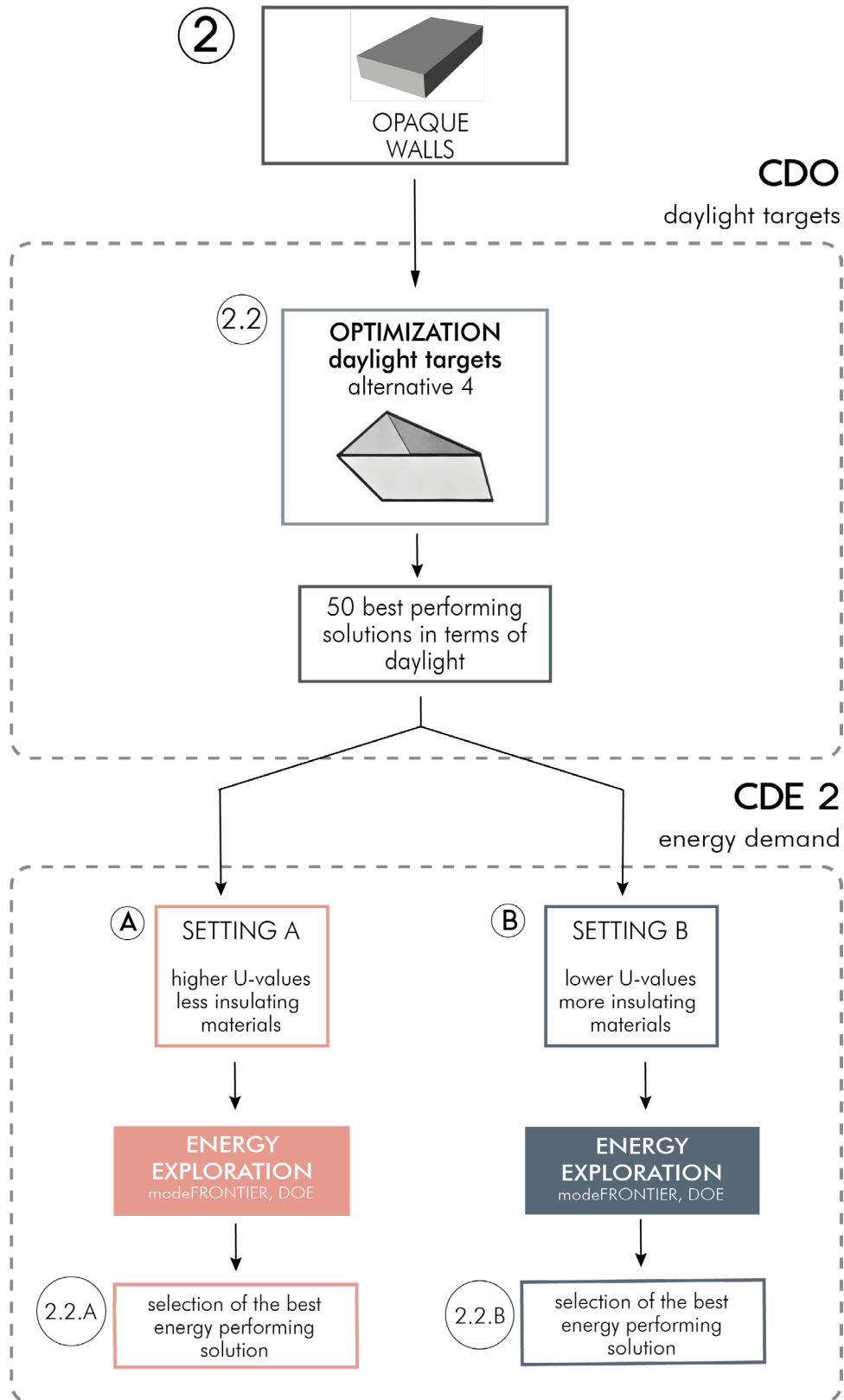


Figure 119 First proposed and adopted CDO workflow applied on Case Study variation 2

The comparison between the visual and thermal performances obtained from the optimization process on Case Study variation 1 and 2, has important implications for the development of a new, more integrated process.

Mainly two observations emerge:

First, the final designs on the Case Study variation 1 (with curtain walls), appear to be significantly different from the ones obtained from the investigation on Case Study variation 2 (with all opaque façades). As conclusion from this differentiation, a more effective way to proceed and ensure an optimal final design, would be to introduce the variation of the construction material already from the CDE.

Secondly, looking at the Case Study variation 1, the energy results show that for the use of less insulating materials (higher U-values, setting A), the heating load is the bigger portion of the total energy demand. While, the energy performances produce a higher cooling than heating load, when calculated with more insulating construction materials (lower U-values, setting B). This observation is valid also for Case Study variation 2 (2.2.A and 2.2.B).

However, the CDE carried out before the CDO process, did not take into account different thermal properties of the material. The significant differences found using setting A and B in the energy performance, imply that including a more specific setting for thermal properties from the Design Exploration is important for the decision of the concept alternative at the end of the Computational Design Exploration.

During the CDE, it is important to consider all the criteria important for the design and give to each criteria a different weight based on the priorities in the design. Therefore, an updated workflow is proposed and discussed in the following section.

## 6.2 NEW PROPOSED WORKFLOW

From the previous consideration a more integrated CDE workflow is proposed (Figure 120). The new process advises to evaluate each concept alternative for both the variations of the Case Study and applying once the less insulating construction materials and once the construction materials with lower U-values. Since during the conceptual phase many geometrical material properties are not yet defined, with the new proposed method a wide range of design possibilities is contemplated and taken into consideration.

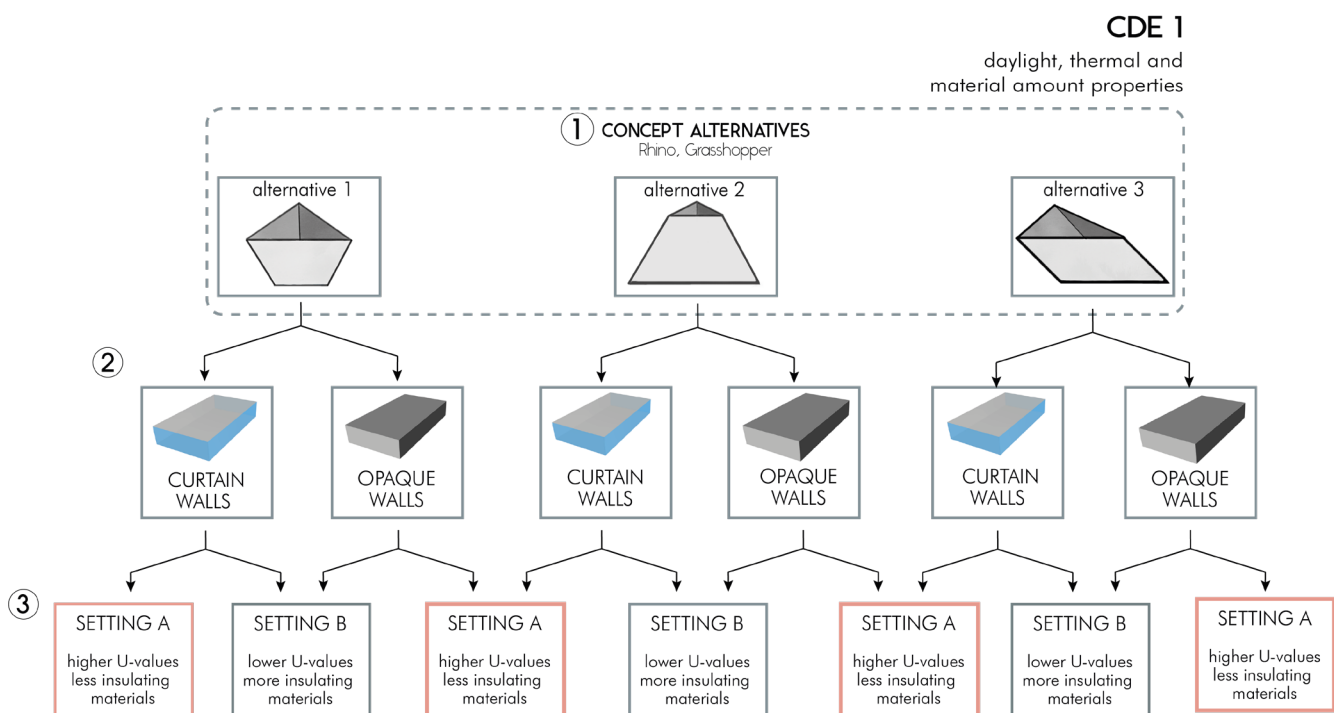


Figure 120 New proposed CDE workflow

At the end of the workflow it is possible to visualise and analyse the design space and identify the best performing concept alternative for each setting combination:

- Opaque walls and setting A
- Opaque walls and setting B
- Curtain walls and setting A
- Curtain walls and setting B

After the sensitivity analysis the user can determine the features that have the

most impact on the targets and come up with a new refined concept alternative, which can be different for each setting. Following from the CDE, the two CDO drafted in *Figure 121* and *Figure 122*, aim to optimise the refined concept alternative to satisfy the performance targets (in this case daylight). A second design exploration (CDE 2) aims to select, between the best designs from the CDO, the solution with lower energy impact.

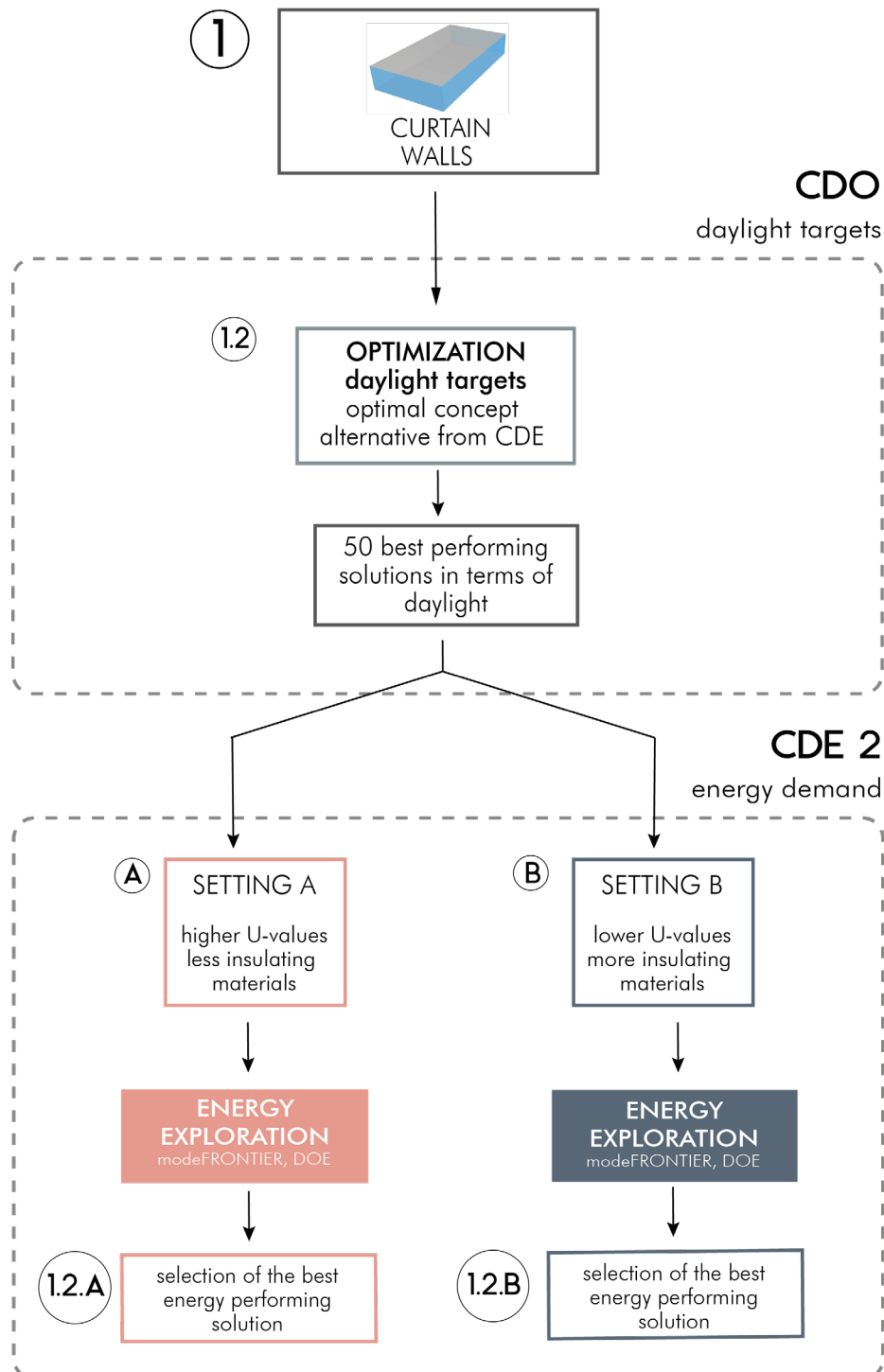


**Figure 121** Final CDE workflow applied on Case Study variation 1

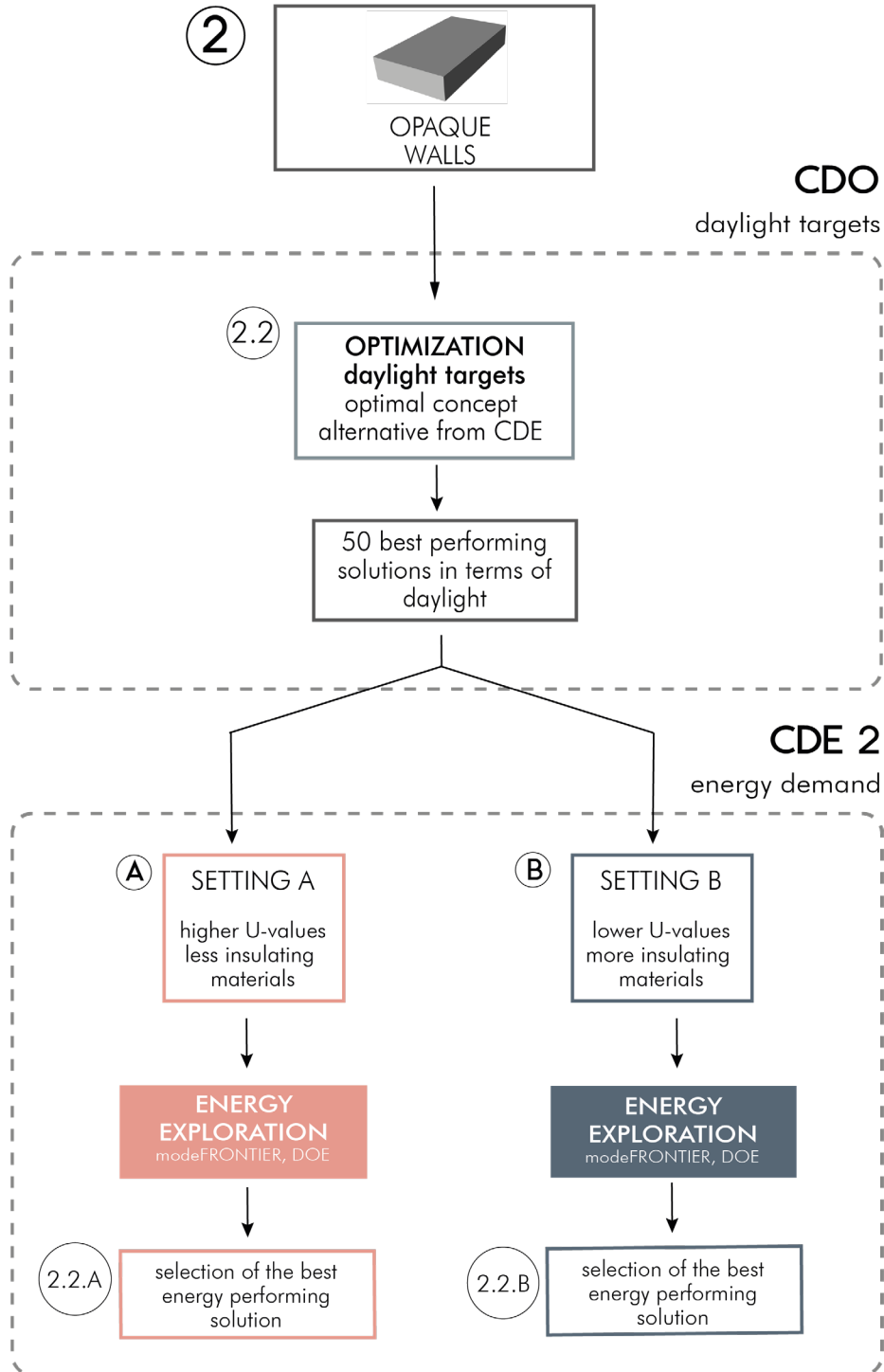


Figure 122 Final CDO workflow applied on Case Study variation 2

The benefits of using this new Computational workflow is that earlier in the design more variables are considered, which enables to include more design possibilities and guide in the decision of a high-performing solution. This approach strives for a minimization of the risk in the concept choice. During the conceptual phase there are still some undefined geometrical and material aspects, therefore introducing more possibilities at the beginning covers more design options.







07





## 7.1 CONCLUSIONS

“In which way can a work-flow, based on computational design exploration and optimization, be a supportive tool for the design decision making of customized large span roofs shading systems? ”

- *Which CDE and CDO workflow can be applied for this research?*

This project was undertaken to propose a computational workflow and evaluate its effectiveness as supportive decision-making tool from the early design stage of large roof shading systems. The proposed Computational Design Exploration is adopted to evaluate three different concept alternatives in terms of daylight and thermal performances. Based on the visualization and analyses of the data, the best morphological performing features of the three alternatives are identified and the design is refined to create an optimal fourth concept. In a second phase, the Computational Design Optimization workflow is applied to obtain high performing solutions in terms of daylight objectives, by varying geometrical and material inputs. 50 configurations are selected as optimal. The post process of the CDO consists of a second CDE, in which the selected samples are evaluated in terms of energy performance. The final shading system is chosen by identifying the input settings that allow the lowest energy consumption. As result, the daylight requirements are fulfilled and the thermal properties are used as final decision criteria.

One of the more significant findings to emerge from this study is that the CDE is an essential step in order to obtain a good solution. It is advised to invest more time and effort in this early step, rather than focus on the late-stage design optimization. The primary formulation of good design concepts is crucial to obtain a high-performing final design. A properly delineated and solid exploration workflow, is the most effective way to approach a multi-objective design problem.

The focus of this study is on large span roof shading systems. Following the steps prescribed by the proposed workflow, the results show that thermal properties of the construction materials are an important factor for the outcome of the Computational Design Exploration. Therefore, changing the insulation of the building would likely lead to different optimal concept alternatives.

The Computational Design workflow (CDE and CDO) used for the New Schiphol Terminal leads to a shading system configuration which enables better visual and thermal conditions in the indoor space, compared to the current roof shading system.

To prove the adaptability and demonstrate the potential of the proposed method, two opposite situations are test. One using the current building design, with three curtain walls, and the second one in which the whole façade is completely opaque. The outcomes show in both cases that the use of the optimal refined concept (alternative 4) improves daylight performances of the indoor space. However, the Case Study with the curtain walls is characterized by high illuminance levels, even when no skylights are present and the ceiling is completely closed. This highly affects the optimization algorithm, which provides optimal designs that exhibit configurations that tend to minimize the roof opening ratio and create self-shading systems. Contrarily, the final design from the workflow applied on the Case Study with all opaque walls, shows a more feasible geometry, which improves the visual comfort of the space yet minimizing the overlit and underlit conditions.

Based on the results obtained from the Computational workflow applied on the two variations of the Case Study and the differentiations in the outcomes, a new Computational Design Exploration workflow is proposed. The new process aims to integrate a wider range of contextual possibilities, such as building configurations and material properties. The advantage in contemplating more possibilities during the exploration phase, lays in the realization of a larger design space, which allows an easier evaluation of the concept alternatives in later phases. The consideration of a large amount of design possibilities reduces the risk of striving for a specific concept based on the wrong design assumptions.

- *Is it possible, using this workflow, to extract general rules and knowledge that can be applied for multiple case studies rather than a specific one only?*

The computational workflow is not only finalized on helping the design selection, but provides also visualization and exploration features. These components assist the learning process of the user and define a new way for creative and informed choices. This efficient set of techniques have many advantages, such as the reduction of time for data and knowledge extraction and the smart identification of robust and reliable designs.

The numerous options to perform statistical analysis provide an effective instrument to determine the correlation effect between variables. The numerous possible investigations and the visual aspect, are the essential factors to obtain insights into the input-input and input-output effects.

In the architectural design process, the experience remains one of the most powerful tools to support the decision making. The proposed computational workflow is not a way to substitute experience, but rather to introduce guidelines to explore the alternatives and assist the decision with data analysis and visualization. The use of a powerful tool which can provide multiple comprehensible graphical data organization and analysis methods, has an essential role in multi-criteria design problems. When the options to select from are numerous, it may be difficult.

The knowledge extracted from the use of the workflow on the Case Study can be used for similar design problems, such as different concept geometries for shading systems for large span roofs. But it is more complex to derive general knowledge applicable to completely different design problems.

However, the process described by the workflow can be adapted for other multi-objective design explorations.

- *Is it beneficial the use of the proposed workflow over the traditional computational design optimization (CDO) conducted in late stages of the project?*

The proposed workflow is intended as tool to carry out a more informed design decision process.

The overall computational workflow adopted is rather different from the traditional method. Generally, the traditional design exploration is guided by experience and is not rigorously proved. Sometimes experience might lead to the choice of a non-optimal design. Some alternatives or features might seem obvious to categorize and their effect easy to predict in advance. However, these pre-judgement can mislead the choice and overshadow other alternatives. Even what it seems logical needs proves.

The new computational workflow allows a computer based design exploration, though the designer 's freedom is still maintained. The proposed workflow assists the decision-making process, without excluding the user's will or his/her autonomy of judgement. The wishes of the user are still respected and the designer is still holding the decision. One of the powerful aspects is the interactive nature of the workflow. The ranking of the concept can still be made in line with the user personal preferences.

The graphical visualizations of the elaborated results and data analysis is very interesting and makes it possible to understand and explain the design features, grab the content of the data and understand the alternatives deeply. With a good understanding of the designs, a valid computational design tool allows the designer to play with the variables, still in line with the main design objectives. These are some of the main features why the use of this modern workflow, supported by valid computational software, can improve the design process, leading to better and optimal solutions.

## 7.2 FUTURE WORK

This study represents only one step in the broad world of computational exploration and optimization. The scope of this study is limited to the application of large span roof shading systems. The number of variables that are analysed is narrowed down to the most essential ones for this particular case. Several questions remain unanswered and the research could be extended in different directions.

- Further studies, which take more or different variables into account, will need to be undertaken. This research focusses mainly on the geometrical morphology of the shading system, and particularly on one concept typology. The final proposed workflow could be applied to other designs in order to determine its effectiveness. More complex shading geometries could be analysed, with the integration of double-curved surfaces and the use of attractor points. However, complex geometries have some limitations when performing daylight and energy simulations with Honeybee and Diva. The complicated geometry adopted results in a time consuming process. The complexity leads to excessive simulation time, up to seven hour per simulation. Before going into excessively complicated geometries, some research and effort is needed in the reduction of the simulation time.
- During the design exploration it has been observed that the energy simulation is the most time-consuming phase of the process. Therefore, during this research it was attempted to solve this issue by substituting the energy simulations with radiation analyses. However, the correlation between solar radiation and energy demand results to be rather complex. Further work is required to establish whether radiations analysis could be a valid alternative to thermal model calculations.
- An extension to this research could implement Photovoltaic panels and Building Integrated Panels in the shading module. The workflow could be used to optimize the energy produced with particular attention to the minimization of self-shading effect, which would reduce the PV panel production. Also, the dynamic shading option could be an interesting study to conduct.
- This research clearly concentrates the attention on the CDE and CDO workflow rather than on evaluating the interaction effects

of the input variables on the performances. Further research is needed to better understand the correlation between variables. If the research focuses on the knowledge extraction deriving from the use of the workflow, a more effective method would be to reduce the number of variables and constrain the objectives to one main performance aspect (for instance only daylight requirements). Realizing a more specific study is expected to provide better insight in the application field.

- In future investigations, it is suggested to compare the results obtained in this thesis with the ones obtained following the same process, but using different computational tools. modeFRONTIER is the software used for this study with the power of the selection of pilOPT, a multi-strategy self-adapting algorithm. The adoption of a different multidisciplinary design optimization (MDO) platform instead of modeFRONTIER, or another optimizer algorithm could be an interesting study to conduct.

- For the completion of this study, the final proposed workflow needs to be tested and its validity proved. The suggested process can still be improved and generalized to obtain a fully integrated, holistic method, suitable for every kind of multi-objective design problem.





08





## 8.1 APPENDIX A

## The electromagnetic theory

Maxwell explains the light as a combination of electric and magnetic waves which travels together, perpendicularly to the propagation direction and to each other.

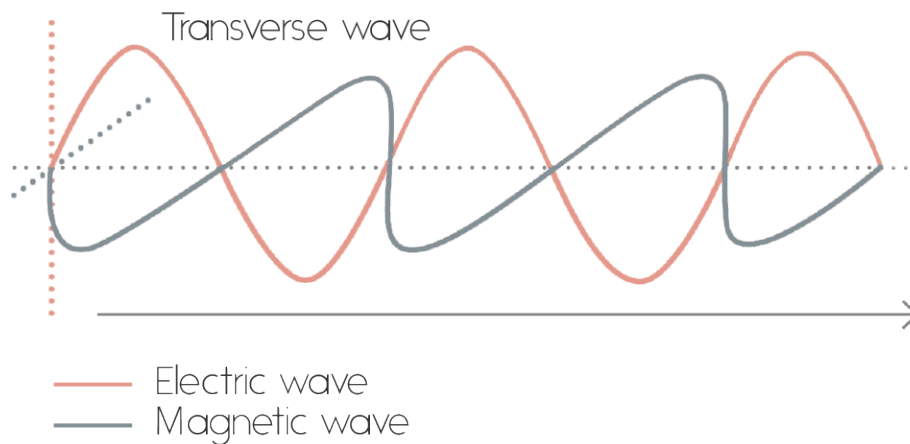


**Figure 123** Electromagnetic wave. Source: van Bommel & Rouhana, 2016

The electromagnetic nature of light allows its propagation not only through matter, but also through vacuum (van Bommel & Rouhana, 2016). A wave is characterized by mainly four properties:

- The speed of light ( $c$ ) is approximately 300.000 km/s
- Wavelength ( $\lambda$ ), which is the distance between one peak (or bottom) and the successive one
- Peak amplitude ( $a$ ), the length from the equilibrium line to the crest (or lowest point) of the wave
- Frequency ( $f$ ) is the ratio between the speed of light and the wavelength, its unit is Herz (Hz)

$$f = \frac{c}{\lambda}$$

When a light wave strikes a metal the electromagnetic field changes, as a reaction the electrons start to vibrate. In response to the increase of the wave intensity, the vibration of the electrons of the metal increases. At certain frequency the electrons get ejected from the metal and the higher the frequencies, the bigger the kinetic energy of the electrons that have been ejected. Each metal surface is different and necessitates a specific minimum frequency in order to eject its electrons.

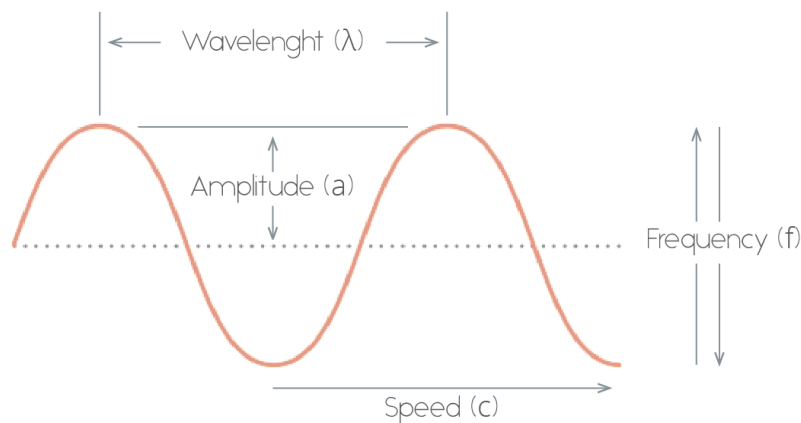


**Figure 124** Characteristics of light wave. Source: van Bommel & Rouhana, 2016

The wave theory was accepted until the end of the 19th century, however it could not explain some phenomena like the black body radiation or the photoelectric effect (Jagielski, 2009). Later in time, Einstein developed the quantum theory based on the alternative of 'quantization of energy' from Max Planck.

### The quantum theory

Einstein in 1905 defined the quantum theory based on Planck's idea. This theory assumed that radiation is emitted in forms of indivisible particles called quanta or photons when talking about visible light. These particles are energy packets, each photon carries the same amount of energy, which depends from the light frequency. The following equation is called the Planck - Einstein relation and defined the energy carried by each quantum as:

$$E = hf$$

Where

- **E** is the photon energy

- $h$  is the Planck's constant defined as  $6.63 \times 10^{-34}$  joule · second (J·s)
- $f$  is the frequency

When the photon hits another material, its energy is transferred to the material's electrons. If the frequency is high enough (and so is the quantum energy), the electrons are ejected. If the quantum energy is higher than the one necessary to eject the electrons, the left over energy is transformed in kinetic energy possessed by the escaped electrons.

Results of Photoelectric Experiments*				
Frequency of Incident Light (Hz)	Kinetic Energy of Released Electrons (J)			
	Cesium	Sodium	Tungsten	
(Red) $4.5 \times 10^{14}$	None emitted	None emitted	None emitted	
(Orange) $5.0 \times 10^{14}$	$0.109 \times 10^{-19}$	None emitted	None emitted	
(Green) $5.5 \times 10^{14}$	$0.440 \times 10^{-19}$	$0.120 \times 10^{-19}$	None emitted	
(Blue) $6.0 \times 10^{14}$	$0.772 \times 10^{-19}$	$0.451 \times 10^{-19}$	None emitted	

\*These results are the same for all intensities of light illuminating the metal surface.

**Table 50** Results of Photoelectric experiments. Source: <https://web.phys.ksu.edu/fascination/Chapter17.pdf>

A greater number of photons emitted by the source means an higher intensity of the light. The more the intensity, the higher the number of electrons released by the metal. In conclusion the frequency is representative of the photon energy and determines if the electrons are ejected and which is their kinetic energy, the light intensity represents the number of photons emitted per second and determines the number of electrons ejected. Despite this theory gave answer to many questions, still some phenomena could no be explained like the light diffraction and interference.

## The duality of light

In 1924 De Broglie came up with the wavelength theory, which states that the nature of light is dependent from its wavelength. De Broglie combined the wave and particle theory explaining how, depending from particular circumstances, the wave or particle nature may prevail.

$$\lambda = \frac{h}{p}$$

Where

- $\lambda$  is the de Broglie wavelength, given by  $\lambda=c/f$  (c is the speed of light in vacuum, f is the frequency of the light) (m)
- $h$  is the Planck's constant, which is defined as  $6.63 \times 10^{-34}$  joule · second (J·s)
- $p$  is the momentum of a photon, given by  $p=mv$  (m is the mass of a particle, v is the velocity of a particle) (kg·m/s)

The de Broglie wavelength is directly proportional to the momentum of a particle, the greater the momentum, the smaller the wavelength and vice versa.

## Refraction

When a beam of light travelling in a medium encounter another material with a different density, and with angle of incidence other than perpendicular, the light rays direction changes (or bent). The changing in direction of the light beam strictly depends on the variation in speed from one medium to the other, and it also depends on the angle of incidence.

This phenomenon is represented by Snell's law, which discloses the relation between the refraction indexes of the two mediums ( $n_1, n_2$ ), the incidence angle ( $\theta_i$ ) and the refraction angle ( $\theta_r$ ).

$$n_i \cdot \text{sine}(\theta_i) = n_r \cdot \text{sine}(\theta_r)$$

$$n = \frac{c}{v}$$

Where

- $n$  is the index representing the refraction
- $c$  is the light speed measured in the vacuum

- $v$  is the light speed when travelling in the considered medium

The same law can be expressed using the speed of light travelling through the two materials ( $c_i, c_r$ ).

$$c_i \cdot \sin(\theta_i) = c_r \cdot \sin(\theta_r)$$

The behaviour of light is also dependent on the structural properties of the material of incidence. The materials can be divided in three categories: smooth, rough and mixed surfaces (Pinterić, 2017):

- Completely **smooth surfaces** produce specular reflections and transmissions because the orientation of the surface is homogeneous, so  $|\theta_i| = |\theta_r|$ .

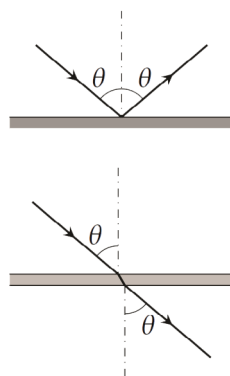


**Figure 125** Smooth surface, specular reflection and transmission. Source: Pinterić, 2017

- **Rough surfaces** are characterized by irregularities, the light refraction angle depends on the point of incidence. The result is a diffuse reflection and no beam is created.

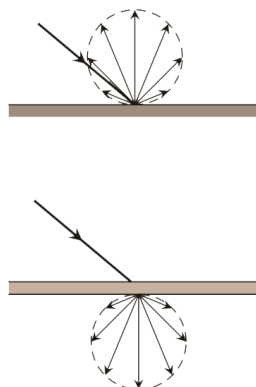


**Figure 126** Rough surface, diffuse reflection and transmission. Source: Pinterić, 2017

- Mostly the materials have surfaces properties in between smooth and rough, so the reflections and transmissions are called glossy. The beam is not created, but the direction of the reflected or transmitted rays are concentrated in an area close to the specular direction.

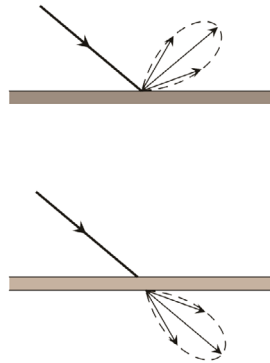


**Figure 127** Real surface, glossy reflection and transmission. Source: Pinterić, 2017

## Diffraction

The phenomenon of diffraction concerns, as the one of refraction, the bending (or changing of direction) of the beam of light. In this case, the deviation of the light rays is due to the interference with an obstacle or the passage through a hole. When a beam of light face up an obstacle or a tiny hole, two or more waves can come closer and when they finally meet they create interference. Diffraction is complex and can produce constructive or destructive interference.

- **Constructive interference** appears when two waves encounter and they are aligned (their phase difference is a multiple of  $2\pi$ ). In this case they sum up, producing a third wave with greater amplitude.

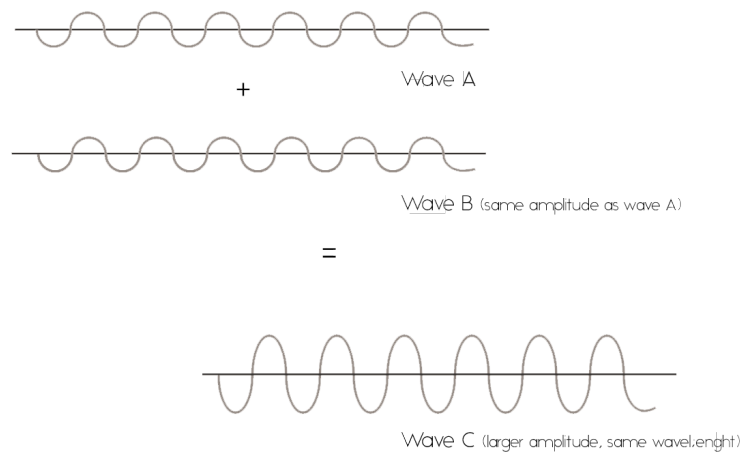


**Figure 128** Constructive interference.

- **Destructive interference**, on the other hand, appears when two waves meet when they are out of phase (the phase difference is multiple of  $\pi$ ,  $3\pi$ ,  $5\pi$  etc.) . In this case the final result is a wave with lower amplitude. In case the two waves have same amplitude, the final result is the elimination of the wave.

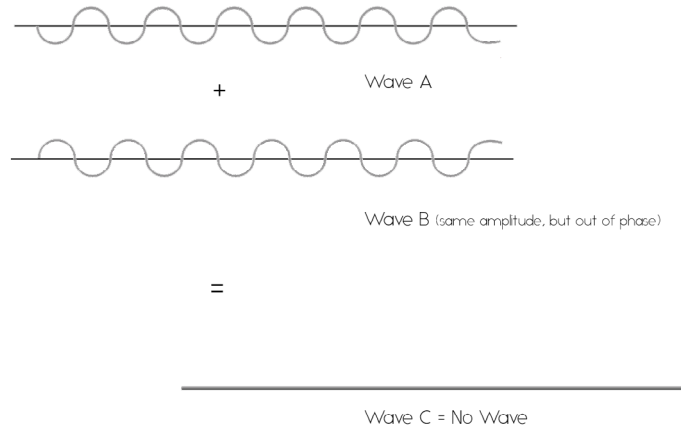


**Figure 129** Destructive interference.

## 8.2 APPENDIX B

### 8.2.1 SAINT-GOBAIN PRODUCTS

Finishing material for the skylight module used for the daylight simulation.

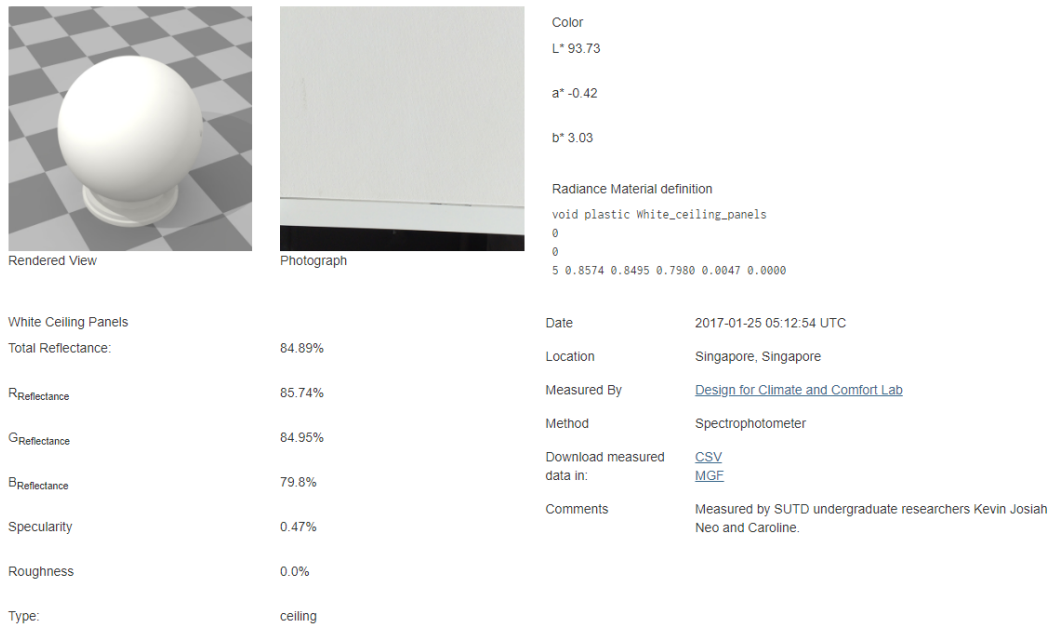


**Figure 130** White ceiling panels used for skylights. Source: <http://spectraldb.com/materials/1392>

## 8.3 APPENDIX C

### PARAMETRIC MODEL

#### Geometry reference building

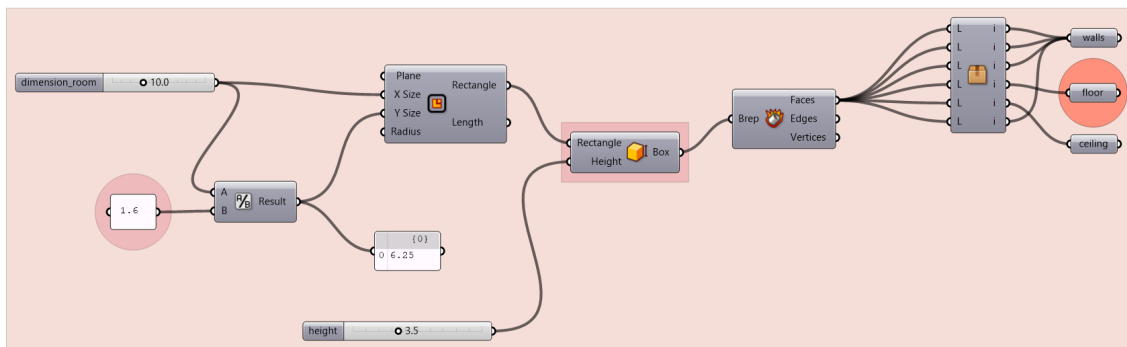


**Figure 131** Reference building geometry

The building geometry is built as rectangular floor plan, with the long side on the x-direction and the short side following the y-direction. The y-axis represents the north orientation. The geometry has a base dimensions of 10 \* 6.25m, which is then extruded with a height of 3.5 m. The space is used as single zone to perform the energy simulations. From this rectangular prism are extracted the walls, floor and ceiling surfaces, to which are assigned thermal and visual properties, as shown in....

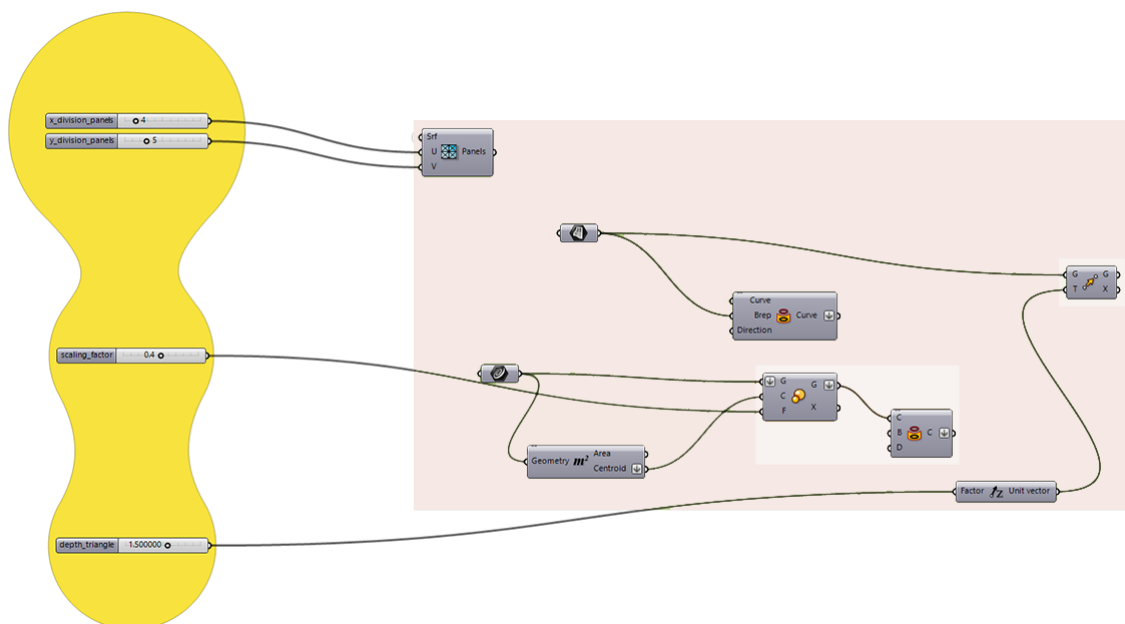


**Figure 132** Basic geometry as starting definition of the three alternatives

## Modules of the shading system

The ceiling/roof surface is divided in panels, which are controlled by the *x\_division\_panels* and *y\_division\_panels* sliders that can vary the number of divisions in the x and y directions. The *depth\_triangle* can modify the height of the shading modules, projecting the triangular elements on the z-direction. Lastly, the parameter *scaling\_factor* can scale down the dimension of the triangular element creating the protrusion of alternative 1 and 2.

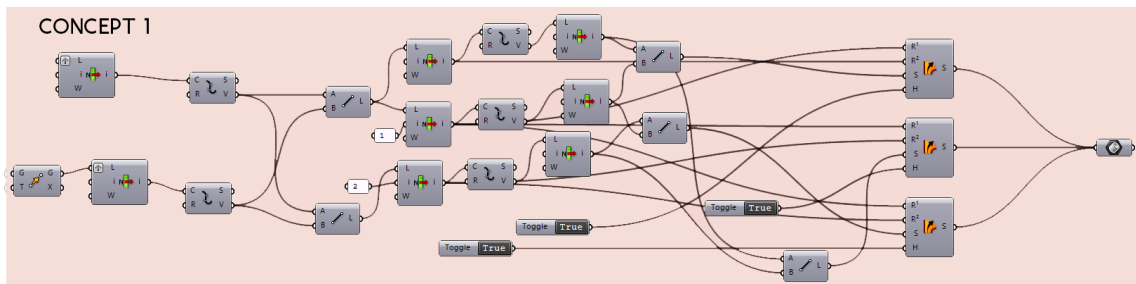


Figure 133 Construction of alternative concept 1

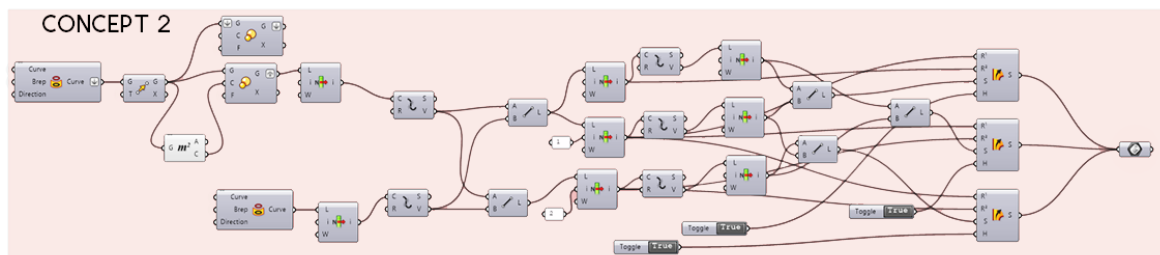


Figure 134 Construction of alternative concept 2

Alternative 1 and 2 are constructed as surfaces between following rails, connecting the two grid of triangular panels on the x,y-plane at different height.

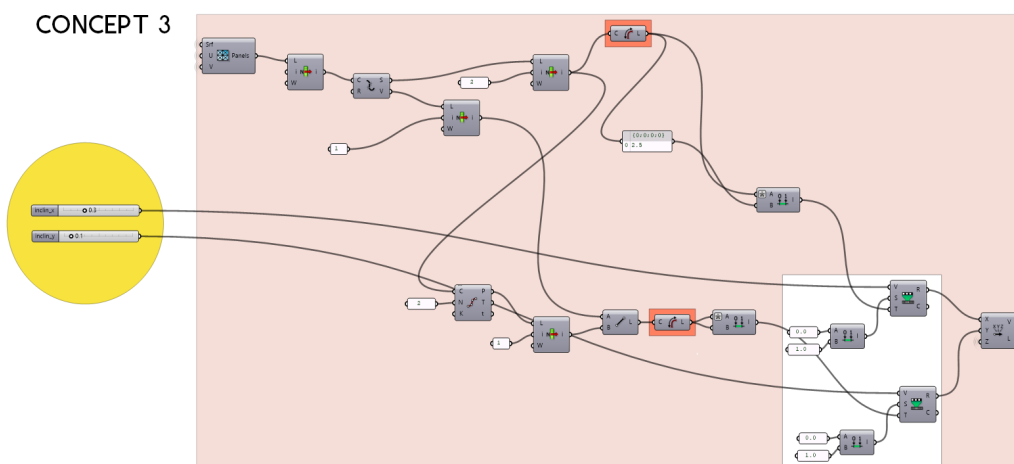
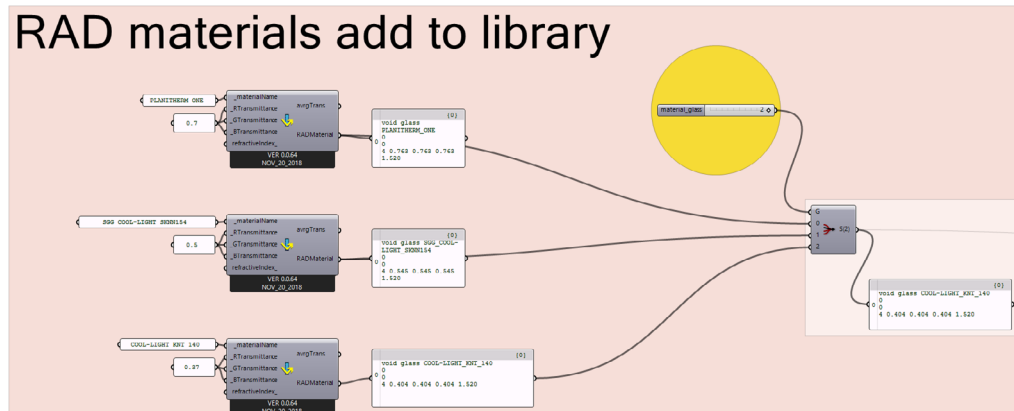


Figure 135 Construction of inclinations for alternative concept 3



(*shading\_area*) is calculated.

### Radiance skylights material



**Figure 138** Definition of Radiance materials

The daylight simulations require the assignment of radiance materials to each surface. The glazing material assigned is customized and the typology is chosen from the Saint-Gobain glass product guide (2013). The value representative for the glazing for the Radiance analysis is the VT.

The slider *material\_glass* determines which glazing option is picked and applied as skylight material.

### DIVA daylight simulations

DIVA 4 - DAYLIGHT SIMULATIONS		
floor	GenericFloor_20	fixed
walls	GenericInteriorWall_50	fixed
roof/ceiling	GenericCeiling_80	fixed
shading	SheetMetal	fixed
skylights	0 - SGG PLANITHERM ONE	variable
	1 - SGG COOL-LITE SKN 154	
	2 - SGG COOL-LITE KNT 140	

**Table 51** DIVA input Radiance materials

The daylight simulations are run using the plug-in DIVA 4. A Radiance material has been assigned to each surface as shown in *Table 7* and *Table 10*.

Material properties:

- GenericFloor\_20 - reflectance of 20%,
- GenericInteriorWall50 - reflectance of 50%
- GenericCeiling\_80 - reflectance of 80%
- SheetMetal \_ reflectance of 90%

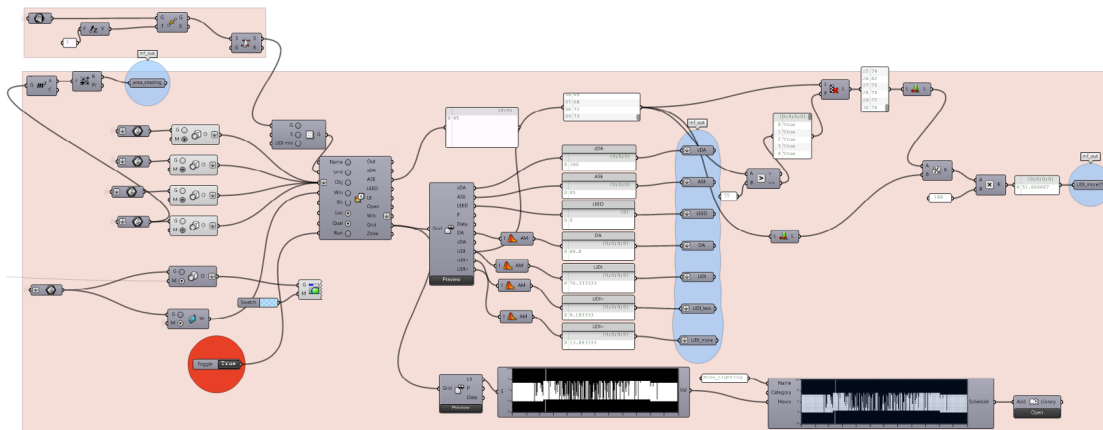


**Figure 139** Daylight simulation in DIVA 4

The grid defined for the DIVA simulations is the floor surface at 1 meter elevation. The grid has a sensor point at 1 meter from each other, with a total of 62 sensor points. The weather data sets used is the ASHRAE IWEC2 which contains data representative of a “typical year” for international locations including Amsterdam, Netherlands (NLD\_Amsterdam.062400\_IWEC retrieved from the energyplus website: [https://energyplus.net/weather-location/europe\\_wmo\\_region\\_6/NLD//NLD\\_Amsterdam.062400\\_IWEC](https://energyplus.net/weather-location/europe_wmo_region_6/NLD//NLD_Amsterdam.062400_IWEC)). The daylight indexes calculated are annual values, thus the design is evaluated for the whole year.

The outputs calculated are the following:

- sDA - spatial daylight autonomy (on *paragraph 2.4.2*)
- ASE - annual sunlight exposure, is the percentage of area with more than 250 hours with more than 1000 lux
- DA - daylight autonomy (on *paragraph 2.4.2*)

- UDI - useful daylight illuminance (on *paragraph 2.4.2*)
- UDI,underlit - percentage of time in which the grid receives less than 100 lux (on *paragraph 2.4.2*)
- UDI,overlit - percentage of time during the year in which the overlit conditions are met (>2000 lux) (on *paragraph 2.4.2*)
- UDI,75 - this score indicates the percentage of analysis surface area that during the year are in the UDI range (100-2000 lux) for at least -75% of the time.

Furthermore, also the total area of the shading system is recorded.

The lighting schedule derived from the daylight simulation is used as input in the energyply calculation to measure the light energy needed to reach the daylight threshold of 300 lux. The lighting load is 5 W/m<sup>2</sup>. The dimming option is on, thus the lighting are turned off or on whether the daylighting target is reached or not. When the illuminance target is met only with natural light, the lighting system is off, while when the illuminance is lower than the threshold the system considers the fixtures on.

### DIVA radiation analysis

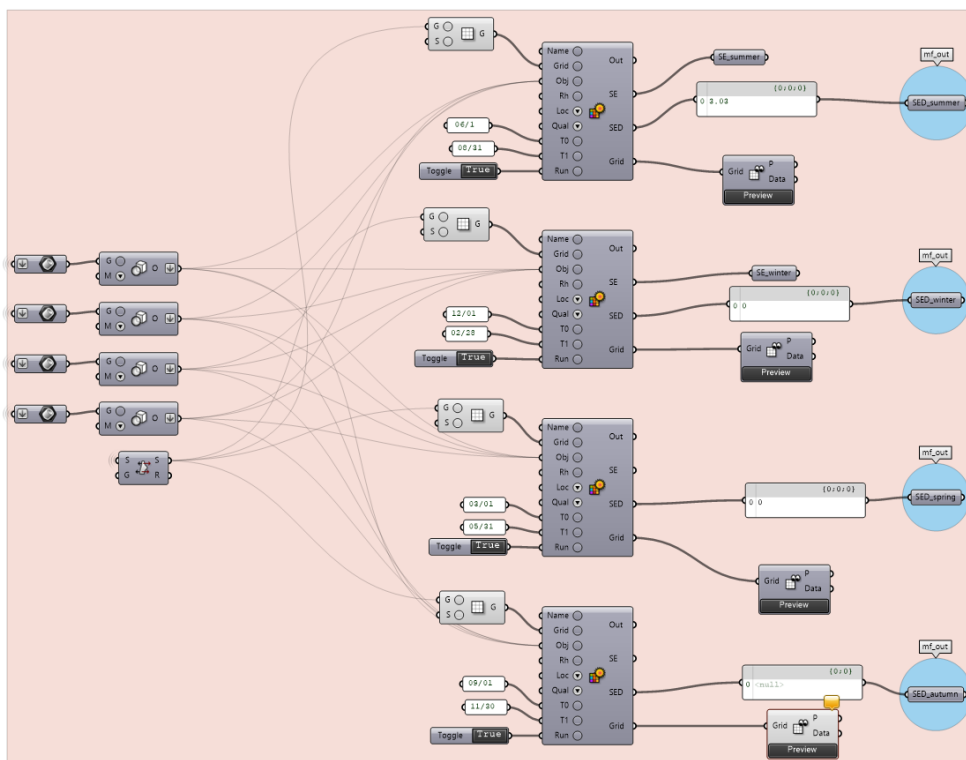


Figure 140 Solar radiation simulation in DIVA 4



## 8.4 APPENDIX D

The multi-analysis chart below (see *Table 52*, displays the grade and weight assigned to each criteria for the concept selection after have carried out the computational design exploration.

PARTIAL SCORES		ALTERNATIVE 1	ALTERNATIVE 2	ALTERNATIVE 3	WEIGHT
DAYLIGHT PERFORMANCE	DA	1	4	3	3
	ASE	2	4	3	3
	UDI	2	3	4	3
	UDI_less	1	4	3	1
	UDI_overlit	4	2	3	2
	UDI_more75	2	3	4	3
MATERIAL AMOUNT	area_glass	4	1	2	1
	area_shading	2	1	4	1
ENERGY PERFORMANCE	lights_elec_energy	1	4	3	1
	tot_cooling	2	4	3	2
	tot_heating	4	1	2	3
	tot_energy	4	1	2	3

**Table 52** Multi-criteria analysis table with scores for each criteria and weights

## 8.5 APPENDIX E

### 8.5.1 HISTORY CHARTS 1.2

History charts of computational design optimization 1.2.

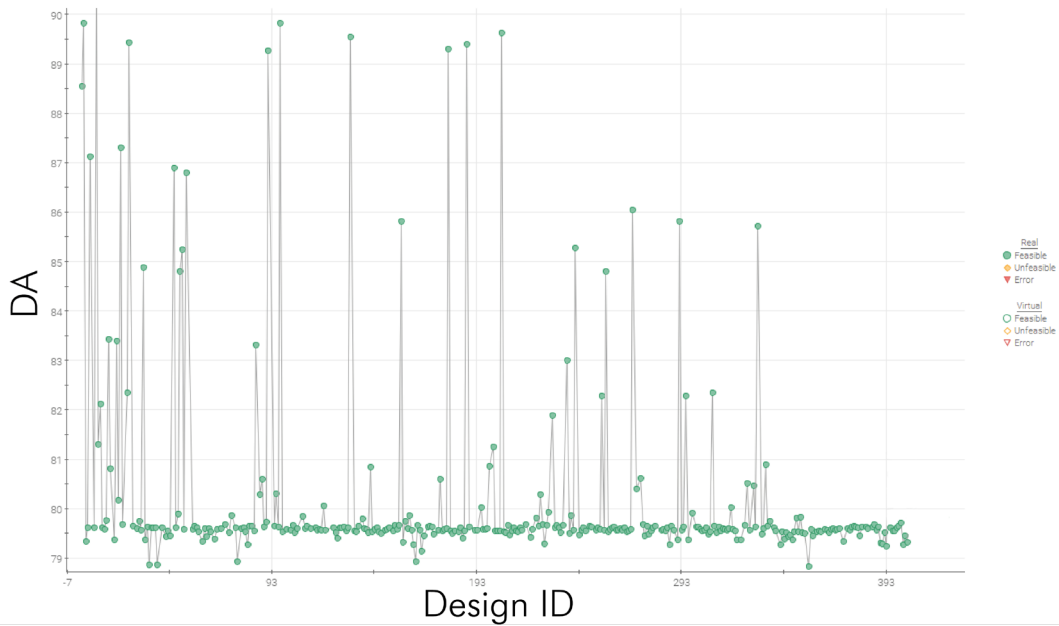


**Figure 142** History chart of the optimization algorithm converging to constrain DA

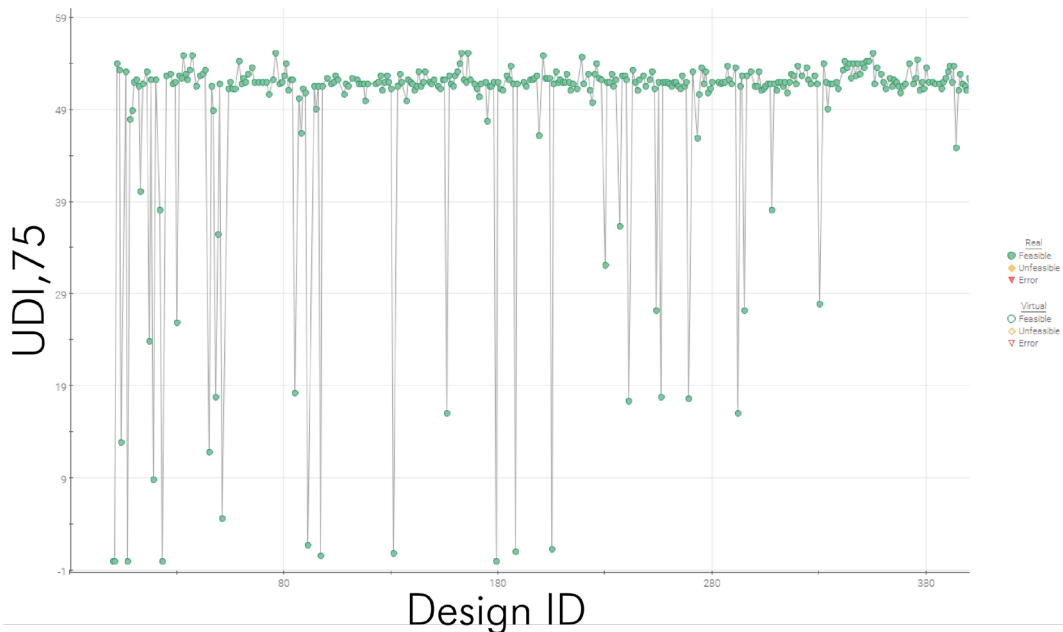
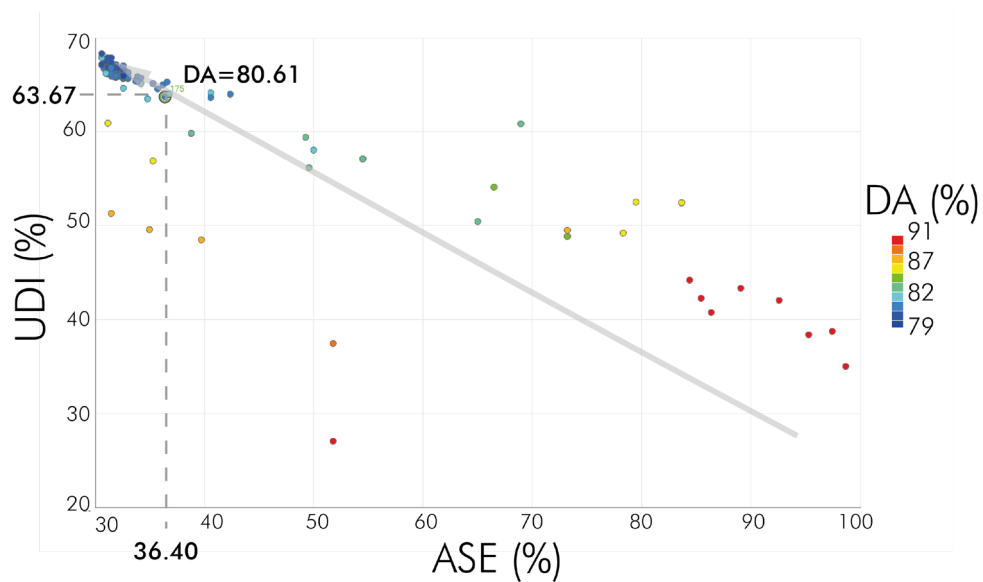
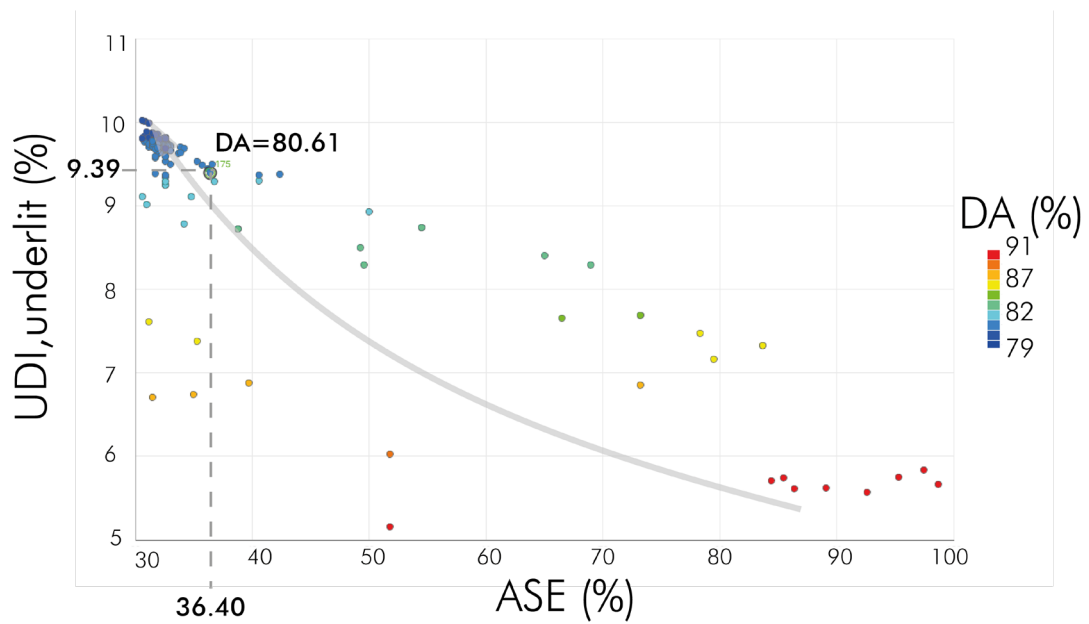
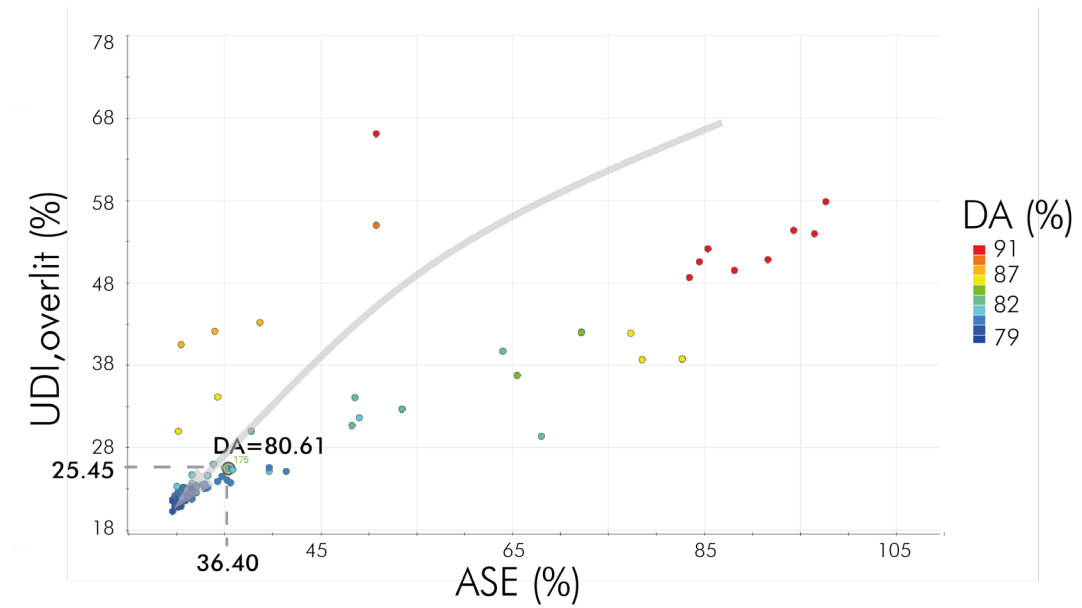


**Figure 143** History chart of the optimization algorithm converging to maximize UDI,75

### 8.5.2 BUBBLE CHARTS 1.2



### 8.5.3 PEARSON CORRELATION STRENGTH

The Pearson correlation formula is the following (modeFRONTIER User Guide, n.d):

$$\rho_{X,Y} = \frac{\text{cov}(X, Y)}{\sigma_X \sigma_Y} = \frac{E[(X - \mu_X)(Y - \mu_Y)]}{\sigma_X \sigma_Y}$$

The Strength of Association expressed by the correlation coefficients is explained in the following table (*Table 53*):

Strength of Association	Positive	Negative
Low	0.1 to 0.3	-0.1 to -0.3
Medium	0.3 to 0.5	-0.3 to -0.5
High	0.6 to 1.0	-0.6 to -1.0

**Table 53** Pearson correlation strength (modeFRONTIER User Guide, n.d)



## 8.6 REFERENCES

**Al Dakheel, J., & Aoul, K. T.** (2017). Building Applications , Opportunities and Challenges of Active Shading Systems: A State-Of-The-Art Review. <https://doi.org/10.3390/en10101672>

**Alkhayat, J.** (2013). Design strategy for adaptive kinetic patterns : creating a generative design for dynamic solar shading systems, (September).

**Athienitis, A., & O'Brien, W.** (Eds.). (2015). Modeling, Design, and Optimization of Net-Zero Energy Buildings. <https://doi.org/https://ebookcentral-proquest-com.tudelft.idm.oclc.org>

**Baker, N., & Steemers, K.** (2014). Daylight design of buildings: A handbook for architects and engineers. Hoboken: Taylor and Francis.

**Bertoldi, P.,** López Lorente, J., & Labanca, N. (2016). Energy Consumption and Energy Efficiency Trends in the EU-28 2000-2014. <https://doi.org/10.2788/03373>

**Berk Ekici, C. C., & Michela Turrin, I. S. S.** (2019). Performative computational architecture using swarm and evolutionary optimisation: A review. *Building and Environment* , 147, 356–371. Retrieved from [https://ac.els-cdn.com/S0360132318306413/1-s2.0-S0360132318306413-main.pdf?\\_tid=6de46557-b576-4ab8-8b42-2baf9e4b0c37&acdnat=1541064443\\_11b292ea720a0b0b2e809efe8659ac25](https://ac.els-cdn.com/S0360132318306413/1-s2.0-S0360132318306413-main.pdf?_tid=6de46557-b576-4ab8-8b42-2baf9e4b0c37&acdnat=1541064443_11b292ea720a0b0b2e809efe8659ac25)

**Bianchi, L.,** Dorigo, M., Gambardella, L. M., & Gutjahr, W. J. (2009). A survey on metaheuristics for stochastic combinatorial optimization, 239–287. <https://doi.org/10.1007/s11047-008-9098-4>

**Bogenstätter, U.** (2000). Prediction and optimization of life-cycle costs in early design. *Building Research & Information*, 28:5-6, 376–386. <https://doi.org/10.1080/096132100418528>

**Bommel, W. van, & Rouhana, A.** (2016). The science of lighting: A guide about the nature and behaviour of light (second ed.). Philips Lighting University.

**Carlucci, S.,** Causone, F., De Rosa, F., & Pagliano, L. (2015). A review of indices for assessing visual comfort with a view to their use in optimization processes to support building integrated design. *Renewable and Sustainable Energy Reviews*.

**Chudley, R., & Greeno, R.** (2014). Building construction handbook (10th ed.). *Building Construction Handbook (10th ed.)*. Taylor & Francis Group. Retrieved from <https://tudelft.on.worldcat.org/search?databaseList=638&queryString=chudley+building+#/oclc/879025882>

**David, M.,** et al., Assessment of the thermal and visual efficiency of solar shades. *Building and Environment*, 2011. 46(7): p. 1489-1496

**Drozdowski, Z.** (2011). The Adaptive Building Initiative: The Functional Aesthetic of Adaptivity. *Architectural Design*, 81(6), 118–123. doi:10.1002/ad.1329

**Edwards, L.,** & Torcellini, P. (2002). A literature review of the effects of natural light on building occupants. National Renewable Energy Laboratory. <https://doi.org/10.2172/15000841>

**Erlendsson, O.** (2014). *Daylight Optimization : A Parametric Study of Atrium Design*. Stockholm.

**Figueiro, M. G.** (2013). An Overview of the Effects of Light on Human Circadian Rhythms: Implications for New Light Sources and Lighting Systems Design. *Journal of Light & Visual Environment*, 37(2\_3), 51–61. <https://doi.org/10.2150/jlve.IEIJ130000503>

**Flöry S,** Schmiedhofer H, Reis M (2012) *Goat*. Rechenraum, Vienna, AUT

**Heinzelmann, F.** (2018). Design method for adaptive daylight systems for buildings covered by large (span) roofs. Eindhoven. Retrieved from [https://pure.tue.nl/ws/files/96860270/20180612\\_Heinzelmann.pdf](https://pure.tue.nl/ws/files/96860270/20180612_Heinzelmann.pdf)

**Imbert, F.,** Frost, K. S., Fisher, A., Witt, A., Turre, V., & Koren, B. (2013). Concurrent Geometric, Structural and Environmental Design: Louvre Abu Dhabi. *Advances in Architectural Geometry 2012*, 77–90. [https://doi.org/10.1007/978-3-7091-1251-9\\_6](https://doi.org/10.1007/978-3-7091-1251-9_6)

**IES, Approved** Method: IES Spatial Daylight Concurrent Geometric, Structural and Environmental Design: Louvre Abu Dhabi. *Advances in Architectural Geometry 2012*, 77–90. [https://doi.org/10.1007/978-3-7091-1251-9\\_6](https://doi.org/10.1007/978-3-7091-1251-9_6)

**International Energy** Agency (IEA) Solar Heating and Cooling Programme, E. conservation in B. & C. S. (2000). *Daylight in Buildings - A source book on daylighting systems and components*.

**Jagielski, B.** (2009). *Elements of the wave-particle duality of light*. University of Oslo.

**Jakubiec, J. A.,** & Reinhart, C. (2012). The 'adaptive zone' – a alternative for assessing glare throughout daylighted spaces. *Lighting Research & Technology*, 44 (2), 149–170.

**Imbert, F.,** Frost, K. S., Fisher, A., Witt, A., Turre, V., & Koren, B. (2013). Concurrent Geometric, Structural and Environmental Design: Louvre Abu Dhabi. *Advances in Architectural Geometry 2012*, 77–90. [https://doi.org/10.1007/978-3-7091-1251-9\\_6](https://doi.org/10.1007/978-3-7091-1251-9_6)

3-7091-1251-9\_6

**Kamsteeg, A. C.** (2016). Authenticity of light: transformation of historic buildings with structural glass components. Delft University of Technology.

**Karagianni, L. K.** (2015). Additive manufacturing by daylight: Towards a customized shading device. Delft University of Technology.

**Kolarevic, B.** (2003). Computing the Performative in Architecture. Proceedings Autonomy (sDA) and Annual Sunlight Exposure (ASE). 2012, Illuminating Engineering Society.

**Kolarevic, B.** (2003). Computing the Performative in Architecture. Proceedings of the 21th ECAADe Conference: Digital Design, Graz, Austria, 457–464.

**Koziel, S.,** & Yang, X.-S. (Eds.). (2011). Computational Optimization, Methods and Algorithms. In Studies in Computational Intelligence. Springer. <https://doi.org/10.1007/978-3-642-20859-1>

**Lechner, N.** (2015). Heating, Cooling, Lighting: Sustainable Design Methods for Architects. Wiley (4th ed., Vol. 91). Hoboken, New Jersey: John Wiley & Sons, Inc. <https://doi.org/10.1109/28.54258>

**Leftheriotis, G.,** & Yianoulis, P. (2012). Glazings and Coatings. In Comprehensive Renewable Energy (Vol. 3, pp. 313–356). Patras, Greece: Elsevier Ltd. <https://doi.org/10.1016/B978-0-08-087872-0.00310-3>

**León, L. E. L. P. de.** (2016). Shading Design Workflow for Architectural Designers. Delft University of Technology.

**Lewy, A.J.;** Sack, R.L.; Singer, C.M. "Immediate and delayed effects of bright lights on human melatonin production: shifting dawn and dusk shifts the dim light melatonin onset (DLMO)." 1985. In: Wurtman, R.J. et al. (Eds), pp. 253–259.

**Lighting at work** Health and Safety Guidance HSG38 (Sudbury: HSE Books) (1998)

**Lu, C. L.,** Li, Q. S., Huang, S. H., Chen, F. B., & Fu, X. Y. (2012). Large eddy simulation of wind effects on a long-span complex roof structure. Jnl. of Wind Engineering and Industrial Aerodynamics, 100, 1–18. <https://doi.org/10.1016/j.jweia.2011.10.006>

**Mardaljevic, J.,** Andersen, M., Roy, N., & Christoffersen, J. (2012). Daylighting, Artificial Lighting and Non-Visual Effects Study for a Residential Building. VELUX Corporation. Retrieved from <http://lrt.sagepub.com/content/early/2013/06/18/1477153513491873.abstract>

**Mardaljevic, J.,** L. Heschong, and E. Lee, Daylight metrics and energy savings. Lighting Research & Technology, 2009. 41(3): p. 261-283

**Moloney, J.** (2011). *Designing Kinetics for Architectural Facades - State Change*.

**M H Morgan** (translator), *Vitruvius: Ten Books on Architecture* (New York: Dover Publications, New York, 1960), p. 170.

**Nabil, A.** and J. Mardaljevic, Useful daylight illuminances: A replacement for daylight factors. *Energy and Buildings*, 2006. 38(7): p. 905-913

**Nelson, D.** (2016). *Energy Efficient Lighting | WBDG - Whole Building Design Guide*. Retrieved from <https://www.wbdg.org/resources/energy-efficient-lighting>

**Nguyen, A. T.;** Reiter, S.; Rigo, P. A review on simulation-based optimization methods applied to building performance analysis. *Applied Energy* 113 (2014) 1043–1058

**Norbert, L.** (2015). *Heating, Cooling, Lighting : Sustainable Design Methods for Architects*. Wiley (4th ed.). Hoboken, New Jersey: John Wiley & Sons, Inc. <https://doi.org/10.1109/28.54258>

**Olbina, S.** and Y. Beliveau, Developing a transparent shading device as a daylighting system. *Building Research and Information*, 2009. 37(2): p. 148-163

**Osterhaus, W. K. E.** (2005). Discomfort glare assessment and prevention for daylight applications in office environments. *Solar Energy*, 79(2), 140–158. <https://doi.org/10.1016/j.solener.2004.11.011>

**Osterhaus, W.K.E.,** Design Guidelines for Glare-free Daylit Work Environments, in 11th European Conference on Lighting - Lux Europe. 2009: Istanbul (TR)

**Ott Biolight** Systems, Inc. (October 1997). "Ergo Biolight Report." California: Ott Biolight Systems, Inc

**Ott, J.N.** (1982). *Light, Radiation, and You*. Connecticut: Devin-Adair Publishers

**Pahl, G.,** Beitz, W., Feldhusen, J., & Grote, K. H. (2007). *Engineering design: a systematic approach*. (K. Wallace & L. Blessing, Eds.) (Third edit). Verlag, London: Springer.

**Pardalos PM,** Resende MGC. (2002) *Handbook of applied optimization*. Oxford University Press

**Pinterić, M.** (2017). *Building Physics: from physical principles to international standards*. Maribor: Springer. <https://doi.org/10.1007/978-3-319-57484-4>

**Riccobono, A.** (2013). Architectural design in the digital era, identifying computer influences and new expressive trends in current architecture. Dottorato di Ricerca in "Recupero dei Contesti Antichi e Processi Innovativi nell'Architettura XXIV CicloUnivesita degli studi di Palermo. <https://doi.org/http://hdl.handle.net/10447/91050>

**Robbins, Claude L.** (1986). *Daylighting Design and Analysis*. New York: Van Nostrand Reinhold Company; pp. 4-1

**Ruck, N** & Aschehoug, Øyvind & Aydinli, S & Christoffersen, Jens & Edmonds, Ian & Jakobiak, Roman & Kischkoweit-Lopin, M & Klinger, M & Lee, Eleanor & Courret, Gilles & Michel, L & Scartezzini, Jean-Louis & Selkowitz, Stephen. (2000). *Daylight in Buildings - A source book on daylighting systems and components*.

**Rutten, D.** (2013). Galapagos: On the Logic and Limitations of Generic Solvers. *Architectural Design* Volume 83, Issue 2, 132-135. <https://doi.org/https://doi.org/10.1002/ad.1568>

**Sadeghi, G.,** Sani, R. M., & Wang, Y. (2015). Symbolic Meaning of Transparency in Contemporary Architecture : An Evaluation of Recent Public Buildings in Famagusta, (December), 385-401.

**Samant, S. R.** . ( 2011 ). (2011). A parametric investigation of the influence of atrium facades on the daylight performance of atrium buildings . PhD thesis , University of Nottingham . [https://doi.org/http://eprints.nottingham.ac.uk/12303/1/PhD\\_thesis.pdf](https://doi.org/http://eprints.nottingham.ac.uk/12303/1/PhD_thesis.pdf)

**Suk, J. Y.,** Schiler, M., & Kensek, K. (2013). Development of new daylight glare analysis methodology using absolute glare factor and relative glare factor. *Energy and Buildings*, 64, 113-122. <https://doi.org/10.1016/j.enbuild.2013.04.020>

**Szokolay, S.** (2014). *Introduction to architectural science: the basis of sustainable design* -2nd ed. <https://doi.org/10.4324/9781315852409>

**Tedeschi, A.** (2014). *AAD\_Algorithms-Aided Design: Parametric Strategies using Grasshopper*. Le Penseur

**Todd, A.** (2011). Europe. 1E. 1E News & Community, Nightwatchman, Software Lifecycle Automation. 2018<https://www.1e.com/news-insights/blogs/europes-energy-efficiency-economy/>

**Tourre, V.,** & Miguet, F. (2010). Lighting Intention Materialization with a Light-Based Parametric Design Model. *International Journal of Architectural Computing*, 8(4), 507-524. <https://doi.org/10.1260/1478-0771.8.4.507>

**Turrin, M.,** Von Buelow, P., & Stouffs, R. (2011). Design explorations of performance driven geometry in architectural design using parametric modeling and genetic algorithms. *Advanced Engineering Informatics*, 25(4), 656-675.

<https://doi.org/10.1016/j.aei.2011.07.009>

**Turrin, M.,** Stouffs, R., & Sariyildiz, S. (2010). Parametric design of the Vela roof: performance oriented exploration of design alternatives. ASCAAD 2010: Proceedings of the 5th International Conference of the Arab Society for Computer Aided Architectural Design.

**Turrin, M.** (2014). Performance assessment strategies: a computational framework for conceptual design of large roofs. Delft University of Technology, Delft.

**van der Linden, A. C.,** Erdtsieck, P., Kuijpers-van Gaalen, L., & Zeegers, A. (2016). Building physics (second).

**Vierlinger, R.** (2015). Multi Objective Design Interface. <https://doi.org/10.13140/RG.2.1.3401.0324>

**VIRACON. (2015).** Product guide.

**Wang, J.** (2002). Improved engineering design alternative selection using fuzzy sets. *International Journal of Computer Integrated Manufacturing*, 15(1), 18–27. [https://doi.org/10.1016/0047-259X\(82\)90081-1](https://doi.org/10.1016/0047-259X(82)90081-1)

**Wang, W.,** Zmeureanu, R., & Rivard, H. (2005). Applying multi-objective genetic algorithms in green building design optimization. *Building and Environment*, 40, 1512–1525. <https://doi.org/10.1016/j.buildenv.2004.11.017>

**Wienold, J.,** & Christoffersen, J. (2006). Evaluation methods and development of a new glare prediction model for daylight environments with the use of CCD cameras. *Energy and Buildings*, 38(7), 743–757. <https://doi.org/10.1016/j.enbuild.2006.03.017>

**Wortmann, T.** (2018). Efficient , Visual , and Interactive Architectural Design Optimization with Model-based Methods. <https://doi.org/10.13140/RG.2.2.15380.55685>

**Yang, D.,** Sun, Y., di Stefano, D., & Turrin, M. (2017). A computational design exploration platform supporting the formulation of design alternatives, 35–42.

**Yang, D.,** Ren, S., Turrin, M., Sariyildiz, S., & Sun, Y. (2018). Multi-disciplinary and multi-objective optimization problem re-formulation in computational design exploration : A case of conceptual sports building design. *Automation in Construction*, 92(October 2017), 242–269. <https://doi.org/10.1016/j.autcon.2018.03.023>

**Zumtobel. (2018).** The lighting handbook: your concise reference book.

<https://doi.org/10.1021/jp902267g>

## STANDARDS

**NEN-EN 12464-1.** (2011). Light and lighting - Lighting of work places - Part 1: Indoor work places, 1.

•

## 8.7 LIST OF FIGURES

<b>Figure 1</b>	Energy consumption per sector in the European Union in 2015. Source: Eurostat EU-28, 2015.	1
<b>Figure 2</b>	The MacLeamy curve. Source: <a href="http://danieloverbey.blogspot.com/2018/02/five-diagrams-every-design-team-should.html">http://danieloverbey.blogspot.com/2018/02/five-diagrams-every-design-team-should.html</a>	3
<b>Figure 3</b>	Louvre Abu Dhabi. Source: Mohamed Somji © louvre abu dhabi	5
<b>Figure 4</b>	Interior spaces of Louvre Abu Dhabi; effect of 'rain of light'. Source: Roland Halbe © louvre abu dhabi	5
<b>Figure 5</b>	Future development process	8
<b>Figure 6</b>	Research approach	11
<b>Figure 7</b>	Galapagos SA and GA interface. Source: Vierlinger, 2015	22
<b>Figure 8</b>	Conceptual 2D phase space and relative 3D fitness landscape. Source: Rutten, 2013	22
<b>Figure 9</b>	Simulated annealing solver progression. Source: Rutten, 2013	23
<b>Figure 10</b>	Evolutionary solver progression. Source: Rutten, 2013	23
<b>Figure 11</b>	Goat's component and graphical user interface. Source: Vierlinger, 2015	24
<b>Figure 12</b>	Octopus different visualization of trade-off space. Source: <a href="https://www.grasshopper3d.com/group/octopus">https://www.grasshopper3d.com/group/octopus</a>	24
<b>Figure 13</b>	Opossum components in Grasshopper. Source: Thomas Worthmann	25
<b>Figure 14</b>	Opossum graphical user interface. Source: Thomas Worthmann	26
<b>Figure 15</b>	Design Space Exploration framework. Source: Reinhard Koenig	26
<b>Figure 16</b>	modeFrontier visualization of the candidates. Source: <a href="https://">https://</a>	

<a href="http://www.esteco.com/sites/default/files/design_space45.png">www.esteco.com/sites/default/files/design_space45.png</a>	27
<b>Figure 17</b> Sun Path In North Hemisphere. Source: <a href="https://www.nachi.org/building-orientation-optimum-energy.htm">https://www.nachi.org/building-orientation-optimum-energy.htm</a>	29
<b>Figure 18</b> Circadian rhythm. Source: <a href="https://ouraring.com/find-your-own-circadian-rhythm/">https://ouraring.com/find-your-own-circadian-rhythm/</a>	30
<b>Figure 19</b> Solar spectrum. UV, Visible and Infrared wavelengths. Source: Lechner, 2015	32
<b>Figure 20</b> The greenhouse effect. Source: Lechner, 2015	32
<b>Figure 21</b> Electromagnetic spectrum. Source: van Bommel & Rouhana, 2016	33
<b>Figure 22</b> Daylight sources. Source: <a href="https://www.velux.com/deic/daylight/daylighting">https://www.velux.com/deic/daylight/daylighting</a>	34
<b>Figure 23</b> Light behaviour. Source: <a href="http://weeklisciencequiz.blogspot.com/2011/09/when-light-meets-matter.html">http://weeklisciencequiz.blogspot.com/2011/09/when-light-meets-matter.html</a>	34
<b>Figure 24</b> Light behaviour for non-transparent (left) and transparent material (right). Source: Pinterić, 2017	36
<b>Figure 25</b> Energy use distribution for generic buildings. Source: Norbert, 2015	37
<b>Figure 26</b> Indication of the energy and electrical demand savings possible with daylighting. Source: Norbert, 2015	37
<b>Figure 27</b> Daylight factor. Source: <a href="http://www.nzeb.in/knowledge-centre/passive-design/daylighting/">http://www.nzeb.in/knowledge-centre/passive-design/daylighting/</a>	41
<b>Figure 28</b> Range of lighting levels. Source: van Bommel & Rouhana, 2016	44
<b>Figure 29</b> Hormones production related to the circadian rhythm. Source: Brainard, 2002	50
<b>Figure 30</b> Spectral energy distribution of an incandescent lamp (2800 K). Source: van Bommel & Rouhana, 2016	52
<b>Figure 31</b> Spectral energy distribution of daylight (5000 K). Source: van Bommel & Rouhana, 2016	52
<b>Figure 32</b> Impact of colours. Source: <a href="https://www.tcpi.com/psychological-impact-light-color/">https://www.tcpi.com/psychological-impact-light-color/</a>	53
<b>Figure 33</b> Kruithof curve, modern version. Source: Wikipedia	54
<b>Figure 34</b> Glass properties. Source: <a href="http://www.nzeb.in/knowledge-centre/passive-design/fenestration/">http://www.nzeb.in/knowledge-centre/passive-design/fenestration/</a>	57
<b>Figure 35</b> Position of shading device. Source: <a href="https://designbuilder.co.uk/helpv1/Content/_Window_shading_internal_1.htm">https://designbuilder.co.uk/helpv1/Content/_Window_shading_internal_1.htm</a>	59
<b>Figure 36</b> Grasshopper and modeFRONTIER workflow. Adapted from: Yang, Ren, Turrin, Sariyildiz & Sun, 2018	71
<b>Figure 37</b> Conventional design process. Adapted from Yang, Ren, Turrin, Sariyildiz & Sun, 2018	72

<b>Figure 38</b>	Relation between design exploration and optimization phases. Source: Yang, Ren, Turrin, Sariyildiz & Sun, 2018	73
<b>Figure 39</b>	Computational Design Exploration	76
<b>Figure 40</b>	Computational Design Optimization workflow	77
<b>Figure 41</b>	Parametric surface triangulation (Monkey Saddle). Source: CC BY-SA 4.0 ( <a href="https://creativecommons.org/licenses/by-sa/4.0">https://creativecommons.org/licenses/by-sa/4.0</a> )	83
<b>Figure 42</b>	Concept alternative 1	84
<b>Figure 43</b>	Concept alternative 2	84
<b>Figure 44</b>	Concept alternative 3	84
<b>Figure 45</b>	Principle of concepts of group 1	85
<b>Figure 46</b>	Logical and geometrical construction of alternative 1 and 2	86
<b>Figure 47</b>	Logical and geometrical construction of alternative 3	86
<b>Figure 48</b>	Example of logical and geometrical construction of a full shading system	87
<b>Figure 49</b>	Examples of concept alternatives applied to reference building.	87
<b>Figure 50</b>	Reference building orientation	89
<b>Figure 51</b>	Input variables displayed	92
<b>Figure 52</b>	Input variables inclination x and y for concept alternative 3	93
<b>Figure 53</b>	Computational Design Exploration workflow constructed and used with modeFRONTIER	95
<b>Figure 54</b>	4D bubble chart of all the three concept alternatives. Relation DA, UDI, alternative (colour) and scaling_factor (diameter)	97
<b>Figure 55</b>	Bubble chart of all the three concept alternatives. Relation DA, UDI and alternative (colour)	98
<b>Figure 56</b>	CDE Bubble chart _ alternatives behavior regarding heating energy demand and UDI	98
<b>Figure 57</b>	CDE Bubble chart _ alternatives behavior regarding tot energy demand and UDI	99
<b>Figure 58</b>	CDE _ Bubble chart alternatives comparison _ relation between energy demand and glass area	100
<b>Figure 59</b>	CDE _ Bubble chart alternative comparison _ relation between energy demand, glass area and glass material	100
<b>Figure 60</b>	Bubble chart showing the relation between the UDI,overlit, the	

area of glass and the glazing material	101
<b>Figure 61</b> Bubble chart showing relation between UDI, overlit, lights energy and glass material	102
<b>Figure 62</b> Clusters parallel coordinates chart _ hierarchical clustering of the three concept alternatives	102
<b>Figure 63</b> Cluster parallel chart filtering only concept alternative 1	104
<b>Figure 64</b> CDE _ Bubble chart alternative 1 _ relation between energy demand, module depth and scaling factor	105
<b>Figure 65</b> Cluster parallel chart filtering only concept alternative 2	106
<b>Figure 66</b> CDE _ Bubble chart alternative 2 _ relation between energy demand, shading module depth and glass material	107
<b>Figure 67</b> Cluster parallel chart filtering only concept alternative 3	108
<b>Figure 68</b> CDE _ Bubble chart alternative 3 _ relation between heating energy, shading area and glass material	109
<b>Figure 69</b> CDE _ Bubble chart alternative 3 _ relation between heating energy, glass area and glass material	110
<b>Figure 70</b> Section view of the three initial concept alternatives for CDE (1-3) and final optimal alternative concept 4	113
<b>Figure 71</b> 3D view of the three initial concept alternatives for CDE (1-3) and final optimal concept alternative 4	114
<b>Figure 72</b> Render of the Terminal, front view. Source: ©KAAN Architecten	120
<b>Figure 74</b> Terminal floor plan with highlight of the space considered for the simulation. Source: ©KAAN Architecten	121
<b>Figure 73</b> Top view of the New Schiphol Terminal. Source: ©KAAN Architecten	121
<b>Figure 75</b> Exploded view of the Terminal and highlight of the space considered for the optimization. Source: ©KAAN Architecten	122
<b>Figure 76</b> Dimensions of the analysed space	122
<b>Figure 77</b> Dimension of the area considered scaled down four times. Model used for computational workflow.	123
<b>Figure 78</b> Render of the main entrance of the Terminal. Source: ©KAAN Architecten	123
<b>Figure 79</b> Original and scaled dimensions of the roof shading module	124
<b>Figure 80</b> Workflow part 1 - case study variation 1 _ three curtain walls	125
<b>Figure 81</b> Workflow part 2 - case study variation 2 _ opaque walls	126

<b>Figure 82</b>	Example of alternative concept 4 applied to New Schiphol Terminal. Prospective views and top view	127
<b>Figure 83</b>	Perspective views of the model of the Terminal - variation 1	128
<b>Figure 84</b>	Perspective views of the model of the case study with three curtain walls and completely opaque roof	131
<b>Figure 85</b>	Line graph of monthly values of energy demand _ step 1.1.A of the workflow Case Study variation 1	135
<b>Figure 86</b>	Line graph of monthly values of energy demand _ step 1.1.B of the workflow Case Study variation 1	138
<b>Figure 87</b>	Line graph of monthly values of energy demand _ step 1.1.A and 1.1.B of the workflow Case Study variation 1	139
<b>Figure 88</b>	modeFRONTIER logical computational optimization workflow _ step 1.2 of the workflow Case Study variation 1	142
<b>Figure 89</b>	Case Study orientation and direction of the inclination in x and y direction	143
<b>Figure 90</b>	Pie chart design summary _ optimization step 1.2	144
<b>Figure 91</b>	History chart of the optimization algorithm converging to minimize ASE	144
<b>Figure 93</b>	Parallel chart of feasible designs from optimization 1.2, filtered to meet the daylight targets	145
<b>Figure 92</b>	Bubble chart with designs converging to the optimization targets _step 1.2 of the workflow of Case Study variation 1	145
<b>Figure 94</b>	Top and perspective view of design no. 1 _ optimization 1.2	147
<b>Figure 95</b>	Correlation matrix chart displaying Pearson correlation coefficients between the selected variables _ step 1.2.A	149
<b>Figure 96</b>	Bubble chart showing relation between cooling, heating and total energy demand of the 50 selected designs _ step 1.2.A	150
<b>Figure 97</b>	Perspective view of the final selected design _ step 1.2.A	151
<b>Figure 98</b>	Correlation matrix chart displaying Pearson correlation coefficients between the selected variables _ step 1.2.B	152
<b>Figure 99</b>	Bubble chart showing relation between cooling, heating and total energy demand of the 50 selected designs _ step 1.2.B	152
<b>Figure 100</b>	Perspective views of the model of the Terminal - variation 2	155
<b>Figure 101</b>	Pie chart design summary _ optimization step 2.2	159

<b>Figure 102</b>	Bubble chart showing relation between DA, UDI,75 and ASE _ optimization step 2.2	160
<b>Figure 103</b>	Bubble chart showing relation between UDI,75, DA and depth_ triangle _ optimization step 2.2	160
<b>Figure 104</b>	Bubble chart showing relation between UDI,75, DA and scaling factor _ optimization step 2.2	161
<b>Figure 105</b>	Correlation matrix chart displaying Pearson correlation coefficients between the selected variables _ step 2.2	161
<b>Figure 106</b>	Parallel chart of feasible designs from optimization 2.2, filtered to meet the daylight targets	162
<b>Figure 107</b>	Top and perspective view of design no. 1 _ optimization 2.2	164
<b>Figure 108</b>	Top and perspective view of design no. 5 _ optimization 2.2	164
<b>Figure 109</b>	Correlation matrix chart displaying Pearson correlation coefficients between the selected variables _ step 2.2.A	165
<b>Figure 110</b>	Bubble chart showing relation between cooling, heating and total energy demand _ optimization step 2.2.A	166
<b>Figure 111</b>	Top and perspective view of the final selected design _ step 2.2.A	167
<b>Figure 112</b>	Correlation matrix chart displaying Pearson correlation coefficients between the selected variables _ step 2.2.A	168
<b>Figure 113</b>	Bubble chart showing relation between cooling, heating and total energy demand _ optimization step 2.2.B	169
<b>Figure 114</b>	Top and perspective view of the final selected design _ step 2.2.B	170
<b>Figure 115</b>	Workflow Case Study variation 1 _ performance outputs comparison	172
<b>Figure 116</b>	Workflow Case Study variation 2 _ performance outputs comparison	173
<b>Figure 117</b>	First proposed and adopted CDE workflow	180
<b>Figure 118</b>	First proposed and adopted CDO workflow applied on Case Study variation 1	181
<b>Figure 119</b>	First proposed and adopted CDO workflow applied on Case Study variation 2	182
<b>Figure 120</b>	New proposed CDE workflow	184
<b>Figure 121</b>	Final CDE workflow applied on Case Study variation 1	185
<b>Figure 122</b>	Final CDO workflow applied on Case Study variation 2	186
<b>Figure 123</b>	Electromagnetic wave. Source: van Bommel & Rouhana, 2016	202

<b>Figure 124</b>	Characteristics of light wave. Source: van Bommel & Rouhana, 2016	203
<b>Figure 125</b>	Smooth surface, specular reflection and transmission. Source: Pinterić, 2017	206
<b>Figure 126</b>	Rough surface, diffuse reflection and transmission. Source: Pinterić, 2017	206
<b>Figure 127</b>	Real surface, glossy reflection and transmission. Source: Pinterić, 2017	207
<b>Figure 128</b>	Constructive interference.	207
<b>Figure 129</b>	Destructive interference.	208
<b>Figure 130</b>	White ceiling panels used for skylights. Source: <a href="http://spectraldb.com/materials/1392">http://spectraldb.com/materials/1392</a>	209
<b>Figure 131</b>	Reference building geometry	210
<b>Figure 132</b>	Basic geometry as starting definition of the three alternatives	210
<b>Figure 133</b>	Construction of alternative concept 1	211
<b>Figure 134</b>	Construction of alternative concept 2	211
<b>Figure 135</b>	Construction of inclinations for alternative concept 3	211
<b>Figure 137</b>	Alternative selection	212
<b>Figure 136</b>	Construction of alternative concept 3	212
<b>Figure 138</b>	Definition of Radiance materials	213
<b>Figure 139</b>	Daylight simulation in DIVA 4	214
<b>Figure 140</b>	Solar radiation simulation in DIVA 4	215
<b>Figure 141</b>	Energy simulations in EnergyPlus through ARCHSIM	216
<b>Figure 142</b>	History chart of the optimization algorithm converging to constrain DA	218
<b>Figure 143</b>	History chart of the optimization algorithm converging to maximize UDI,75	218

## 8.8 LIST OF TABLES

<b>Table 1</b>	Daylight comfort indexes. Source: Carlucci, Causone, De Rosa, & Pagliano, 2015	38
<b>Table 2</b>	Illuminance average values. Source: Lighting at work Health and Safety Guidance HSG38 (Sudbury: HSE Books) (1998)	40
<b>Table 3</b>	UDI illuminance limit values. Source: Carlucci et al., 2015	43
<b>Table 4</b>	Illuminance Uniformity recommended in standards for indoor spaces. Source: Slater & Boyce, 1990	45
<b>Table 5</b>	Comparison of CGI and DGP indexes. Source: Jakubiek & Reinhart, 2012	49
<b>Table 6</b>	Table summarizing the features of precedent buildings with large roof shading systems	61
<b>Table 7</b>	Input variables of reference building for CDE	90
<b>Table 8</b>	Input settings in Grasshopper for the CDE	91
<b>Table 9</b>	Variables inclination_x and inclination_y explained	92
<b>Table 10</b>	Reference glass products. Source: Saint-Gobain Glass, 2013	93
<b>Table 11</b>	Multi-criteria analysis table with weighted scores for each criteria	112
<b>Table 12</b>	Weighted scores total score for each alternative and partial for each performance	113
<b>Table 13</b>	Material areas of the current roof shading system	128
<b>Table 14</b>	Lighting requirements for interior airports transportation areas. Source: NEN-EN 12464-1:2011 en	129
<b>Table 15</b>	Input daylight simulation _ step 1.1 of the workflow Case Study variation 1	130
<b>Table 16</b>	Output values daylight simulation _ step 1.1 of the workflow Case Study variation 1	130
<b>Table 17</b>	Output values of daylight simulation from Terminal with closed roof	131
<b>Table 18</b>	Input values energy simulation _ step 1.1.A of the workflow Case Study variation 1. Based on data of the project provided by ABT	133
<b>Table 19</b>	Output energy simulation _ step 1.1.A of the workflow Case Study variation 1	134
<b>Table 20</b>	Monthly values of energy demand _ step 1.1.A of the workflow Case Study variation 1	134
<b>Table 21</b>	Input values energy simulation _ step 1.1.B of the workflow Case	

Study variation 1. Based on data of the project provided by ABT	136
<b>Table 22</b> Output values energy simulation _ step 1.1.B of the workflow Case Study variation 1	137
<b>Table 23</b> Monthly values of energy demand _ step 1.1.B of the workflow Case Study variation 1	137
<b>Table 24</b> Settings for computational design optimization _ step 1.2 of the workflow Case Study variation 1	140
<b>Table 25</b> Outputs and target CDO _ step 1.2 of the workflow of Case Study variation 1	141
<b>Table 26</b> Targets of the CDO_ step 1.2 of the workflow of Case Study variation 1	141
<b>Table 27</b> Input variables of the CDO _ step 1.2 of the workflow of Case Study variation 1	142
<b>Table 28</b> Input variables inclination in x and y direction	143
<b>Table 29</b> Summary of the output from daylight optimization of the best 50 designs _ step 1.2	146
<b>Table 30</b> Five best designs from the computational optimization _ step 1.2 of the workflow of Case Study variation 1	147
<b>Table 31</b> Input settings for best energy performing solution _ step 1.2.A of the workflow Case Study 1	150
<b>Table 32</b> Daylight performances and material amount of the final selected design _ step 1.2.A	151
<b>Table 33</b> Energy performances of the final selected design _ step 1.2.A	151
<b>Table 34</b> Input settings for best energy performing solution _ step 1.2.B of the workflow Case Study variation 1	153
<b>Table 35</b> Daylight performances and material amount of the final selected design _ step 1.2.B	153
<b>Table 36</b> Energy performances of the final selected design _ step 1.2.B	154
<b>Table 37</b> Output values daylight simulation _ step 2.1 of the workflow Case Study variation 2	156
<b>Table 38</b> Output values energy simulation _ step 2.1.A of the workflow Case Study variation 2	156
<b>Table 39</b> Output values energy simulation _ step 2.1.B of the workflow Case Study variation 2	157
<b>Table 40</b> Summary of the output from daylight optimization of the best 50 designs _ step 2.2	162
<b>Table 41</b> Five best designs from the computational optimization _ step 2.2 of	

the workflow of Case Study variation 2	163
<b>Table 42</b> Input settings for best energy performing solution _ step 2.2.A of the workflow Case Study variation 2	166
<b>Table 43</b> Daylight performances and material amount of the final selected design _ step 2.2.A	167
<b>Table 44</b> Energy performance of the final selected design _step 2.2.A	167
<b>Table 45</b> Input settings for best energy performing solution _ step 2.2.B of the workflow Case Study variation 2	169
<b>Table 46</b> Daylight performances and material amount of the final selected design _ step 2.2.B	170
<b>Table 47</b> Energy performance of the final selected design _step 2.2.B	170
<b>Table 48</b> Comparison daylight output Case Study variation 1(step 1.1) and optimization 1.2	174
<b>Table 49</b> Comparison daylight output Case Study variation 2 (step 2.1) and optimization 2.2	175
<b>Table 50</b> Results of Photoelectric experiments. Source: <a href="https://web.phys.ksu.edu/fascination/Chapter17.pdf">https://web.phys.ksu.edu/fascination/Chapter17.pdf</a>	206
<b>Table 51</b> DIVA input Radiance materials	215
<b>Table 52</b> Multi-criteria analysis table with scores for each criteria and weights	219
<b>Table 53</b> Pearson correlation strength (modeFRONTIER User Guide, n.d)	222





